# Rapid Increase of Molecular Complexity through C–H and C–C Bond Activation

**Kelvin Ho**

*Thesis submitted in accordance with the requirements of the University of Liverpool for the degree of*
***Doctor of Philosophy***

UNIVERSITY OF LIVERPOOL

**Department of Chemistry**
**Sept 2014**

# Rapid Increase of Molecular Complexity through C–H and C–C Bond Activation

*Kelvin Ho*

## Abstract

The activation of carbon-hydrogen (C–H) and carbon-carbon (C–C) bonds by transition metal catalysts is an attractive strategy to streamline organic synthesis. Herein this manuscript, the two main areas of research are described.

Firstly, it was found that a nickel catalyst can promote the insertion of alkynes into the C–C bond of 3-azetidinones and 3-oxetanones to enable quicker access to pyranones and pyridinones in high yields and excellent regioselectivity.

Secondly, a rhodium-catalysed pyridine directed C–H bond activation enables the rearrangement of 1,6-heptadienes into bicyclo[2.2.1]heptanes in good yields. Importantly, three stereogenic centres are created with complete diastereocontrol in this atom-efficient reaction.

In chapter 1, an overview of the literature on transition metal-catalysed C–C bond activation of four membered rings is described. In chapter 2, our efforts to optimise the catalytic conditions and build the scope of the nickel-catalysed reaction are reported. In chapter 3, the results of the mechanistic investigations of the nickel-catalysed reaction are reported.

Finally in chapter 4, a brief overview of the transition metal-catalysed functionalisation of an alkene C–H bond with another alkene is described. Subsequently, the optimisation of the catalytic conditions and the scope of the diastereoselective carbocyclisation of 1,6-heptadienes triggered by rhodium-catalysed activation of an alkene C–H bond are reported.

# Acknowledgements

I wish to acknowledge the contributions made to me by my primary supervisor, Doctor Christophe Aïssa. Throughout my PhD, Dr Aïssa has been a consistently a great source of help, guidance and enthusiasm for chemistry. Furthermore, Dr Aïssa gave countless hours of his time and has contributed greatly to my scientific development.

I have been very fortunate to have Chris Halsall as my industrial supervisor. His patience is unbelievable and has been a positive influence on my PhD degree. I am grateful for his supervision during my industrial placement at AZ Alderley Park. Furthermore, I have received valuable input from him during our meetings throughout my PhD degree. Chris and along with the other members of the laboratory, have made the experience both productive and enjoyable.

I am forever grateful to all the members of the Aïssa group of both the past and present. I would like to thank Damien Crépin for being an extremely great source of help during the start of my PhD. Throughout my time in the Aïssa group, all of my colleagues have been helpful to me. All have helped to keep my spirits high especially when another failed nickel-catalysed reaction had to happen. I would like to thank Stephanie Yip for her delicious lunches. I am particularly grateful to Dr. Daniel J. Tetlow and Maria Pin-Nó for their contributions to the rhodium-catalysed research project. Together, we managed to publish work of a high standard with great efficiency. I am also thankful to the Evan's group members because they have helped to keep the laboratory lively and dynamic.

I am thankful to all of the technical staff in the chemistry department of Liverpool. Particularly to Dr. Jonathan Iggo and Konstantin for their assistance with my many NMR experiments.

I would like to thank all the members of the place of worship in Manchester. I had a really good time with all of you and I have been very lucky to meet each one of you. I thank God for

such an opportunity. I hope the place of worship can grow in the near future. I am really thankful to Zico Liu for being my “bigger” brother. Thank you all for pushing me to keep going, especially when another failed nickel-catalysed reaction had to happen.

Finally, I am very grateful to my parents and my sister who have provided constant support during these 4 years. I could not have completed my PhD without them. Thank you always for encouraging me to do my best in life.

# Abbreviations and Definitions

| | |
|---|---|
| ν̃ | wavenumber |
| δ | chemical Shift |
| °C | Degree Celsius |
| 1,2-DCE | 1,2-Dichloromethane |
| 1,2-DME | 1,2-Dimethoxyethane |
| BINAP | 2,2'-bis(diphenylphosphino)-1,1'-binaphthyl |
| Bn | Benzyl |
| BnBr | Benzyl Bromide |
| br | Broad |
| calcd | calculated |
| CI | Chemical Ionisation |
| cod | cyclooctadiene |
| coe | cyclooctene |
| d | doublet |
| DMAc | Dimethylacetamide |
| DMAP | 4-Dimethylaminopyridine |
| DMI | 1,3-Dimethyl-2-imidazolidinone |
| DMSO | Dimethyl Sulfoxide |
| DM-SegPHOS | 5,5’-Bis(diphenylphosphino)-4,4’-bi-1,3-benzodioxole |
| DPEPHos | (Oxydi-2,1-phenylene)bis(diphenylphosphine) |
| dppe | 1,2-Bis(diphenylphosphino)ethane |
| dppb | 1,2-Bis(diphenylphosphino)butane |
| ee | Enantiomeric Excess |

| | |
|---|---|
| equiv | equivalent |
| ESI | Electrospray Ionisation |
| EtOAC | Ethyl Acetate |
| $Et_2O$ | Diethyl Ether |
| g | gram |
| GC | Gas Chromatography |
| hr | hour |
| HMBC | Heteronuclear Multiple Bond Correlation |
| HRMS | High Resolution Mass Spectrometry |
| HSQC | Heteronuclear Single-Quantum Correlation |
| Hz | Hertz |
| IMes | 1,3-bis(2,4,6-trimethylphenyl)-imidazolium |
| IPr | 1,3-bis(2,6-diisopropylphenyl)imidazol-2-ylidene |
| IR | Infrared Red |
| J | Coupling Constant |
| m | Multiplet |
| M | Molar |
| LDA | Lithium Diisopropylamide |
| m.p. | melting point |
| mg | miligram |
| MHz | Megahertz |
| min | minute |
| ml | millilitre |
| mmol | millimole |
| MS | Mass Spectroscopy |
| MTBE | Methyl *tert*butyl ether |

| | |
|---|---|
| NaHMDS | Sodium bis(trimethylsilyl)amide |
| nbd | Norbordiene |
| NMR | Nuclear Magnetic Resonance |
| noe | Nuclear Overhauser effect |
| NOESY | Nuclear Overhauser effect spectroscopy |
| PE | Petroleum Ether (40/60) |
| Ph | Phenyl |
| ppm | Part per million |
| q | quadruplet |
| rt | room temperature |
| rac | racemic |
| s | singlet |
| SIPr | 1,3-bis(2,6-diisopropylphenyl)imidazolidin-2-ylidene |
| t | triplet |
| T | Temperature |
| TBAF | Tetra-n-butylammonium fluoride |
| THF | Tetrahydrofuran |
| TLC | Thin Layer Chromatography |

# Table of Contents


Abstract ..... 1

Acknowledgements ..... 2

Abbreviations and Definitions ..... 4

Chapter 1 Carbon–Carbon Bond Activation of Four-Membered Rings ..... 12

1.1 Introduction ..... 12

1.2 Transition metal catalysed C–C σ bond cleavage ..... 15

1.2.1 Cyclobutanones ..... 15

1.2.2 Cyclobutenones and benzocyclobutenones ..... 20

1.2.3 Cyclobutadienones ..... 26

1.2.4 Vinyl-Cyclobutanols and Allenylcyclobutanols ..... 28

1.2.5 Cyclobutenols and benzocyclobutenols ..... 32

1.2.6 Cyclobutanone *O*-Benzoyloximes ..... 34

1.2.7 Biphenylenes ..... 35

1.2.8 Alkylidenecyclobutanes ..... 37

1.3 Conclusion and Outlook ..... 38

1.4 References ..... 44

Chapter 2 Nickel-Catalysed Cycloaddition of 3-Azetinones and 3-Oxetanones with Alkynes ..... 48

2.1 Aim and Hypothesis ..... 48

2.2 Optimisation ..... 49

2.3 Scope of the reaction ..... 58

2.3.1 Cycloaddition of *N*-Boc Azetidinone with alkynes ..... 58

2.3.2 Limitations ..... 70
2.3.2.1 Terminal Alkynes ..... 70
2.3.2.2 Alkynyl pyridines ..... 71
2.3.2.3 Electron-deficient alkynes ..... 72
2.3.2.4 Alkynyl boronate esters ..... 73
2.3.2.5 Propargyl ethers ..... 73
2.3.2.6 Miscellaneous alkynes ..... 78
2.3.3 Cycloaddition of *N*-Benzhydryl azetidinone 76 with alkyne 5b ..... 79
2.3.4 Cycloaddition of *N*-Ts Azetidinones with alkynes ..... 80
2.3.5 Aromatisation to pyridinols ..... 84
2.3.6 Cycloaddition of oxetanones with alkynes ..... 85
2.3.7 Optimisation of the formation of four-membered ring 8 ..... 88
2.3.8 Initial attempts of formal [4+2] cycloaddition of azetidinone with alkenes ..... 92
2.4 Future development of air-stable Ni(II) pre-catalyst ..... 93
2.4.1 Introduction and initial optimisation ..... 93
2.4.2 1,3-Enyne as alkyne surrogate to improve regioselectivity ..... 97
2.4.2.1 Regioselectivity issues with alkyne 5k ..... 97
2.4.2.2 1,3-Enyne as alkyne surrogate ..... 99
2.5 Conclusion ..... 105
2.6 Synthesis of Precursors ..... 106
2.6.1 Synthesis of 3-azetidinones ..... 106
2.6.2 Synthesis of 3-oxetanones ..... 107

2.6.3 Synthesis of alkynes ..... 108

2.7 Experimental Section ..... 114

2.7.1 Synthesis of 3-azetidinones ..... 114

2.7.2 Synthesis of 3-oxetanones and precursor ..... 118

2.7.3 Synthesis of alkynes ..... 119

2.7.4 Nickel(0): Synthesis of pyridinones and pyranones ..... 132

2.7.5 Nickel(II): Synthesis of pyridinones ..... 163

2.7.6 Hydrogenation and Aromatisation ..... 165

2.8 References ..... 169

Chapter 3 Mechanistic Investigations ..... 173

3.1 Introduction ..... 173

3.2 Results and Discussion ..... 183

3.2.1 Re-optimisation of the reaction conditions ..... 183

3.2.2 Rate law with silylated alkyne 74 ..... 185

3.2.2.1 “Initial Burst” Phase ..... 185

3.2.2.2 Kinetic study with silylated alkyne 73 ..... 193

3.2.2.3 NMR studies ..... 197

3.3 Revised Mechanism and Conclusion ..... 201

3.4 Experimental data ..... 203

3.4.1 Kinetic study ..... 203

3.4.1.1 Kinetic study: Ni(cod)2/PPh3 (1:3) ..... 203

3.4.1.2 Kinetic Study: Ni(cod)2/PPh3 (1:2) ..... 215

3.4.2 NMR studies ..... 224

3.4.2.1 Product Inhibition ..... 224

3.4.2.2 Competition Experiment ..... 225

3.4.2.3 Synthesis of 77 ..... 227

3.4.2.4 Catalytic competency of 77 ..... 227

3.4.2.5 Reaction of 77 with excess 73 ..... 227

3.4.2.6 Reaction of 77 with excess 79 ..... 228

3.4.2.7 Reaction of 77 with 70 ..... 229

3.5 References ..... 229

Chapter 4 Transition Metal-Catalysed Functionalisation of an Alkene C–H Bond with another Alkene ..... 231

4.1 Introduction ..... 231

4.1.1 Formation of a metallacycle intermediate via oxidative cyclisation ..... 233

4.1.2 *In situ* formation of metal hydride ..... 235

4.1.3 C–H bond activation ..... 237

4.1.3.1 Oxidative cross coupling ..... 237

4.1.3.2 Group directed C–H activation ..... 240

4.2 Aims and Hypothesis ..... 252

4.3 Optimisation of the reaction ..... 253

4.4 Scope of the reaction ..... 270

4.4.1 Another directing group ..... 273

4.5 Mechanistic studies ..... 273

4.5.1 Deuterium-labelling experiment ..... 275

4.6 Conclusion ..... 282

4.7 Future work ..... 283

4.8 Synthesis of precursors ..... 284

4.9 Experimental ..... 291

4.10 References ..... 322

# Chapter 1 Carbon–Carbon Bond Activation of Four-Membered Rings

## 1.1 Introduction

Carbon–Carbon (C–C) σ bond activation by transition metals is an attractive atom-economical methodology for organic chemists as it can potentially streamline the synthesis to targets of interest.[1] However, C–C activation is thermodynamically unfavourable as a C–C σ bond (90 kcal $mol^{-1}$) is broken to form two weaker metal carbon bonds (20-30 kcal $mol^{-1}$).[1d] Moreover, by comparison of the orbital alignment of C–C π bonds versus C–C σ bonds (Scheme 1), the C–C σ bond orbitals lie along the bond axis and render them less accessible for a good overlap with the incoming orbitals of the transition metal.[2] Whereas for C–C π bonds, the orbitals are more accessible as they are projected out of the C–C axis.

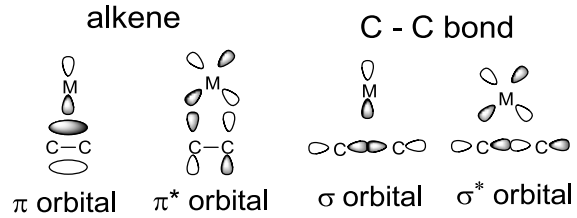


**Scheme 1** Orbital diagram

To overcome the barriers for C-C σ bond activation, substrates with high strain energy are commonly employed as the release of this energy drives the reaction forward. The orbital alignment of C–C σ bonds in strained systems such as 3- or 4-membered rings generally do not

lie in the plane of the ring but are commonly distorted out of plane which allows for increased orbital interaction with the orbitals of the transition metal.[3]

Hence, Wiberg reported that orbitals of the C–C bond of cyclobutane are bent out of plane by approximately 7° (Scheme 2).[4] In cyclohexane, the bond path angles of the C–C bond are closed to ideal. However, the bond path angle in cyclobutane is distorted.

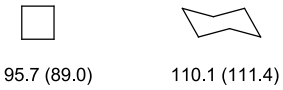


**Scheme 2** Bond path angles

Experimentally, the C–C–C bond angle in cyclobutane is found to be 89°. This large angle deviation from the ideal contributes to the high angle strain in cyclobutane. Furthermore, many C–H bonds are eclipsing which results in high torsional strain. To minimise the torsional strain, the cyclobutane adopts a puckered conformation to reduce some of the eclipsing interactions. Both angle strain and torsional strain contribute to the high ring strain energy observed in cyclobutane as determined theoretically[5] and experimentally[6] (Scheme 3). Therefore, the relief of this high ring strain energy serves as a thermodynamic driving force for the C–C cleavage of cyclobutane. As mentioned earlier, the strength of a typical C–C bond is roughly 90 kcal / mol and it can be seen that the high ring strain of cyclobutane substantially weakens the C–C bond of cyclobutane.

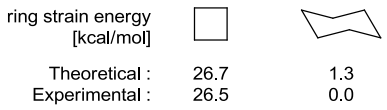


**Scheme 3** Ring strain energy in cyclobutane vs cyclohexane

Due to the aforementioned kinetic and thermodynamic factors of four-membered ring systems, these systems are amenable to cleavage of a C–C σ bond by a variety of transition metals. Three of the most common mechanisms for the C–C bond cleavage are direct oxidative insertion, β-C elimination and [1,2]-shift (Scheme 4).[1k]

On the one hand, the direct oxidative insertion of a transition-metal complex into a four-membered ring system **1** results in the formation of 5-membered ring metallacycle **2**. Metallacycle **2** can then be subjected to a variety of transformations.

On the other hand, transition-metal complexes can activate four-membered ring systems **3** to undergo β-C elimination. β-C elimination is a rearrangement process whereby the relief of ring strain serves as a thermodynamic driving force. The resulting alkyl metal intermediate **4** can then be exploited for further transformations.

Finally, [1,2]-shift is a carbocation rearrangement commonly observed in four-membered ring systems **5**. Unlike, oxidative addition and β-C elimination, the metal never comes in direct contact with the C–C bond cleaved in the process. The resulting metal intermediate **6** can then be subjected to further transformations.

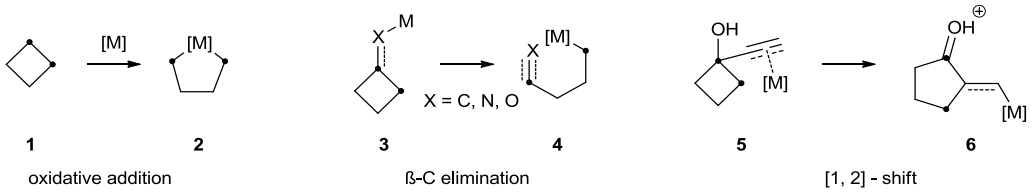


**Scheme 4** Three Common C–C bond cleavage processes

## 1.2 Transition metal catalysed C–C σ bond cleavage

### 1.2.1 Cyclobutanones

In 1994, Ito and co-workers reported the first catalytic C–C bond activation of cyclobutanone **7** (Scheme 5).[7] It was proposed that oxidative insertion of the rhodium catalyst into the less sterically hindered acyl-carbon bond of **7** would afford pentarhodacycle **8**. Under 50 atmospheres of hydrogen, hydrogenolysis of **8** would eventually afford alcohol **9** as product.

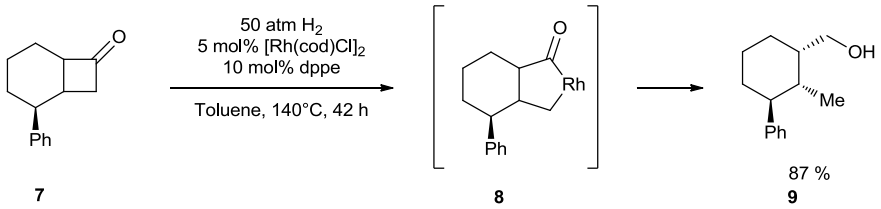


**Scheme 5** Rhodium-catalysed hydrogenolysis of cyclobutanone

After this preliminary work, Murakami and co-workers reported a rhodium-catalysed rearrangement of strained *spiro*-cyclobutanone **10** into cyclohexenone **11** whereby the putative rhodacycle **12** is trapped by another C–C bond cleavage process (Scheme 6).[8] The authors postulated that oxidative insertion of the rhodium catalyst into the acyl-carbon bond of **10** would form the initial pentarhodacycle **12**. Ring enlargement by β-C elimination would then afford heptarhodacycle **13**, which after reductive elimination and isomerisation of the double bond would afford cyclohexenone **11** as product.

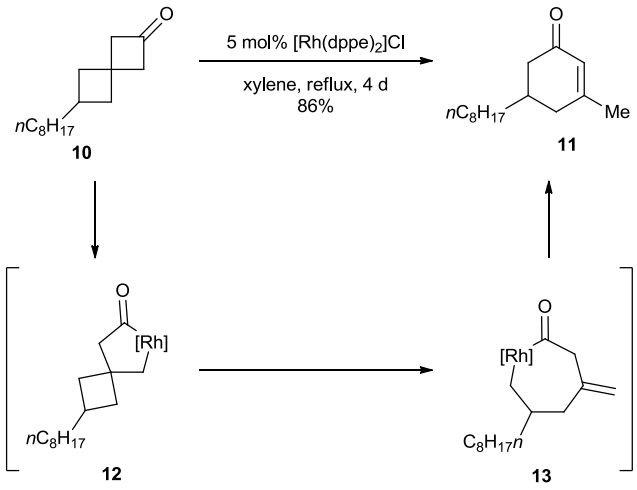


**Scheme 6** Rhodium-catalysed ring opening of spiro-cyclobutanone

Murakami and co-workers also reported some striking ligand effects on the C–C bond cleavage of cyclobutanone **14** (Scheme 7).[9] With dppe as a ligand, oxidative insertion of the rhodium complex was assumed to be directed by the alkene moiety into bond *b* of **14** to form pentarhodacycle **15.** Subsequent β-H elimination would afford intermediate **16**. Finally, reductive elimination would occur to afford enone **17**. However, with dppp as a ligand, the oxidative insertion of the rhodium complex into bond *a* of **14** would result in the formation of pentarhodacycle **18**, which could then be trapped by intramolecular insertion of the alkene to afford the tricyclic intermediate **19**. Finally, reductive elimination would afford the tricyclic ketone **20**. Recently, Cramer and co-workers have reported the enantioselective variation of the same sequence of elementary steps.[10]

Murakami and co-workers also reported a change of reactivity of cyclobutanone **14** with a nickel-catalyst (Scheme 7).[11] Oxidative cyclisation of the ketone and alkene moiety by the nickel catalyst would afford nickelapentacycle **21**. Afterwards, ring enlargement by β-C elimination would afford intermediate **22**. Finally, reductive elimination would afford tricyclic ketone **23** as the product. Later, the same group reported an enantioselective version of this reaction.[12] The different transformations of **14** highlight the ongoing research in C–C activation

to generate a diverse range of structures and the difference in reactivity induced by different catalysts.

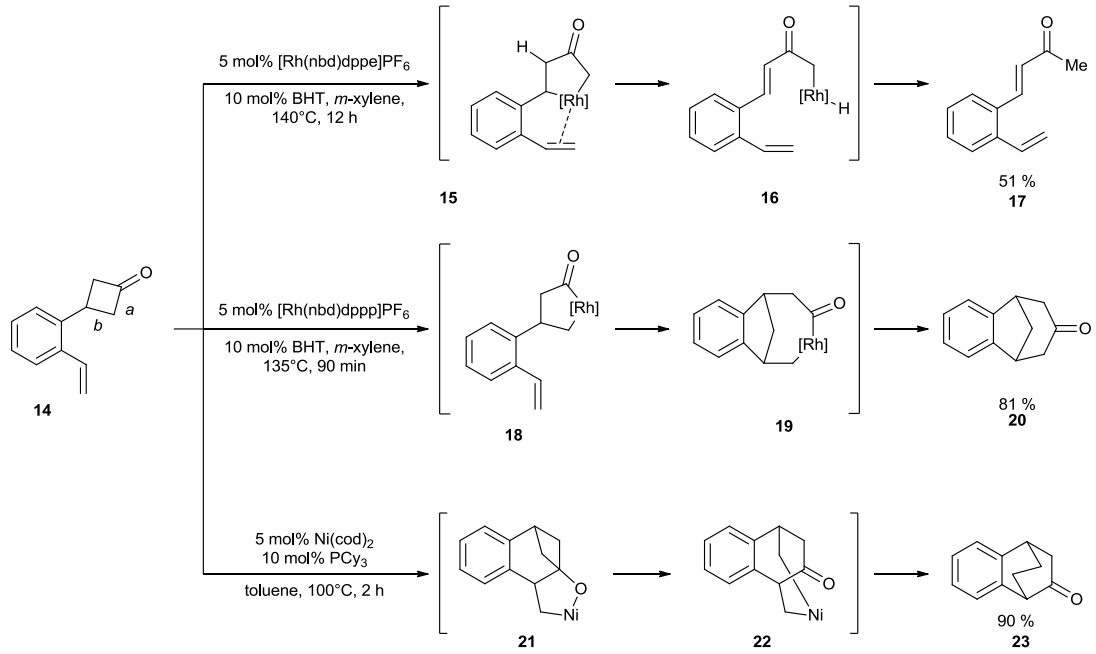


**Scheme 7** Different catalytic systems

In 2006, Murakami and co-workers extended the reaction to a formal nickel catalysed [4+2+2] cycloaddition to form eight membered rings **26** (Scheme 8).[13] It is proposed that it would begin by the initial oxidative cyclisation of the diyne **24**, the ketone **25** and the nickel catalyst to afford nickelaheptacycle **27**. Afterwards, ring enlargement by β-C elimination would give intermediate **28**. Finally, reductive elimination would afford cyclooctadienone **26**. Symmetrical diynes which processed either internal or terminal alkynes proceeded in good yields. Several modifications to the tether were tolerated under the reaction conditions. Furthermore, non-symmetrical diynes proceeded with excellent regioselectivity under a Ni/IPr catalyst system.

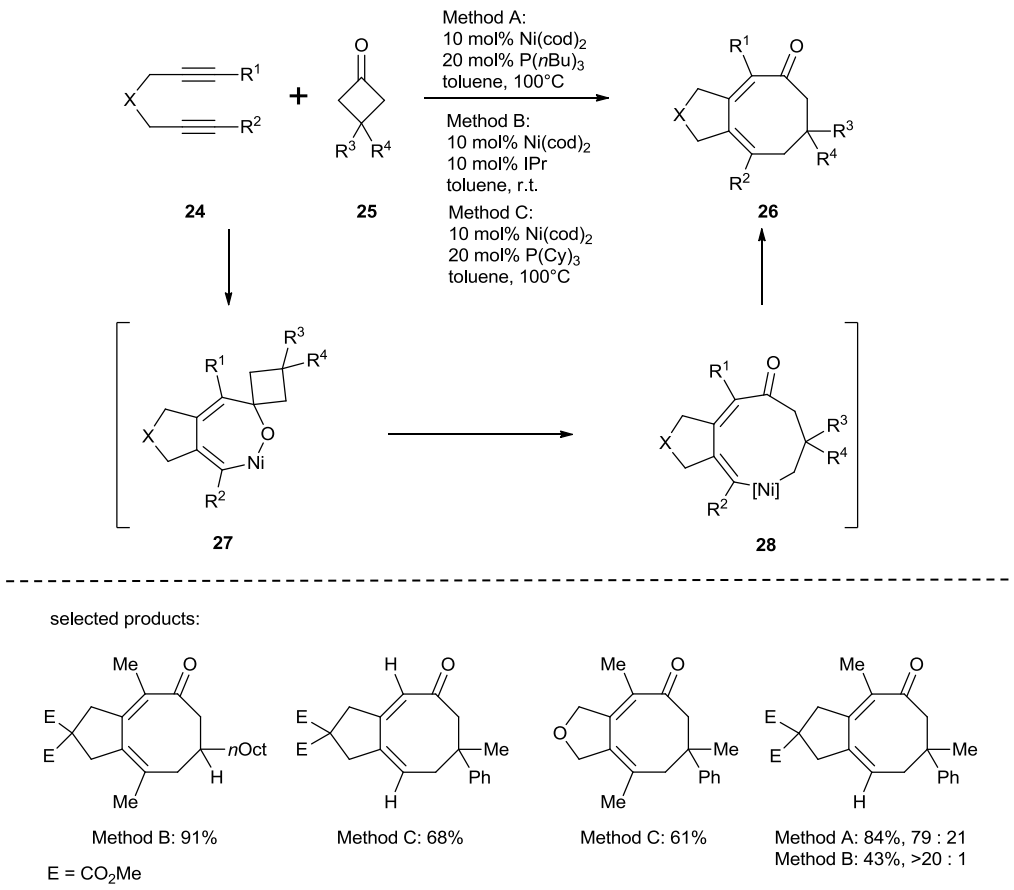


**Scheme 8** Nickel-catalysed [4+2+2] cycloaddition of cyclobutanones and diynes

Wender and co-workers reported a rhodium catalysed [6+2] cycloaddition of vinylcyclobutanones **29** to form eight-membered ring systems **30** (Scheme 9).[14] Theoretical studies suggest the formation of rhodacycle **31** happens first.[15] Afterwards, ring opening via β-carbon elimination and concomitant cleavage of bond *b* would afford rhodacycle **32**. Then reductive elimination would occur to afford product **30**. Several eight-membered ring ketones were formed in good to excellent yields.

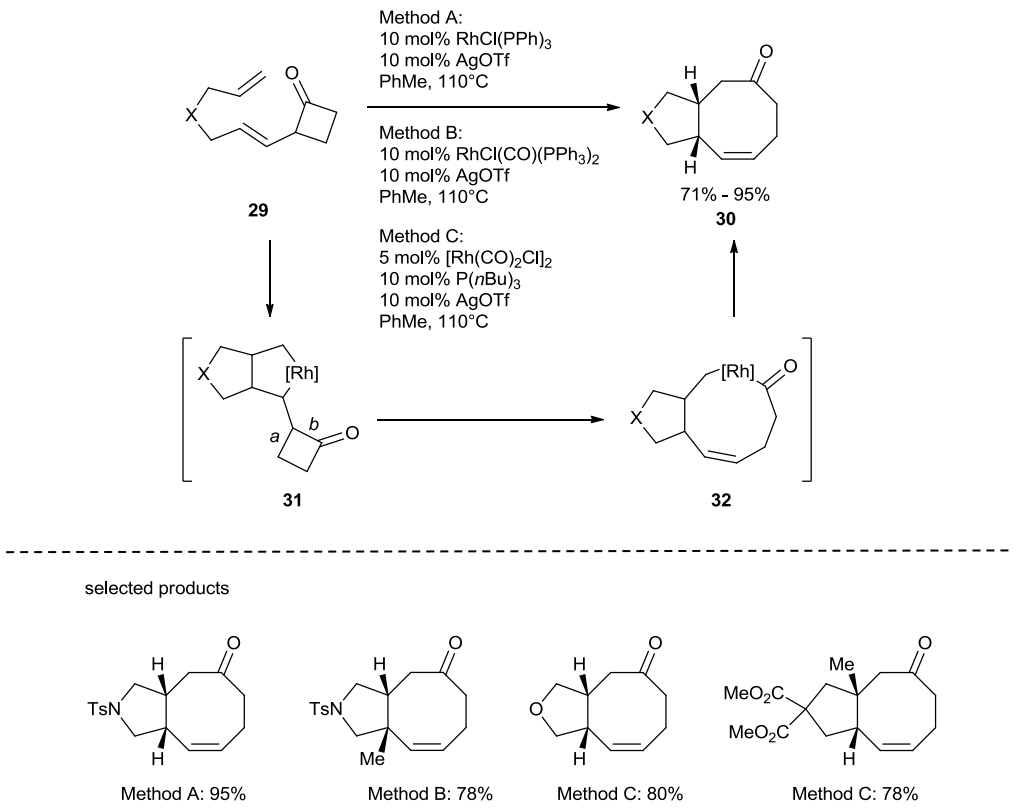


**Scheme 9** Rhodium-catalysed [6+2] cycloaddition

Rhodium-catalysed addition of boronic acids to a carbonyl moiety have been reported to proceed through an organorhodium intermediate which would undergo a 1,2-addition to the carbonyl moiety.[16] Organorhodium intermediates can also add across an alkyne triple bond to generate an alkenyl rhodium intermediate.[17] From these work, Murakami and co-workers reported a rhodium-catalysed ring expansion towards seven-membered-ring ketones **33** which involves the exploitation of the initial formation of the alkenyl rhodium intermediate **35** and C–C bond cleavage (Scheme 10).[18] The initial vinyl rhodium species **35,** arising from the regioselective carborhodation of alkyne **33,** would undergo an intramolecular 1,2-addition to the ketone which would result in the formation of rhodium alkoxide **36**. Subsequent regioselective β-C elimination would afford intermediate **37**. Then hydrolysis would afford ketone **34**. While several seven-membered ring ketones were synthesised in good to high

yields, the authors found that additional substitution on the cyclobutanone prevented the formation of the desired product.

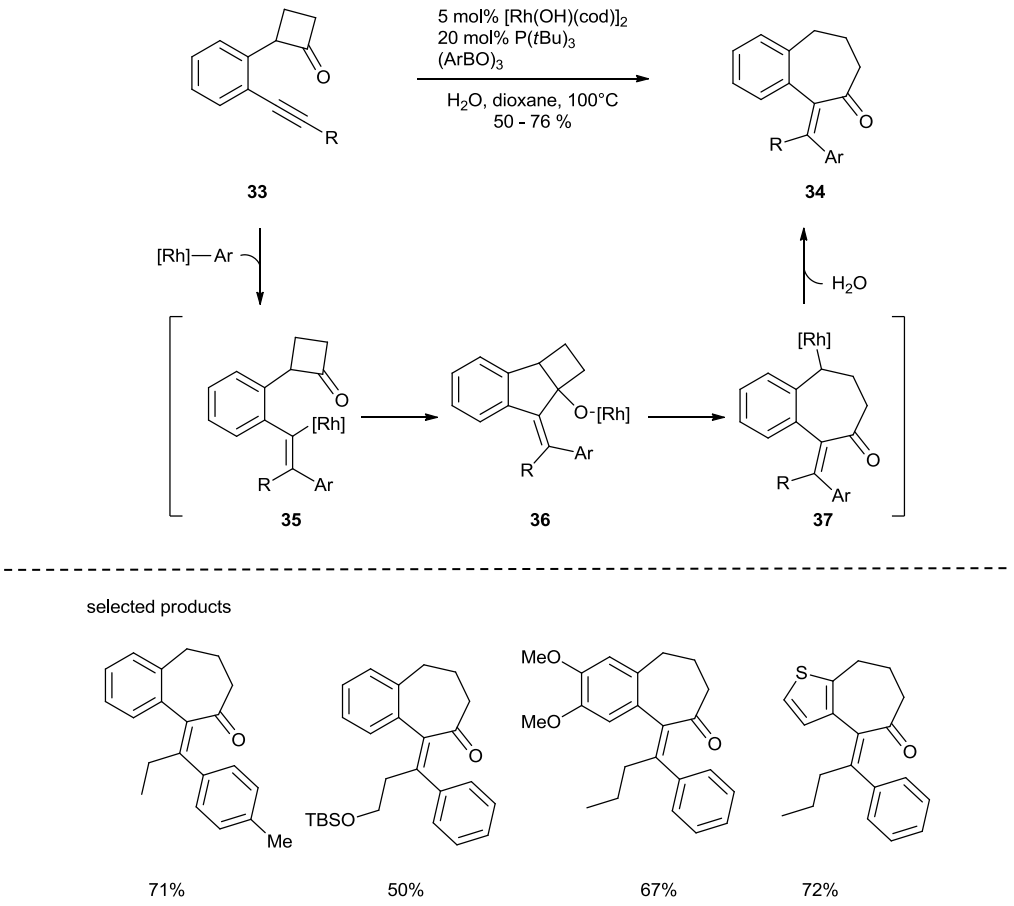


**Scheme 10** Intramolecular 1,2-addition of vinyl rhodium species

### 1.2.2 Cyclobutenones and benzocyclobutenones

Liebeskind and Huffman reported a rhodium-catalysed insertion into cyclobutenone **38** to form eight-membered ring ketones **39** whereby both oxidative insertion and β-C elimination processes had taken place (Scheme 11).[19] Therefore, it was postulated that oxidative insertion of rhodium complex into cyclobutenone **38** would form rhodacycle **40**. Subsequent ring enlargement by β-C elimination would then trap rhodacycle **40** and as a result would form

intermediate **41**. This would then be followed by reductive elimination to afford cyclooctadienone **39** in a 90% yield.

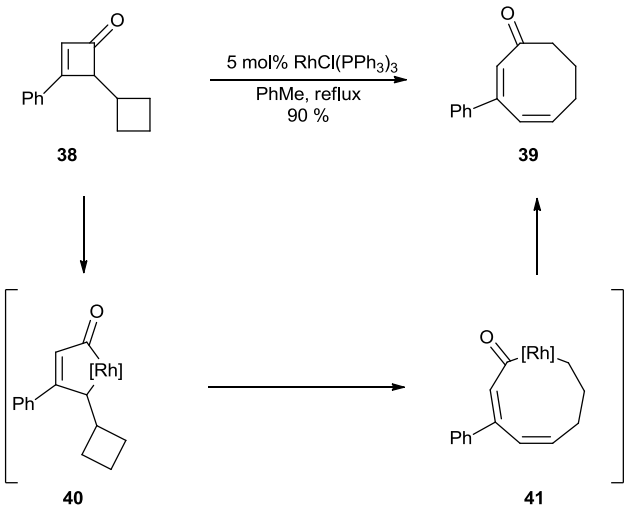


**Scheme 11** Rhodium-catalysed insertion into cyclobutenone

Liebeskind and Huffman reported a nickel-catalysed annulation of cyclobutenones **42** with alkynes to form phenols **43** (Scheme 12).[20] Initial cleavage of the acyl-carbon bond of cyclobutenone **42** would result in the formation of intermediate **44** or **45**. Insertion of alkyne would form intermediate **46**. Reductive elimination and aromatisation would then afford phenol **43**.

Electron-rich substituents on the cyclobutenone were found to be unfavourable under the reaction conditions as decomposition will occur. The insertion of various non-symmetrical internal alkynes proceeded in moderate to good yields. However, the regioselectivity of the alkyne insertion was generally poor. More recently, Harrity and Auvinet reported the nickel-catalysed annulation of cyclobutenones and alkynylboronates which proceeded with excellent regioselectivity.[21] In 2007, Kondo and co-workers reported an improved substrate scope to also include electron poor alkenes with a rhodium catalyst.[22]

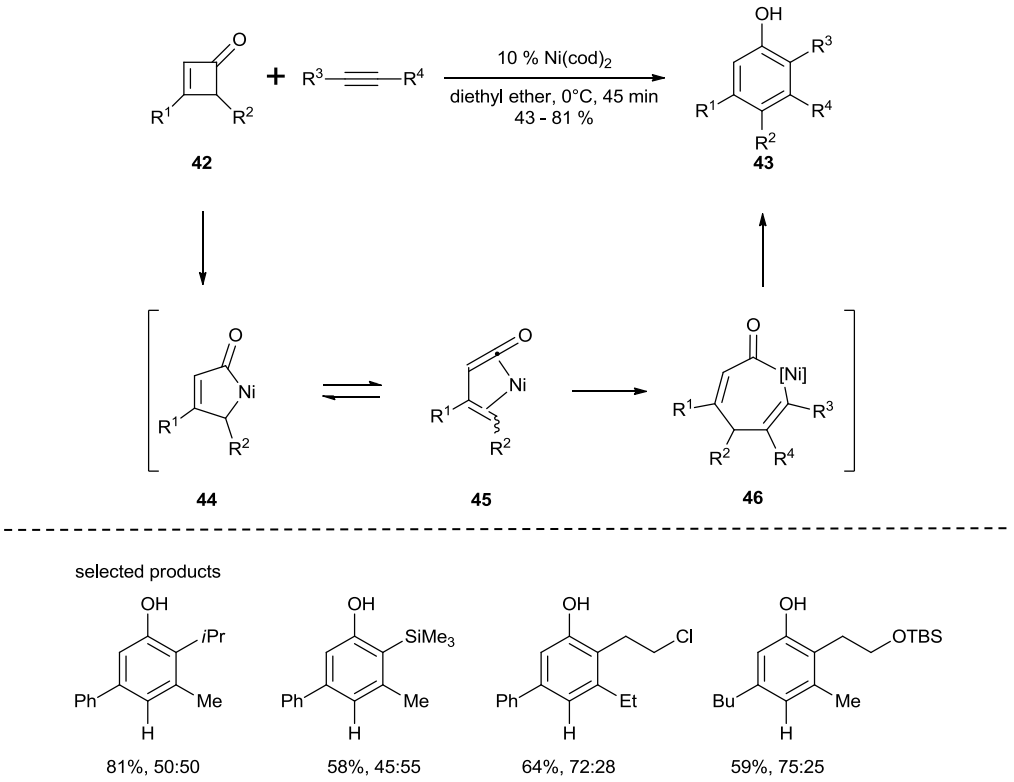


**Scheme 12** Nickel-catalysed annulation of cyclobutenone with alkyne

Mitsudo and co-workers reported a rhodium-catalysed transformation of cyclobutenones **47** with alkenes to afford product **51** or **52** depending on the atmosphere (Scheme 13).[23] In the presence of the rhodium-catalyst, either intermediate **48** or **49** would form from the initial acyl-carbon bond cleavage. Insertion of the alkene fragment would form intermediate **50**. When the reaction was carried out under an atmosphere of Ar, decarbonylation would then be followed by reductive elimination to afford product **51**. However, when the reaction was carried out under 30 atmospheres of CO, the amount of product arising from decarbonylation was reduced and the direct reductive elimination would occur to form mainly product **52**.

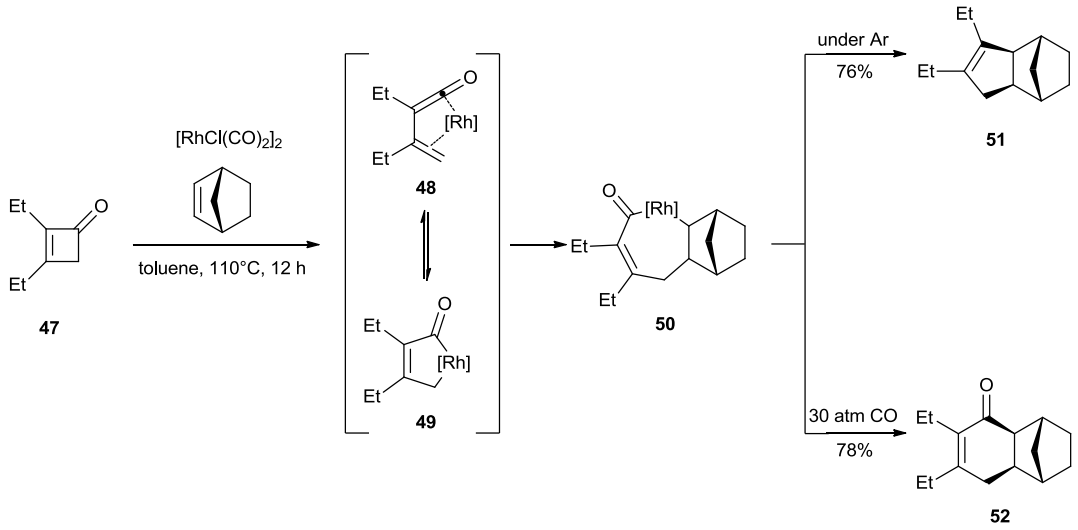


**Scheme 13** Atmosphere dependent rhodium-catalysed transformations of cyclobutenones

In the previous examples, the rhodium catalyst is postulated to undergo oxidative insertion into the acyl –C $sp^3$ bond. In the subsequent examples, the rhodium is postulated to undergo oxidative insertion into the acyl–C $sp^2$ bond. Dong and co-workers reported a rhodium-catalysed intramolecular alkene insertion into benzocyclobutenone **53** to form tricyclic ketone **54** (Scheme 14).[24] Interestingly, the major product comes from the rhodium insertion into the C–C $sp^2$ bond. To account for their results, the authors proposed that the pendant alkene would direct the oxidative insertion of the rhodium catalyst into the more sterically hindered bond of **53** to form rhodacycle **55** and intramolecular alkene insertion would then form intermediate **56**. Finally, reductive elimination would afford product **54**. An enantioselective version of this reaction was later reported by the same group.[25] Furthermore, this methodology was used as a key step in the total synthesis of the proposed structure of cycloinumakiol **59** (Scheme 15).[26]

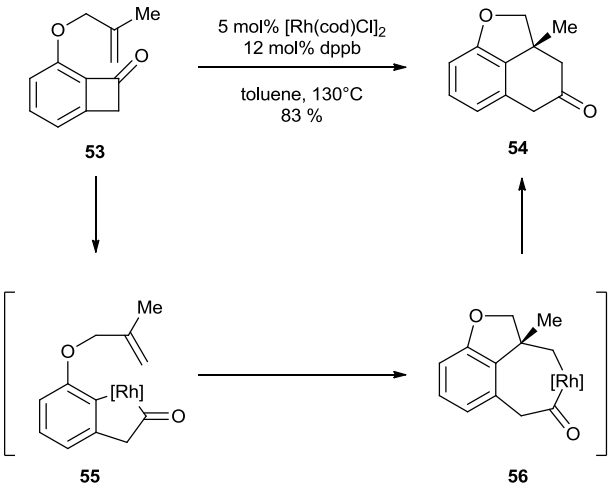


**Scheme 14** Rhodium-catalysed intramolecular alkene insertion into cyclobutanone

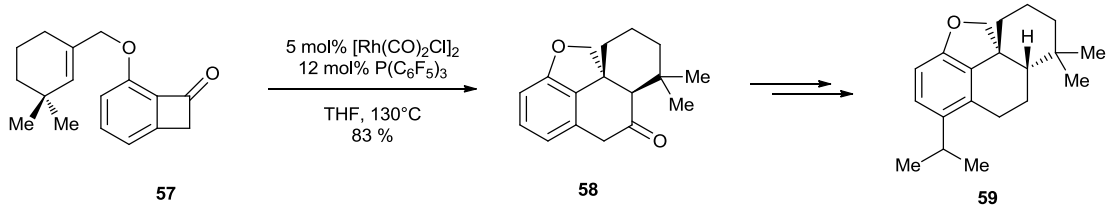


**Scheme 15** Total synthesis of proposed structure of cycloinumakiol

This work was later extended to include alkyne insertion to form either a β-napthol **63** or indene **64** (Scheme 16).[27] It is proposed the tether alkyne would direct the oxidative insertion of the rhodium catalyst into the more sterically hindered bond of **60** would form rhodacycle **61**. Intramolecular alkyne insertion would form intermediate **62**. Finally, reductive elimination and aromatisation would afford β-napthol **63** when the reaction was carried out in a sealed tube in dioxane at 130°C. However, if the reaction was carried out in xylene under reflux under Argon, decarbonylation of intermediate **62** and then reductive elimination would afford indene **64**.

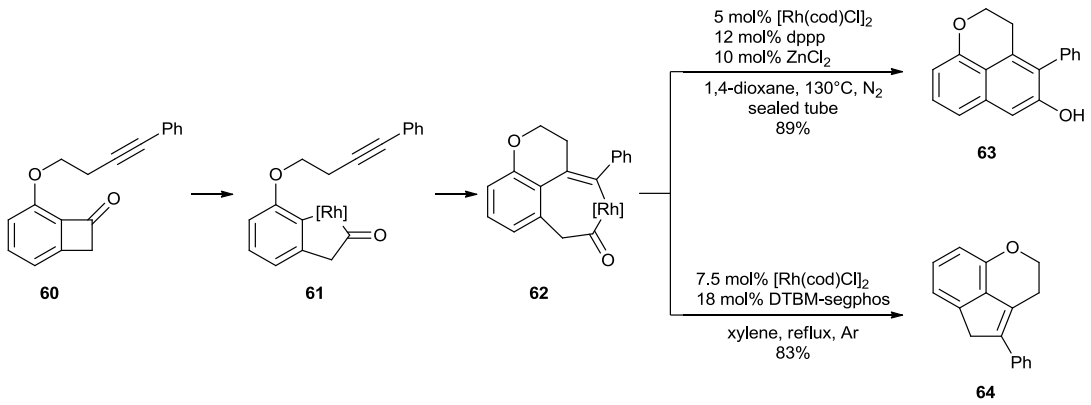


**Scheme 16** Rhodium-catalysed intramolecular alkyne insertion into cyclobutanone

Liebeskind and co-workers reported experimental evidence of the oxidative insertion of a rhodium complex into the C–C bond of cyclobutenone **65** (Scheme 17) and the C–C bond of benzocyclobutenone **68** (Scheme 18).[28] The insertion into either cyclobutenone or benzocyclobutenone requires high temperatures which is a common requirement for rhodium-catalysed reactions. Furthermore, the oxidative insertion into benzocyclobutenone **68** was shown to happen at both the more and the least sterically hindered acyl–carbon bond and Liebeskind found that the ratio of **69** and **70** is different depending on the time of the reaction. Equilibrium is reached after 5 days, and **69** and **70** were obtained in almost equimolar ratio. This equilibration demonstrates the oxidative insertion is a reversible process. Murakami and co-workers reported the oxidative addition into the least sterically hindered C–C bond of benzocyclobutenone **68** to occur at room temperature which is likely facilitated by the electron rich ligand (Scheme 19).[29]

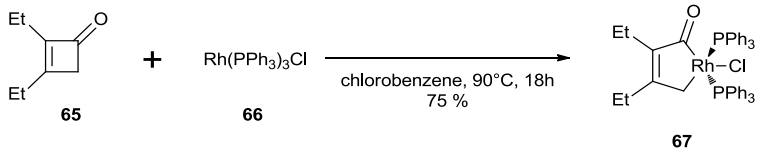


**Scheme 17** Oxidative addition of rhodium into a C–C bond of cyclobutenone

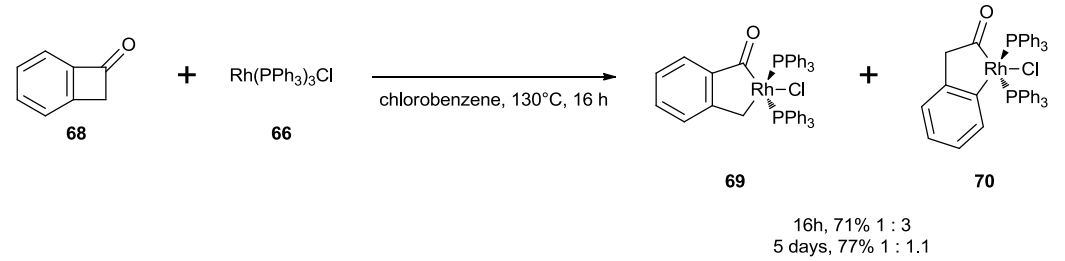


**Scheme 18** Oxidative addition of rhodium into a C–C bond of benzocyclobutenone

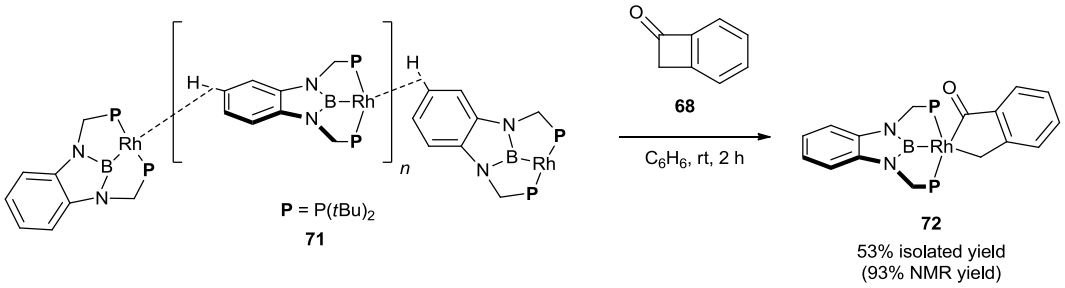


**Scheme 19** Experimental proof of the oxidative addition into the C–C bond

### 1.2.3 Cyclobutadienones

Mitsudo and co-workers reported a ruthenium-catalysed intermolecular decarbonylative cycloaddition of cyclobutadienone **73** with alkene to form cyclopentenone **74** (Scheme 20).[30] It was necessary to carry the reaction under three atmospheres of CO because external CO was assumed to be required to suppress complete decarbonylation of cyclobutadienone **73** to the corresponding alkyne. Furthermore, 70% scrambling was observed when the reaction was carried out with labelled $^{13}CO$. Therefore, it was proposed the oxidative insertion of the ruthenium catalyst was directed by the alkoxy substituent into bond *b* over bond *a* to form pentarhodacycle **75**. Subsequent decarbonylation would afford intermediate **76**. Afterwards, stereoselective alkene insertion would form intermediate **77**. This would then undergo reductive elimination to give product **74**. Various substituted cyclobutadienones were tolerated under the reaction conditions. Also, the use of ethene as a coupling partner was effective.

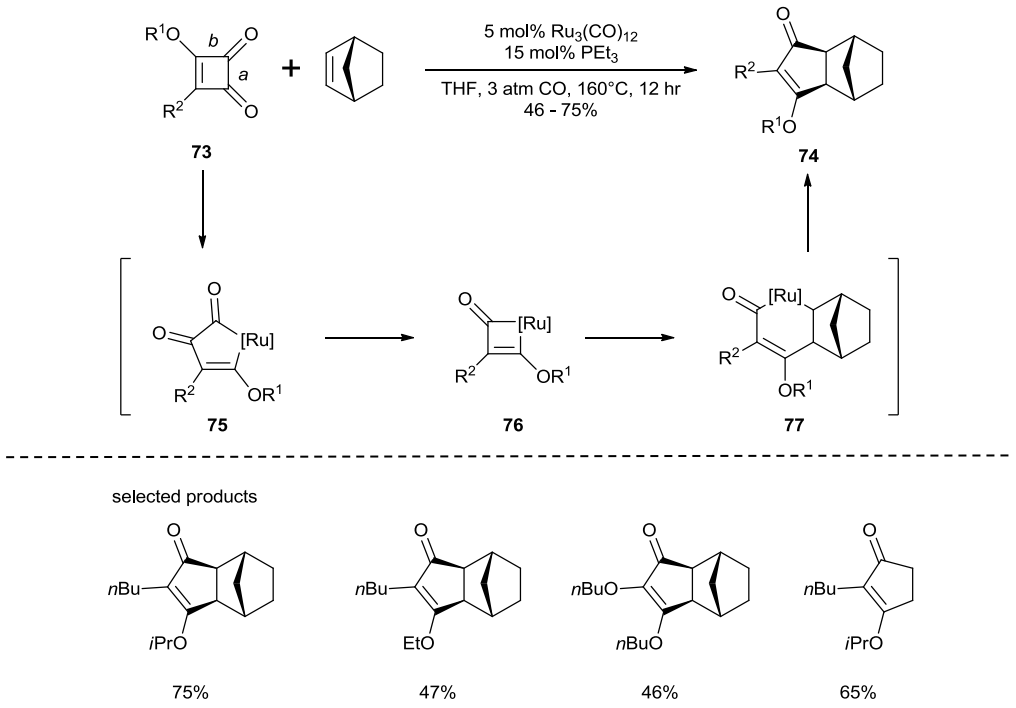


**Scheme 20** Ruthenium-catalysed intermolecular decarbonylative cycloaddition

Yamamoto and co-workers reported a rhodium-catalysed intramolecular decarbonylative cycloaddition of cyclobutadienone **78** with pendant alkene to cyclopentenone **79** (Scheme 21).[31] It was proposed that if X is a heteroatom, it would direct the oxidative insertion of the rhodium complex into bond *a* of **78** to form pentarhodacycle **80**. However, reactivity was still observed when X was methine. Regardless, subsequent decarbonylation would afford intermediate **81**. Afterwards, alkene insertion followed by reductive elimination would afford product **79**. Unlike the intermolecular decarbonylative decoupling reported by Mitsudo and co-workers, no external CO was necessary.[30]

Various substitution patterns on the alkene system were tolerated. However, *gem*-disubstituted alkenes were the most reactive. Cyclobutadienone bearing aromatic or alkyl substituents were tolerated. Furthermore, modifications to the tether did not affect the overall reactivity.

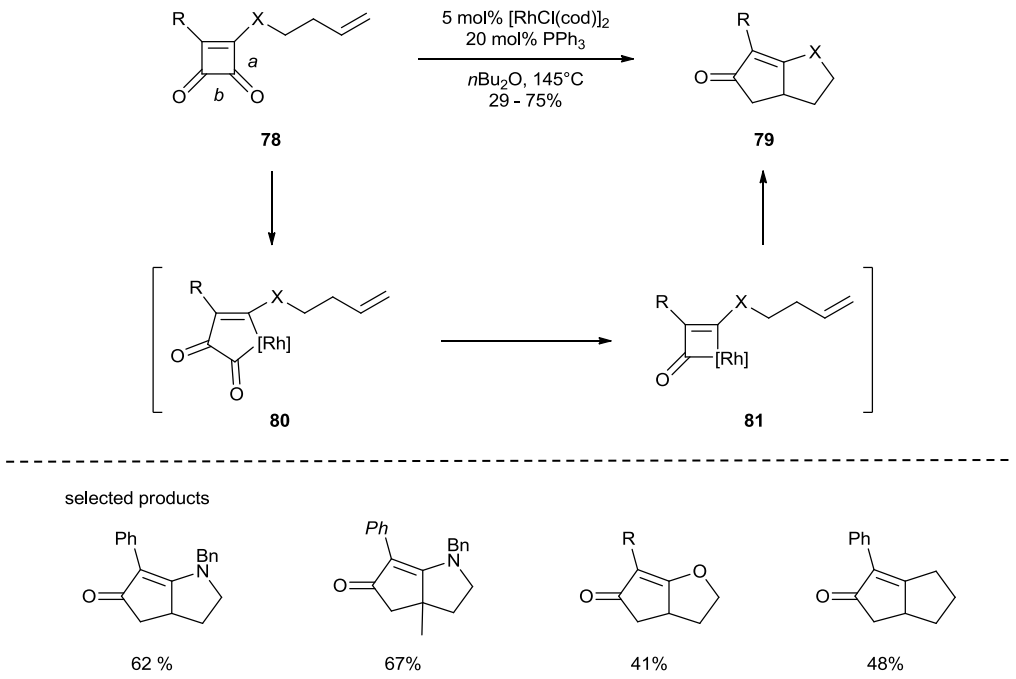


**Scheme 21** Rhodium-catalysed intramolecular decarbonylative cycloaddition

### 1.2.4 Vinyl-Cyclobutanols and Allenylcyclobutanols

Uemura and co-workers reported a regioselective oxidative palladium-catalysed ring opening of cyclobutanols **82** to form bicyclic ketones **85** (Scheme 22).[32] After the formation of the putative palladium alkoxide **83**, ring opening of the least sterically hindered bond *b* via β-C elimination would afford alkylpalladium complex **84**. An intramolecular Mizoroki-Heck reaction would then occur to give product **85**. The presence of base might be vital to facilitate the formation of the palladium alkoxide **83**. Conversely, Clark and Thiensathit reported the ring opening of cyclobutanol **82** proceeded in a different manner under another oxidative palladium catalytic system.[33] The palladium-catalyst would coordinate to the alkene of **82** to form **86**. This would activate the system for ring enlargement by the cleavage of bond *a* via [1,2]-shift which would form intermediate **87**. Afterwards, β-H elimination and isomerisation of the double bond would afford product **88**. Since the report by Clark and Thiensathit, related ring expansions of cyclobutanols have been reported. [34]

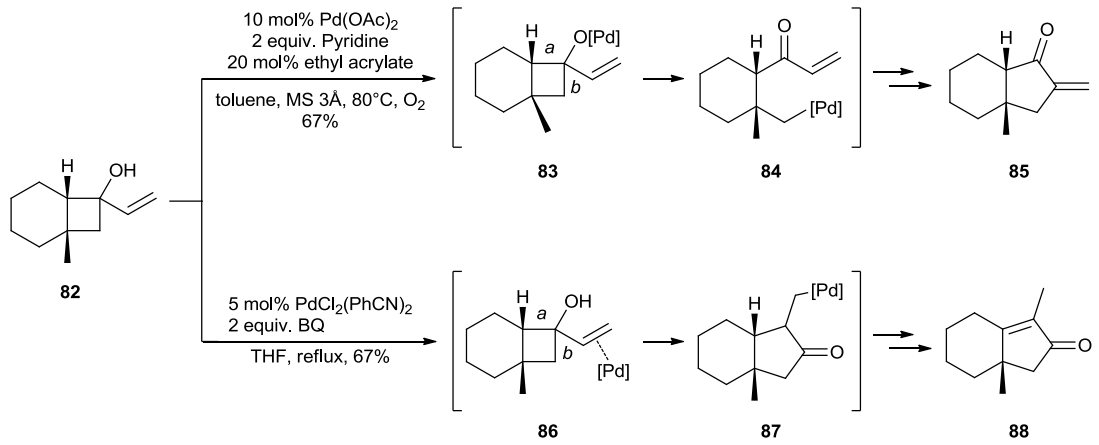


**Scheme 22** Palladium-catalysed ring opening of cyclobutanols

Cramer and Souillart reported an enantioselective rhodium-catalysed domino reaction of cyclobutanols **89** (Scheme 23).[35] After the formation of putative rhodium alkoxide **91**, ring opening via β-C elimination would form intermediate **92**. Then intramolecular oxidative addition of **92** would form intermediate **93**. Afterwards, insertion of the alkene and then reductive elimination would afford product **90**. Various substituents and substitution patterns on the aryl ring were tolerated. Various substituents on the cyclobutanol ring were also tolerated. However, only non-substituted and 1,1-disubstituted alkenes were tolerated under the reaction conditions.

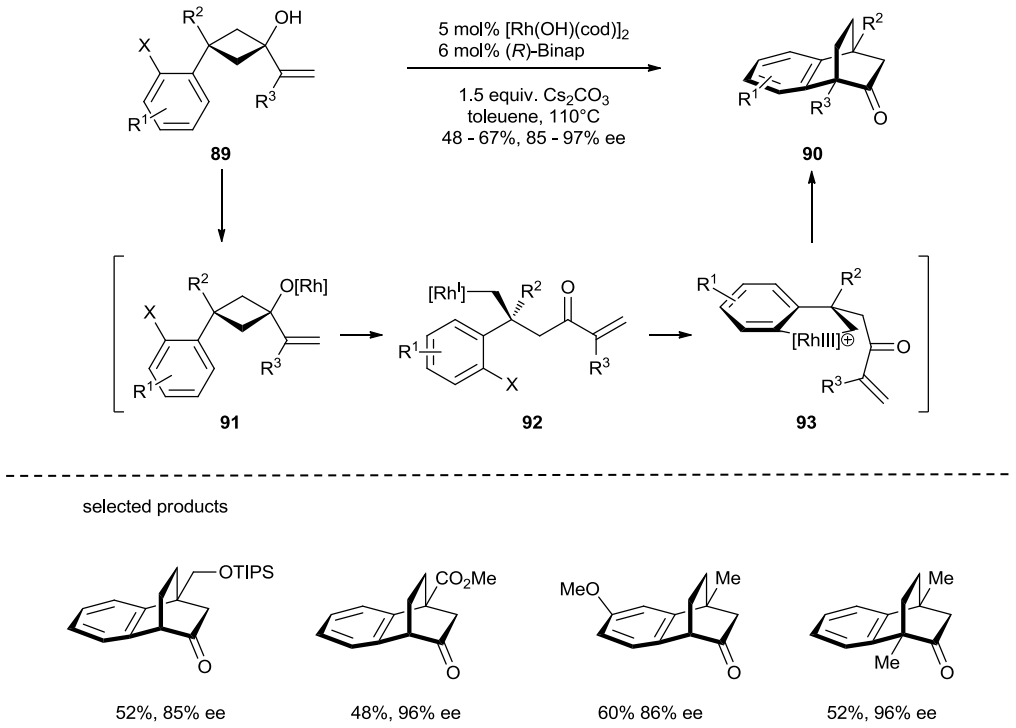


**Scheme 23** Rhodium-catalysed domino-reaction of cyclobutanols

Cramer and Seiser reported a related rhodium-catalysed ring expansion of 1-allenyl cyclobutanols **94** to cyclohexenones **95** (Scheme 24).[36] The mechanism of this reaction is analogous to the rhodium catalysed C–C cleavage of 1-vinyl cyclobutanols. After the formation of the putative rhodium alkoxide **96**, ring enlargement *via* β-C elimination would afford heptarhodacycle **97**. Reductive elimination would give 6-membered ring **98** which would then undergo isomerism to give product **95**. Various functional groups on the cyclobutanol were tolerated under the reaction conditions. Coordinating groups such as the vinyl and pyridyl group required slightly more forced conditions for full conversion. Cyclic substituted allenes and terminal allenes were tolerated under the reaction condition.

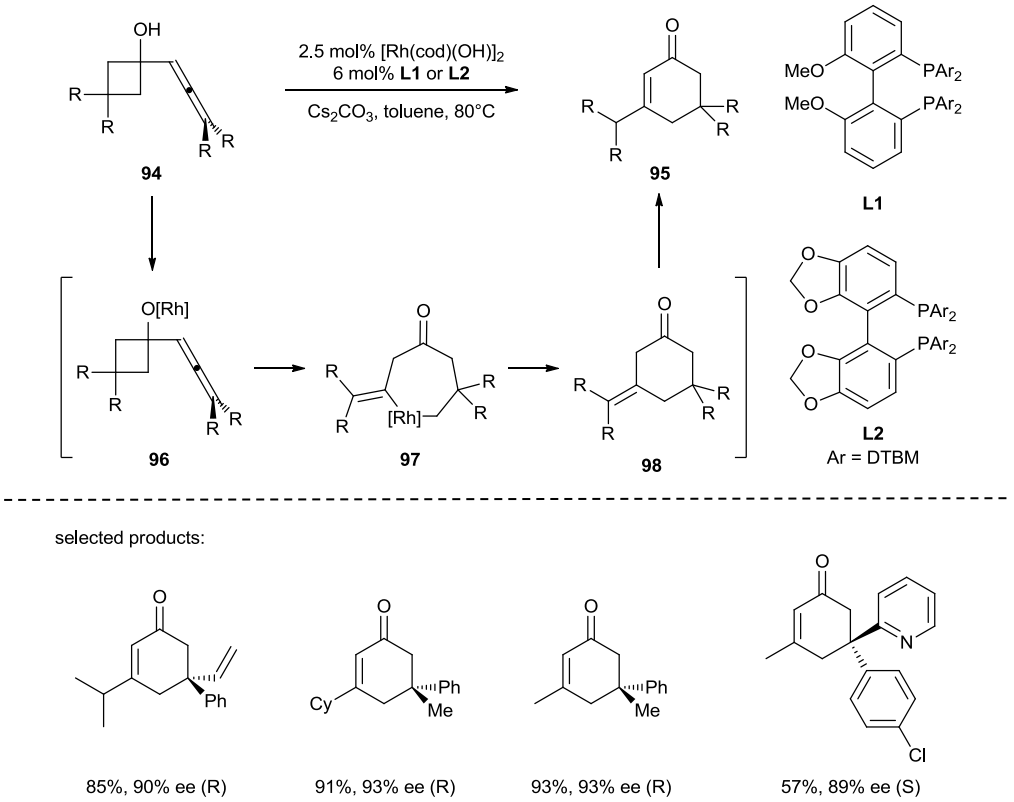


**Scheme 24** Rhodium catalysed ring expansion of 1-allenyl cyclobutanols

Wender and co-workers reported a rhodium-catalysed [6+1] cycloaddition of allenylcyclobutane ether **99** (Scheme 25).[37] The mechanism of the reaction is now different from 1-allenyl cyclobutanols. Since the oxygen is now protected, the rhodium catalyst will first form a π-complex with the allene to form intermediate **102**. It was then proposed that a rhodium-catalysed ring opening of **102** via β-C elimination of the least sterically hindered bond *a* would then occur to form intermediate **103**. Insertion of CO and then reductive elimination would afford product **100**. Occasionally, product **101** arising from the cleavage of the more sterically hindered bond *b* was observed.

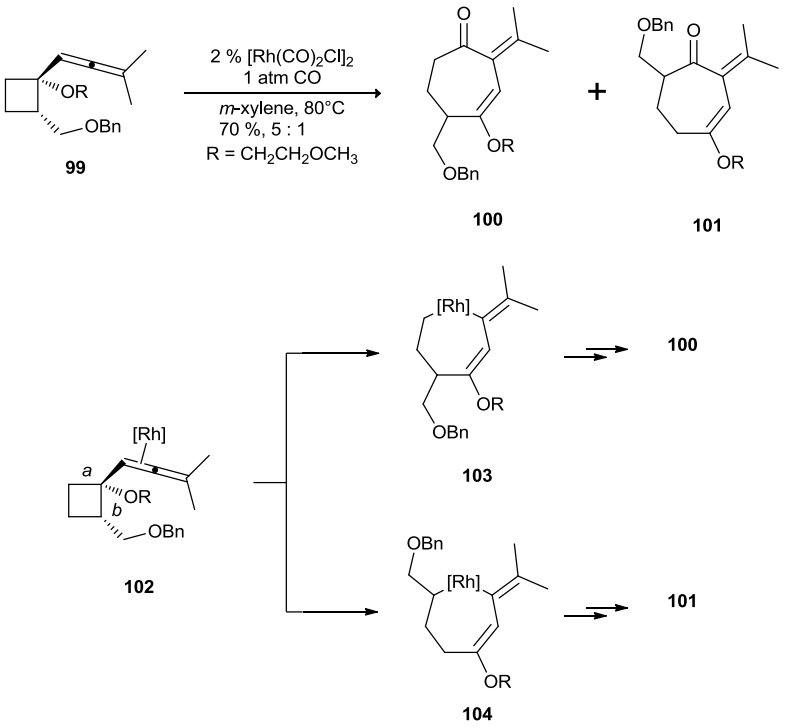


**Scheme 25** Rhodium-catalysed [6+1] cycloaddition

### 1.2.5 Cyclobutenols and benzocyclobutenols

Matsuda and Miura reported a rhodium-catalysed [4+2] annulation of cyclobutenols **105** with alkynes to form tetrasubstituted benzenes **106** (Scheme 26).[38] After the formation of the putative rhodium alkoxide **107**, ring opening of **107** by β-C elimination would form alkenylrhodium complex **108**. Insertion of alkyne into the rhodium-carbon bond would form rhodium complex **109**. Subsequent nucleophilic addition to the ketone would afford cyclohexadiene **110**. Protonation would afford alcohol **111**. Finally, dehydration would afford tetra-substituted benzene **106**. Several tetrasubstituted benzenes were synthesised in a high yield. Silylated alkyne was tolerated and preceded with excellent regioselectivity but poor reactivity. Modification of the reaction conditions improved the yield but slightly diminished the regioselectivity. The insertion of various other non-symmetrical internal alkynes proceeded with good to high regioselectivity.

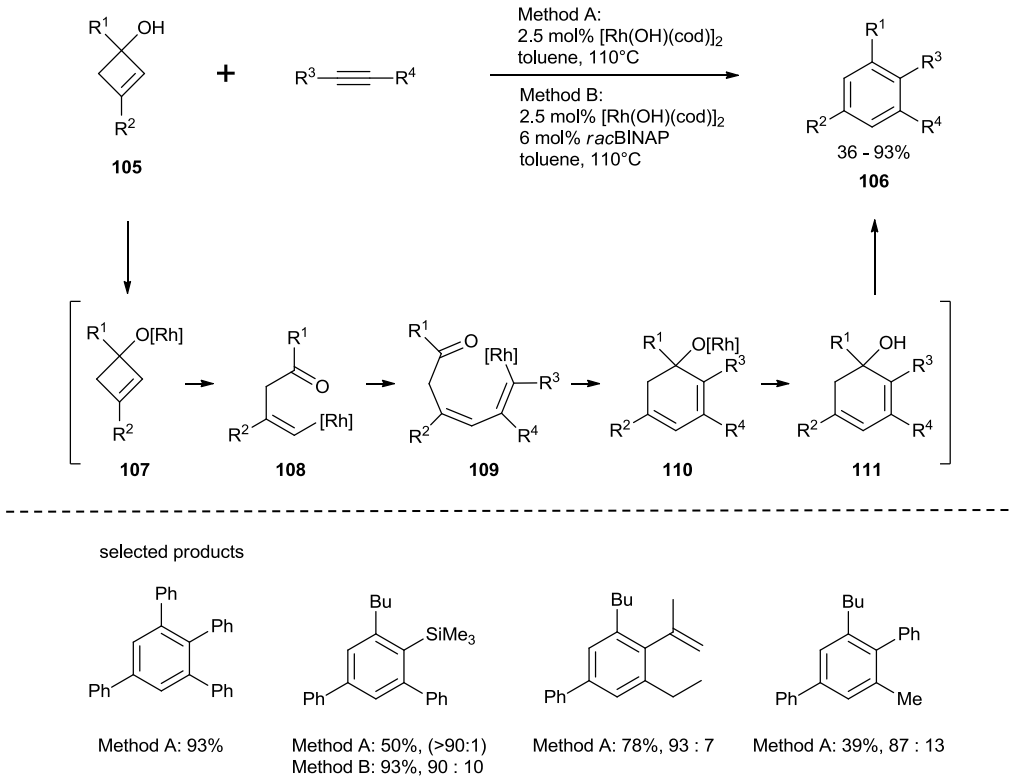


**Scheme 26** Rhodium-catalysed [4+2] annulation

Murakami and co-workers reported a rhodium-catalysed benzannulation of alkyne and benzocyclobutenols **112** (Scheme 27).[39] Recent theoretical studies by Morokuma and co-workers reported that after the formation of rhodium alkoxide **114**, cleavage of bond *a* would occur preferentially over bond *b* because the extra π-bond interaction of the benzene ring of the substrate with the rhodium catalyst would stabilise the transition state to form intermediate **115**.[40] Afterwards, alkyne insertion would form alkenylrhodium complex **116**. Subsequent nucleophilic addition to the ketone and protonation would afford dihydronaphthalene **113**. Interestingly, unlike the examples with cyclobutanol as reported by Matsuda and Miura,[38] the major product is not the aromatised naphthalene.

Various functional groups on the aryl ring were tolerated under the reaction conditions. Alteration of the electronic character of the aryl ring had no significant effect in the reaction outcome. Furthermore, the insertion of non-symmetrical alkynes proceeded with moderate to

excellent regioselectivity. Different functional groups on the alkyne were tolerated but terminal alkynes were not.

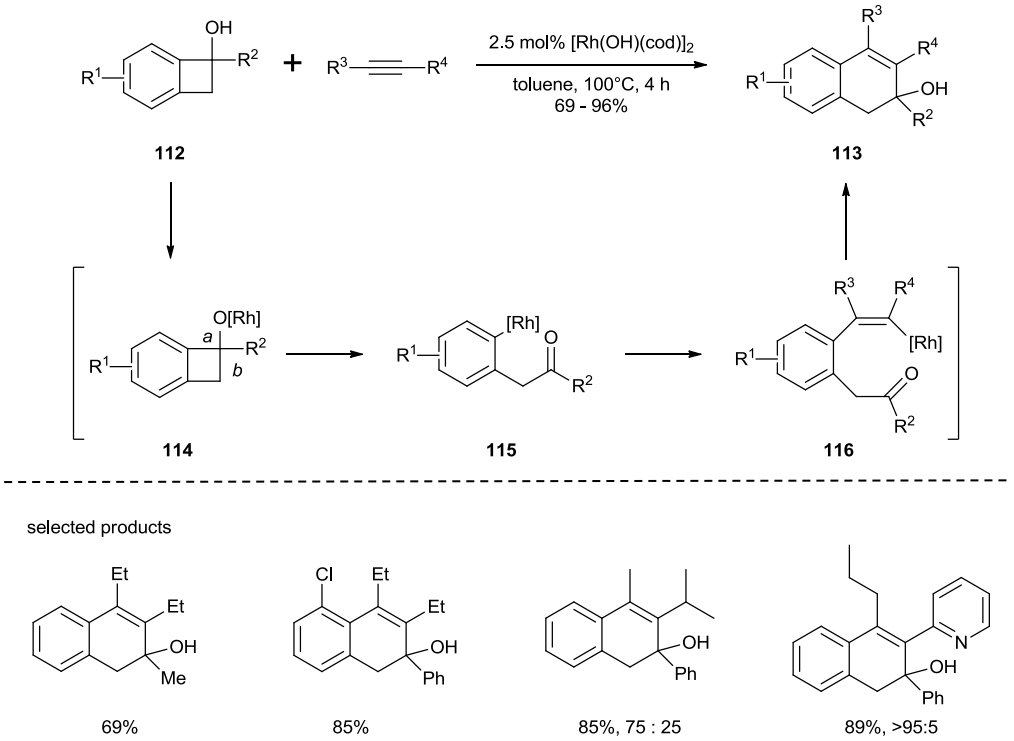


**Scheme 27** Rhodium-catalysed benzannulation of benzocyclobutenol and alkyne

### 1.2.6 Cyclobutanone *O*-Benzoyloximes

Uemura and co-workers reported ligand effects in the palladium-catalysed ring opening of cyclobutane **117** (Scheme 28).[41] Oxidative insertion into the N–O bond of the oxime would form intermediate **120**. With PPFCyA as a ligand, bond *a* of intermediate **120** was postulated to be broken via β-C elimination which would form intermediate **121**. Intramolecular cyclisation followed by β-H elimination would then afford **118**. However, with BINAP as a ligand, bond *b* of intermediate **120** was assumed to be preferentially broken via β-C elimination which would form intermediate **122**. Subsequent β-H elimination would afford **119**.

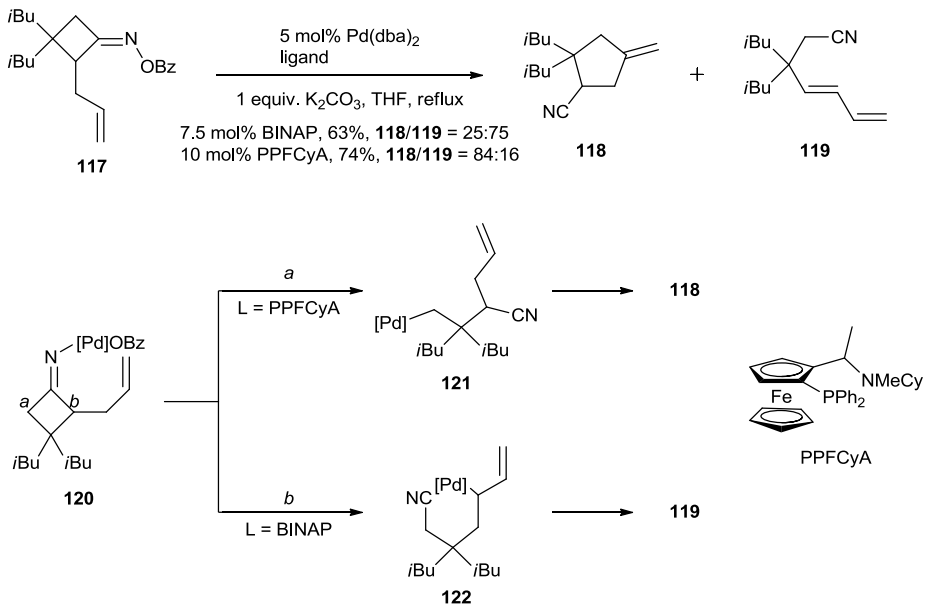


**Scheme 28** Ligand effects in the ring opening of cyclobutane **117**

### 1.2.7 Biphenylenes

Products resulting from the stoichiometric cleavage of a C–C σ bond of biphenylene **123** by the oxidative insertion of a transition metal complex have been isolated and characterised.[42] However, it wasn't until 1990 that Vollhardt and co-workers demonstrated the first catalytic C–C σ bond cleavage of biphenylene **123** (Scheme 29).[43] Oxidative insertion of the nickel catalyst into the strained C–C bond of biphenylene **123** would form intermediate **125**. Dimerisation of intermediate **125** would form intermediate **126**. Subsequent reductive elimination would afford dimer **124**.

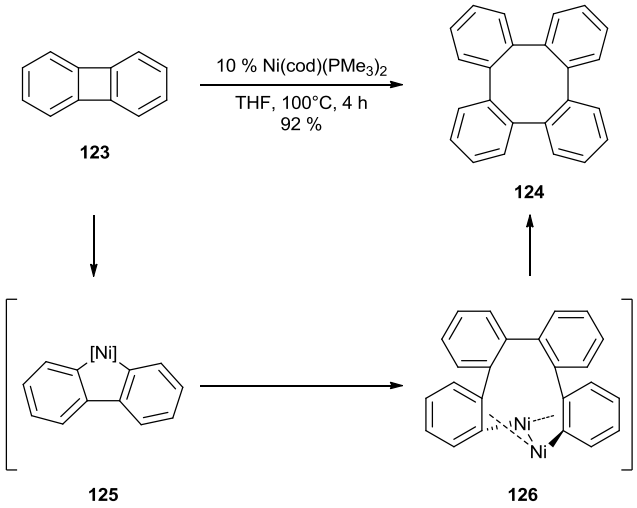


**Scheme 29** Nickel-catalysed dimerisation of biphenylene

Jones and co-workers reported a nickel-catalysed [4+2] cycloaddition of biphenylene **123** with alkynes to form phenanthrenes **127** (Scheme 30).[42,44] Oxidative insertion of the nickel catalyst **128** into **123** would form intermediate **129**. Insertion of the alkyne would form intermediate **130**. Reductive elimination would afford **127**. No cyclotrimerisation was observed. The hemi-labile ligand was found to be essential for the catalytic cycle. Interestingly, when dippe (1,2-bis(diisopropylphosphino)ethane) was used as a ligand, 6 mol% of $O_2$ was required to make the reaction catalytic.[45]

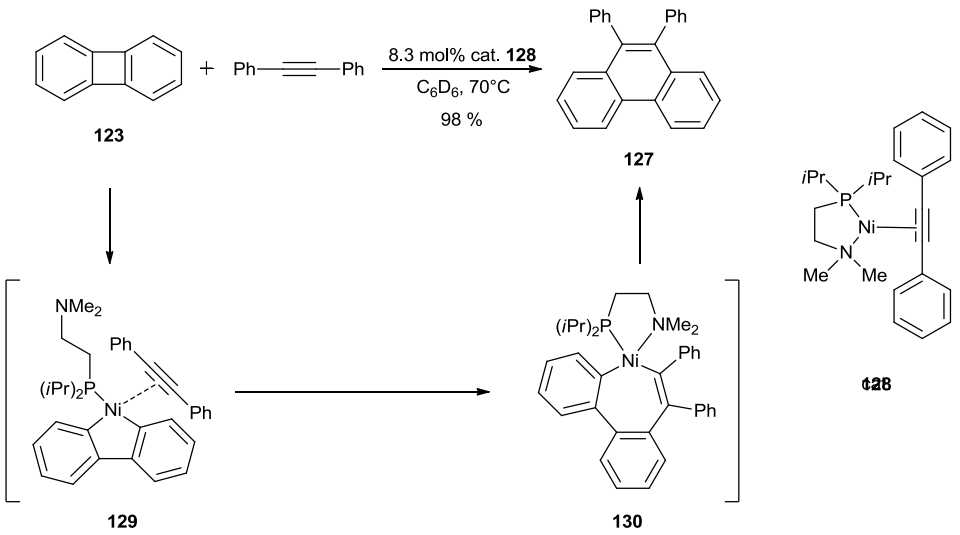


**Scheme 30** Nickel-catalysed [4+2] cycloaddition

### 1.2.8 Alkylidenecyclobutanes

Aissa and co-workers reported a rhodium-catalysed a C–H / C–C bond activation sequence to form 8-membered ring ketones **132** (Scheme 31).[46] Subtle modifications to the catalytic system were required for optimal yields. Mechanistically, initial C–H activation of **131** would give intermediate **133**. This would then be followed hydrometalation onto the alkylidenecyclobutane to give intermediate **134**. Subsequent ring enlargement by β-C elimination to trap intermediate **134** would give intermediate **135**. Afterwards, reductive elimination would afford product **132**. Mono-substitution and *gem*-diphenyl substitution on the cyclobutane ring were tolerated under the reaction conditions. Tetra-substitution on the alkene resulted in no reaction under various rhodium-catalysed conditions. Furthermore, various modifications on the tether were also compatible.

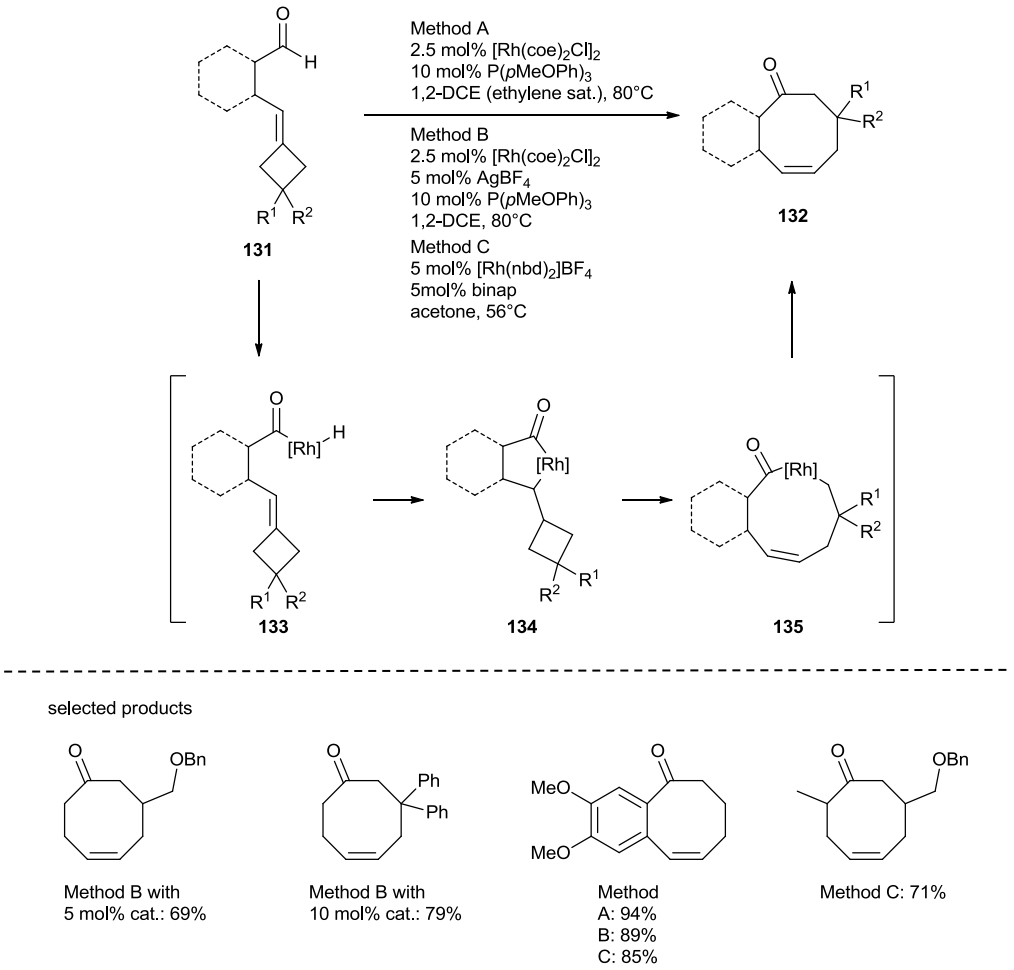


**Scheme 31** Rhodium-catalysed C–H / C–C bond activation sequence

## 1.3 Conclusion and Outlook

Transition metal catalysed C–C cleavage of four-membered cabocycles is an area of extensive research. This has led to the discovery of many different intermolecular and intramolecular restructuring of the carbon framework. C–C cleavage via oxidative addition, β-C elimination or [1,2] shift are common mechanistic processes used to explain the reaction outcome.

However, C–C bond cleavage of small heterocycles had been studied less extensively. The ring strain energy in cyclobutane **136** is similar to the ring strain energy in oxetane **137** and azetidine **138** by both experimental and computational studies (Scheme 32).[47]

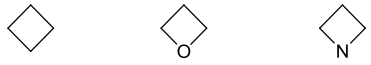


| | **136** | **137** | **138** |
|---|---|---|---|
| Theoretical (kcal / mol): | 25.7 | 24.9 | 25.4 |
| Experimental (kcal / mol): | 26.5 | 25.2 | 26.2 |

**Scheme 32** Ring strain energies

In 2010, Aissa and co-workers reported the first example of a C–C bond cleavage of a small heterocycle **139** (Scheme 33).[46] Replacing the alkylidenecyclobutane moiety with alkylideneazetidine moiety still resulted in the formation of the desired 8-membered ring **140** in good yields. The mechanistic pathway was proposed to be identical to the all carbon equivalent whereby the C–C bond *a* of intermediate **142** was broken to eventually afford 8-membered ring ketone **140**. Despite the increased loading in catalyst, this work demonstrated the viability of C–C bond cleavage of small heterocycles.

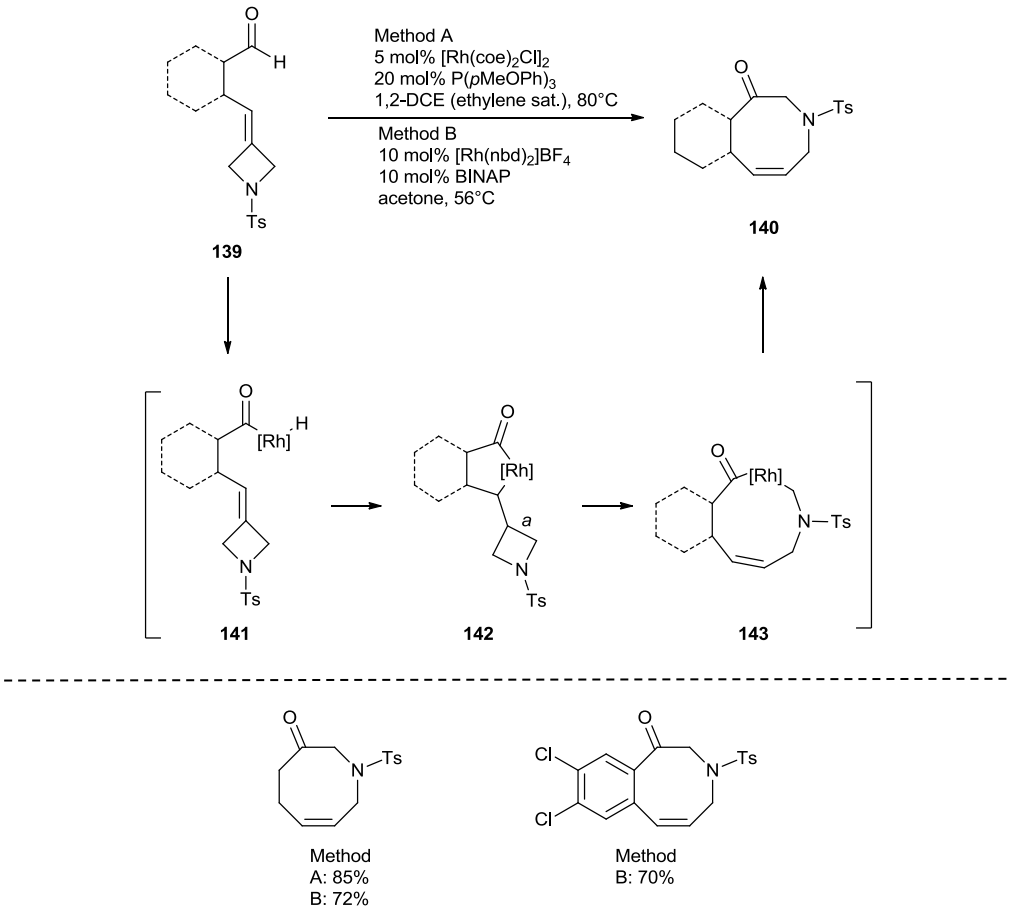


**Scheme 33** Rhodium-catalysed C–H / C–C bond activation sequence of alkylideneazetidines

Afterwards, we became curious about whether or not other small heterocycles can undergo selective C–C cleavage. In 2005, Murakami and co-workers reported the first intermolecular insertion of alkyne into cyclobutanone **144** to afford the corresponding cyclohexenone **145** in a formal [4+2] cycloaddition with a nickel-catalyst (Scheme 34).[48] Therefore it is proposed, the nickel catalyst would coordinate to both the ketone and the alkyne to form intermediate **146**. Then oxidative cyclisation would afford nickelapentacycle intermediate **147**. Afterwards, ring enlargement by β-C elimination would afford nickelaheptacycle **148**. Finally, reductive elimination would afford cyclohexenone **145**. Various cyclohexenones were successfully synthesised in moderate to excellent yields. The insertion of non-symmetrical alkynes proceeded with good and consistent regioselectivity regardless of the electronic properties of the alkyne.

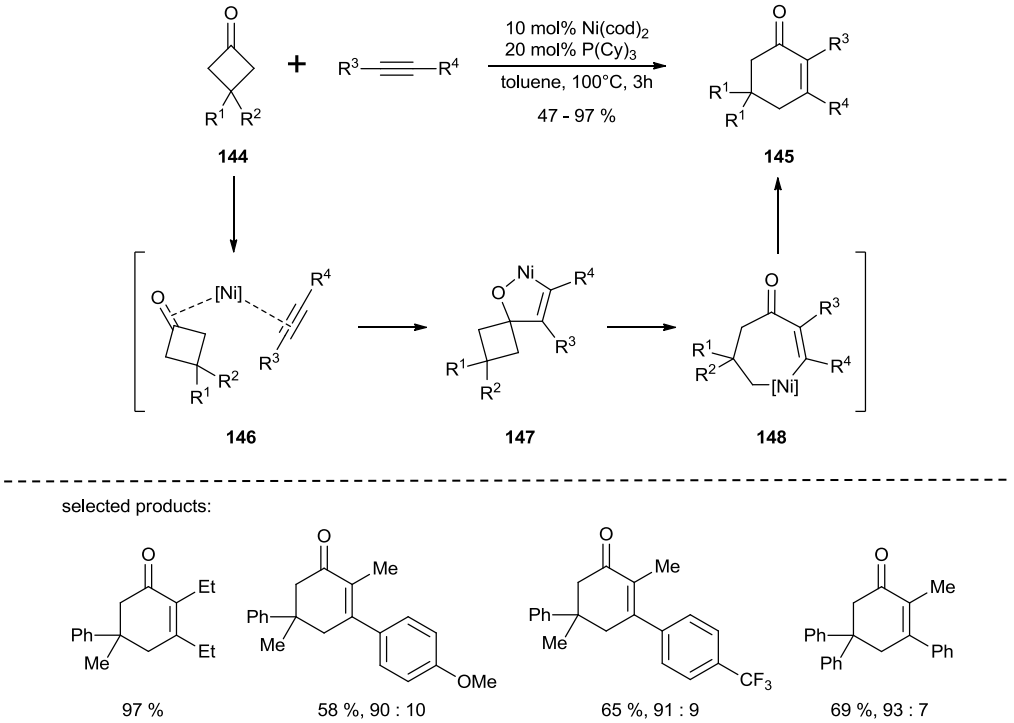


**Scheme 34** Nickel-catalysed alkyne insertion into cyclobutanone

Drawing inspiration from Murakami's work, it was of interest to determine if azetidinone **149** could behave like cyclobutanone **144** in a transition-metal catalysed [4+2] cycloaddition with alkyne **150** to generate pyridinone **151** (Scheme 2).

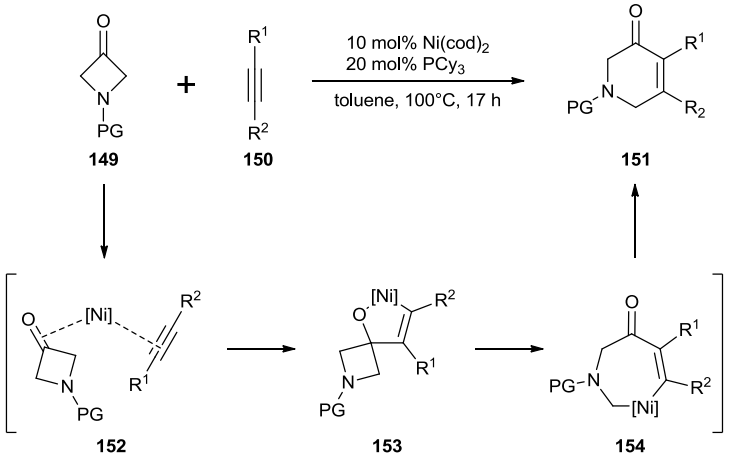


**Scheme 35** Hypothesis

Drawing an analogy to the proposed mechanism of the [4+2] cycloaddition of cyclobutanone **144** with an alkyne, it was hypothesised that the nickel-catalyst will first associate azetidinone **149** and alkyne **150** to form intermediate **152**. Afterwards, oxidative cyclisation would form nickelapentacycle **153**. Ring enlargement by β-C elimination will form nickelaheptacycle **154**. Finally, reductive elimination should afford desired product **151**.

This work towards the synthesis of pyridinones **151** would offer an alternative approach to the other methods already published. The approach by ring closing metathesis is generally low yielding as the formation of a tetra-substituted alkene is difficult (Scheme 36).[49] Alternatively, a relay metathesis approach can circumvent this issue but requires a more advanced substrate (Scheme 37). [50]

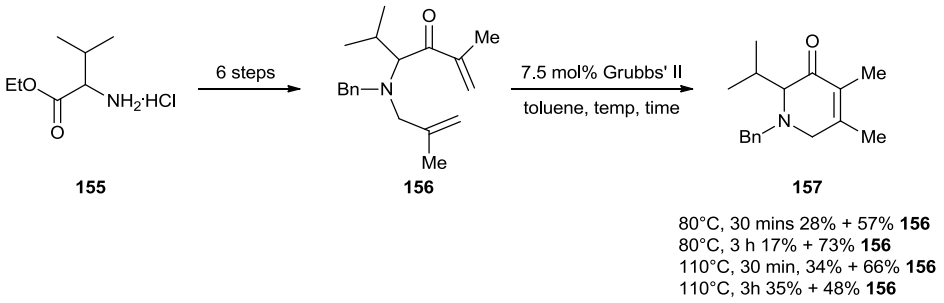


**Scheme 36** Ring closing metathesis

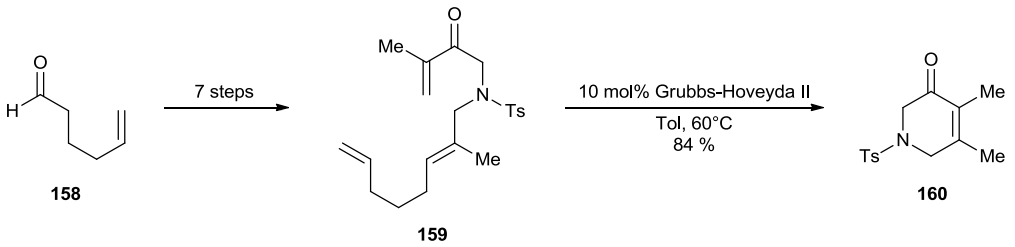


**Scheme 37** Relay metathesis

Another approach towards pyridinones **164** is by a palladium-catalysed intramolecular Heck-type reaction of oxime **162** as reported by Tong and co-workers (Scheme 38).[51] After the palladium step, acid hydrolysis of oxime **163** is then carried out to furnish pyridinone **164**.

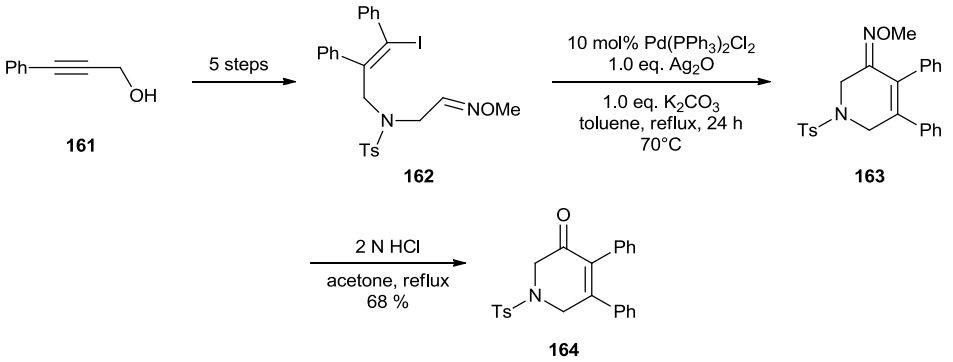


**Scheme 38** Palladium catalysed Heck-type reaction

In light of what is known in the literature towards the synthesis of pyridinones **151**, the formal [4+2] cycloaddition of azetidinone **149** and alkyne **150** should offer a more direct approach. Furthermore, this method can also be seen as a rapid build-up of molecular complexity. Furthermore, the formal [4+2] cycloaddition is seen as a convergent synthesis rather than a linear synthesis. As a result, the overall steps required to synthesise pyridinones **151** are reduced.

In this context, the initial aims of the work presented herein were to:

a.) To validate the hypothesis of the insertion of an alkyne into the C–C bond of azetidinone to give pyridinones **151**

b.) Optimise the reaction

c.) Examine the scope

d.) Investigate the mechanism of the reaction

During the development of the work presented in this thesis, Murakami and co-workers reported an example of C–C cleavage of 3-azetidinol **165** to form tetralone **166** (Scheme 39).[52] After the formation of rhodium alkoxide **167**, oxidative addition into the carbon-bromine bond would form rhodacycle **168**. C–C cleavage of bond *a* via β-C elimination would afford heptarhoacycle **169**. Finally, reductive elimination would generate tetralone **166**.

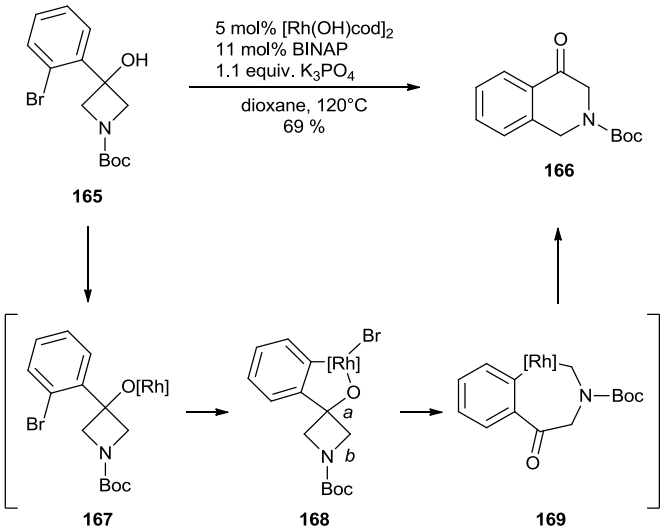


**Scheme 39** Rhodium catalysed formation of tetralone

## 1.4 References

1.) For recent reviews on C–C bond activation, see: a) I. Nakamura, Y. Yamamoto, *Adv. Synth. Catal.* **2002**, *344*, 111–129; b) M. E. van der Boom, D. Milstein, *Chem. Rev.* **2003**, *103*, 1759–1792; c) T. Nishimura, S. Uemura, *Synlett* **2004**, 201–216; d) C.-H. Jun, *Chem. Soc. Rev.* **2004**, *33*, 610–618; e) T. Satoh, M. Miura, in *Topics in Organometallic Chemistry*, Vol. 14, (Ed: S. Murai), Springer: Berlin, **2005**, 1–20; f) M. Murakami, M. Makino, S. Ashida, T. Matsuda, *Bull. Chem. Soc. Jpn.* **2006**, *79*, 1315–1321; g) M. Rubin, M. Rubina, V. Gevorgyan, *Chem. Rev.* **2007**, *107*, 3117–3179; h) T. Seiser, N. Cramer, *Org. Biomol. Chem.* **2009**, *7*, 2835–2840; i) M. Murakami, T. Matsuda, *Chem. Commun*. **2011**, *47*, 1100–1105; j) C. Aïssa, *Synthesis* **2011**,

3389–3407; k) T. Seiser, T. Saget, D. N. Tran, N. Cramer, *Angew. Chem. Int. Ed.* **2011**, *50*, 7740–7752; l) K. Ruhland, *Eur. J. Org. Chem.* **2012**, 2683–2706; m) G. Dong, *Synlett* **2013**, *24*, 1–5.

2.) M. Murakami, Y. Ito, In *Topics In Organometallic Chemistry*, (Ed: S. Murai), Springer: New York, **1999**, 97-129

3.) B. Rybtchinski, D. Milstein, *Angew. Chem. Int. Ed*. **1999**, *38*, 870 – 883

4.) K. B. Wiberg, *Acc. Chem. Res.* **1996**, *29*, 229–234.

5.) P. R. Khoury, J. D. Goddard, W. Tam, *Tetrahedron* **2004**, *60*, 8103–8112.

6.) K. B. Wiberg, *Angew. Chem. Int. Ed. Engl.* **1986**, *25*, 312–322.

7a.) M. Murakami, H. Amii, Y. Ito, *Nature* **1994**, *370*, 540–541; b) M. Murakami, H. Amii, K. Shigeto, Y. Ito, *J. Am. Chem. Soc.* **1996**, *118*, 8285–8290

8.) M. Murakami, K. Takahashi, H. Amii, Y. Ito, *J. Am. Chem. Soc.* **1997**, *119*, 9307–9308.

9.) M. Murakami, T. Itahashi, Y. Ito, *J. Am. Chem. Soc.* **2002**, *124*, 13976–13977.

10 .) E. Parker, N. Cramer, *Organometallics* **2014**, *33*, 780−787.

11.) M. Murakami, S. Ashida, *Chem. Commun.* **2006**, 4599–4601.

12.) L. Liu, N. Ishida, M. Murakami, *Angew. Chem. Int. Ed.* **2012**, *51*, 2485–2488.

13a.) M. Murakami, S. Ashida, T. Matsuda, *J. Am. Chem. Soc.* **2006**, *128*, 2166–2167.; b) S. Ashida, M. Murakami, *Bull. Chem. Soc. Jpn.* **2008**, *81*, 885–893.

14.) P. A. Wender, A. G. Correa, Y. Sato, R. Sun, *J. Am. Chem. Soc.* **2000**, *122*, 7815–7816.

15.) M. M. Montero-Campillo, J. Rodríguez-Otero, E. M. Cabaleiro-Lago, *Tetrahedron* **2008**, *64*, 6215–6220.

16a.) M. Sakai, M. Ueda, N. Miyaura, *Angew. Chem. Int. Ed.* **1998**, *37*, 3279–3281; b) M. Ueda, N. Miyaura, *J. Org. Chem.* **2000**, *65*, 4450–4452; c) A. Takezawa, K. Yamaguchi, T. Ohmura, Y. Yamamoto, N. Miyaura, *Synlett* **2002**, 1733–1735.

17a.) T. Hayashi, K. Inoue, N. Taniguchi, M. Ogasawara, *J. Am. Chem. Soc.* **2001**, *123*, 9918–9919; b) M. Lautens, M. Yoshida, *J. Org. Chem.* **2003**, *68*, 762–769.

18.) T. Matsuda, M. Makino, M. Murakami, *Angew. Chem. Int. Ed.* **2005**, *44*, 4608–4611.

19.) M. A. Huffman, L. S. Liebeskind, *J. Am. Chem. Soc.* **1993**, *115*, 4895–4896.

20.) M. A. Huffman, L. S. Liebeskind, *J. Am. Chem. Soc.* **1991**, *113*, 2771–2772.

21.) A.-L. Auvinet, J. P. A. Harrity, *Angew. Chem. Int. Ed.* **2011**, *50*, 2769–2772.

22.) T. Kondo, M. Niimi, M. Nomura, K. Wada, T. Mitsudo, *Tetrahedron Lett.* **2007**, *48*, 2837–2839.

23.) T. Kondo, Y. Taguchi, Y. Kaneko, M. Niimi, T.-A. Mitsudo, *Angew. Chem. Int. Ed.* **2004**, *43*, 5369–5372.

24.) T. Xu, G. Dong, *Angew. Chem. Int. Ed.* **2012**, *51*, 7567–7571.

25.) T. Xu, H. M. Ko, N. a Savage, G. Dong, *J. Am. Chem. Soc.* **2012**, *134*, 20005–20008.

26.) T. Xu, G. Dong, *Angew. Chem. Int. Ed.* **2014**, early view

27.) P.-H. Chen, T. Xu, G. Dong, *Angew. Chem. Int. Ed.* **2014**, *53*, 1674–1678.

28a.) M. A. Huffman, L. S. Liebeskind, W. T. Pennington, *Organometallics* **1990**, *9*, 2194–2196; b) M. A. Huffman, L. S. Liebeskind, W. T. Pennington, *Organometallics* **1992**, *11*, 255–266.

29.) Y. Masuda, M. Hasegawa, M. Yamashita, K. Nozaki, N. Ishida, M. Murakami, *J. Am. Chem. Soc.* **2013**, *135*, 7142–7145.

30.) T. Kondo, A. Nakamura, T. Okada, N. Suzuki, K. Wada, T. Mitsudo, *J. Am. Chem. Soc.* **2000**, *122*, 6319–6320.

31.) Y. Yamamoto, S. Kuwabara, H. Hayashi, H. Nishiyama, *Adv. Synth. Catal.* **2006**, *348*, 2493–2500.

32.) T. Nishimura, K. Ohe, S. Uemura, *J. Am. Chem. Soc.* **1999**, *121*, 2645–2646.

33.) G. R. Clark, S. Thiensathit, *Tetrahedron Lett.* **1985**, *26*, 2503–2506.

34a.) M. Yoshida, Y. Komatsuzaki, H. Nemoto, M. Ihara, *Org. Biomol. Chem.* **2004**, *2*, 3099–3107 and references cited; (b) J. P. Markham, S. T. Staben, F. D. Toste, *J. Am. Chem. Soc.* **2005**, *127*, 9708–9709.

35.) L. Souillart, N. Cramer, *Chem. Sci.* **2014**, *5*, 837–840.

36.) T. Seiser, N. Cramer, *Angew. Chem. Int. Ed.* **2008**, *47*, 9294–9297.

37.) P. A. Wender, N. M. Deschamps, R. Sun, *Angew. Chem. Int. Ed.* **2006**, *45*, 3957–3960.

38.) T. Matsuda, N. Miura, *Org. Biomol. Chem.* **2013**, *11*, 3424–3427.

39.) N. Ishida, S. Sawano, Y. Masuda, M. Murakami, *J. Am. Chem. Soc.* **2012**, *134*, 17502–17504.

40.) L. Ding, N. Ishida, M. Murakami, K. Morokuma, *J. Am. Chem. Soc.* **2014**, *136*, 169–178.

41.) T. Nishimura, Y. Nishiguchi, Y. Maeda, S. Uemura, *J. Org. Chem.* **2004**, *69*, 5342–5347.

42.) C. Perthuisot, B. L. Edelbach, D. L. Zubris, N. Simhai, C. N. Iverson, C. Müller, T. Satoh, W. D. Jones, *J. Mol. Catal. A: Chem.* **2002**, *189*, 157–168 and references cited therein

43.) H. Schwager, S. Spyroudis, K. P. C. Vollhardt, *J. Organomet. Chem.* **1990**, *382*, 191–200.

44.) C. Müller, R. J. Lachicotte, W. D. Jones, *Organometallics* **2002**, *21*, 1975–1981.

45.) B. L. Edelbach, R. J. Lachicotte, W. D. Jones, *Organometallics* **1999**, *18*, 4040–4049.

46.) D. Crépin, J. Dawick, C. Aïssa, *Angew. Chem. Int. Ed.* **2010**, *49*, 620–623.

47.) R. D. Bach, O. Dmitrenko, *J. Org. Chem.* **2002**, *67*, 3884–3896 and references cited therein

48a.) M. Murakami, S. Ashida, T. Matsuda, *J. Am. Chem. Soc.* **2005**, *127*, 6932–6933; b) M. Murakami, S. Ashida, T. Matsuda, *Tetrahedron* **2006**, *62*, 7540–7546

49.) K. Yoshida, F. Kawagoe, K. Hayashi, S. Horiuchi, T. Imamoto, A. Yanagisawa, *Org. Lett.* **2009**, *11*, 515–518.

50a.) T. J. Donohoe, J. F. Bower, J. A. Basutto, L. P. Fishlock, P. A. Procopiou, C. K. A. Callens, *Tetrahedron* **2009**, *65*, 8969–8980; b) T. J. Donohoe, L. P. Fishlock, J. A. Basutto, J. F. Bower, P. A. Procopiou, A. L. Thompson, *Chem. Commun.* **2009**, 3008–3010.

51.) H. Liu, L. Wang, X. Tong, *Chem. Commun.* **2011**, *47*, 12206–12208.

52.) N. Ishida, S. Sawano, M. Murakami, *Chem. Commun.* **2012**, *48*, 1973–1975.

# Chapter 2 Nickel-Catalysed Cycloaddition of 3-Azetinones and 3-Oxetanones with Alkynes

## 2.1 Aim and Hypothesis

As mentioned in the previous section, Aïssa and co-workers reported the first example of C–C bond cleavage of small heterocycles.[1] Afterwards, we became curious about whether or not other small heterocycles can undergo selective C–C cleavage. As discussed in the previous section, Murakami and co-workers reported the nickel-catalysed insertion of alkyne **2** into cyclobutanone **1** to form cyclohexenone **3** (Scheme 1).[2] As a result, a variety of cyclohexenones were synthesised via this methodology.

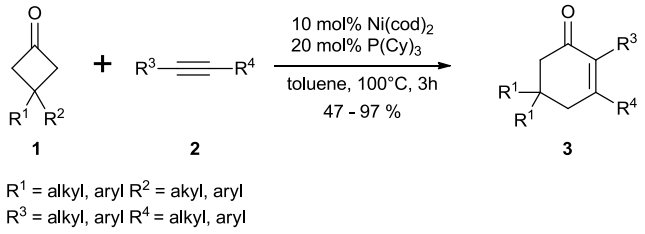


**Scheme 1** Nickel-catalysed insertion of alkyne **2** into cyclobutanone **1**

From this work, it was therefore of interest to determine if azetidinone **4** could behave like cyclobutanone **1** in a transition-metal catalysed [4+2] cycloaddition with alkyne **5** to generate pyridinone **6** (Scheme 2).

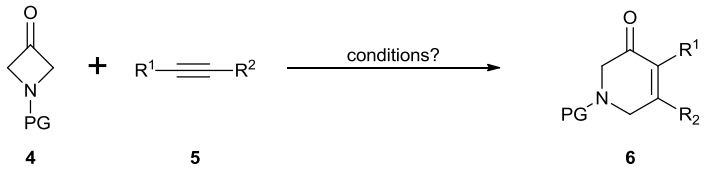


**4** **5** **6**

**Scheme 2** Hypothesis

## 2.2 Optimisation

Using the conditions described by Murakami and co-workers,[2] treatment of commercially available *N*-Boc-Azetidinone **7** with diphenylacetylene **5a** in the presence of 10 mol% $Ni(cod)_2$ and 20 mol% $PCy_3$ in toluene at 100°C gave the expected six-membered ring **6a** but also a four-membered ring **8** in a near 1:1 ratio (Scheme 3). Both products were characterised by $^{1}H$ and $^{13}C$ NMR, IR and HRMS.

The formation of the four-membered ring **8** is believed to be a result of a Boc-group directed C–H bond activation to form intermediate **9**. Afterwards, hydrometalation onto alkyne **5a** would form intermediate **10**. Finally, reductive elimination would give four-membered ring **8**.

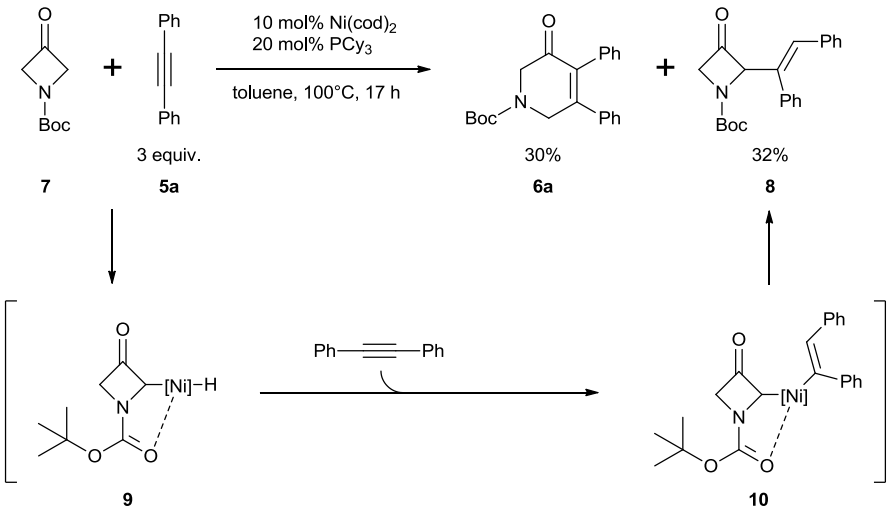


**Scheme 3** Initial screen with azetidinone **7** under Murakami's conditions

A screening of ligands was then carried out to optimise the formation of **6a** (Table 1). Phosphines with alkyl groups tend to favour the formation of **8** (Table 1, Entry 1-3). Ligands with *ortho* substitution (Table 1, Entry 4 and 5) have large cone angles and inhibited the reaction. Ligands with a heteroatom (Table 1, Entry 6 and 7) appear to be somewhat tolerated with electron poor L3[3] (Table 1, Entry 7) favouring high selectivity towards **6a** but with incomplete conversion. Electron poor triphenylphosphite (Table 1, Entry 8) was found to be ineffective. $PPh_3$ (Table 1, Entry 9) had some selectivity towards **6a**. Modifying the *para* substituents on the phenyl ring (Table 1, Entry 10-12) showed that the electronic effects[4] had little influence on the formation of **6a** or **8** except for P(*p*-$ClC_6H_4)_3$ (Table 1, Entry 13) which led to high selectivity towards **6a** but with incomplete conversion.

**Table 1** Ligand Screening

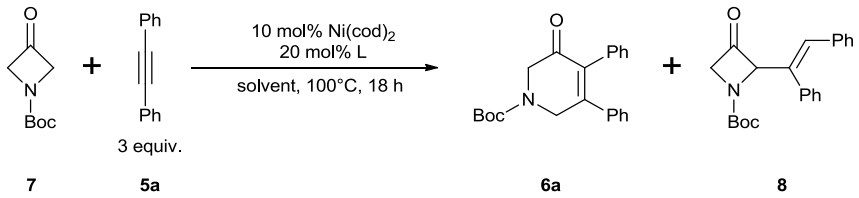


| Entry | Ligand (20 mol%) | Conversion (%) | **6a/8** | $v_{co}$ ($cm^{-1}$) | Cone angle (q) |
|---|---|---|---|---|---|
| 1. | $PCy_3$ | 100 | 50 : 50 | 2056.4 | 170 |
| 2. | $P^tBu_3$ | 95 | 21 : 79 | 2056.1 | 182 |
| 3. | $P(Ph_2)Me$ | 100 | 21 : 79 | 2067.0 | 136 |
| 4. | L1 | 55 | 50 : 50 | 2066.1 | |
| 5. | $P(o\text{-}MeC_6H_4)_3$ | 0 | 0 : 0 | 2066.6 | 194 |
| 6. | L2 | 94 | 37 : 63 | | |
| 7. | L3 | 44 | 100 : 0 | 2078.4 | |
| 8. | $P(OPh)_3$ | 7 | 100 : 0 | 2085.3 | 128 |
| 9. | **$PPh_3$** | **100** | **59 : 41** | **2068.9** | **145** |
| 10. | **$P(p\text{-}MeOC_6H_4)_3$** | **100** | **71 : 29** | **2066.1** | **145** |
| 11. | $P(p\text{-}MeC_6H_4)_3$ | 100 | 50 : 50 | 2066.7 | 145 |
| 12. | **$P(p\text{-}CF_3C_6H_4)_3$** | **>97** | **61 : 39** | | **145** |
| 13. | $P(p\text{-}ClC_6H_4)_3$ | 50 | 100 : 0 | 2072.8 | 145 |
| 14. | dppe | 0 | 0 : 0 | | |
| 15. | dppb | 36 | 100 : 0 | | |
| 16. | Xantphos | <5% | 100 : 0 | | |
| 17. | L4 | 0 | 0 : 0 | | |
| 18. | IPr | 0 | 0 : 0 | | |
| 19. | SIPr | 0 | 0 : 0 | | |

[a] $\gamma_{CO}$ ($cm^{-1}$) of $Ni(CO)_3L$ in $CH_2Cl_2$

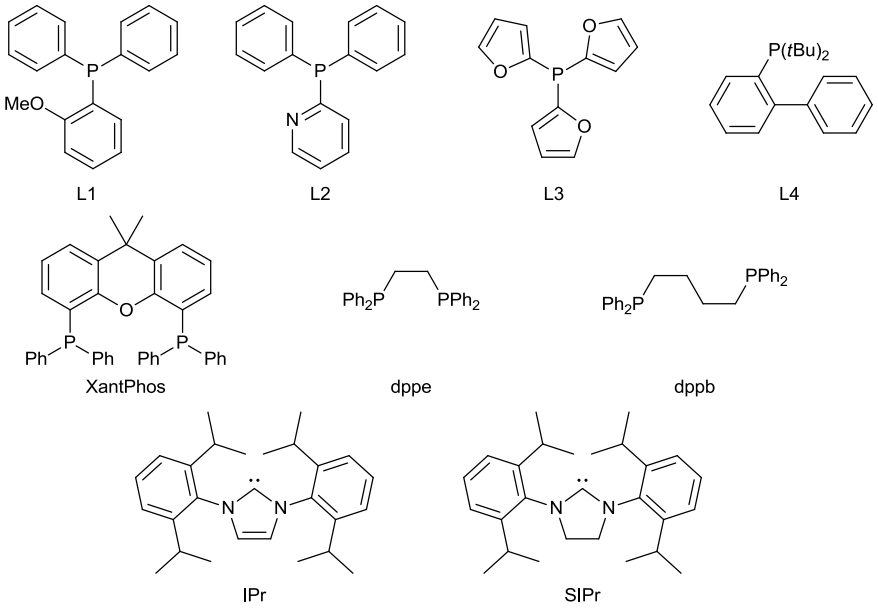


Analysis of the various properties of the phosphines revealed there is no correlation between product selectivity and the electronic properties of the ligand (Table 2). Carrying out the reaction with P*t*Bu$_3$ as the ligand gave the same selectivity as PPh$_2$Me despite both ligands being electronically ($\nu_{CO}$) different. In fact, PPh$_2$Me has similar electronic properties to PPh$_3$ and P(*p*MeOC$_6$H$_4$)$_3$ but the selectivity obtained with PPh$_2$Me is reversed compared to the latter two phosphines. Furthermore, the selectivity observed with the ligand P*t*Bu$_3$ is the same as with PPh$_2$Me despite the huge difference in cone angle between the two ligands. This illustrates that there is no correlation between the cone angle and product selectivity.

**Table 2** Comparison

| | P*t*Bu$_3$ | PPh$_2$Me | PPh$_3$ | P(*p*MeOC$_6$H$_4$)$_3$[a] |
|---|---|---|---|---|
| $\nu_{CO}$ (cm$^{-1}$) | 2056.1 | 2067.0 | 2068.9 | 2066.1 |
| Cone angle (θ) | 182 | 136 | 145 | 145[a] |
| Conversion (%) | 100 | 100 | 100 | 100 |
| Selectivity (**6a**:**8**) | 21 : 79 | 21 : 79 | 59 : 41 | 71 : 29 |

[a] assumed that para-substitution will have no effect on the cone angle

Bidentate ligand, dppe (Table 1, Entry 14) proved to be ineffective. However, dppb (Table 1, Entry 15) displayed some reactivity with complete selectivity towards **6a**. A much more rigid bidentate ligand, Xantphos (Table 1, Entry 16), was found to be ineffective. Hemi labile ligand, L4 (Table 1, Entry 17) was also ineffective. None of the NHCs tested led to the formation of an active catalyst (Table 1, entry 18 and 19). Despite P(*p*-$MeOC_6H_4)_3$ and P(*p*-$CF_3C_6H_4)_3$ displaying slightly better selectivity towards **6a**, $PPh_3$ was chosen for the subsequent solvent screening since it is a much cheaper ligand.

A screening of anhydrous solvents was then carried out with $PPh_3$ as ligand to optimise the formation of **6a** (Table 3). Carrying out the reaction in toluene (Table 3, Entry 1) resulted in little selectivity. However, carrying out the reaction in dioxane (Table 3, Entry 2) increased the selectivity for **6a.** However, using MeCN (Table 3, Entry 3) showed better selectivity for **8** and 1, 2-DCE (Table 3, Entry 4) gave no conversion.

**Table 3** Initial anhydrous solvent screen

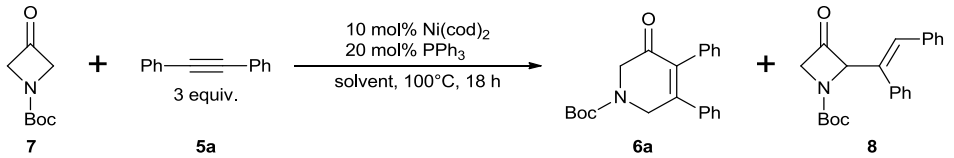


| Entry | Solvent | Conversion | **6a**/**8** |
|---|---|---|---|
| 1. | Toluene | 100% | 59 : 41 |
| 2. | Dioxane | 93% | 91 : 9 |
| 3. | MeCN | 100% | 33 : 67 |
| 4. | 1, 2-DCE | 0% | 0 : 0 |

During the study of alkyne insertion into cyclobutanones, Murakami and co-workers reported that 3 equivalents of alkyne were sometimes necessary in order to compensate for alkyne

oligomerisation. Therefore, with dioxane as solvent, a study was commenced to determine the optimal loading of alkyne (Table 4). In our study, lowering the alkyne stoichiometry from 3 equivalents (Table 4, Entry 1) to 1.5 equivalents (Table 4, Entry 2) resulted in only a slight decrease in selectivity for **6a** but with a better isolated yield. Reducing the loading of alkyne to 1.1 equivalents (Table 4, Entry 3) resulted in a further slight decrease in selectivity for **6a** but with a similar isolated yield. However, a loading of 1.5 equivalents of alkyne was used in further screening as it was a low alkyne loading with good selectivity towards **6a**.

**Table 4** Alkyne loading screening in dioxane

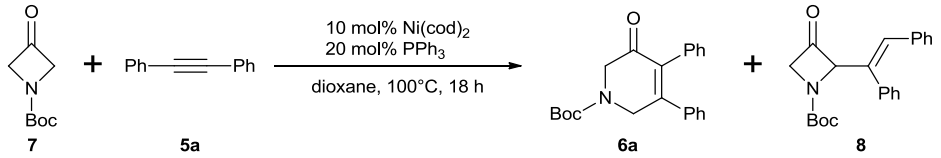


| Entry | Alkyne (eq.) | Conversion | **6a**/**8** | Yield of **6a** (%) |
|---|---|---|---|---|
| 1 | 3 | 96% | 91 : 9 | 69 |
| 2 | 1.5 | 100% | 86 : 14 | 80 |
| 3 | 1.1 | 100% | 83 : 17 | 78 |

Afterwards, the solvent screen was resumed with a loading of 1.5 equivalents of alkyne (Table 5). Using 2-pentanone (Table 5, Entry 1) led to a good selectivity towards **8** but, *c*-pentanone (Table 5, Entry 2) displayed poor selectivity for either **6a** or **8**. Both 2-MeTHF (Table 5, Entry 3) and 1,2-DME (Table 5, Entry 4) led to a good selectivity towards **8**. However, THF (Table 5, Entry 5) started to re-orientate the selectivity towards **6a**. MTBE (Table 5, Entry 6) led to a good selectivity towards **6a**. However, no solvent that was screened was able to match or exceed the performance of dioxane in orientating the selectivity towards **6a**. It is noteworthy that most of the solvents used in this second screening were used directly from bottles exposed to air and moisture. Hence, it was thought "wet" solvents might display better

selectivity towards **8**. When "wet" dioxane (Table 5, Entry 7) was used, lower selectivity towards **6a** was observed.

**Table 5** Further solvent screen with 20 mol% $PPh_3$

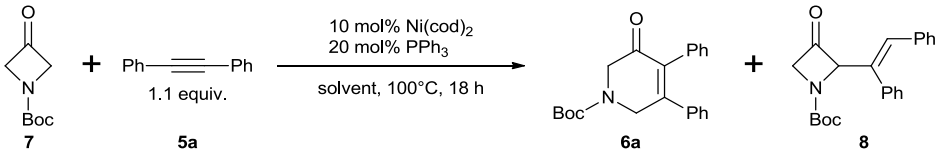


| Entry | Solvent | Conversion | 6a/8 |
|---|---|---|---|
| 1. | 2-pentanone* | >95% | 24 : 76 |
| 2. | *c*-Pentanone* | >95% | 40 : 60 |
| 3. | 2-MeTHF* | >95% | 19 : 81 |
| 4. | 1,2-DME* | >95% | 29 : 71 |
| 5. | THF | >95% | 56 : 44 |
| 6. | MTBE* | >95% | 75 : 25 |
| 7. | Dioxane* | >95% | 71 : 29 |

*wet solvents used

A study on the stoichiometry and ratio of $Ni(cod)_2/PPh_3$ was carried out in anhydrous dioxane (Table 6). Carrying out the reaction with 5 mol% $Ni(cod)_2$ and 10 mol% $PPh_3$ (Table 6, Entry 1) or 5 mol% $Ni(cod)_2$ and 10 mol% $PPh_3$ (Table 6, Entry 2) gave incomplete conversion. Changing the stoichiometry of $PPh_3$ with respect to $Ni(cod)_2$ (Table 6, Entry 3-6) revealed that selectivity for **6a** is optimal when the stoichiometry of $PPh_3$ is greater than 20 mol% with respect to 10 mol% $Ni(cod)_2$ with isolated yields greater than 69%. As expected, with 10 mol% $Ni(cod)_2$ and 20 mol% $PPh_3$, reducing the alkyne loading from 1.5 equivalents to 1.1 equivalents (Table 6, Entry 4 vs 7) reduced the selectivity towards **6a**. However, when the loading of $PPh_3$ was then increased to 30 mol% (Table 6, Entry 8), the selectivity towards **6a** is very high with an average

isolated yield of 81%. In the end, further optimisation towards **6a** was carried out with 10 mol% $Ni(cod)_2$ and 30 mol% $PPh_3$.

**Table 6** Study on the influence of stoichiometry

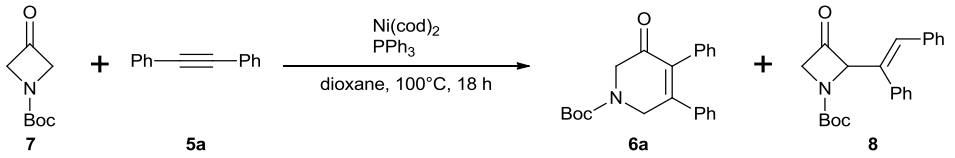


| Entry | Alkyne (eq.) | Ni (mol %) | $PPh_3$ (mol %) | Conversion | **6a**/**8** | Yield of **6a** (%)[a] |
|---|---|---|---|---|---|---|
| 1. | 1.5 | 5 | 10 | 18% | 100 : 0 | |
| 2. | 1.5 | 5 | 15 | 0% | 0 : 0 | |
| 3. | 1.5 | 10 | 10 | 93% | 81 : 19 | |
| 4. | 1.5 | 10 | 20 | >95% | 83 : 17 | 79 |
| 5. | 1.5 | 10 | 30 | >95% | 87 : 13 | 85 |
| 6. | 1.5 | 10 | 40 | >95% | 91 : 9 | |
| 7. | 1.1 | 10 | 20 | >95% | 78 : 22 | 77 |
| 8. | 1.1 | 10 | 30 | >95% | 90 : 10 | 81 |

[a]Isolated yield of an average of 2-3 runs

Lowering the concentration from 0.22M to 0.1M resulted in incomplete conversion and increasing the concentration had no effect over the timescale of the reaction. Therefore, the concentration used in the subsequent optimisations was kept at 0.22M.

Temperature effects were then studied (Table 7). Increasing the temperature to 120°C gave virtually identical results to that obtained at 100°C (Table 7, Entry 1 vs 2). With dioxane, variable conversions were obtained when the temperature was lowered to 80°C (Table 7, Entry 3 and 4). With 2-pentanone (Table 7, Entry 5 and 6), variable conversions were also obtained but the selectivity towards **6a** is much higher suggesting that the formation of **8** is a

higher energy pathway. Carrying out the reaction in dioxane and at 90°C allowed for a high selectivity towards **6a** (Table 7, Entry 7 and 8). When 20% of $PPh_3$ was used (Table 7, entry 7), an isolated yield of 84% of **6a** was obtained. A 90% isolated yield of **6a** was obtained when 30% $PPh_3$ (Table 7, entry 8) was used.

**Table 7** Temperature effects on C–C activation

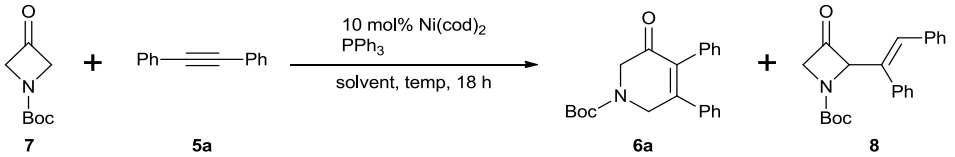


| Entry | Temp (°C) | **5a** (eq.) | $PPh_3$ (mol %) | Solvent | Conv. | **6a/8** | Yield of **6a** (%)[a] |
|---|---|---|---|---|---|---|---|
| 1. | 100 | 1.5 | 30 | Dioxane | >95% | 91 : 9 | |
| 2. | 120 | 1.5 | 30 | Dioxane | >95% | 91 : 9 | |
| 3. | 80 | 1.5 | 30 | Dioxane | >95% | 100 : 0 | |
| 4. | 80 | 1.5 | 30 | Dioxane | 63%[b] | 100 : 0 | |
| 5. | 80 | 1.5 | 30 | 2-Pentanone | 71% | 100 : 0 | |
| 6. | 80 | 1.5 | 30 | 2-Pentanone | >95%[b] | 83 : 17 | |
| 7. | 90 | 1.1 | 20 | Dioxane | >95% | 94 : 6 | 84 |
| 8. | 90 | 1.1 | 30 | Dioxane | >95% | >95 : <5 | 90 |

[a] Isolated yield of an average of 2-3 runs; [b] reaction left over the weekend

Attempts to use $Ni(PPh_3)_2Cl_2$/Zn instead of $Ni(cod)_2$ proved unsuccessful, giving only unreacted starting material or trace formation of **3**. $Ni(PPh_3)_4$ also failed to give any reaction. Blank tests without $Ni(cod)_2$ and without both $Ni(cod)_2$ and $PPh_3$ resulted in no conversion therefore confirming it is a Ni-catalysed reaction. Therefore, the optimised condition was set at 10 mol% $Ni(cod)_2$, 30 mol% $PPh_3$ in dioxane at 90°C. The azetidinone and alkyne were added sequentially after the formation of the active catalyst.

## 2.3 Scope of the reaction

### 2.3.1 Cycloaddition of *N*-Boc Azetidinone with alkynes

With the optimised reaction condition in hand, the scope of the reaction was examined (Table 8). The insertion of symmetrical alkynes diphenylacetylene **5a** and 4-octyne **5b** into azetidinone **7** proceeded in high yields to give **6a** and **6b** respectively. With unsymmetrical alkyne, the insertion of 1-phenyl-1 propyne **5c** proceeded with good regioselectivity as determined from isolated yields of **6c** and **11c**. Furthermore, the isomers were easily separable by standard flash column chromatography. The regioselectivity of insertion of other non-symmetrical alkynes **5d – 5i** was good. However, the reactivity of non-symmetrical alkynes **5h** and **5i** was not initially reproducible. However, the addition of a solution of both azetidinone **7** and the alkyne in dioxane (0.29 mM) gave reproducible results. Furthermore, despite the increase of the steric bulk on the alkyl substituent (Table 8, entries 8 and 9), only a small erosion of the regioselectivity was observed. The regiochemistry of all isomers was determined by NOESY and HMBC experiments (Scheme 4).

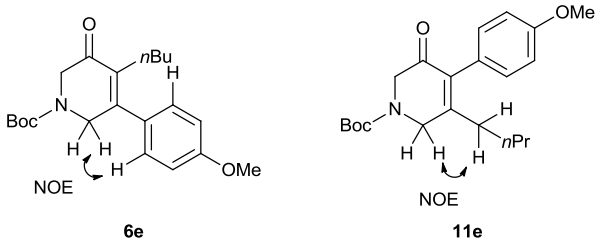


**Scheme 4** NOESY experiments

The results obtained with alkynes **5e** and **5g** suggest that electronic differentiation had little influence on the regioselectivity. This was confirmed with the reaction involving **5j**. On this substrate, both substituents of the alkyne were differentiated only electronically and displayed identical steric hindrance. The two isomers **6k** and **11k** were not separable by

column chromatography but from crude NMR, the regioisomers ratio was established as almost equimolar. Comparison of alkynes **5k** and **5l**, revealed that the increase of steric differentiation between the substituents resulted in improved regioselectivity.

**Table 8** Alkyne scope

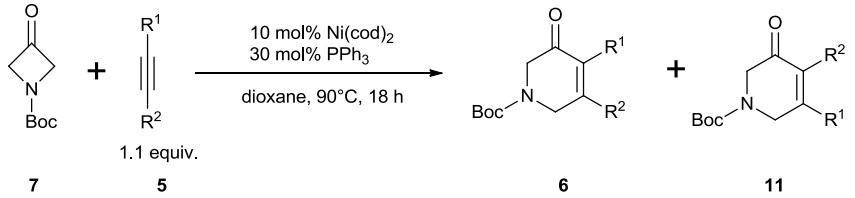


| Entry | Alkyne **5** | Major Product **6** | Ratio (**6** / **11**)[a] | Yield[b] |
|---|---|---|---|---|
| 1 | 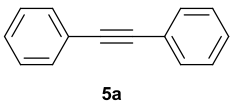 **5a** | 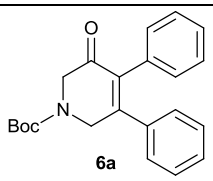 **6a** | | 90 |
| 2 | 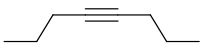 **5b** | 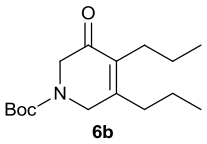 **6b** | | 88 |
| 3 | 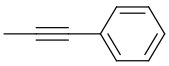 **5c** | 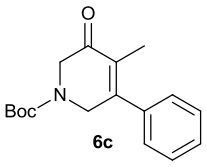 **6c** | 87 : 13 | 92 |
| 4 | 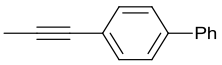 **5d** | 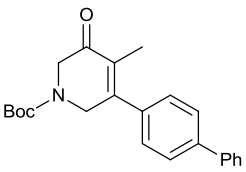 **6d** | 91 : 9 | 91 |
| 5 | 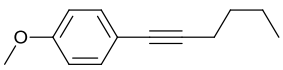 **5e** | 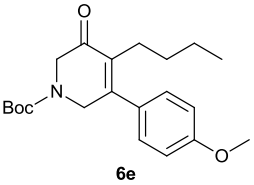 **6e** | 89 : 11 | 89 |

| | | | | |
|---|---|---|---|---|
| 6 | 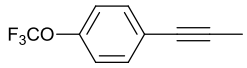 **5f** | 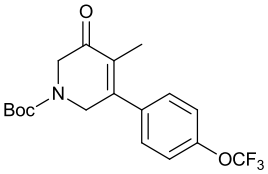 **6f** | 90:10 | 69[e] |
| 7 | 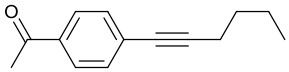 **5g** | 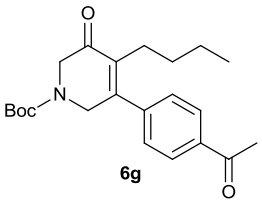 **6g** | 89 : 11 | 99 |
| 8 | 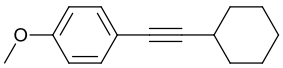 **5h** | 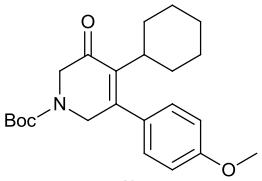 **6h** | 86 : 14 | 88[c] |
| 9 | 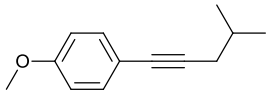 **5i** | 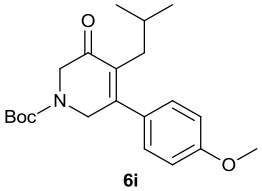 **6i** | 84 : 16 | 91[c] |
| 10 | 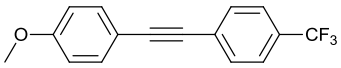 **5j** | 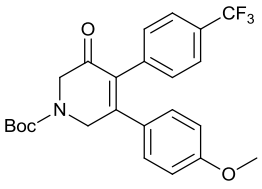 **6j** | 55 : 45 | 82[d] |
| 11 | 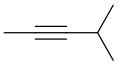 **5k** | 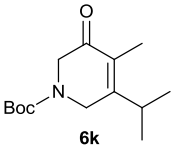 **6k** | 60 : 40 | 90[d] |
| 12 | 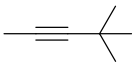 **5l** | 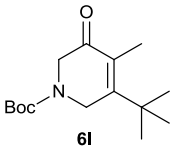 **6l** | >99: 1 | 87[d] |

[a] Unless otherwise stated, this ratio was determined from the isolated yields of separated regioisomers **6** and **11**. [b]Combined isolated yields of **6** and **11.** [c] Alkyne and Azetidinone were premixed. [d] Ratio determined by $^{1}$H NMR spectroscopy on an inseparable mixture of **6** and **11**. [e] Yield of major isomer

By comparison of the experimental results of nickel-catalysed reductive coupling of simple internal alkynes (alkyl-C≡C-alkyl and alkyl-C≡C-aryl) and aldehydes, the regioselectivities that were obtained followed the same trend as the results we obtained.[5] Jamison and co-workers reported the nickel-catalysed reductive coupling of alkyne **5c** with aldehyde **12** (Scheme 5).[5f] The coupling proceeded with a similar regioselectivity as the insertion of alkyne **5c** into azetidinone **7**. Furthermore, the major isomer has the Me group appear nearest to the C(O)–C bond.

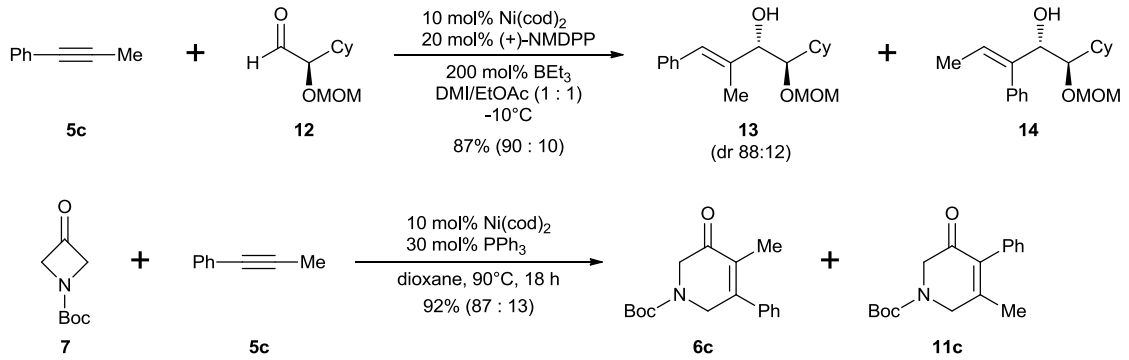


**Scheme 5** Comparison of our result with the result reported by Jamison

Furthermore, computation studies of nickel-catalysed reductive couplings of simple alkynes and aldehydes revealed the energy of the transition states are affected by the orientation of the alkyne (Scheme 6).[6] It was calculated that transition state **19a** is lower than transition state **19b** purely because of steric effects. This study suggests the steric repulsion between the alkyne substituent and the aldehyde is more influential than between the alkyne substituent and the nickel-phosphine catalyst in the oxidative cyclisation step. Due to the greater steric repulsion between the alkyne substituent and the aldehyde, the lowest transition state has the smallest alkyne substituent next to the aldehyde. Therefore, this subtle difference would then explain why some alkynes added onto the aldehyde with good regioselectivity.

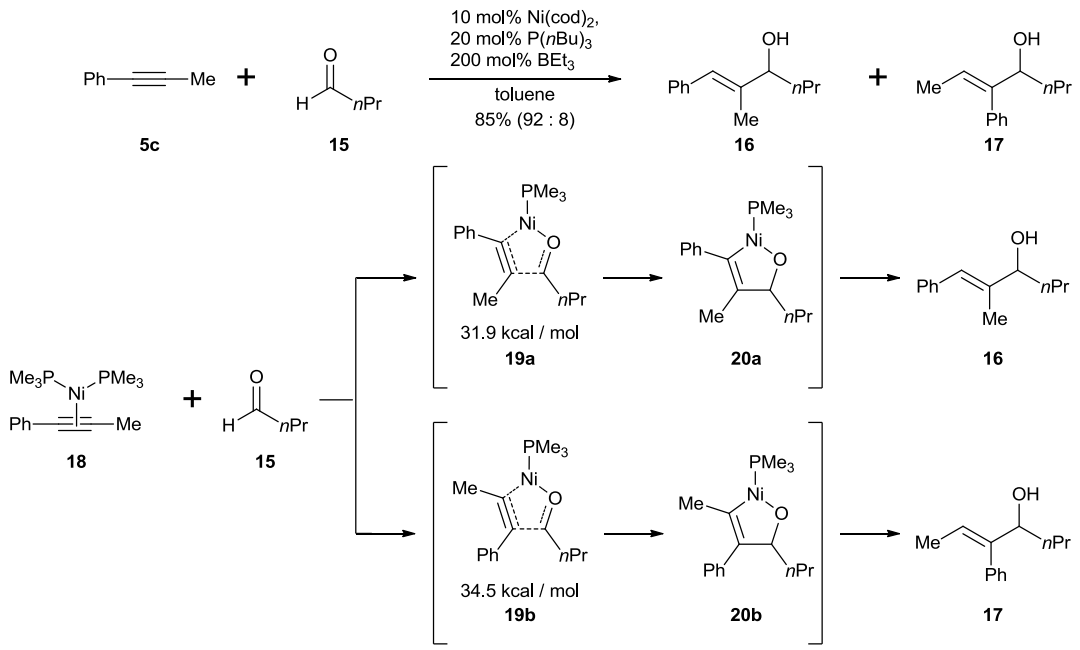


**Scheme 6** Experimental and theoretical study of nickel-catalysed reductive coupling

Therefore, from the work done on nickel-catalysed reductive couplings of simple internal alkynes and aldehydes, we proposed the regioselectivity of the insertion of alkynes **5c-5l** are determined by the steric differentiation between the substituents of the alkyne.

For the mechanism, we propose that prior to the oxidative cyclisation, the alkyne has two orientations whereby the small alkyne substituent in **21** or the large alkyne substituent in **24** can be in proximity to the azetidinone (Scheme 7). For the major regioisomer, the minimisation of the steric interaction between the Boc protective group on the azetidinone and the large alkyne substituent would afford metallacycle **22**. Ring enlargement by β-C elimination would then afford nickelaheptacycle **23**. Finally, reductive elimination would afford product **6**.

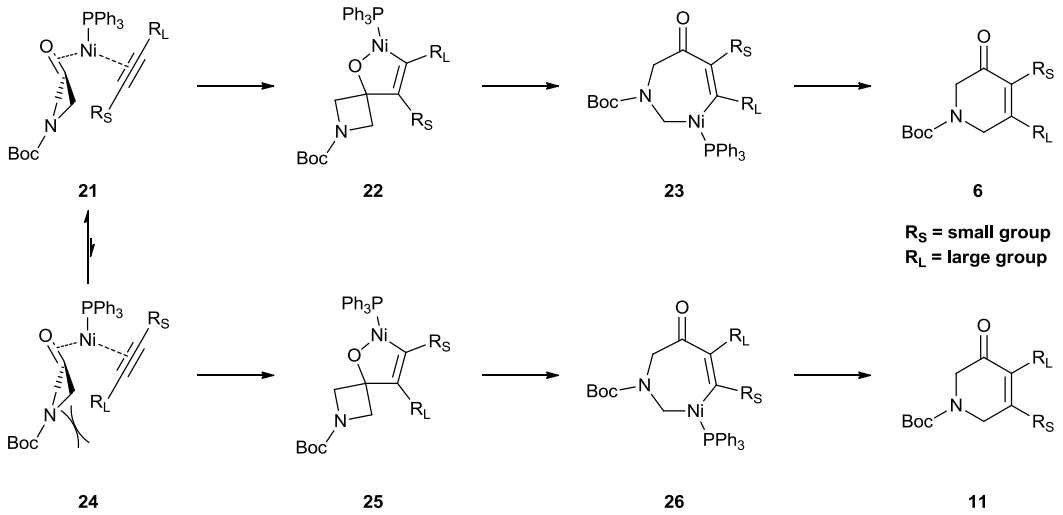


**Scheme 7** Steric differentiation to explain the formation of the regioisomer

There appears to be some correlation between regioselectivity and steric differentiation (Scheme 8). A-values are derived from the energy for the interconversion of a monosubstituted cyclohexane ring and these values can be used as a measure of the steric bulk of a substituent.[7] Comparison of the difference in A-value for alkyne **5k**, **5c** and **5l** indicates that the greater the difference, the better the regioselectivity. However, comparison of alkyne **5c** and **5h** suggests the regioselectivity is not completely influenced by the steric differentiation between the two substituents. Both have a phenyl group conjugated to the alkyne and therefore, the phenyl group could behave as a directing group.

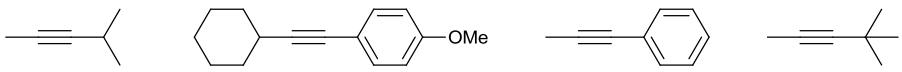


| | **5k** | **5h** | **5c** | **5l** |
|---|---|---|---|---|
| A values (kcal / mol) | Me : 1.74<br>*i*Pr : 2.21 | Cy : 2.2<br>Ph : 2.8* | Me : 1.74<br>Ph : 2.8 | Me : 1.74<br>*t*Bu : 4.7 - 4.9 |
| Difference | 0.47 | 0.6 | 1.06 | 2.96 - 3.16 |
| Regioselectivity | 55:45 | 86 : 14 | 87 : 13 | >99 : 1 |

*assumed that para-substitution on benzene to have little influence on A-values

**Scheme 8** Correlation between regioselectivity and steric differentiation

Furthermore, insertion of 1,3-enynes into azetidinone **7** proceeded successfully (Table 9). Enyne **5m** was found to insert with good regioselectivity which suggests the alkene moiety can behave as a directing group. However, enyne **5n** was found to insert with poor regioselectivity which suggests both the alkene and the aryl substituent can complete as a directing group. This could also explain why the insertion of alkynes **5c – 5i** proceeded with near consistent regioselectivity. Furthermore, both directing groups appear to be able to over-ride or minimise any steric influences.

**Table 9** Insertion of 1,3 enyne

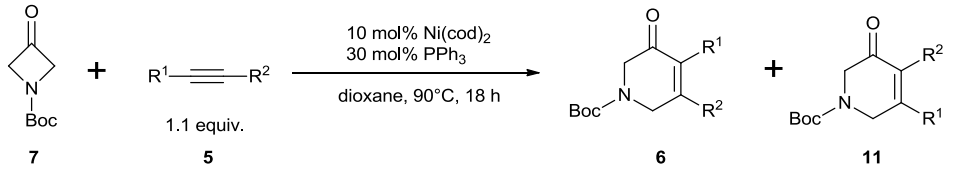


| Entry | Alkyne **5** | Major Product **6** | Ratio (**6** : **11**)[a] | Yield (%)[b] |
|---|---|---|---|---|
| 1 | 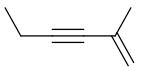 **5m** | 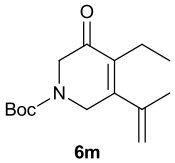 **6m** | 88 : 12 | 88 |
| 2 | 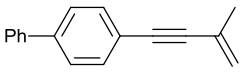 **5n** | 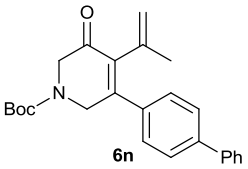 **6n** | 60 : 40 | 86[c] |

[a] Unless otherwise stated, this ratio was determined from the isolated yields of separated regioisomers **6** and **11**. [b]Combined isolated yields of **6** and **11.** [c] Ratio determined by $^{1}$H NMR spectroscopy on an inseparable mixture of **6** and **11**.

According to a computational study, the insertion of 1,3-enynes into aldehydes could proceed via one of three pathways (Scheme 9). [6b] From the modelled example of the reductive coupling of 1, 3-butenyne and acetaldehyde, the oxidative cyclisation is the rate determining step.

Coupling at the alkene was calculated to have a high activation energy. By comparison, coupling at the alkyne was calculated to be lower in energy. Pathway A is the 1,4 attack to enyne. Pathway B is the 1,2 attack to enyne. Finally, pathway C is the 1,2 attack to enyne to form the minor regioisomer. It is calculated the activation energy to the transition state in pathway A is the lowest out of the three pathways. Furthermore, it is calculated the extra $\eta^3$-allyl/metal interaction in pathway A lowers the energy of the transition state. Interestingly, the authors reported that the activation energy barrier for coupling with 1,3 enynes is lower than coupling with simple alkynes. Therefore, 1,3 enynes should be more reactive as a coupling partner.

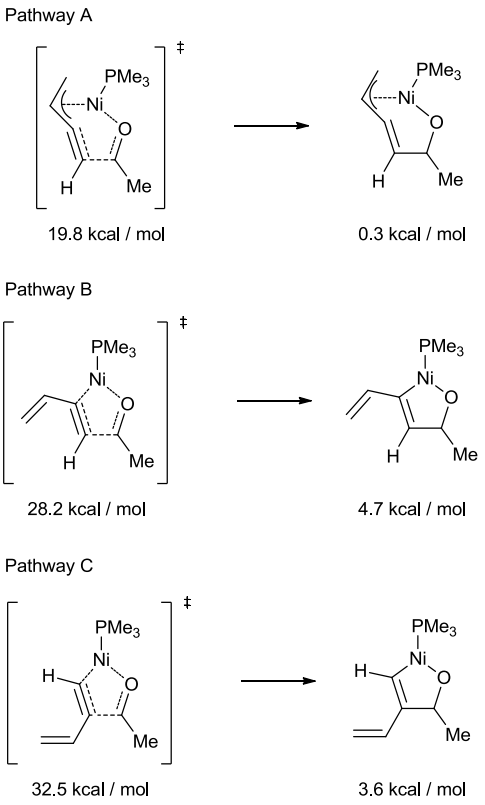


**Scheme 9** Theoretical study of the nickel-catalysed reductive coupling of 1,3-enyne with aldehydes

Therefore, based on the computational study, enyne **5n or 5m** will first form complex **27** whereby the alkene or aryl will coordinate to the nickel metal centre (Scheme 10). Then oxidative cyclisation would occur to give metallacycle **28** which subsequently would undergo β-C elimination to give metallacycle **29**. Then reductive elimination would afford pyridinone **6** as the major isomer with the vinyl group in the β-position to the carbonyl.

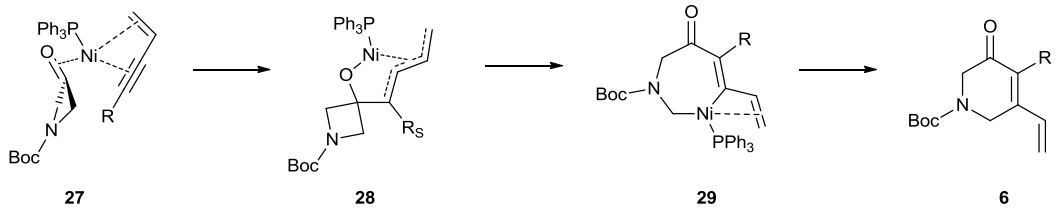


**Scheme 10** Directing group effects to explain the formation of the major regioisomer

Experimental results of the reductive coupling of enynes with aldehydes also proceeded with similar regioselectivities if the other alkyne substituent is an alkyl group.[8] When the other alkyne substituent is an aryl group, the regioselectivity tended to be better rather than worse.[8a] To exemplify this, Montgomery and co-workers reported a nickel catalysed reductive coupling of enyne **30** and aldehyde **31** which proceeded in an excellent regioselectivity (Scheme 11) whereas with the nickel-catalysed cycloaddition developed in this thesis, the insertion of **5n** into **7** proceeded with poor regioselectivity (Scheme 12).[5e]

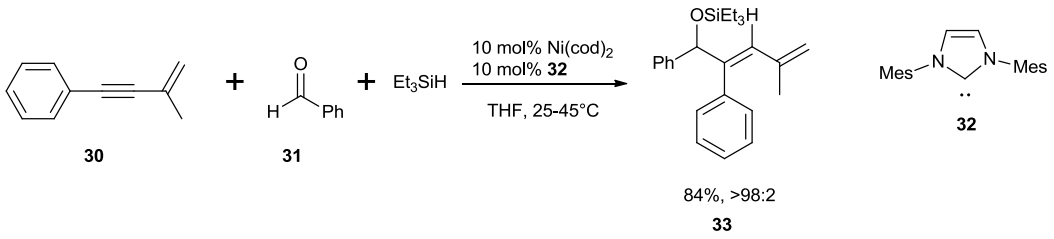


**Scheme 11** Nickel catalysed reductive couplings of enyne and aldehyde

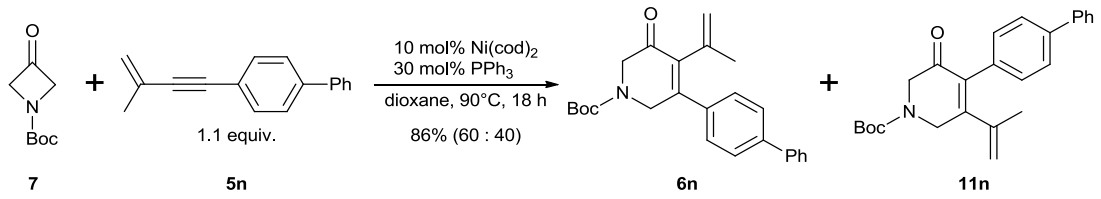


**Scheme 12** Nickel catalysed [4+2] cycloaddition of enyne and azetidinone

The reaction of silylated alkynes was unexpected as none worked in the nickel-catalysed insertion into cyclobutanone as reported by Murakami and co-workers.[2] However, insertion of alkyne **5o** proceeded in a high yield and with excellent regioselectivity.[9] Even with a larger silyl group **5p**, the insertion still proceeded in an excellent yield and regioselectivity. Slightly diminished regioselectivity of the insertion was observed with alkyne **5q**. It appears that if an aryl group is conjugated to the silylated alkyne, the directing group effect of the aryl group and the preference of the silicon being in the α-position will make the insertion more regioselective. However, insertion of alkyne **5r** and **5s** failed to take place.

**Table 10** Silylated alkyne scope

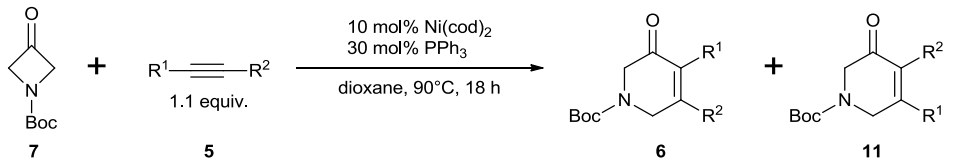


| Entry | Alkyne **5** | Major Product **6** | Ratio **6 / 11**[a] | Yield **6** (%)[b] |
|---|---|---|---|---|
| 1 | 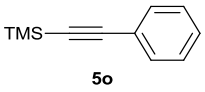 **5o** | 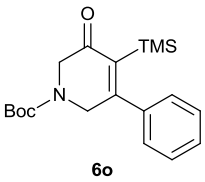 **6o** | 97 : 3 | 91 |
| 2 | 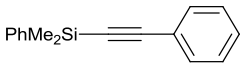 **5p** | 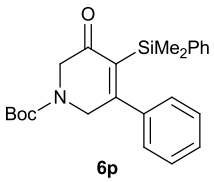 **6p** | 97 : 3 | 98 |
| 3 | 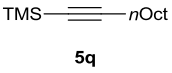 **5q** | 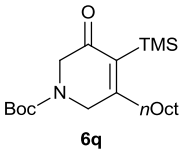 **6q** | 80 : 20[c] | 78[d] |
| 4 | 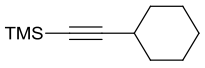 **5r** | 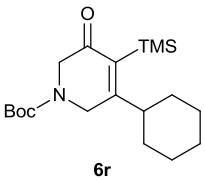 **6r** | n / a | 0 |
| 5 |  **5s** | 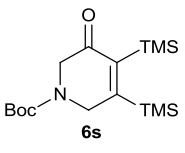 **6s** | n / a | 0 |

[a] Unless otherwise stated, this ratio was determined from the isolated yields of separated regioisomers **6** and **11**. [b]Combined isolated yields of **6** and **11.** [c] Ratio determined by $^{1}$H NMR spectroscopy on an inseparable mixture of **6** and **11**. [d] 1.5 equiv. of alkyne was used

Furthermore, the nickel-catalysed reductive coupling reactions with silylated alkynes generally proceeded with better regioselectivity when compared to the more simple alkynes. As a

representative example, Jamison and co-workers reported the reductive coupling of alkynes **5** with aldehydes **34** to afford allylic alcohol **35** proceeded with superior regioselectivities when silylated alkynes are used (**35b** and **35d**) compared to when 1-phenyl-1-propyne is used (**35a** and **35c**) (Scheme 13).[5b]

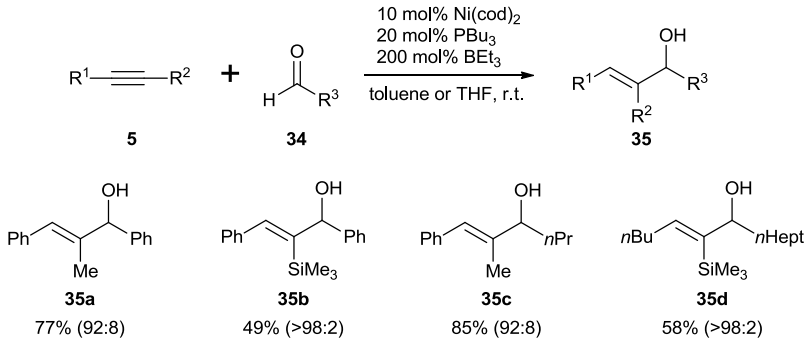


**Scheme 13** Comparison of the reductive coupling of silylated and simple alkynes with aldehydes

The principles used to explain the regioselectivity outcome are different with silylated alkynes. By looking at the axial strain values and comparing the outcome between the alkyne insertion of **5k** and **5o** revealed that steric differentiation was more or less irrelevant with respect to silylated alkynes (Scheme 14). If steric differentiation was important, insertion of alkyne **5k** should have proceeded with better regioselectivity than alkyne **5o**.

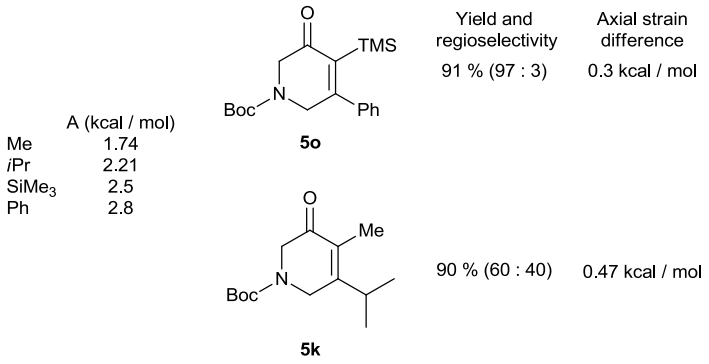


**Scheme 14** Axial strain values

Therefore, electronic effects are likely to be the prevalent factor in the highly regioselective insertion of silylated alkynes. Nickel-alkynes complexes have been studied extensively.[10] The $^{13}C$ NMR of a nickel-silylated alkyne complex **36** shows there is a large chemical shift difference between the two carbons of the coordinated alkyne which reveals the alkyne is significantly polarised. Compared to 1-phenyl-1-propyne, the chemical shift difference between the two coordinated alkyne carbons of complex **37** is significantly smaller as judged by $^{13}C$ NMR (Scheme 15). The greater polarisation in silylated alkynes might facilitate the proposed oxidative cyclisation step and its direction appears to dictate the regioselectivity.

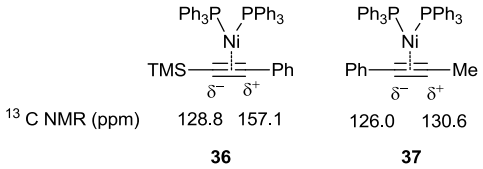


**Scheme 15** Polarisation exhibited in known nickel alkyne complexes

### 2.3.2 Limitations

#### 2.3.2.1 Terminal Alkynes

Terminal alkynes **38** and **39** were ineffective in the reaction (Scheme 16). It is believed that the cyclotrimerisation pathway is also operating. Regardless, there are examples of nickel-catalysed reactions whereby a terminal alkyne has been successfully incorporated.[5a,e,h,11] Furthermore, Kumar and Louie reported a successful insertion of *tert*butylacetylene **40** into azetidinone **7** under modified reaction conditions (Scheme 17).[12] The requirement of an increased loading of alkyne was necessary due to competing co-oligomerisation. Furthermore, slow addition of the alkyne and a reaction temperature of 100°C were necessary. The successful insertion of *tert*butylacetylene might be imputed to size of the *tert*butyl substituent

on the acetylene which makes it harder for another acetylene molecule to coordinate to the metal centre.

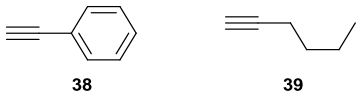

**38** **39**

**Scheme 16** Terminal alkynes attempted

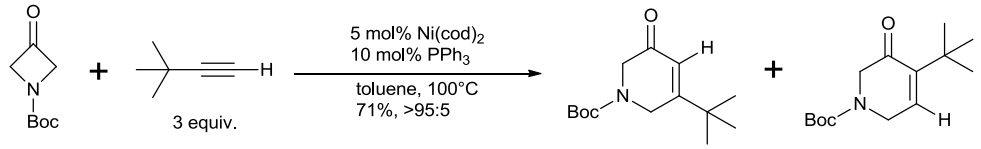


**7** **40** **41** **42**

**Scheme 17** Kumar and Louie example

### 2.3.2.2 Alkynyl pyridines

No reaction was observed when an alkyne conjugated to a pyridine was used (Scheme 18). Furthermore, there are examples in the literature of substrates containing heterocyclic moieties which were tolerated in nickel-catalysed reactions (Scheme 19).[13] The success of these reactions suggest that the pyridine on alkyne **43** and **44** makes the alkyne more electron poor and as a result will bind stronger to the nickel centre and render the desired catalytic pathway inactive. Alternatively, the pyridine could coordinate to the nickel-catalyst and render the catalyst inactive.

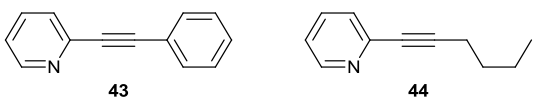


**43** **44**

**Scheme 18** Alkynes conjugated to a pyridine attempted

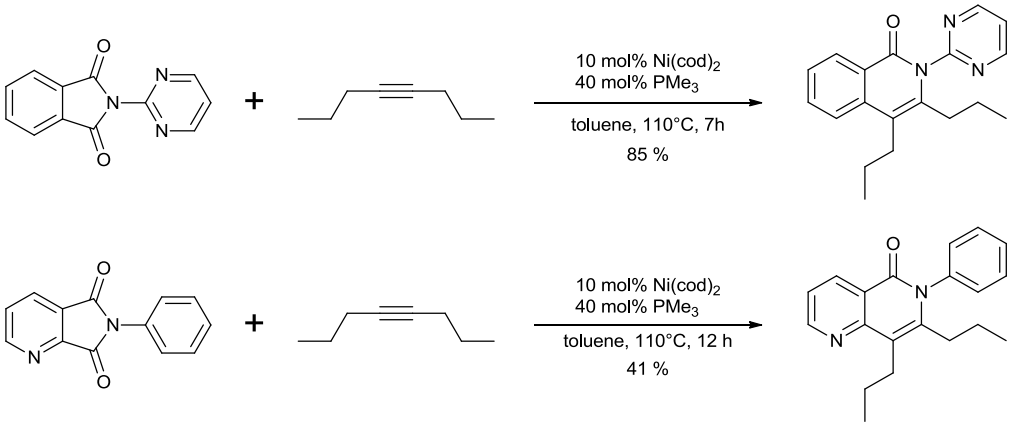


**Scheme 19** Heterocyclic moieties tolerated in nickel-catalysed reactions

### 2.3.2.3 Electron-deficient alkynes

Electron deficient alkynes **45** – **47** were then examined (Scheme 20). However, the formation of the desired six-membered ring was never observed. This is likely due to the stronger binding of electron deficient alkynes to the nickel centre.[6] Interestingly, there is a report of a nickel catalysed alkynoate insertion.[5g] Montgomery and co-workers reported the reductive coupling of enone **48** and alkynoate **49** which was carried out at room temperature to give ketone **50** as the major regioisomer (Scheme 21). Large excess of **49** was not required nor was careful control of reagent addition necessary. Surprisingly, no homocoupling products were observed.

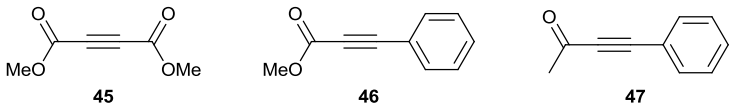


**Scheme 20** Alkyne conjugated to electron withdrawing functional group

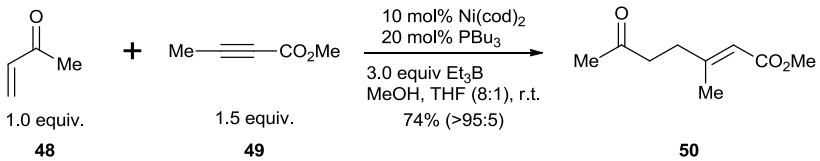


**Scheme 21** Successful nickel catalysed coupling of enone and alkynoate

### 2.3.2.4 Alkynyl boronate esters

Alkynyl boronate esters were then studied (Scheme 22). With alkyne **5t**, the insertion into **7** took place with 73% conversion. Product **6t** that was isolated identified to have had the pinacolborane moiety cleaved off and was isolated in a yield of 44%. Attempts to insert alkyne **5u** into azetidinone **7** were unsuccessful.

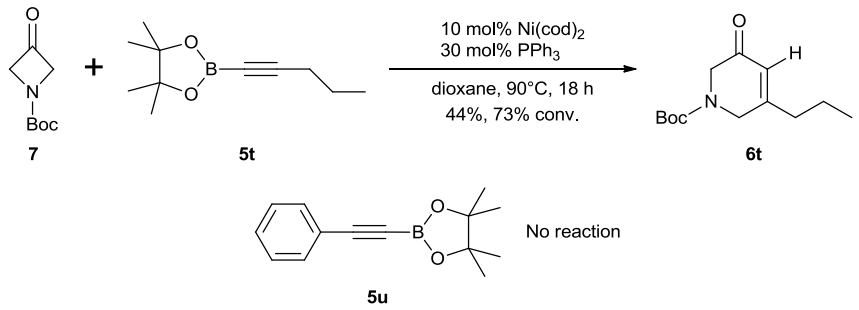


**Scheme 22** Studied of alkynyl boronate esters

### 2.3.2.5 Propargyl ethers

Non-symmetrical propargyl ethers were then examined (Table 11). No asymmetrical propargyl alkynes (Table 11, Entry 1-3) were found to successfully insert into azetidinone **7**. When the propargyl oxygen atom was replaced with a methine (Table 11, Entry 1 vs 4), there was full conversion with an isolated yield of 72% but with poor regioselectivity. Homologation of the carbon chain between the alkyne and the oxygen (Table 11, Entry 5) resulted in reactivity. Unfortunately, poor regioselectivity was observed. These results suggest oxygen is a poor directing group.

**Table 11** Alkynes with a heteroatom

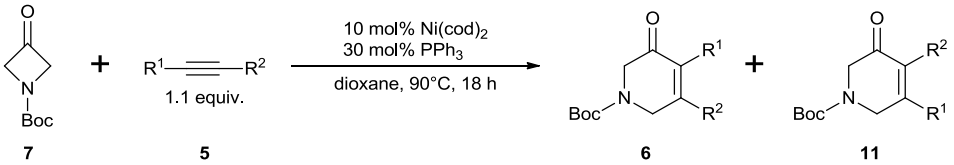


| Entry | Alkyne **5** | Major Product **6** | Ratio (**6**/**11**) | Yield (%) |
|---|---|---|---|---|
| 1 | 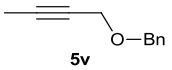 **5v** | 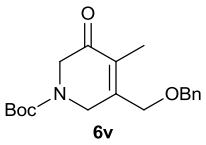 **6v** | n/a | 0 |
| 2 | 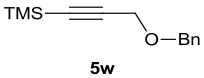 **5w** | 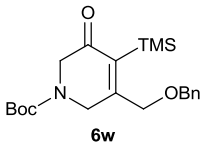 **6w** | n/a | 0 |
| 3 | 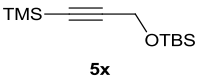 **5x** | 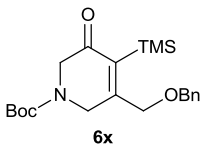 **6x** | n/a | 0 |
| 4 | 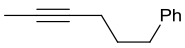 **5y** | 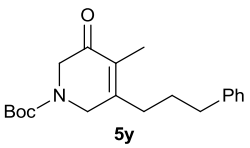 **5y** | 58 : 42 | 75% |
| 5 | 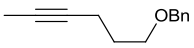 **5z** | 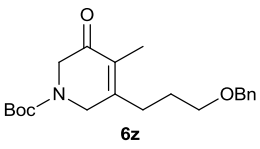 **6z** | 55 : 45 | 91% |

However, Jamison and co-workers reported a nickel-catalysed coupling of non-symmetrical propargylic ether **51** with aldehydes **52** to afford allylic alcohol **53** at -25°C (Scheme 23).[5d] This result indicates that the ligand or the reaction temperature could be influential factors.

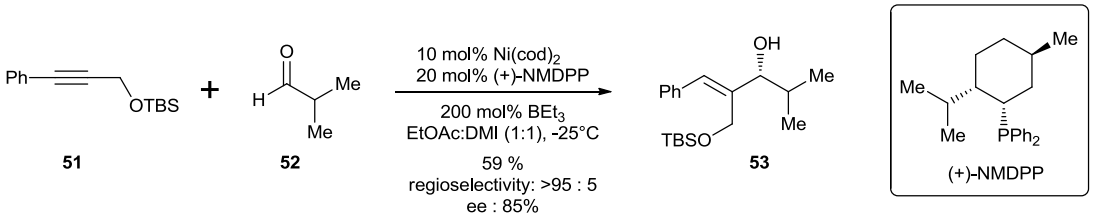


**Scheme 23** Nickel-catalysed reductive coupling of aldehyde **52** and propargyl ether **51**

A competition experiment was then carried out to determine if the catalytic system is rendered inactive by propargyl ethers (Scheme 24). Previously, the insertion of 4-octyne **6b** into **7** proceeded in an excellent yield. However, no reaction occurred when 0.55 equivalent of 4-octyne **5b** was added to the nickel catalyst, **7** and 0.55 equivalent of alkyne **5v**. Even when the loading of both alkynes were increased to 1.1 equivalent, there was still no reaction. Therefore, propargyl ethers might bind more strongly to the nickel-catalyst than 4-octyne **5b** and render the catalyst inactive.

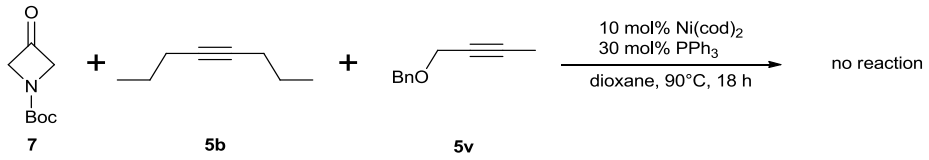


**Scheme 24** Competition experiment

Due to the lack of reactivity with propargyl ether **5v**, it was of interest to see if another transition metal catalytic system could effect the insertion (Table 12). However, no catalytic systems examined were successful. However, the temperature of the reaction was likely to be too low as there are reports of several rhodium catalysed C–C bond cleavage of four-membered rings which require a higher temperature.[14]

**Table 12** Attempted insertion of alkyne **5v** into azetidinone **7**

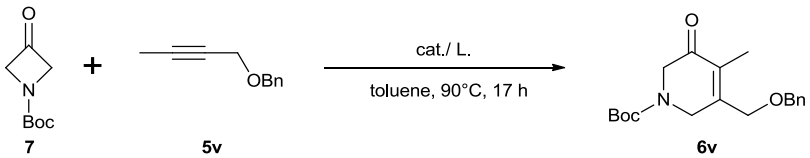


| Entry | Cat. (mol%) | Ligand (mol%) | Result |
|---|---|---|---|
| 1 | $Pd_2dba_3$ (5) | $PPh_3$ (20) | No reaction |
| 2 | $[Rh(CO)_2Cl]_2$ (5) | none | Decomp |
| 3 | $[Rh(CO)_2Cl]_2$ (5) | $PPh_3$ (20) | No reaction |
| 4 | $[Rh(CO)_2Cl]_2$ (5) | dppp (10) | No reaction |
| 5 | $[Rh(cod)_2]BF_4$ (10) | none | No reaction |

Out of curiosity, it was of interest to then see if propargylic ether **5w** could insert into azetidinone **7** (Table 13). Due to the lack of reactivity with propargylic ether **5v** by a nickel catalyst, it was of interest to see if another transition metal could catalyst the insertion of silylated equivalent **5w** into **7**. However, a brief screen of different catalytic systems revealed no catalytic system could effect successful [4+2] cycloaddition.

**Table 13** Attempted insertion of alkyne **5w** into azetidinone **7**

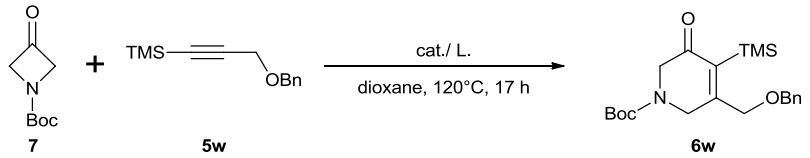


| Entry | Cat. | Ligand | Result |
|---|---|---|---|
| 1 | $Ru_3(CO)_{12}$ | none | No reaction |
| 2 | $Ru_3(CO)_{12}$ | $PPh_3$ | No reaction |
| 3 | $Pd(OAc)_2$ | 2x$PPh_3$ | No reaction |
| 4 | $Sc(OTf)_3$ | none | No reaction |

The insertion of propargylic ethers **5aa** into azetidinone **7** was then studied (Scheme 25). Carrying out the reaction with an increased loading of catalyst and at a lower reaction temperature gave rise to a regioselective insertion of alkyne **5aa** into azetidinone **7** to form **6aa**. Furthermore, another product **54** was formed from the cleavage of the Boc-group.

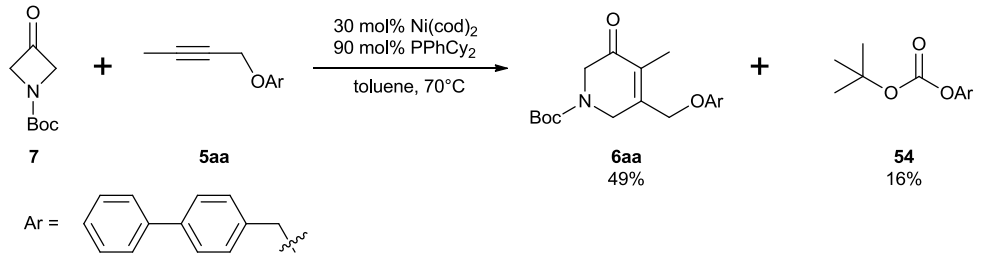


**Scheme 25** Insertion of alkyne **5aa** into azetidinone **7**

Attempts to reduce the loading of catalyst were then carried out by Jet-Sing Lee (Table 14). Reattempting the reaction with the increased loading of catalyst (Table 14, Entry 1) reproduced the initial result. When the loading of catalyst was reduced, no formation of the cleaved product **54** was observed. Instead, the other regioisomer **11aa** was observed and both isomers were isolated in a ratio of 50:50 (Table 14, Entry 2). With $PPh_3$ (Table 14, Entry 3), the selectivity towards **6aa** improved. Changing the solvent to dioxane (Table 14, Entry 4) did make a difference to the outcome. Changing the ligand to 30 mol% of $PPh_2Cy$ (Table 14, Entry 5) and carrying the reaction out in dioxane improved the selectivity towards **6aa** a little. However, with 30 mol% $PPhCy_2$ as ligand (Table 14, Entry 6) in dioxane slightly reduced the selectivity towards **6aa** and suffered from poor reactivity.

**Table 14** Catalytic loading screen

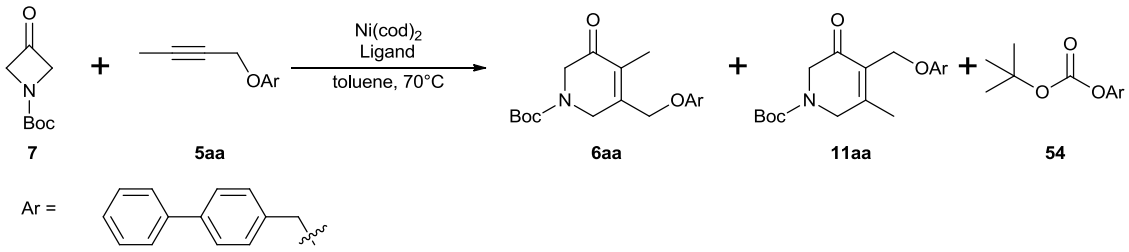


| Entry | Ni (mol %) | L (mol %) | Temp (°C) | (**6aa**/**11aa**)[a] | Yield (%)[b] | Yield **54** (%)[c] |
|---|---|---|---|---|---|---|
| 1 | 30 | $PPhCy_2$ (90) | 70 | 100 : 0 | 68 | 32 |
| 2 | 10 | $PPhCy_2$ (30) | 70 | 50 : 50 | 40 | 0 |
| 3 | 10 | $PPh_3$ (30) | 60 | 69 : 31 | 56 | 0 |
| 4[d] | 10 | $PPh_3$ (30) | 60 | 68 : 32 | 71 | 0 |
| 5[d] | 10 | $PPh_2Cy$ (30) | 60 | 72 : 28 | 41 | 0 |
| 6[d] | 10 | $PPhCy_2$ (30) | 60 | 64 : 36 | 17 | 0 |

[a] Ratio determine by $^1$H NMR of the crude material; [b] Combined isolated yield of **6aa** and **11aa**; [c] Isolated yield; [d] in dioxane

### 2.3.2.6 Miscellaneous alkynes

Several other alkynes were then tested and were found to remain inert or decomposed under the optimised conditions (Scheme 26). Propargyl alcohols **55**-**58** were ineffective. Ynamides **59** and **60** were unproductive. Alkynol **61** also failed to insert. Halogen directly attached to the alkyne **62** or an alkyne with the halogen further along a tether **63** failed to give rise to the desired 6-membered ring. However, there have been examples in the literature of nickel-catalysed reactions whereby chloro[15], protected alcohol,[15] mono-protected amines[5f] functional groups are tolerated. An example of this is the report by Liebeskind and Huffman on a nickel-catalysed annulation of cyclobutenones **64** with alkynes **65** to form phenols **66** (Scheme 27). [15]

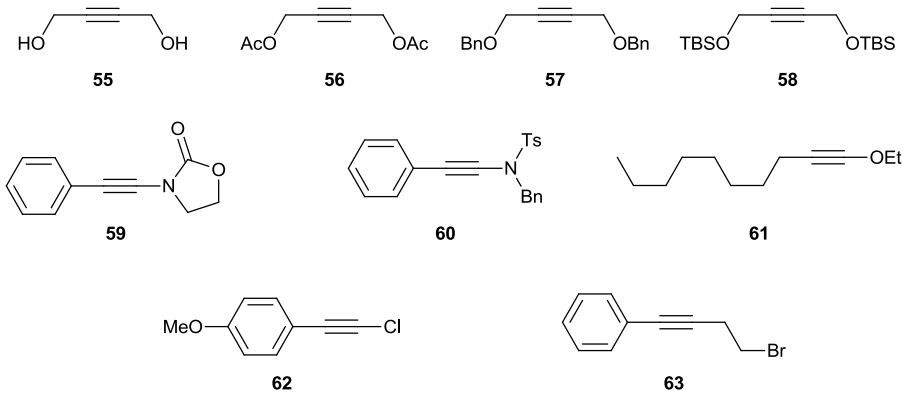


**Scheme 26** Ineffective alkynes

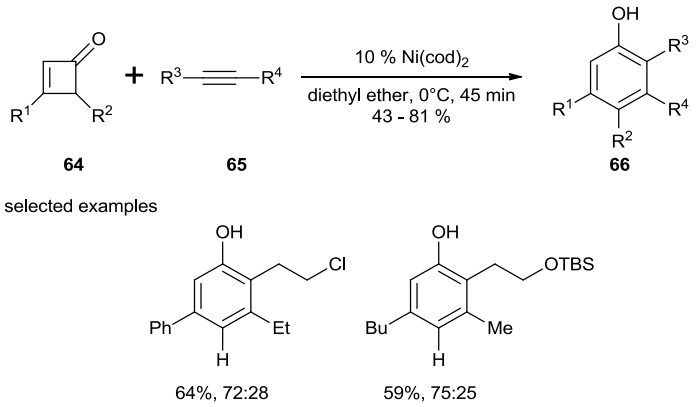


**Scheme 27** Nickel-catalysed reaction that tolerated hetero-functionality on the alkyne

### 2.3.3 Cycloaddition of *N*-Benzhydryl azetidinone 76 with alkyne 5b

The insertion of alkyne **5b** into azetidinone **67** was then examined (Scheme 28). However, no reactivity was observed with our optimised reaction conditions. In 2012, Murakami and co-workers examined this reaction and reported a 82% isolated yield of the desired pyridinone **68** when carried out with 10 mol% $Ni(cod)_2$, 20 mol% $PCy_3$ and in toluene at room temperature.[16]

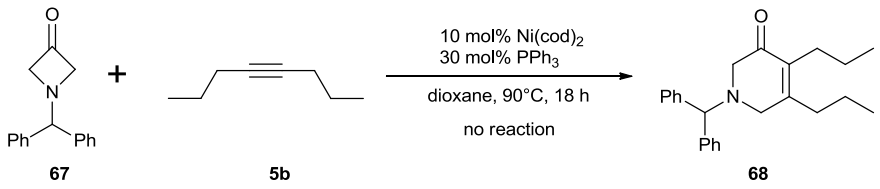


**Scheme 28** Insertion of azetidinone **67**

### 2.3.4 Cycloaddition of *N*-Ts Azetidinones with alkynes

Harsher conditions were required when *N*-Ts-azetidinone **69** was used in the place of *N*-Boc-Azetidinone **7** for full conversion (Table 15). Insertion of alkyne **5b** proceeded in good yields in 1 hour. Insertion of alkyne **5c** required a higher catalyst loading and proceeded with a lower regioselectivity. The higher temperature might explain the poorer outcome in regioselectivity.

**Table 15** Screen with *N*-Ts-azetidinone **69**

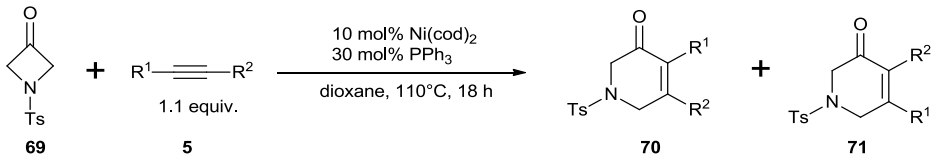


| Entry | Alkyne | Major Product **70** | Ratio (**70**/**71**) | Yield[a] |
|---|---|---|---|---|
| 1 | 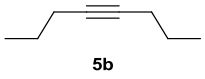 **5b** | 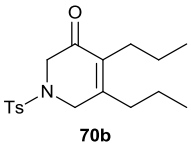 **70b** | | 73 |
| 2 | 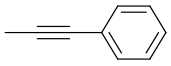 **5c** | 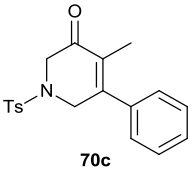 **70c** | 83 : 17 | 75[b] |

[a] combined isolated yield. [b] 20 mol% $Ni(cod)_2$, 80 mol% $PPh_3$, 1.5 equiv. of 2b, dioxane, 100°C.

The reaction also worked with α-substituted azetidinones **72** (Table 16). Insertion of symmetrical alkynes **5a** and **5b** proceeded in excellent yields. In the cycloaddition to form **73b**, the enantiomeric purity was slightly eroded with an ee of 97%. Good regioselectivity was observed in the insertion of alkyne **5c**. Finally with silylated alkyne **5o**, the regioselectivity was high but more decomposition was noted. Notably, the results in the regioselectivity were comparable to the results obtained with *N*-Boc-Azetidinone **7**.

**Table 16** α-substituted *N*-Ts-azetidinone

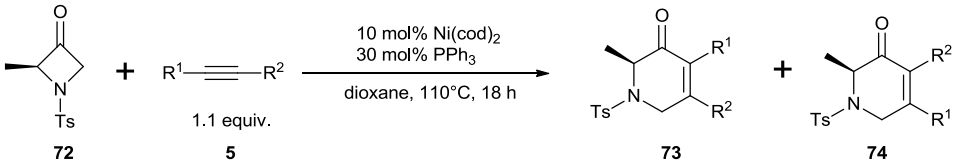


| Entry | Alkyne | Major Product **73**[a] | Ratio (**73**/**74**)[b] | Yield (%)[c] |
|---|---|---|---|---|
| 1 | 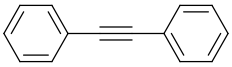 **5a** | 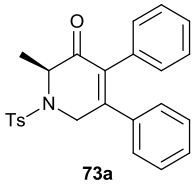 **73a** | n/a | 92 |
| 2 |  **5b** | 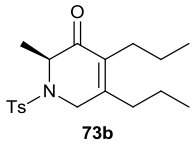 **73b** | n/a | 91[c] |
| 3 | 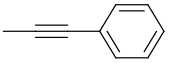 **5c** | 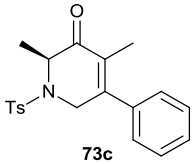 **73c** | 93 : 7 | 99 |
| 5 | 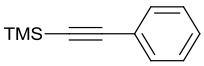 **5o** | 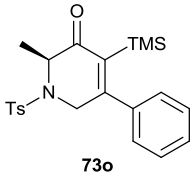 **73o** | >95 : 5 | 71[d] |

[a] **72** has an ee of >99% as determined by HPLC [a] Unless otherwise stated, this ratio was determined from the isolated yields of separated regioisomers **73** and **74**. [b] Combined isolated yields of **73** and **74.** [c] ee of product is 97% as determined by HPLC. [d] Only **73o** was isolated

The principles discussed to explain the regioselectivity of the alkyne insertion into *N*-Boc-azetidinone **7** appears to be equally applicable here. After the oxidative cyclisation to form intermediate **75**, the ring opening proceeded exclusively with the least sterically hindered C–C

bond broken to form intermediate **78** rather than intermediate **77** (Scheme 29). Finally, reductive elimination would afford product **73** as the major isomer.

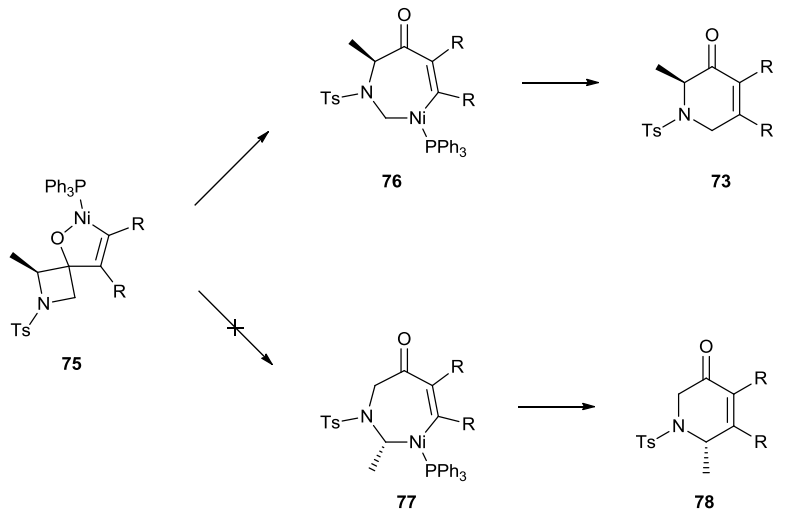


**Scheme 29** C–C cleavage of the least sterically hindered C–C bond

The insertion of 4-octyne **5b** into azetidinone **79** proved to be unsuccessful as no reaction was observed. Large α-substitution appears to hinder the reaction. However, Murakami and co-workers reported that after a slight modification to the reaction conditions, the insertion of alkyne **5l** into azetidinone **81** proceeded with an isolated yield of 56% of pyridinone **82** (Scheme 31).[16]

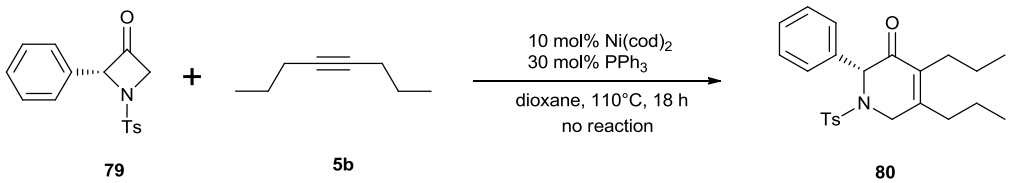


**Scheme 30** Failed insertion of alkyne **5b** into azetidinone **79**

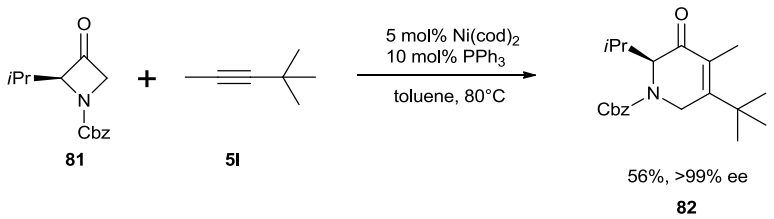


**Scheme 31** Insertion of alkyne **5l** into azetidinone **81**

The insertion of alkyne **5b** into azetidinone **83** was then studied (Table 17). With $PPh_3$ as ligand (Table 17, Entry 1), trace amounts of pyridinone **84** was formed as judged from the $^1H$ NMR spectra of the crude. Attempts to use nitrogen based ligands (Table 17, Entry 2 and 3) did not give rise to the formation of **84**.

**Table 17** Attempted insertion of alkyne **5b** into azetidinone **83**

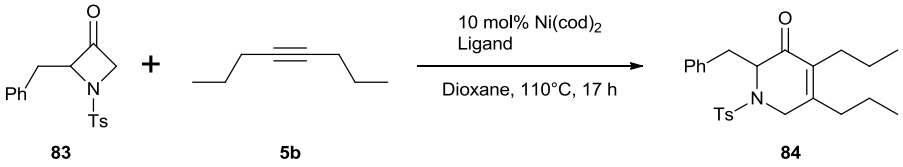


| Entry | Ligand | mol % | Result |
|---|---|---|---|
| 1 | $PPh_3$ | 30 | trace |
| 2 | Phen | 15 | trace |
| 3 | Bipy | 15 | No reaction |

### 2.3.5 Aromatisation to pyridinols

Several research groups have demonstrated the transformation of pyridinones to the corresponding pyridinols. However, no procedures were reported to deprotect the Boc group and aromatise the deprotected pyridinone to give the corresponding pyridinol. Aromatisation using DDQ as the aromatising agent was ineffective as no reaction occurred even after two nights at rt (Scheme 32). It was found acid hydrolysis of the Boc group of pyridine **6a** give a mixture of **85a** and **86a** (Scheme 33). Complete consumption of **6a** always occurs after 18 hrs and usually, mostly **86a** is formed but the mixture ratio could never be reproduced. Therefore, it became of interest to force the formation towards **85a**. A report on the use of $NaNO_2$ in the presences of wet $SiO_2$ as a aromatisation agent of 1,2-dihydroquinolines was reported.[17] Consequently, a procedure was developed to successfully transform pyridinones **6a** to the corresponding pyridinols **85** (Scheme 34). Firstly, acid hydrolysis of the Boc group followed by a $NaNO_2$ mediated aromatisation and subsequent neutralisation with triethylamine furnished the desired pyridinol **92** in a one pot process in good yields. Synthesis of **85d** and **85o** required another batch of $NaNO_2$ and allowed to stir for a further hour prior to quenching with $Et_3N$. For the synthesis of **85f**, the solution was diluted with $CH_3CN$ prior to addition of $NaNO_2$. The role of $CH_3CN$ is currently unclear but it did allow the aromatisation to be carried out within 1 hour. Compounds **85f**, **85h** and **85o** are not fully characterised in this thesis. Nonetheless, the examples given demonstrate the functional group tolerance of this methodology.

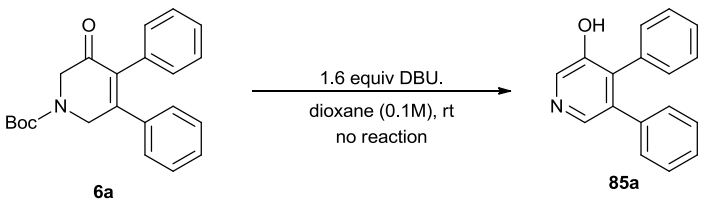


**Scheme 32** Aromatisation with DDQ

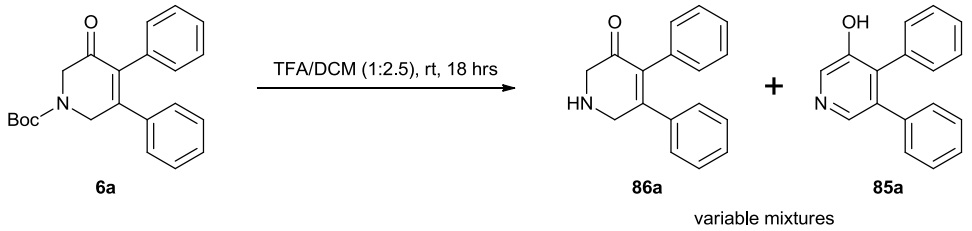


**Scheme 33** Initial attempts on aromatisation

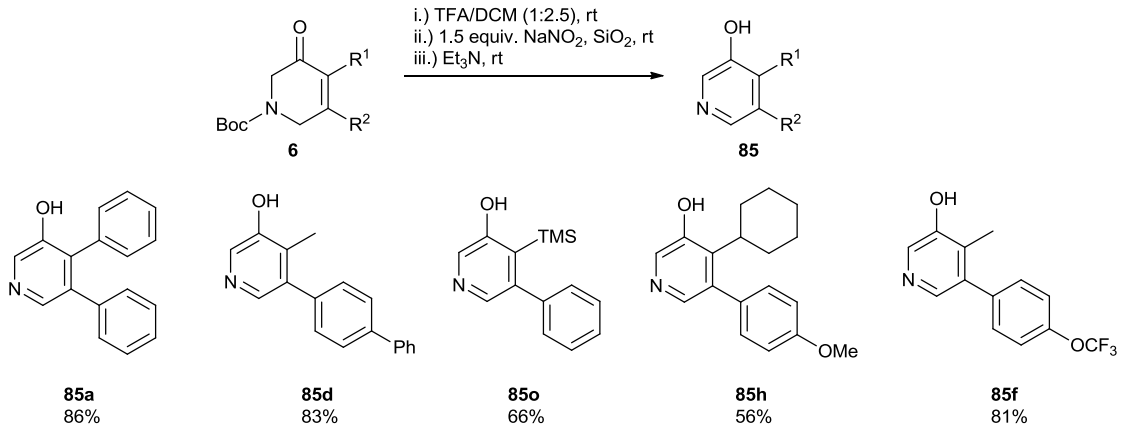


**Scheme 34** Aromatisation of pyridinones to corresponding pyridinols

### 2.3.6 Cycloaddition of oxetanones with alkynes

Using the same optimised conditions as those reported with *N*-Boc-azetidinone **7** allowed the insertion of alkyne **5** into commercially available 3-oxetanone **87** (Table 18). Insertion of alkyne **5a** proceeded in high yields. Insertion of alkyne **5g** proceeded with a lower regioselectivity when compared to the insertion of the same alkyne into *N*-Boc-azetidinone **7**. The poorer regioselectivity might be due to the less steric hindrance of the oxygen of the oxetane when compared to the larger carbamoyl group of then *N*-Boc-azetidinone **7**. Due to the different behaviour of silylated alkynes, alkyne **5o** still proceeded with excellent regioselectivity.

**Table 18** Insertion of alkyne into oxetanone

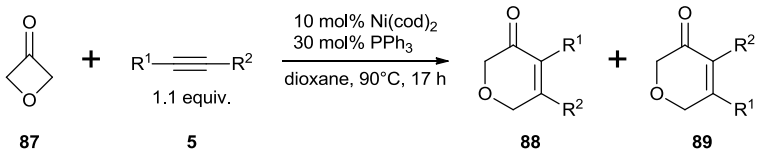


| Entry | Alkyne **5** | Major Product **88** | Ratio (**88**/**89**)[a] | Yield (%)[b] |
|---|---|---|---|---|
| 1 | 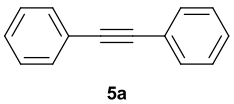 **5a** | 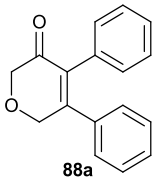 **88a** | n/a | 82 |
| 2[c] | 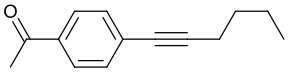 **5g** | 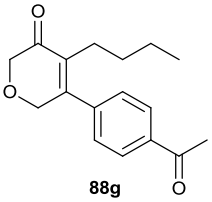 **88g** | 79 : 21 | 92 |
| 3 | 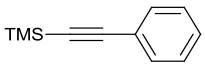 **5o** | 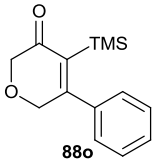 **88o** | 96 : 4 | 99 |

[a] Unless otherwise stated, this ratio was determined from the isolated yields of separated regioisomers **88** and **89**. [b] Combined isolated yields of **88** and **89**. [c] Alkyne and Azetidinone were premixed.

It was found that α-substituted oxetanone **90** underwent the nickel-catalysed cycloaddition, whereby the ring opening of the oxetanone proceeded with less regioselectivity. Products arising from the C–C cleavage of both the least and the most sterically bonds were isolated under the standard reaction conditions. The insertion of 4-octyne **5b** into **90** with the optimised reaction condition proceeded to give two isomers **91** and **92** in a 4:1 ratio with 32% recovered starting material (Table 19, entry 1). On increasing the catalytic loading to 20 mol% $Ni(cod)_2$ and 40 mol% $PPh_3$, the conversion was complete with an isolated yield of 70% of **91** and 14% yield of **92** (Table 19, entry 2). The insertion of diphenylacetylene **5a** into **90** was then

studied with the higher catalyst loading of 20 mol% $Ni(cod)_2$ and 40 mol% $PPh_3$. An isolated yield of 42% of **93** and combined mass recovery of 33% which contained **94** and recovered **90** was achieved (Scheme 35). Due to the difficulty in separating **94** from **90**, no characterisation of **94** was carried out. The lower reactivity with **5a** might be imputed to the lower reactivity of **5a** in general.

**Table 19** Nickel catalysed ring opening of α-substituted oxetanones and 4-octyne

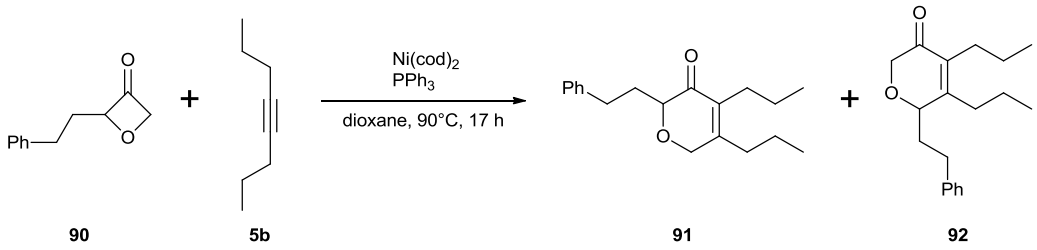


**90** **5b** **91** **92**

| $Ni(cod)_2$ (mol %) | $PPh_3$ (mol %) | **90** (%)[a] | **91** (%)[b] | **92** (%)[b] |
|---|---|---|---|---|
| 10 | 30 | 32 | 44 | 11 |
| 20 | 40 | n/a[c] | 70 | 14 |

[a] recovered starting material. [b] isolated yield. [c] all starting material consumed

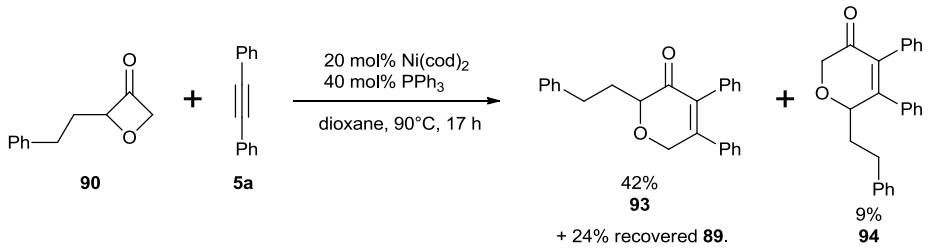


**Scheme 35** Nickel catalysed ring opening of α-substituted oxetanones and diphenylacetylene

The ring opening of α-substituted oxetanones proceeded differently when compared to α-substituted azetidinones. Whereas α-substituted azetidinones proceeded with cleavage of only the least sterically hindered bond, α-substituted oxetanones proceeded with the cleavage of preferentially the least sterically hindered bond (Scheme 36). The steric crowding provided

by the protecting group of the azetidinone might contribute to the selective C–C bond cleavage. The mechanistic proposal for the ring opening of oxetanone **90** is as follows. The oxidative cyclisation would form intermediate **95** and then the ring opening could either proceed with the least sterically hindered C–C bond or the more sterically hindered bond broken to form intermediate **96** and **98** respectively**.** Finally, reductive elimination would then afford product **97** or **99** respectively.

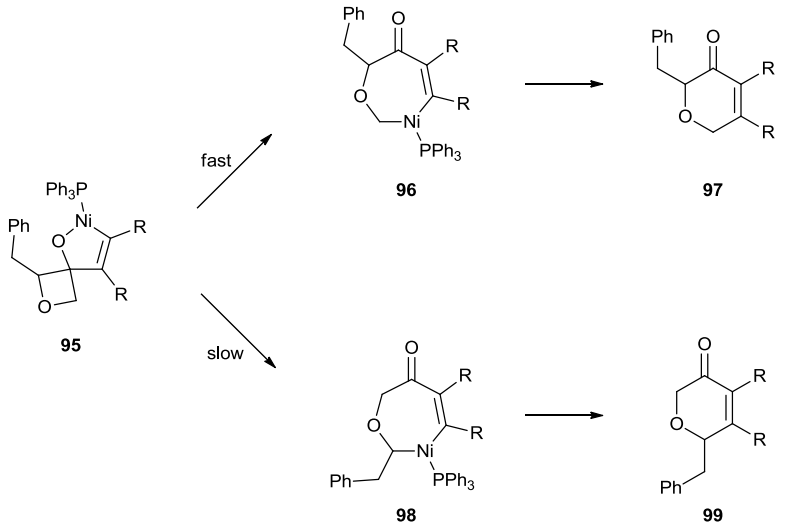


**Scheme 36** Mechanistic proposal for the ring opening of α-substituted oxetanones

### 2.3.7 Optimisation of the formation of four-membered ring 8

During the optimisation of pyridinone **6a**, solvent effects were found to be significant in the selectivity between pyridinone **6a** and four-membered ring **8**. Previously, carrying out the reaction in 2-MeTHF at 100°C gave good selectivity towards **8**. However, carrying out the reaction in 2-MeTHF at 90°C resulted in only the formation of **6a** (Scheme 37). Therefore, the reaction pathway towards **8** operates at a higher temperature.

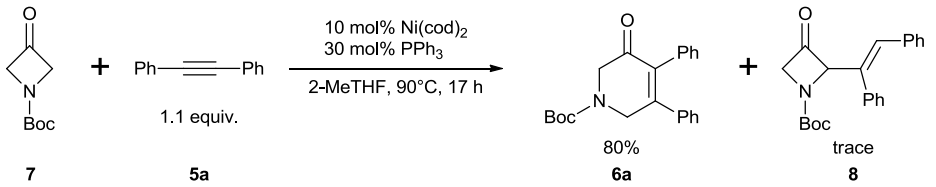


**Scheme 37** Carrying out the reaction in 2-MeTHF

A screen of different conditions was then carried out to optimise the selectivity towards four-membered ring **8** (Table 20). Previously, it was noted that alkyl phosphines generally gave good selectivity towards four-membered ring **8**. As most alkyl phosphines are liquid and air-sensitive, it was of interest to see if there was a solid alkyl phosphine alternative.

The replacement of one of the phenyl rings of $PPh_3$ with a cyclohexyl ring (Table 20, Entry 1) gave a slight increase in selectivity towards **8**. The replacement of another phenyl ring with a cyclohexyl ring (Table 20, Entry 2) resulted in the selectivity towards **8** becoming comparable to those observed with alkyl phosphines (Table 1, Entry 2 and 3).

Increasing or decreasing the loading of $PPhCy_2$ (Table 20, Entry 3 and 4) had little effect on the selectivity but with 20 mol% $PPhCy_2$, the selectivity towards **8** was slightly better. The reduction of alkyne loading (Table 20, Entry 5 – 7) had little detriment in the selectivity towards **8**. However, 1.5 equivalent of alkyne was used in further screening as it is a low alkyne loading with good selectivity towards **8**.

**Table 20** Optimisation Table

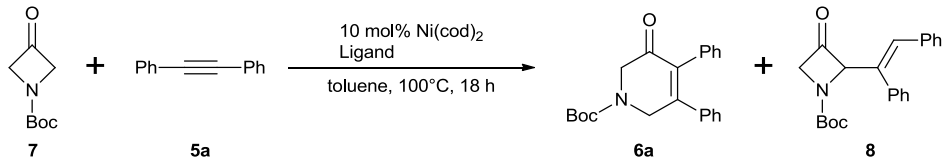


| Entry | Alkyne (equiv.) | Ligand | mol % | Conversion | **6a**/**8** |
|---|---|---|---|---|---|
| 1 | 3 | $Ph_2PCy$ | 20 | >95% | 43 : 57 |
| 2 | 3 | $PhPCy_2$ | 20 | >95% | 19 : 81 |
| 3 | 3 | $PhPCy_2$ | 10 | >95% | 22 : 78 |
| 4 | 3 | $PhPCy_2$ | 30 | >95% | 21 : 79 |
| 5 | 2 | $PhPCy_2$ | 20 | >95% | 20 : 80 |
| 6 | 1.5 | $PhPCy_2$ | 20 | >95% | 20 : 80 |
| 7 | 1.1 | $PhPCy_2$ | 20 | >95% | 21 : 79 |

A screening of different solvents which previously displayed a good selectivity toward the four-membered ring **8** was then carried out (Table 21). Toluene (Table 21, Entry 1) gave good selectivity and reactivity toward **8**. Carrying out the reaction in 2-pentanone (Table 21, Entry 2) gave identical selectivity as before (Table 4, Entry 1) but with poorer conversion. 2-MeTHF (Table 21, Entry 3) gave near identical selectivity as before (Table 4, Entry 3) with full conversion and an isolated yield of 63%. Also, 2-pentanone and 2-MeTHF was used directly out of a bottle exposed to air and moisture. Isopropanol (Table 21, Entry 4) gave full conversion but with no selectivity. Increasing the temperature did not enhance the selectivity towards **8**. Therefore, the optimised condition for the synthesis of **8** was 10 mol% $Ni(cod)_2$, 20 mol% $PPhCy_2$ and in toluene at 100°C.

**Table 21** Solvent screen

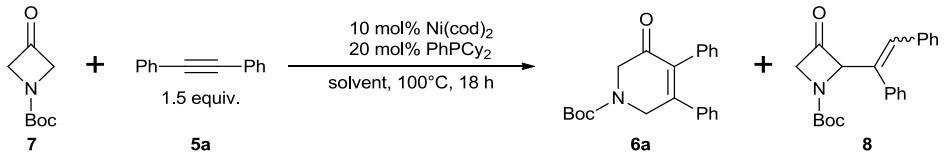


| Entry | Solvent | Conversion (%) | **6a**/**8**[a] |
|---|---|---|---|
| 1 | Toluene | >95 | 20 : 80 |
| 2[b] | 2-pentanone | 25 | 24 : 76 |
| 3[b] | 2-MeTHF | >95 | 18 : 82 |
| 4 | isopropanol | >95 | 50 : 50 |

[a] Ratio determined by $^{1}$H NMR spectroscopy on a crude mixture of **6** and **11** [b] wet solvent

With the optimised reaction condition in hand, the insertion of symmetrical alkyne **100** was found to proceed with poor selectivity for **102** (Scheme 38). A near 1:1 isolated ratio of **101** and **102** was observed. Furthermore, carrying out the reaction with 4-octyne **5b** in toluene resulted in a 62% isolated yield of pyridinone **6b**. 1-Phenyl-1-propyne **5c** resulted in an 88% conversion to pyridinones **6c** and **11c**. Neither alkyne **5b** nor **5c** reacted to form the corresponding four-membered ring. Attempts to incorporate the terminal alkyne phenylacetylene **38** were unsuccessful. Therefore, the methodology towards the four-membered ring appears to be restricted to only bis-aryl alkynes.

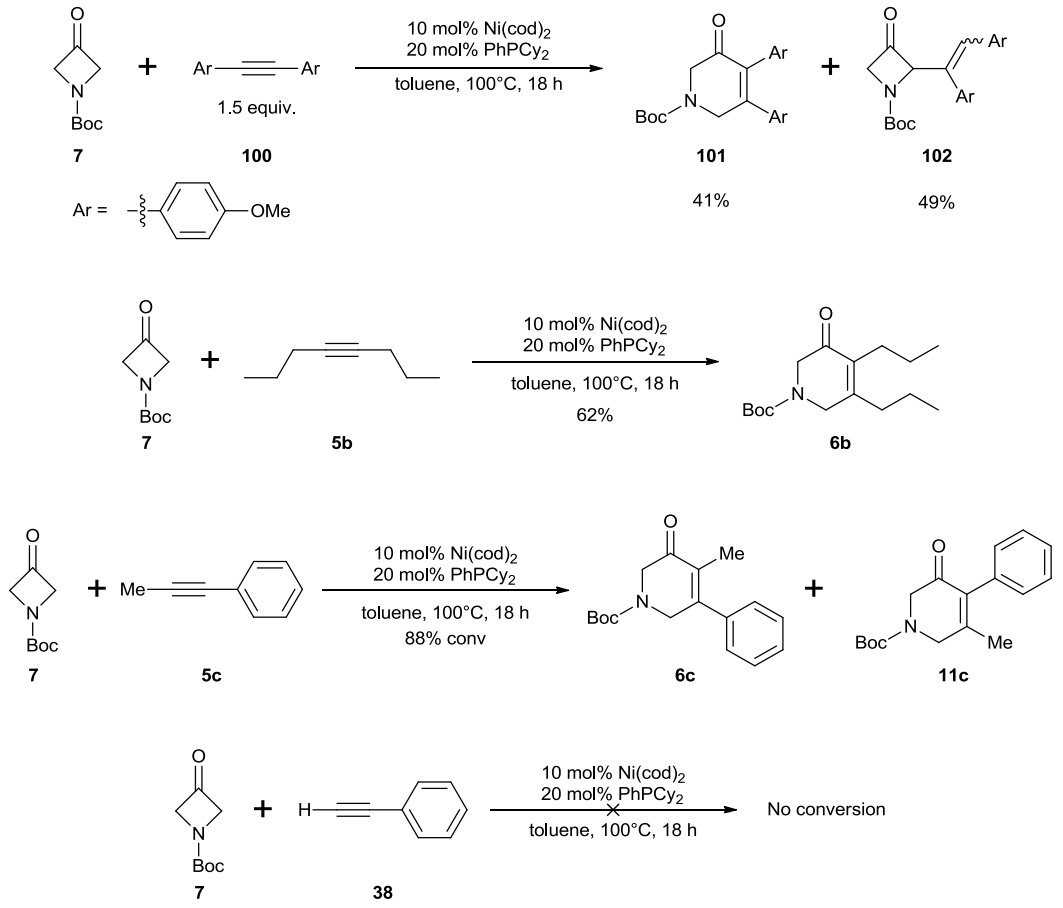


**Scheme 38** Nickel catalysed reaction of azetidinone **7** and alkyne **5**

### 2.3.8 Initial attempts of formal [4+2] cycloaddition of azetidinone with alkenes

Jamison and co-workers reported a nickel catalysed coupling of aldehydes **104** with alkenes **103** (Scheme 39).[18] After a screen of different ligands, $PPhCy_2$ was found to give a good selectivity for allylic product **105** over homoallylic product **106**.

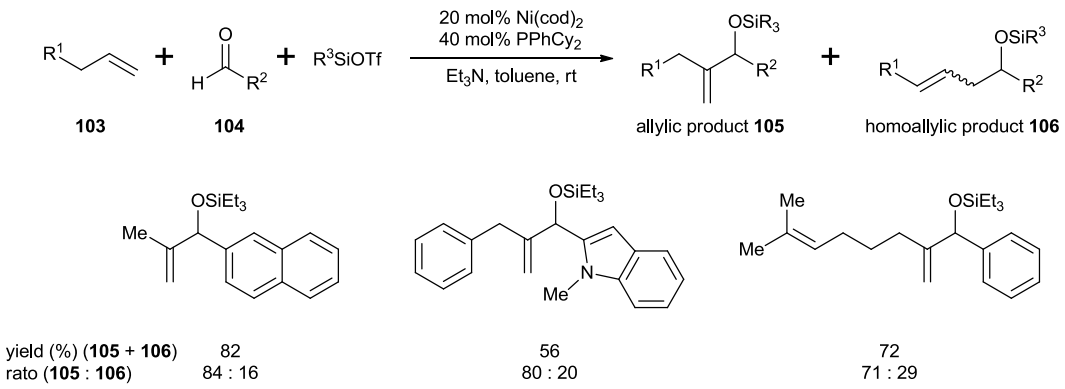


**Scheme 39** Nickel catalysed coupling of aldehydes with alkenes

It was then decided to see if the insertion of alkenes into *N*Boc-azetidinone **7** was possible with the optimised reaction condition used for the synthesis of four-membered ring **8** (Scheme 40). However, no reactivity took place with ethylacrylate **107**. Also, no reactivity took place with alkenes **108** and **109**, even when the temperature of the reaction was increased to 120°C.

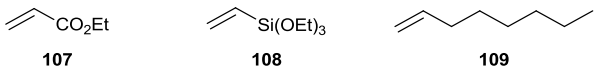


**107** **108** **109**

**Scheme 40** Alkenes screened

## 2.4 Future development of air-stable Ni(II) pre-catalyst

### 2.4.1 Introduction and initial optimisation

$Ni(cod)_2$ is an air sensitive complex which is required to be stored cold under an inert atmosphere and is handled inside a glovebox. However, there are many commercially available nickel-catalysts which can be conveniently stored outside of the glovebox. There are reports of commercially air-stable Ni(II) pre-catalysts that can be reduced by a reducing agent *in situ* to become the active Ni(0).[19] We then became interested to see if we can find a commercially available and air stable Ni(II) pre-catalyst that can do the [4+2] cycloaddition of azetidinone with alkyne. This would primarily allow the reaction to be setup and be carried on

the benchtop which would circumvent the need for a glovebox. Secondly, this method could potentially improve the scope of the methodology.

The commercially available and air stable $Ni(PCy_3)_2Cl_2$ was chosen as it exhibits better air stability than $Ni(PPh_3)_2Cl_2$. Zinc was chosen as the reducing agent as it can be stored outside the glovebox. It was found that no activation was necessary and the zinc can be used directly out of a bottle which has been exposed to air and moisture. The initial optimisation with $Ni(PCy_3)_2Cl_2$ began with 50 mg of azetidinone **7** and 1.1 equivalents of alkyne **5b** at 60°C. It was found that the conversion was low when the reaction was carried out in toluene (Table 22, Entry 1). However, THF or *i*PrOH (Table 22, Entry 2 and 3) gave full conversion in both cases and a 72% isolated yield of pyridinone **6b** was obtained with *i*PrOH. Interestingly, formation of the desired $Ni(PPh_3)_2Cl_2$ can be achieved by mixing $NiCl_2 \bullet 6H_2O$ and $PPh_3$ together in a suitable solvent. Unfortunately, THF and EtOH proved to be poor solvents (Table 22, Entry 4 and 5). On the other hand, *i*PrOH allowed at least a reasonable conversion to **6b** (Table 22, Entry 6). Furthermore, the last 3 entries suggest that the excess water from the $NiCl_2 \bullet 6H_2O$ is potentially detrimental to the reaction. As a result, the initial formation of $Ni(PCy_3)_2Cl_2$ from $NiCl_2 \bullet 6H_2O$ might require better examination.

**Table 22** Optimisation with **5b**

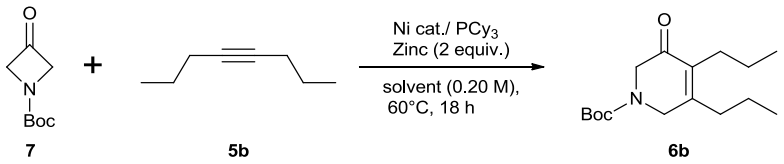


| Entry | Ni cat. (10 mol%) | $PCy_3$ (mol%) | Solvent | Conv. | Isolated yield of **6b** (%) |
|---|---|---|---|---|---|
| 1 | $Ni(PCy_3)_2Cl_2$ | 0 | Toluene | trace | |
| 2 | $Ni(PCy_3)_2Cl_2$ | 0 | THF | >95% | |
| 3 | $Ni(PCy_3)_2Cl_2$ | 0 | *i*PrOH | >95% | 72% |
| 4 | $NiCl_2•6H_2O$ | 20 | THF | 6% | |
| 5 | $NiCl_2•6H_2O$ | 20 | EtOH | <5% | |
| 6 | $NiCl_2•6H_2O$ | 20 | *i*PrOH | 77% | |

With these promising results in hand, we became interested to see if the insertion of alkyne **5c** could proceed with good regioselectivity. Therefore, the study with 50 mg of azetidinone **7** and 1.1 equivalents of alkyne **5c** was carried out (Table 23). However, a mixture of $NiCl_2•6H_2O/PCy_3$ was ineffective (Table 23, entry 1). Carrying out the reaction with $Ni(PCy_3)_2Cl_2$ at 80°C was ineffective in either THF or *i*PrOH (Table 23, entry 1 and 2). $Ni(PPh_3)_2Br_2$, is a more air-stable nickel pre-catalyst than $Ni(PPh_3)_2Cl_2$ and can be stored for at least several months outside of the glovebox without loss of activity. $Ni(PPh_3)_2Br_2$ proved to be an effective pre-catalyst and good conversion towards **6c** was observed at 80°C in both THF and *i*PrOH (Table 23, entry 4 and 5). Furthermore, the insertion of **5c** proceeded with good regioselectivity in both solvents. On reducing the temperature to 60°C and the loading of $Ni(PPh_3)_2Br_2$ to 5 mol%, the reaction proceeded with excellent conversion towards **6c** and the regioselectivity was maintained (Table 23, entry 6 and 7). Carrying out the reaction at 40°C in THF gave poorer conversion (Table 23, entry 8). However in *i*PrOH at 40°C, the regioselectivity remained unchanged and an isolated yield of 84% of **6c** was obtained (Table 23, entry 9). Furthermore,

the reaction can be carried out successfully on a 500 mg scale and **7** was isolated in a 83% yield (Table 23, entry 10).

**Table 23** Optimisation with **5c**

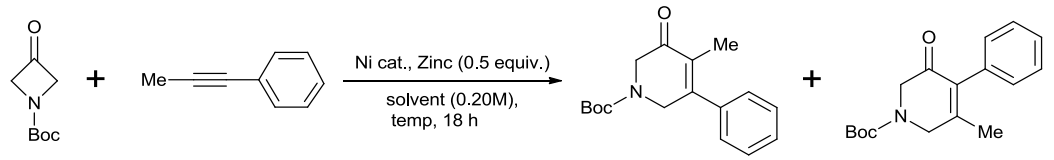


**7** **5c** **6c** **11c**

| Entry | Ni. cat. | mol % | Solvent | Temp. (°C) | Conv. | Ratio of **6c**/**11c** | **6c** (%)[a] |
|---|---|---|---|---|---|---|---|
| 1[b] | $NiCl_2$•$6H_2O$ | 10 | *i*PrOH | 60 | trace | n/a | |
| 2 | $Ni(PCy_3)_2Cl_2$ | 10 | THF | 80 | <5% | n/a | |
| 3 | $Ni(PCy_3)_2Cl_2$ | 10 | *i*PrOH | 80 | 20% | n/a | |
| 4 | $Ni(PPh_3)_2Br_2$ | 10 | THF | 80 | 85% | 88 : 12 | |
| 5 | $Ni(PPh_3)_2Br_2$ | 10 | *i*PrOH | 80 | 82% | 86 : 14 | |
| 6 | $Ni(PPh_3)_2Br_2$ | 5 | THF | 60 | 92% | 90 : 10 | |
| 7 | $Ni(PPh_3)_2Br_2$ | 5 | *i*PrOH | 60 | >95% | 89 : 11 | |
| 8 | $Ni(PPh_3)_2Br_2$ | 5 | THF | 40 | 60% | 91 : 9 | |
| 9 | $Ni(PPh_3)_2Br_2$ | 5 | *i*PrOH | 40 | >95% | 89 : 11 | 84 |
| 10[c] | $Ni(PPh_3)_2Br_2$ | 5 | *i*PrOH | 40 | >95% | 90 : 10 | 83 |

[a] Isolated yield, [b] 20 mol% $PCy_3$ also used to form the catalyst, [c] carried out on a 500 mg scale

### 2.4.2 1,3-Enyne as alkyne surrogate to improve regioselectivity

#### 2.4.2.1 Regioselectivity issues with alkyne 5k

Matsubara and co-workers reported a nickel-catalysed reaction involving the insertion of alkyne **5k** into **110** which proceeded with a better regioselectivity when compared to the insertion of alkyne **5k** into azetidinone **7** with our original optimised reaction conditions (Scheme 41).[20]

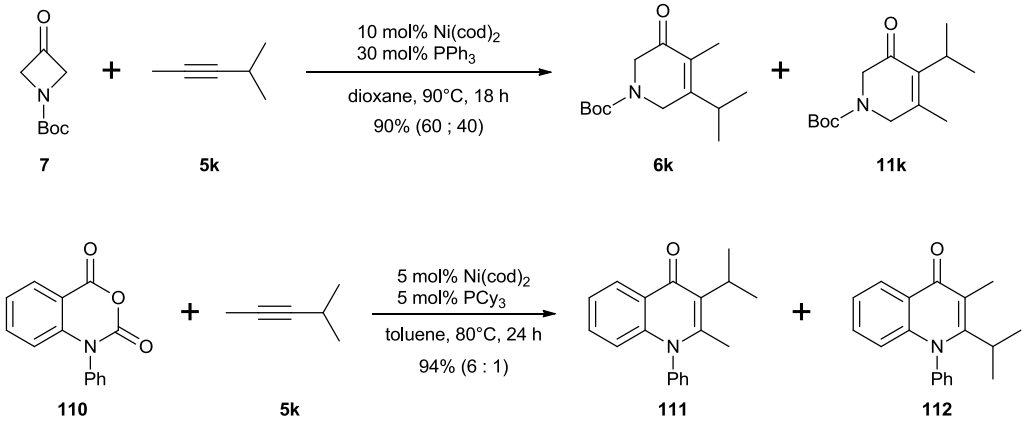


**Scheme 41** Nickel-catalysed insertion of alkyne **5k**

Therefore, a screen was carried out to determine if the regioselectivity of the insertion of alkyne **5k** into azetidinone **7** could be improved (Table 24). From entry 2 onwards, the work was carried out by Daniel J. Tetlow and Jet-Sing Lee. On changing the ligand from $PPh_3$ (Table 24, Entry 1) to $PCy_3$ (Table 24, Entry 2), the regioselectivity switched but the selectivity remained poor. Any changes to the alkyne equivalents, solvent or temperature did little to influence the regioselectivity (Table 24, Entry 3-6). Using $P(OMe)_3$ as the ligand reversed the regioselectivity towards **6k** with a better selectivity towards **6k** than $PPh_3$ but suffers from a poorer conversion (Table 24, Entry 7 vs 1). However, triphenyl phosphite (Table 24, Entry 8) had no reactivity. Afterwards, several other ligands were screened and a trend was noticed.

With the exception of L1 (Table 24, Entry 9) which proceeded with full conversion and with one of the highest regioselectivities, large phosphines tend to erode the regioselectivity and can actually cause the regioselectivity to reverse (Table 24, Entry 10 – 15).

**Table 24** Insertion of alkyne **5k** into azetidinone **7**

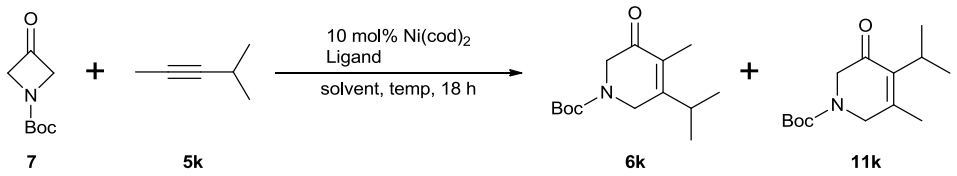


**7** **5k** **6k** **11k**

| Entry | Alkyne equiv. | Ligand (mol %) | Solvent | Temp ($^{o}$C) | Ratio | Conv. (%) |
|---|---|---|---|---|---|---|
| 1 | 1.1 | $PPh_3$ (30) | Dioxane | 90 | 60 : 40 | 100 |
| 2 | 1.1 | $PCy_3$ (30) | Dioxane | 90 | 45 : 55 | 100 |
| 3 | 1.5 | $PCy_3$ (30) | Dioxane | 90 | 43 : 57 | 99 |
| 4 | 1.5 | $PCy_3$ (30) | Toluene | 90 | 43 : 57 | 92 |
| 5 | 1.1 | $PCy_3$ (30) | Dioxane | 70 | 44 : 56 | 100 |
| 6 | 1.1 | $PCy_3$ (30) | Dioxane | 40 | 44 : 56 | 100 |
| 7 | 1.1 | $P(OMe)_3$ (30) | Dioxane | 60 | 69 : 31 | 45 |
| 8 | 1.1 | $P(OPh)_3$ (30) | Dioxane | 60 | - | 0 |
| 9 | 1.1 | L1 (30) | Dioxane | 40 | 67 : 33 | 100 |
| 10 | 1.1 | L2 (30) | Dioxane | 40 | 63 : 37 | 85 |
| 11 | 1.1 | L3 (30) | Dioxane | 40 | 62 : 38 | 100 |
| 12 | 11 | $PPh_3$ (30) | Dioxane | 40 | 58 :42 | 100 |
| 13 | 1.1 | L4 (30) | Dioxane | 40 | 55 : 45 | 100 |
| 14 | 1.1 | L5 (30) | Dioxane | 40 | 53 : 47 | 100 |
| 15 | 1.1 | $PCy_3$ (30) | Dioxane | 40 | 44 : 56 | 100 |

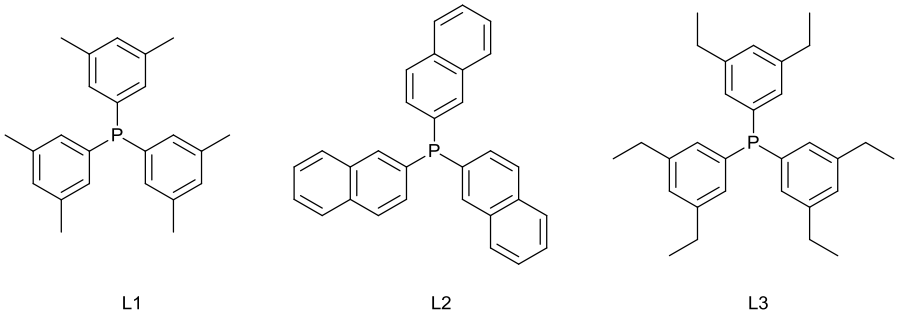

L1 L2 L3

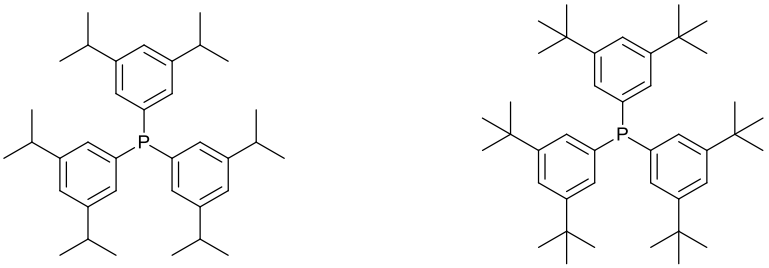

L4 L5

### 2.4.2.2 1,3-Enyne as alkyne surrogate

In 2008, Fagnou and co-workers reported a rhodium-catalysed indole synthesis (Scheme 42).[21] However, it was found that there is little regiocontrol in the coupling of acetanilide **113** with asymmetrical alkyne **114** to afford unsymmetrical 2,3-aliphatic-substituted indole **115** and **116**.

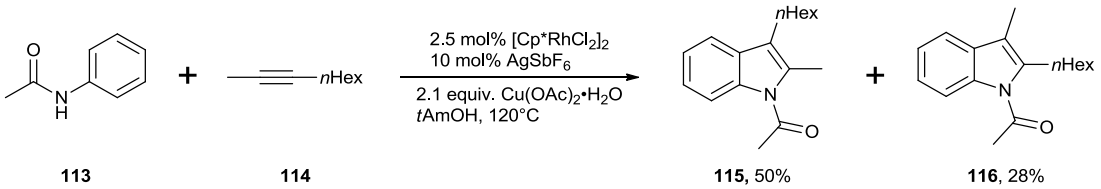


**113** **114** **115,** 50% **116**, 28%

**Scheme 42** Rhodium-catalysed indole synthesis.

In order to circumvent this problem, Fagnou and co-workers reported a highly regioselective coupling of alkyne **118** with acetanilide **117** by a rhodium-catalyst (Scheme 43).[22] The highly regioselective coupling of alkyne **118** is attributed to the vinyl moiety acting as a directing

group. Afterwards, the vinyl moiety can then be converted by hydrogenation (Scheme 44). As a result, good regiocontrol in the synthesis of various unsymmetrical 2,3-aliphatic-substituted indoles **120** is achieved.

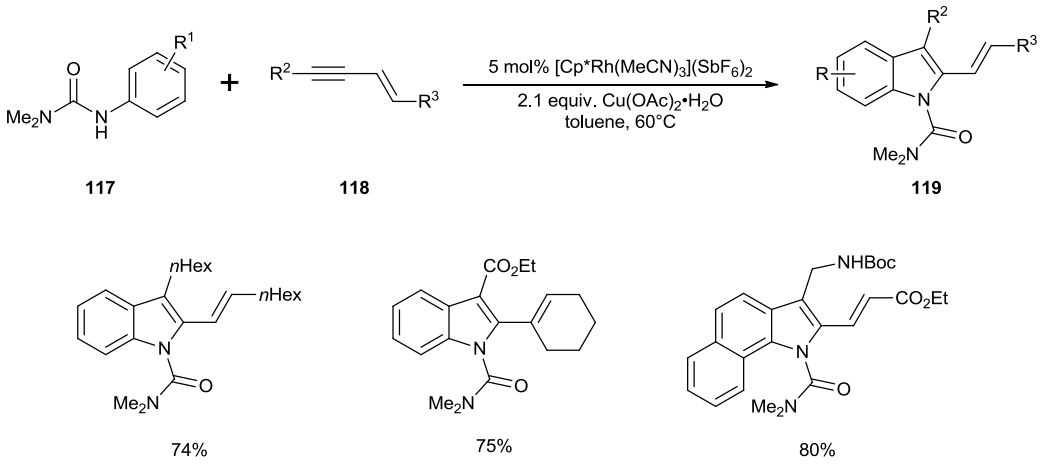


**Scheme 43** Rhodium-catalysed indole synthesis.

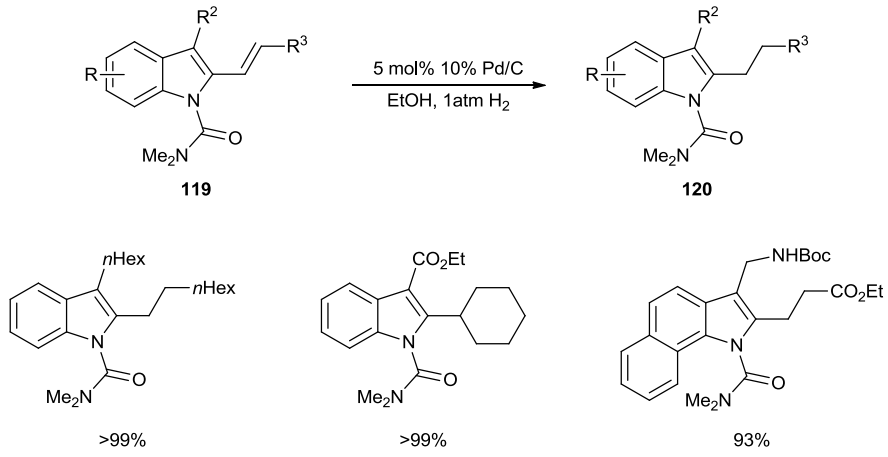


**Scheme 44** Hydrogenation

Therefore, we became interested to see if enyne **5m** can circumvent the low regiocontrol problem observed with non-symmetrical alkyl alkynes. Also, it was of interest if an air-stable nickel pre-catalyst can be used to effect the insertion of alkyne **5m** into azetidinone **69** on a 50 mg scale of **69** (Table 25). It was found that 10 mol% of the catalyst and 50 mol% of Zinc at

60°C gave full conversion with a combined isolated yield of 75% and a regioselectivity of 88:12 (Table 25, entry 1). However, reduction of the loading of Ni/Zn reduced the conversion (Table 25, entry 2 and 3). Reducing the Ni/Zn ratio also reduced the conversion which is not too surprising, as the reaction is a suspension (Table 25, entry 4 and 5). When the temperature was increased to 80°C, full conversion was observed but the isolated yield was rather low (Table 25, entry 6). A brief screen of alternative solvents revealed that THF and 2-MeTHF gave slightly better regioselectivities but the difference is not significant (Table 25, entry 7-12). Furthermore, the reaction can be carried out in THF at 40°C but with poorer conversion (Table 25, entry 13). Using a solvent mixture of *i*PrOH/THF (1:1) at 60°C did not allow the reaction to go to complete conversion but a good regioselectivity was obtained (Table 25, entry 14). When the reaction carried out on a 150 mg scale of **69**, the loading of Ni/Zn can be reduced to 1:2 but the regioselectivity decreased (Table 25, entry 15). This result was then reproduced (Table 25, entry 16).

**Table 25** Optimisation with **5m**

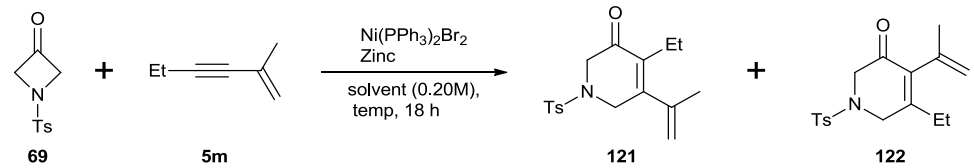


**69** **5m** **121** **122**

| Entry | Ni. (mol %) | Zinc (mol %) | Solvent | Temp. (°C) | Conv. | Yield [a] | Ratio (**121**/**122**) |
|---|---|---|---|---|---|---|---|
| 1 | 10 | 50 | *i*PrOH | 60 | >95% | 75% | 88 : 12 |
| 2 | 5 | 25 | *i*PrOH | 60 | 88% | 53% | 88 : 12 |
| 3 | 3 | 15 | *i*PrOH | 60 | 34% | 21% | 87 : 13 |
| 4 | 5 | 20 | *i*PrOH | 60 | 86% | 50% | 88 : 12 |
| 5 | 5 | 10 | *i*PrOH | 60 | 45% | 30% | 86 : 14 |
| 6 | 5 | 20 | *i*PrOH | 80 | >95% | 61% | 88 : 12 |
| 7 | 5 | 20 | MeCN | 60 | 50% | 21% | 88 : 12 |
| 8 | 5 | 20 | THF | 60 | >95% | 74% | 89 : 11 |
| 9 | 5 | 20 | Acetone | 60 | 44% | 33% | 88 : 12 |
| 10 | 5 | 20 | Toluene | 60 | 0% | n/a | n/a |
| 11 | 5 | 20 | 1,2-DCE | 60 | <10% | n/a | n/a |
| 12 | 5 | 20 | 2-MeTHF | 60 | 56% | 39% | 90 : 10 |
| 13 | 5 | 20 | THF | 40 | 55% | 41% | 91 : 9 |
| 14 | 5 | 20 | iPrOH/THF[b] | 60 | 80% | 61% | 92:8 |
| 15[c] | 5 | 10 | THF | 60 | >95% | 79% | 83:17 |
| 16[c] | 5 | 10 | THF | 60 | >95% | 83% | 77:23 |

[a] Combined isolated yield of **121** and **122**. [b] 1:1 solvent ratio. [c] On 150 mg scale of **69**

Furthermore, the *in situ* formation of $Ni(PPh_3)_2Br_2$ can be achieved by the direct mixing of $NiBr_2 \bullet xH_2O$ and $PPh_3$. The insertion of alkyne **5m** into azetidinone **69** on a 200 mg scale of **69**

was found to proceed to give **121** in 69% yield and **122** on 13% yield (Scheme 45). The experiment was setup without the requirement of a glovebox. Also, this result will allow the screening of ligands to be carried out with ease.

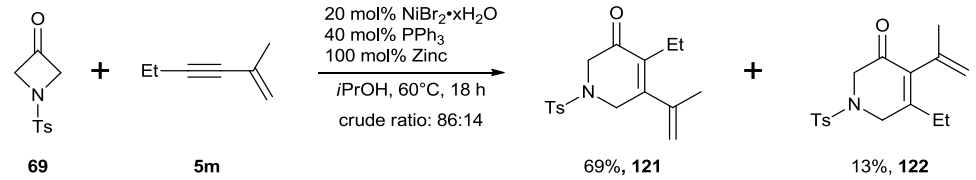


**Scheme 45** The *in situ* formation of $Ni(PPh_3)_2Br_2$

Akin to the work by Fagnou, hydrogenation of pyridinone **121** formed **123** (Scheme 46). The product of the hydrogenation was shown to be pure as judged by $^1H$ NMR and used directly in the next reaction. Prolonged hydrogenation led to a variety of unidentified side products. After the filtration to remove the palladium catalyst, **123** was aromatised with potassium *tert*butoxide to give pyridinol **124** in a 43% yield over two steps. Therefore, the aromatisation step requires some more optimisation.

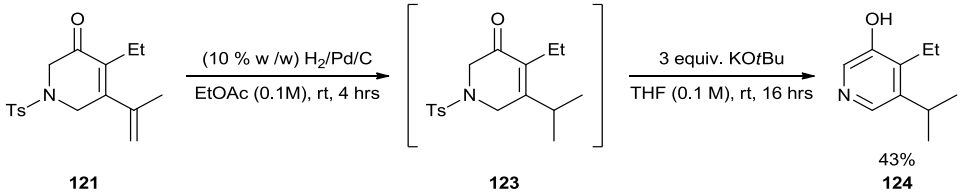


**Scheme 46** Hydrogenation, deprotection and aromatisation

Therefore, some optimisation of the aromatisation was carried out on model substrate **70b** (Table 26). Organic bases $Et_3N$ and imidazole were ineffective regardless of temperature (Table 26, entry 1-4). The aromatisation with 3 equiv. KO*t*Bu in THF without an aqueous workup furnished the desired product in a 58% but the yield could be higher as the column leaked (Table 26, entry 5). Increasing the equivalents of KO*t*Bu to 5 increased the isolated yield to 92% (Table 26, entry 6). However, with 3 equiv. KO*t*Bu in THF that involves initial purification

by standard aqueous workup with a saturated solution of brine resulted in an isolated yield of 42% (Table 26, entry 7). Using a saturated solution of $NH_4Cl$ instead resulted in an isolated yield of 63% (Table 26, entry 8).

**Table 26** Model substrate for aromatisation

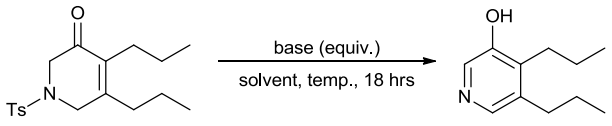


**70b** **125**

| Entry | Base (equiv.) | Solvent | Temp (°C) | Workup | Isolated yield (%) |
|---|---|---|---|---|---|
| 1 | $Et_3N$ (3) | DCM | rt | None | 0 |
| 2 | $Et_3N$ (3) | DCM | 40 | None | 0 |
| 3 | Imidazole (3) | DCM | rt | None | 0 |
| 4 | Imidazole (3) | DCM | 40 | None | 0 |
| 5 | KO*t*Bu (3) | THF | rt | None | 58[a] |
| 6 | KO*t*Bu (5) | THF | rt | None | 92 |
| 7 | KO*t*Bu (3) | THF | rt | Brine | 42 |
| 8 | KO*t*Bu (3) | THF | rt | $NH_4Cl$ | 63 |

[a] column leaked

This initial work with the air-stable nickel pre-catalyst demonstrates the reaction can now be set up outside of the glovebox on the benchtop. However, much work remains to optimise the conditions. On the other hand, it is clear that the ligand on the nickel can have a significant influence on the success on the reaction. Furthermore, the regioselectivity of the insertion of non-symmetrical alkynes are in in line with those observed when the mixture of air sensitive $Ni(cod)_2/PPh_3$ was used.

## 2.5 Conclusion

The [4+2] cycloaddition of four-membered ring heterocycles with alkynes has been successfully developed. This rapid build-up of six-membered heterocycles offers an alternative approach to previous approaches.[23] Initially, the choice of ligand and solvent were critical to minimise the formation of the four-membered ring. Upon re-examination, the four-membered ring is found to be both substrate specific and temperature dependent. Furthermore, the reaction towards six-membered ring **127** proceeded smoothly with various azetidinones and oxetanones (Scheme 47). Furthermore, α-substitution on the small heterocycle is tolerated providing the substituent is not too large. The insertion of various alkynes proceeded with good regioselectivity. Moreover, the insertion of silylated alkynes proceeded successfully.

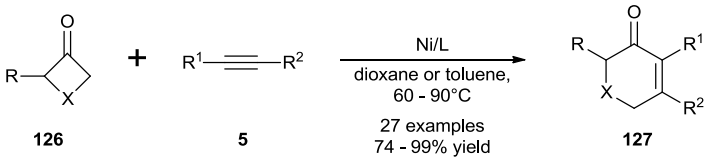


**Scheme 47** Summary of the [4+2] cycloaddition

The development of setting up the reaction without the need for a glovebox with an air-stable Ni(II) pre-catalyst is of interest. Furthermore, seeking to improve upon the original scope will be of interest. To determine if the regioselectivity of the alkyne insertion can be improved or even reversed will be of synthetic importance.

As alluded to, since the publication of some of the work which has been presented in this thesis,[24] the groups of Murakami[16] and Louie[12] have published similar results which indicate that small heterocycles are indeed competent partners in C–C activation reactions.

## 2.6 Synthesis of Precursors

### 2.6.1 Synthesis of 3-azetidinones

The synthesis of azetidinone **69** was easily achieved in a two-step procedure from 3-hydroxyazetidine hydrochloride **S1** (Scheme 48). Compound **S2** was obtained by mono-protection with 1 equivalent of tosyl chloride in methanol and three equivalents of triethylamine following a modification to the original reaction procedure.[25] Afterwards, carrying out a standard Swern oxidation[26] afforded azetidinone **69** in 69% yield.

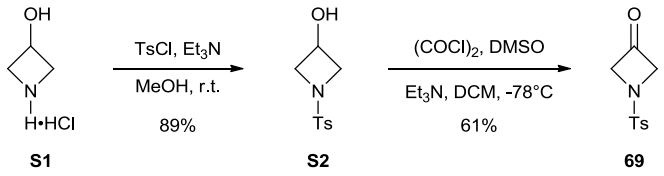


**Scheme 48** Synthesis of azetidinone **69**

The synthesis of azetidinone **72**, **79** and **83** began with the corresponding commercially available amino acid **S3**, **S5** and **S8** (Scheme 50 - 49). The protection with tosyl chloride of **S5** to give **S6** was carried out in a 54% yield. Carboxylic acids **S3**, **S6**, **S8 w**ere first transformed to the corresponding acyl chloride. All volatiles were removed on the high vacuum line to minimise the inclusion of water. Afterwards, trimethylsilyldiazomethane was added to form diazo **S4**, **S7** and **S9** which could be purified by flash column chromatography or used directly in the next step. Then the copper catalysed N–H insertion formed azetidinone **72** in 84% yield from **S4**, **79** in 48% yield from **S7** and **83** in 38% yield over 3 steps from **S8**.

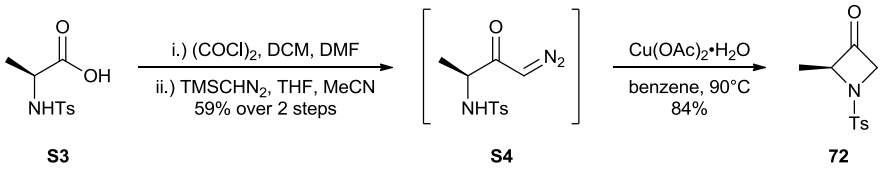


**Scheme 49** Synthesis of α-aryl azetidinone

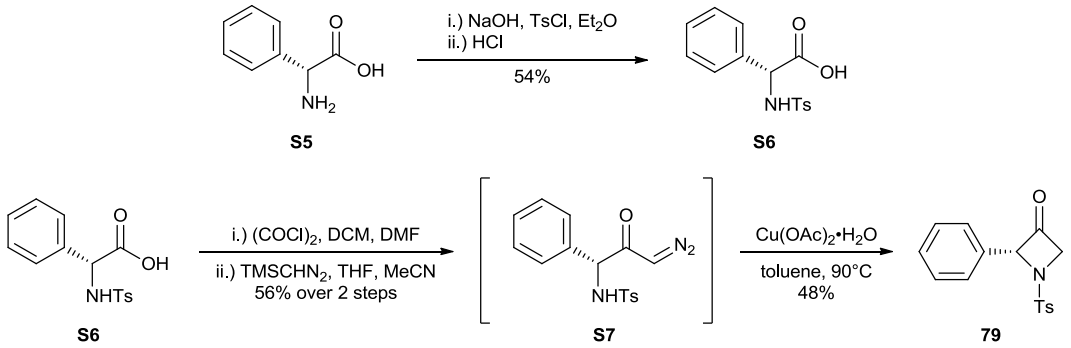


**Scheme 50** Synthesis of α-aryl azetidinone

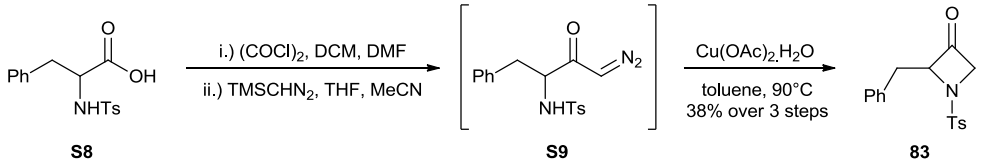


**Scheme 51** Synthesis of α-substituted azetidinone

## 2.6.2 Synthesis of 3-oxetanones

The gold catalyst **S11** was generated by a salt metathesis of the commercially available phosphine gold chloride **S9** with silver bis(trifluoromethanesulfonyl)imide in DCM at rt. The silver chloride was separated by filtration and the catalyst was of good quality as judged by $^{31}P$ NMR. **S14** was made by Dr Christophe Aissa and is not described in this thesis. Afterwards, the synthesis of α-substituted oxetanone **90** was carried out by following the procedure described by Zhang and co-workers (Scheme 53).[27] The synthesis began with the in situ formation of the lithium acetylide. Aldehyde **S12** was then added to form propagryl alcohol **S13** which was then isolated after workup. Afterwards, the TMS group was cleaved by TBAF to give the terminal alkyne **S14**. Finally, the gold-catalysed synthesis was carried out to give **90** in a 51% yield.

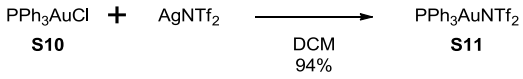


**Scheme 52** Synthesis of gold complex

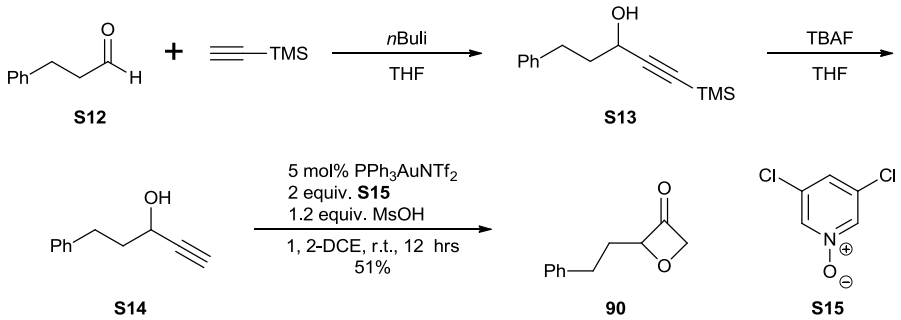


**Scheme 53** Synthesis of α-substituted oxetanone

### 2.6.3 Synthesis of alkynes

The synthesis of alkynes **5e**, **5g-j**, **63** and **100** were achieved by a Sonogashira reaction (Table 27).[24] In each case, the palladium-catalysed coupling of an aryl halide with a terminal alkyne in THF proceeded in good to high yields.

**Table 27** Sonogashira reaction

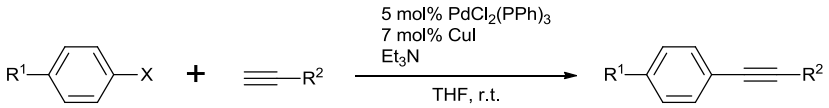


| Entry | $R^1$ | X | $R^2$ | Alkyne | Yield |
|---|---|---|---|---|---|
| 1 | MeO | I | *n*Bu | 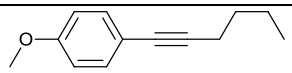 **5e** | Quant |
| 2[a] | $CH_3C(O)$ | Br | *n*Bu | 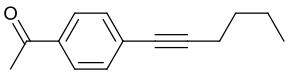 **5g** | 89% |
| 3 | MeO | I | Cy | 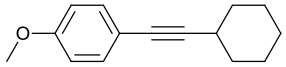 **5h** | 81% |
| 4 | MeO | I | *i*Bu | 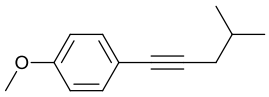 **5i** | Quant |
| 5 | MeO | I | *p*$CF_3$Ph | 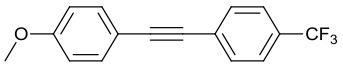 **5j** | Quant |
| 6 | H | I | -$CH_2CH_2$Br | 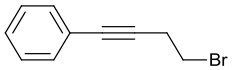 **63** | 86% |
| 7 | MeO | I | *p*MeOPh | 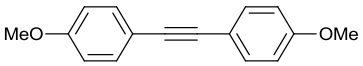 **100** | 70% |

[a] 3 mol% $Pd(PPh_3)_4$ and 3mol% CuI were used

With 2-iodopyridine, the Sonogashira reaction was slightly more difficult (Table 28). Regardless, the desired product was still isolated in moderate to good yields.

**Table 28** Sonohashira reaction with 2-iodopyridine

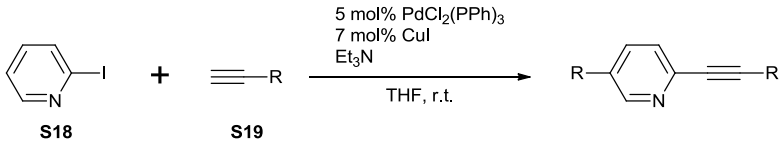


| Entry | R | Alkyne | Result |
|---|---|---|---|
| 1 | Ph | 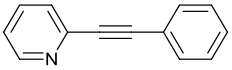 **43** | 73% |
| 2 | *n*Butyl | 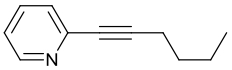 **44** | 58% |

The syntheses of propargylic alkynes **56 – 58** and **5v** were carried out in one step from commercially available starting materials (Scheme 54). Alkyne **57** and **5v** were synthesised by benzylation with benzyl bromide **S23** as the electrophile. Alkyne **56** was synthesised by acetylation with acetyl chloride **S21** as the electrophile. Alkyne **58** was synthesised by silylation with *tert*-butyldimethylsilyl chloride **S22** as the electrophile.

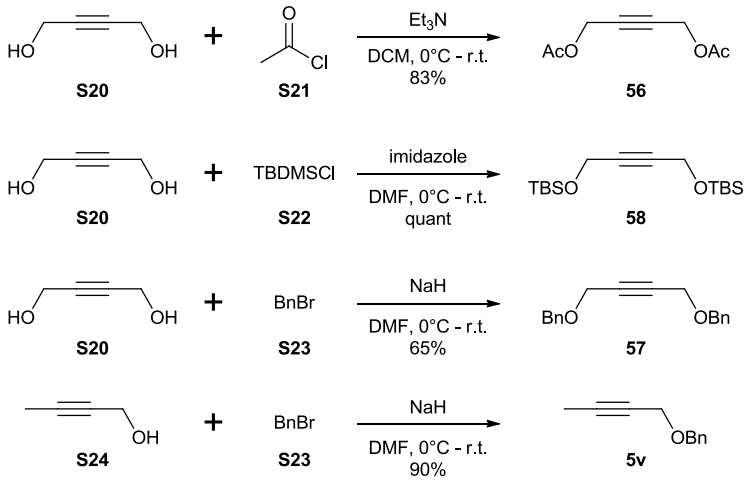


**Scheme 54** Synthesis of propargylic alkynes

The synthesis of alkyne **5d** began with a modified Ohira-Bestmann using trimethylsilyldiazomethane on aldehyde **S25** to form terminal alkyne **S26** and was isolated in a 91% yield (Scheme 55). Afterwards, deprotection of alkyne **S26** with *n*BuLi and subsequent trapping with iodomethane afforded desired alkyne **5d** in 90% yield. The synthesis of alkyne **5n** was a Sonogashira reaction between **S26** and 2-bromopropene **S27** to form **5n** in 86% yield.

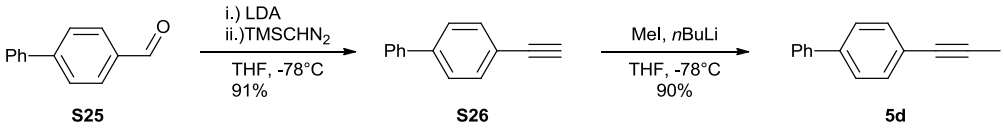


**S25** **S26** **5d**

**Scheme 55** Synthesis of alkyne **5d**

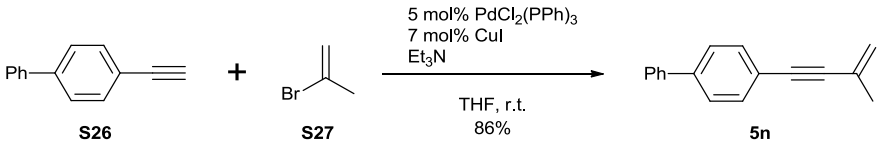


**S26** **S27** **5n**

**Scheme 56** Synthesis of alkyne 5n

The syntheses of alkyne **5f**, **5p**-**r**, **5y**, **61** and **62** were carried out in one step from commercially available alkynes (Table 29). In all cases, treatment of alkyne **S28** with *n*BuLi as the base formed the anion. The anion was then trapped with an electrophile to furnish the desired alkyne. For the synthesis of alkyne **61**, an additive was required (Table 28, entry 6).

**Table 29** Synthesis of alkyne

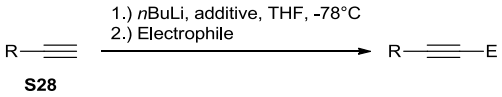


| Entry | **S28** | Electrophile | Additive | Product | Yield (%) |
|---|---|---|---|---|---|
| 1 | 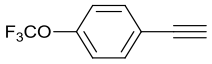 | MeI | n/a | 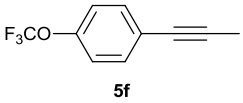 **5f** | 44 |
| 2 | 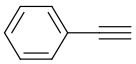 | $SiMe_2PhCl$ | n/a | 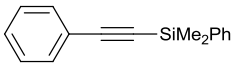 **5p** | Quant. |
| 3 |  | TMSCl | n/a |  **5q** | 96 |
| 4 | 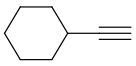 | TMSCl | n/a | 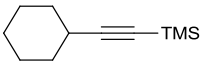 **5r** | 91 |
| 5 | 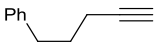 | MeI | n/a | 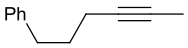 **5y** | 93 |
| 6 |  | $nC_8H_{17}Br$ | HMPA | 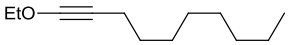 **61** | 65 |
| 7 | 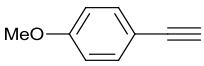 | NCS | n/a | 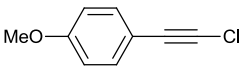 **62** | 76 |

The synthesis of alkyne **5w** and **5z** began from the corresponding commercially available alkyne **S29** and **S31** (Scheme 57). The benzylation of alkyne **S29** with benzyl bromide as the electrophile gave terminal alkyne **S30** whereby the silyl group was cleaved. Afterwards, the silyl group was reintroduced by trapping the terminal alkyne anion with trimethylsilyl chloride to form alkyne **5w**.[28] On the hand, the benzylation of alkyne **S31** with benzyl bromide as the electrophile gave terminal alkyne **S32**. The anion of **S32** was generated by treatment with *n*Buli. Subsequent trapping of the terminal alkyne anion with methyl iodide gave alkyne **5z** in 87% yield.

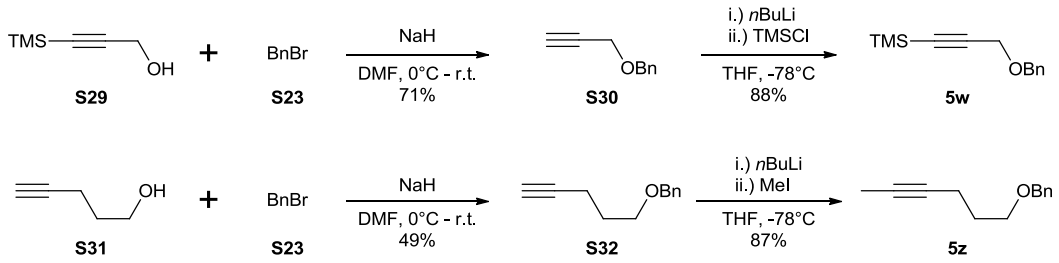


**Scheme 57** Synthesis of alkyne **5w** and **5z**

The synthesis of ynamide **59** and **60** started with the silver-catalysed bromination of phenylacetylene **38** (Scheme 58). The bromide **S33** was then used directly in the next step without purification by flask column chromatography. Then a copper-catalysed coupling was carried out to form the ynamide. Both ynamides were synthesised by the following the procedure by Liu.[29]

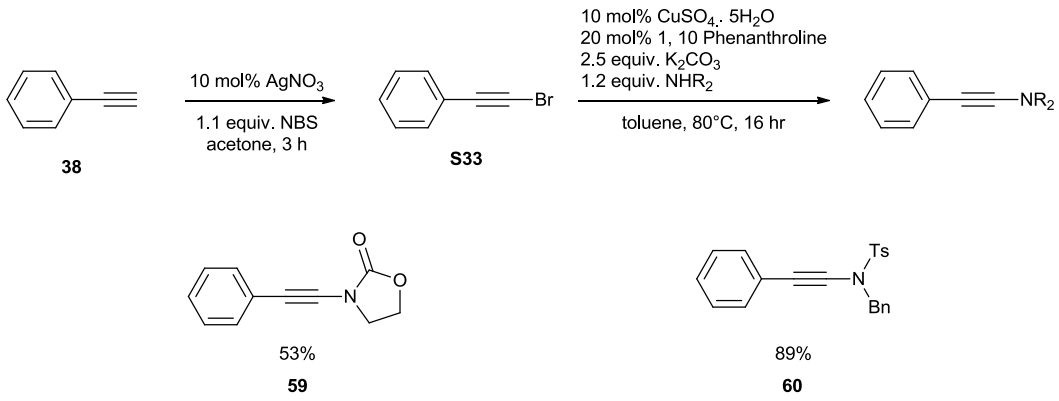


**Scheme 58** Synthesis of ynamides **59** and **60**

## 2.7 Experimental Section

**General**. Otherwise noted, all reactions were carried out in flame-dried glassware under dry nitrogen atmosphere. The solvents were purified with the solvent purification system Pure Solv MD-6 (THF, $Et_2O$, $CH_2Cl_2$, benzene, toluene, hexane). Dry dioxane was purchased from Aldrich. All commercially available compounds were used as received. Flash chromatography: Merck silica gel 60 (230-400 mesh) with petroleum ether (PE, 40–60°C) and EtOAc or Et2O analytical grade. NMR: spectra were recorded on a Bruker DRX 500, Bruker DPX 400, and Bruker AVANCE 400 spectrometers in CDCl3; chemical shifts (δ) are given in ppm relative to TMS. The solvent signals were used as references and the chemical shifts converted to the TMS scale ($CDCl_3$: $\delta_C$ = 77.0 ppm; residual $CHCl_3$ in $CDCl_3$: $\delta_H$ = 7.24 ppm). IR: PerkinElmer Spectrum 100 FT-IR spectrometer, wavenumbers ($\tilde{\nu}$) in $cm^{-1}$. HRMS at the University of Liverpool: VG7070E (CI), micromass LCT mass spectrometer (ES+). Melting points: Griffin melting point apparatus (not corrected). Elemental analyses: University of Liverpool. Optical rotations were measured on a PerkinElmer 343plus polarimeter.

### 2.7.1 Synthesis of 3-azetidinones

**Compound 69**

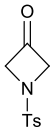


A round-bottom flask was charged with 3-hydroxyazetidine hydrochloride (1000 mg, 9.13 mmol) and suspended in MeOH (9 ml). Triethylamine (1.9 ml, 13.69 mmol) was added dropwise at 0°C and after the addition, the clear solution was allowed to stir at rt for 20 mins. Afterwards, tosyl chloride (1740 mg, 9.13 mmol) and triethylamine (1.9 ml, 13.69 mmol) were

added and allowed to stir at rt overnight. Afterwards, all volatiles were removed and then partitioned between EtOAc and $H_2O$. Extraction from the aqueous layer was carried out three times with EtOAc. The organic layer was then washed with $H_2O$, a saturated solution of brine, dried over $Na_2SO_4$, filtered and concentrated. Purification by flash column chromatography (PE/EtOAc, 1/1→1/2) gave **S2** (1.86g, 89%) as a white solid. Under $N_2$, DMSO (1.5 mL, 21.2 mmol) in $CH_2Cl_2$ (5 mL) was added to a solution of oxalyl chloride (911 µL, 10.6 mmol) in $CH_2Cl_2$ (25 mL) at –78°C. After 10 minutes of stirring at –78°C, a solution of **S2** (1.86g, 8.16 mmol) in $CH_2Cl_2$ (10 mL) was added. After 20 minutes of stirring at –78°C, triethylamine (5.7 mL, 40.8 mmol) was added rapidly and the mixture was stirred at room temperature during 10 minutes. A saturated solution of $NH_4Cl$ was added to the reaction mixture which was then extracted three times with EtOAc. The organic layer was washed with $H_2O$, a saturated solution of brine, dried over $Na_2SO_4$, filtered and concentrated. Purification by flash column chromatography (PE/EtOAc, 3/1→2/1) gave **69** as a white solid (1.12 g, 61%). This compound is known.[30] $^1$H NMR (500 MHz, $CDCl_3$): $\delta$ = 7.78 (d, *J* = 8.2 Hz, 2H), 7.38 (d, *J* = 8.0 Hz, 2H), 4.61 (s, *4*H), 2.45 (s, 3H).

**Compound 72**

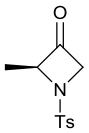


Under $N_2$, a flame-dried Schlenk flask was charged with *N*-Ts-(L)-Alanine **S3** (300 mg, 1.23 mmol), dry DMF (50 µL) and dry DCM (2.4 ml). At 0 °C, $(COCl)_2$ (0.12 ml, 1.36 mmol) was then added drop wise. After stirring at room temperature for 1 hour, all volatiles were removed under high vacuum and THF (3 ml) was then added to the pale yellow oil. Then at 0°C, 2.0 M $TMSCHN_2$ in $Et_2O$ (0.74 ml, 1.48 mmol) was added. After stirring at room temperature for 2 hours, all volatiles were then removed by evaporation and the residue was purified by flash column chromatography (PE/EtOAc, 4/1→2/1) to give **S4** (195 mg, 59 %) as a pale yellow solid.

This compound was diluted in benzene (14 ml), and $Cu(OAc)_2 \bullet H_2O$ (14mg, 0.07 mmol) was added under $N_2$ to this refluxing solution. Immediate evolution of $N_2$ was observed. Completion was reached within 10 minutes stirring at reflux. After evaporation, purification by flash column chromatography (PE/EtOAc, 4/1→2.5/ 1) gave **69** as a white solid (143 mg, 84 %). Enantiomeric excess > 99%.^ m.p. 75–77 °C [lit.: 78–79 °C];[31] $[\alpha]_D^{20}$ = 76.9 (c = 1 in $CHCl_3$) [lit.: 80 (c = 1 in $CHCl_3$)];[31] $^1$H NMR (500 MHz, $CDCl_3$): $\delta$ = 7.75 (d, *J* = 8.3 Hz, 2H), 7.36 (d, *J* = 8.2 Hz, 2H), 4.73 (qd, *J* = 7.1 Hz, 1.2 Hz, 1H), 4.50– 4.41 (m, 2H), 2.43 (s, 3H), 1.42 (d, *J* = 7.0 Hz, 3H); $^{13}$C NMR (125 MHz, $CDCl_3$): $\delta$ = 196.7, 145.0, 131.5, 130.0 (2C), 128.4 (2C), 80.9, 69.5, 21.6, 15.7; IR (neat): $\tilde{\nu}$ = 2978 (w), 2930 (w), 1867 (w), 1825 (s), 1597 (w), 1493 (w), 1444 (w), 1419 (w), 1338 (s), 1323 (m), 1299 (m), 1251 (w), 1238 (w), 1182 (w), 1156 (s), 1132 (s), 1101 (s), 1085 (s), 1051 (s), 1013 (s), 973 (s), 848 (w), 822 (m), 812 (s), 803 (m), 778 (m), 731 (s), 708 (m), 668 (s) $cm^{-1}$; MS (CI): *m/z* (rel. intensity): 257 (100) $[M+NH_4]+$, 240 (7) $[M+H]^+$

^ Determined by chiral HPLC, Chiralpak AD - H Column, *i*PrOH:hexane = 8/92, 1 mL/min, 230 nm on a Agilent technologies 1200 apparatus

**Compound 79**

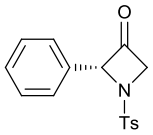


A flask was charged with (*R*)-(-)-2-phenylglycine (1000 mg, 6.62 mmol) and 2M NaOH (8.25 ml). Then TsCl (1.5g, 7.94 mmol) in $Et_2O$ (6.6 ml) was added dropwise. The suspension was then left to stir at rt overnight. Afterwards, conc HCl was added until a pH of 2 was reached. $Et_2O$ was added. The precipitate was then collected by filtration and washed with $Et_2O$ to give **S6** as a white solid (1.1g, 54%). Under $N_2$, a flame-dried Schlenk flask was charged with **S6** (300 mg, 0.98 mmol), dry DMF (2 drops) and dry DCM (2 ml). At 0 °C, $(COCl)_2$ (93 µl, 1.08 mmol) was then added drop wise. After stirring at room temperature for 1 hour, all volatiles were removed under high vacuum and THF (1 ml) was then added to the pale yellow oil. Then at

0°C, 2.0 M $TMSCHN_2$ in $Et_2O$ (1 ml, 2 mmol) was added. After stirring at room temperature for 2 hours, all volatiles were then removed by evaporation and the residue was purified by flash column chromatography (PE/EtOAc, 4/1→2/1) to give **S6** (177 mg, 56 %) as a pale yellow solid. This compound was diluted in toluene (11 ml), and $Cu(OAc)_2 \bullet H_2O$ (11mg, 0.05 mmol) was added under $N_2$ to this refluxing solution. Immediate evolution of $N_2$ was observed. Completion was reached within 10 minutes stirring at reflux. After evaporation, purification by flash column chromatography (PE/EtOAc, 4/1→2.5/ 1) gave **79** as a white solid (77 mg, 48 %). This compound is known.[32]; $^1$H NMR (500 MHz, $CDCl_3$): $\delta$ = 7.80 – 7.75 (m, 2H), 7.39 – 7.28 (m, 7H), 5.73 (d, *J* = 3.9 Hz, 1H), 4.76 (d, *J* = 16.2 Hz, 1H), 4.61 (dd, *J* = 16.2, 4.0 Hz, 1H), 2.44 (s, 3H)

**Compound 83**

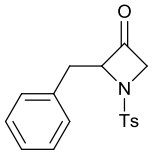


This compound was prepared from *N*-Ts-(DL)-phenylalanine **S8** (500 mg, 1.57 mmol) according to the procedure described for the preparation of **69**. This compound is known.[33] White solid (173 mg, 35%); $^1$H NMR (500 MHz, $CDCl_3$): $\delta$ = 7.73 (d, *J* = 8.2 Hz, 2H), 7.36 (d, *J* = 8.1 Hz, 2H), 7.30 – 7.25 (m, 2H), 7.23 – 7.18 (m, 3H), 4.97 – 4.92 (m, 1H), 4.39 (d, *J* = 16.1 Hz, 1H), 4.15 (d, *J* = 16.1, 4.0 Hz, 1H), 3.15 (dd, *J* = 14.6, 6.9 Hz, 1H), 3.09 (dd, *J* = 14.4, 4.3 Hz, 1H), 2.44 (s, 3H)

### 2.7.2 Synthesis of 3-oxetanones and precursor

**Compound S11**

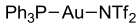

Under $N_2$, DCM (1 ml) was added to silver bis(trifluoromethanesulfonyl)imide (50 mg, 0.1 mmol) and **S9** (39 mg, 0.1 mmol). After 1 hour of stirring at rt, the precipitate was removed by filtration through a celite plug. The plug was washed with DCM. Afterwards, all volatiles were removed to give a **S11** as a white solid (71 mg, 94%). This compound has been described.[34]; $^1$H NMR (500 MHz, $CDCl_3$): $\delta$ = 7.60 – 7.42 (m, 15H); $^{31}$P NMR (202 MHz, $CDCl_3$): $\delta$ = 30.5

**Compound 90**

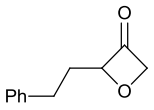


Compound **90** was obtained according to a modified procedure described by Zhang.[27] Under $N_2$, **S15** (307mg, 1.87 mmol) and then MsOH (73µl, 1.12 mmol) were added to a solution of **S14** (150mg, 0.94 ml) in 1,2-DCE (4 ml). Then **S11** (35mg, 0.05 mmol) in 1,2-DCE (4ml) was added. Left to stir at rt overnight. A saturated solution of $NaHCO_3$ was added and extracted three times with DCM. Extracts dried over $Na_2SO_4$, filtered and concentrated. Purification by flash column chromatography (PE/EtOAc, 19/1→9/ 1) gave **90** as a colourless oil (83 mg, 51%). $^1$H NMR (500 MHz, $CDCl_3$): $\delta$ = 7.31 – 7.25 (m, 2H), 7.22 – 7.15 (m, 3H), 5.47 – 5.41 (m, 1H), 5.29 (d, *J* = 14.9 Hz, 1H), 5.24 (dd, *J* = 15.0, 4.2 Hz, 1H), 2.84 – 2.71 (m, 2H), 2.22 – 2.05 (m, 2H).

### 2.7.3 Synthesis of alkynes

**Compound S26**

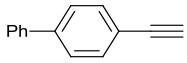


Under $N_2$, a flame-dried RB flask was charged with DIPA (0.5 ml, 3.56 mmol) and THF (10 ml). At 0°C, 2.5M of *n*BuLi in hexanes (1.3 ml, 3.29 mmol) was added. After 10 mins at 0°C, the vessel was cooled to -78°C and 2M of $TMSCHN_2$ in $Et_2O$ (1.65 ml, 3.29 mmol) was added. It was then allowed to stir at -78°C for 30 mins. Afterwards, biphenyl-4-carboxaldehyde (500 mg, 2.74 mmol) in THF (5 ml) was cannulated into the flask. Afterwards, the ice-bath was removed and allowed to warm to rt. After 1h, the reaction was complete and a saturated solution of $NH_4Cl$ was added. Then $Et_2O$ was added and the organic layer was washed with water and a saturated solution of brine. Dried over $Na_2SO_4$, filtered and concentrated. Purification by flash column chromatography (PE/EtOAc, 1/0→60/ 1) gave **S26** as a white solid (452 mg, 91%). This compound has been described.[x] $^1$H NMR (500 MHz, $CDCl_3$): 7.59 – 7.52 (m, 6H), 7.46 – 7.40 (m, 2H), 7.37 – 7.32 (m, 1H), 3.11 (s, 1H).

**Compound 5d**

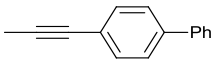


At -20°C, 2.5M of *n*BuLi was added to a solution of **S26** (200 mg, 1.12 mmol) in THF (8 ml). After 40 mins of stirring at -20°C, iodomethane (154 µl, 2.47 mmol) was added. The solution was allowed to stir overnight whilst allowing it to warm to rt. Afterwards, the reaction was quenched with a saturated solution of $NH_4Cl$. $Et_2O$ was added and the organic layer was washed with water and a saturated solution of brine. Dried over $Na_2SO_4$, filtered and concentrated. Purification by flash column chromatography (PE/EtOAc, 60/ 1) gave **5d** as a white solid (194 mg, 90%). This is a known compound. [35]; $^1$H NMR (500 MHz, $CDCl_3$): $\delta$ = 7.57

(d, *J* = 7.8 Hz, 2H), 7.51 (d, *J* = 8.2 Hz, 2H), 7.47 – 7.40 (m, 4H), 7.36 – 7.30 (m, 1H), 2.07 (s, 3H); $^{13}$C NMR (125 MHz, $CDCl_3$): $\delta$ = 140.4, 140.2, 131.9, 128.8, 127.4, 127.0, 126.9, 122.9, 86.5, 79.6, 4.4

**Compound 5e**

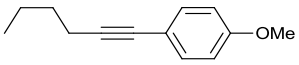


Under $N_2$, a flame-dried round-bottom flask was charged sequentially with $PdCl_2$ (91 mg, 0.5 mmol), $PPh_3$ (224 mg, 0.9 mmol), CuI (130 mg, 0.7 mmol) and MeCN (32 ml). The mixture was stirred at rt for 5 mins to give a dark brown solution. 4-Iodoanisole (4 g, 17.1 mmol), 1-hexyne (2.9 ml, 25.6 mmol) and $Et_3N$ (7.2 mL, 51.3 mmol) were then added. The solution was allowed to stir at rt overnight. The crude mixture was then partitioned between water and $Et_2O$ at room temperature. The organic layer washed with a saturated aqueous solution of $NH_4Cl$, dried over $Na_2SO_4$, filtered and concentrated. Purification by flash chromatography (PE) afforded alkyne **5e** as an orange oil (3.2 g, quantitative). This is a known compound.[36]; $^1$H NMR (500 MHz, $CDCl_3$): $\delta$ = 7.35 – 7.28 (m, 2H), 6.83 – 6.76 (m, 2H), 3.77 (s, 3H), 2.37 (t, *J* = 7.0 Hz, 2H), 1.61 – 1.51 (m, 2H), 1.51 – 1.40 (m, 2H), 0.93 (t, *J* = 7.3 Hz, 3H).

**Compound 5f**

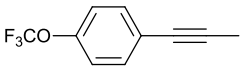


This compound was prepared from 4-(trifluoromethoxy)phenylacetylene **S7** (300 µl, 1.96 mmol) according to the procedure described for the preparation of **5d**. Colourless Oil (251 mg, 64%).; $^1$H NMR (500 MHz, $CDCl_3$): $\delta$ = 7.40 – 7.35 (m, 2H), 7.13 – 7.08 (m, 2H), 2.03 (s, 3H); $^{13}$C NMR (125 MHz, $CDCl_3$): $\delta$ = 148.3 (q, *J* = 1.7 Hz), 132.9, 122.8, 120.8, 120.4 (q, *J* = 257.6 Hz), 86.8, 78.4, 4.3; IR (neat): $\tilde{\nu}$ = 2958 (w), 2922 (w), 2860 (w), 1604 (w), 1507 (m), 1468 (w), 1379

(w), 1251 (s), 1220 (s), 1201 (s), 1161 (s), 1100 (w), 1019 (w), 971 (w), 922 (w), 887 (w), 851 (m), 831 (w), 808 (w), 734 (w), 670 (w), 662 (w) $cm^{-1}$

**Compound 5g**

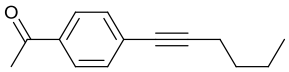

Under $N_2$, a flame-dried Schlenk flask was charged with $Pd(PPh_3)_4$ (697 mg, 0.60 mmol), CuI (115 mg, 0.60 mmol) and *para*bromoacetophenone (4 g, 20.1 mmol). THF (84 ml), $Et_3N$ (32 ml) and 1-Hexyne (3.4 ml, 30.1 mmol) were then added in that order. After stirring at 60°C for 18 hours, the crude mixture was partitioned between water and $Et_2O$ at room temperature. The organic layer washed with a saturated aqueous solution of $NH_4Cl$, dried over $Na_2SO_4$, filtered and concentrated. Purification by flash chromatography (PE → PE/Et2O: 10/1) afforded alkyne **5g** as a pale yellow oil (3.68g, 89%). $^1H$ NMR (500 MHz, $CDCl_3$): $\delta$ = 7.82 (d, *J* = 8.9 Hz, 2H), 7.41 (d, *J* = 7.5 Hz, 2H), 2.53 (s, 3H), 2.39 (t, *J* = 7.0 Hz, 2H), 1.55 (quint, 7.5 Hz, 2H), 1.49–1.39 (m, 2H), 0.91 (t, *J* = 7.3 Hz, 3H); $^{13}C$ NMR (125 MHz, $CDCl_3$): $\delta$ = 197.2, 135.5, 131.5 (2C), 129.1, 128.0 (2C), 94.3, 80.0, 30.5, 26.4, 21.9, 19.1, 13.5; IR (neat): $\tilde{\nu}$ = 2958 (w), 2933 (w), 2873 (w), 2229 (w), 1682 (s), 1601 (s), 1555 (w), 1466 (w), 1428 (w), 1403 (m), 1357 (m), 1329 (w), 1284 (m), 1259 (s), 1178 (m), 1109 (w), 1075 (w), 1015 (w), 956 (m), 838 (s), 738 (w) $cm^{-1}$; MS (CI): *m/z* (rel. intensity): 218 (44) $[M+NH_4]^+$, 201 (100) $[M+H]^+$; elemental analysis (%) calcd for $C_{14}H_{16}O$: C 83.96, H 8.05; found: C 82.89, H 8.26.

**Compound 5h**

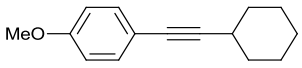

Under $N_2$, a flame-dried Schlenk flask was charged sequentially with $Pd(PPh_3)_2Cl_2$ (37 mg, 0.05 mmol), THF (4 ml), $Et_3N$ (450 µL, 3.2 mmol), CuI (14 mg, 0.07 mmol) and 4-iodoanisole (250 mg, 1.07 mmol). After stirring for 5 minutes, cyclohexylacetylene (181 µL, 1.39 mmol) was

added. After stirring at room temperature for 18 hours, the crude mixture was partitioned between water and $Et_2O$ at room temperature. The organic layer washed with a saturated aqueous solution of $NH_4Cl$, dried over $Na_2SO_4$, filtered and concentrated. Purification by flash chromatography (PE/Et2O: 200/1) afforded alkyne **5h** as an orange oil (188 mg, 81%). This is a known compound.[37] $^1$H NMR (500 MHz, $CDCl_3$): $\delta$ = 7.34 – 7.29 (m, 2H), 6.81 – 6.76 (m, 2H), 3.77 (s, 3H), 2.59 – 2.49 (m, 1H), 1.91 – 1.81 (m, 2H), 1.79 – 1.68 (m, 2H), 1.57 – 1.45 (m, 3H), 1.38 – 1.26 (m, 3H)

**Compound 5i**

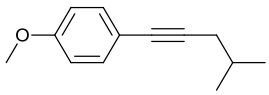

This compound was prepared from 4-iodoanisole (250 mg, 1.07 mmol) and 4-methyl-1-pentyne (163 µL, 1.39 mmol) according to the procedure described for the preparation of **5h**. Orange oil (204 mg, quantitative). $^1$H NMR (500 MHz, $CDCl_3$): $\delta$ = 7.32 (d, *J* = 8.9 Hz, 2H), 6.79 (d, *J* = 9.0 Hz, 2H), 3.77 (s, 3H), 2.26 (d, *J* = 6.5 Hz, 2H), 1.93–1.80 (m, 1H), 1.02 (d, *J* = 6.7 Hz, 6H); $^{13}$C NMR (125 MHz, $CDCl_3$): $\delta$ = 158.9, 132.8 (2C), 116.3, 113.8 (2C), 87.7, 81.1, 55.2, 28.6, 28.3, 22.0; IR (neat): $\tilde{\nu}$ = 2957 (m), 2932 (w), 2905 (w), 2870 (w), 2836 (w), 1607 (m), 1568 (w), 1507 (s), 1464 (m), 1442 (m), 1385 (w), 1368 (w), 1344 (w), 1282 (m), 1245 (s), 1172 (m), 1105 (w), 1035 (m), 830 (s), 800 (w), 665 (w) $cm^{-1}$; elemental analysis (%) calcd for $C_{13}H_{16}O$: C 82.94, H 8.57; found: C 82.17, H 9.01.

**Compound 5j**

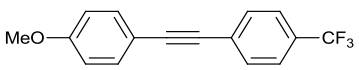


This compound was prepared from commercially available 4-ethynyl-α,α,α-trifluorotoluene (227 µl, 1.37 mmol) and 4-iodoanisole (250 mg, 1.07 mmol) according to the procedure described for the preparation of **5h**. Yellow solid (300 mg, quant). This is a known compound.

[38]; $^1$H NMR (500 MHz, $CDCl_3$): $\delta$ = 7.61 – 7.55 (m, 4H), 7.47 (d, *J* = 8.8 Hz, 2H), 6.88 (d, *J* = 8.8 Hz, 2H), 3.82 (s, 3H).

**Compound 5n**

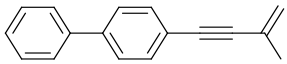

This compound was prepared from commercially available 4-ethynylbiphenyl (150 mg, 0.84 mmol) and 2-bromopropene (112 µL, 1.26 mmol) according to the procedure described for the preparation of **5h**. White Solid (160 mg, 86%). m.p. 70–72°C; $^1$H NMR (500 MHz, $CDCl_3$): $\delta$ = 7.59 (d, *J* = 7.4 Hz, 2H), 7.55 (d, *J* = 8.2 Hz, 2H), 7.51 (d, *J* = 8.2 Hz, 2H), 7.44 (t, *J* = 7.6 Hz, 2H), 7.35 (t, *J* = 7.3 Hz, 1H), 5.42 (s, 1H), 5.31 (s, 1H), 2.01 (s, 3H); $^{13}$C NMR (125 MHz, $CDCl_3$): $\delta$ = 140.8, 140.3, 132.0 (2C), 128.8 (2C), 127.6, 127.0 (2C), 126.93 (2C), 126.86, 122.2, 122.0, 91.2, 88.3, 23.5; IR (neat): $\tilde{\nu}$ = 3056 (w), 3033 (w), 2975 (w), 2920 (w), 2855 (w), 2199 (m), 1671 (m), 1612 (w), 1599 (m), 1581 (w), 1521 (w), 1486 (m), 1448 (m), 1405 (w), 1373 (w), 1316 (m), 1286 (w), 1155 (w), 1113 (m), 1076 (w), 1039 (w), 1006 (m), 976 (w), 893 (m), 840 (s), 761 (s), 721 (m), 692 (s) cm$^{-1}$; elemental analysis (%) calcd for $C_{17}H_{14}$: C 93.54, H 6.46; found: C 92.14, H 6.68.

**Compound 5p**

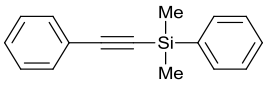


This compound was prepared from Phenylacetylene **38** (300 µl, 2.7 mmol) and chloro(dimethyl)phenylsilane (688 µl, 4.1 mmol) according to the procedure described for the preparation of **5d**. Colourless Oil (660 mg, quantitative).; $^1$H NMR (500 MHz, $CDCl_3$): $\delta$ = 7.71 – 7.65 (m, 2H), 7.51 – 7.47 (m, 2H), 7.40 – 7.36 (m, 3H), 7.33- 7.28 (m, 3H), 0.48 (s, 6H); $^{13}$C NMR (125 MHz, $CDCl_3$): $\delta$ = 137.0, 133.7, 132.1, 129.4, 128.7, 128.2, 127.9, 122.9, 106.8, 92.0, -0.8; IR (neat): $\tilde{\nu}$ = 3068 (w), 3020 (w), 2960 (w), 2158 (m), 1952 (w), 1883 (w), 1817 (w), 1593 (w),

1574 (w), 1488 (m), 1443 (w), 1428 (m), 1407 (w), 1302 (w), 1249 (m), 1219 (w), 1189 (w), 1157 (w), 1118 (m), 1069 (w), 1027 (w), 999 (w), 844 (s), 779 (s), 729 (s), 689 (s), 663 (m) $cm^{-1}$; HRMS (CI): calcd for $(C_{16}H_{16}Si + NH_4)^+$: 254.1360; found: 254.1358

**Compound 5q**




This compound was prepared from 1-decyne (500 µl, 2.77 mmol) and chlorotrimethylsilane (527 µl, 4.16 mmol) according to the procedure described for the preparation of **5d** except at -78°C. This is a known compound.[39] Colourless oil (558 mg, 96%).; $^1$H NMR (500 MHz, $CDCl_3$): $\delta$ = 2.19 (t, *J* = 2.19 Hz, 2H), 1.53 – 1.45 (m, 2H), 1.39 – 1.31 (m, 2H), 1.31 – 1.20 (m, 8H), 0.86 (t, *J* = 6.9 Hz, 3H), 0.12 (s, 9H)

**Compound 5r**


This compound was prepared from cyclohexylacetylene (400 µl, 3.06 mmol) and chlorotrimethylsilane (583 µl, 4.59 mmol) according to the procedure described for the preparation of **5d** except at -78°C. This compound is known. [40] Colourless Oil (505 mg, 91%).; $^1$H NMR (500 MHz, $CDCl_3$): $\delta$ = 2.41 – 2.30 (m, 1H), 1.82 – 1.72 (m, 2H), 1.72 – 1.63 (m, 2H), 1.52 – 1.35 (m, 3H), 1.33 – 1.19 (m, 3H), 0.12 (s, 9H); HRMS (CI): calcd for $(C_{11}H_{20}Si + NH_4)^+$: 198.1673; found: 198.1675

**Compound 5v**

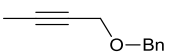


A flamed dried schlenk was charged with 60% NaH (177mg, 4.4 mmol) and DMF (4 ml). At 0°C, 2-butyn-1-ol (300 µl, 4 mmol) was added dropwise. It was then allowed to stir at 0°C for 30

mins. Then, benzyl bromide (525 µl, 4.4 mmol) was added dropwise. Allowed to stir overnight at rt. Quenched with solution of aqueous $NH_4Cl$ and $Et_2O$ was added. Washed three timed with water, a saturated solution of brine, dried over $Na_2SO_4$, filtered and concentrated. Purification by flash chromatography (PE/EtOAc: 1/0→75/1) afforded alkyne **5v** as a colourless oil (579 mg, 90%). This a known compound.[41]; $^1$H NMR (500 MHz, $CDCl_3$): $\delta$ = 7.38 – 7.25 (m, 5H), 4.57 (s, 2H), 4.12 (q, *J* = 2.3 Hz, 2H), 1.86 (t, *J* = 2.2 Hz, 3H)

**Compound 5w**

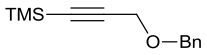


A flamed dried schlenk was charged with 60% NaH (297 mg, 7.42 mmol) and DMF (6.1 ml). At 0°C, 3-(trimethylsilyl)propargyl alcohol (1 ml, 6.77 mmol) was added dropwise. It was then allowed to stir at 0°C for 30 mins. Then, benzyl bromide (900 µl, 7.42 mmol) was added dropwise. Allowed to stir for 2 hours at rt. Quenched with solution of aqueous $NH_4Cl$ and $Et_2O$ was added. Washed three timed with water, a saturated solution of brine, dried over $Na_2SO_4$, filtered and concentrated. Purification by flash chromatography (PE/$Et_2O$: 40/1→33/1) afforded alkyne **S30** as a colourless oil (701 mg, 71%). At -78°C, 1.7M of *n*BuLi (2.4 ml, 4.10 mmol) was added to a solution of **S30** (500 mg, 3.42 mmol) in THF (3.4 ml). After 15 mins of stirring at -78°C, trimethylsilylchloride (651 µl, 5.13 mmol) was added. The solution was allowed to stir for 15 mins at -78°C. Then the ice-bath was removed and allowed to stir at rt for 30 mins. Afterwards, the reaction was quenched with a saturated solution of $NH_4Cl$. $Et_2O$ was added and the organic layer was washed with water and a saturated solution of brine. Dried over $Na_2SO_4$, filtered and concentrated. Purification by flash column chromatography (PE/$Et_2O$, 66/1→50/1) gave **5w** as a colourless oil (653 mg, 88%).; $^1$H NMR (500 MHz, $CDCl_3$): $\delta$ = 7.37 – 7.25 (m, 5H), 4.58 (s, 2H), 4.15 (s,2H), 0.18 (s, 9H); $^{13}$C NMR (125 MHz, $CDCl_3$): $\delta$ = 137.4, 128.4, 128.2, 127.9, 101.4, 91.6, 71.5, 57.9, -0.2; IR (neat): $\tilde{\nu}$ = 3066 (w), 3031 (w), 2960

(w), 2898 (w), 2174 (w), 1455 (w), 1350 (w), 1250 (m), 1088 (m), 1076 (m), 1028 (w), 994 (m), 841 (s), 760 (m), 737 (m), 697 (m) $cm^{-1}$

**Compound 5x**

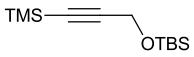


A flame-dried schlenk was charged with TBSCl (244mg, 1.6 mmol) and imidazole (202mg, 3.0 mmol). Then dissolved in DMF (0.85 ml) and 3-(trimethylsilyl)propargyl alcohol (200µl, 1.3 mmol) was added. Allowed to stir at rt overnight. Afterwards, $Et_2O$ was added. Washed three timed with water, a saturated solution of brine, dried over $Na_2SO_4$, filtered and concentrated. Purification by flash chromatography (PE/$Et_2O$: 1/0→100/1) afforded **5x** as a colourless oil (191 mg, 58%).; $^1$H NMR (500 MHz, $CDCl_3$): $\delta$ = 4.29 (s, 2H), 0.89(s, 9H), 0.14 (s, 9H), 0.10 (s, 6H); $^{13}$C NMR (125 MHz, $CDCl_3$): $\delta$ = 104.5, 89.6, 52.3, 25.8, 18.3, -0.3, -5.1; IR (neat): $\tilde{\nu}$ = 2957 (w), 2929 (w), 2899 (w), 2332 (w), 2178 (w), 1472 (w), 1463 (w), 1408 (w), 1390 (w), 1362 (w), 1251 (m), 1092 (m), 1003 (m), 939 (w), 831 (s), 776 (m), 759 (m), 722 (w), 699 (w), 668 (w) $cm^{-1}$; HRMS (CI): calcd for $(C_{12}H_{26}OSi_2 + NH_4)^+$: 243.1595; found: 243.1602

**Compound 5y**

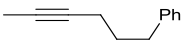


This compound was prepared from 5-phenyl-1-pentyne (200 µl, 1.32 mmol) and iodomethane (123 µl, 1.98 mmol) according to the procedure described for the preparation of **5d** except at -78°C. Colourless oil (195 mg, 93%).; $^1$H NMR (500 MHz, $CDCl_3$): $\delta$ = 7.30 – 7.23 (m, 2H), 7.20 – 7.14 (m, 3H), 2.69 (t, *J* = 7.6 Hz, 2H), 2.17 – 2.09 (m, 2H), 1.82 – 1.74 (m, 5H); $^{13}$C NMR (125 MHz, $CDCl_3$): $\delta$ = 141.8, 128.5, 128.3, 125.8, 78.8, 75.9, 34.8, 30.6, 18.2, 3.5; IR (neat): $\tilde{\nu}$ = 3027 (w), 2919 (m), 2859 (m), 1604 (w), 1497 (m), 1454 (m), 1332 (w), 1080 (w), 1031 (w), 744 (m), 699 (s) $cm^{-1}$

**Compound 5z**

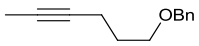


A flamed dried schlenk was charged with 60% NaH (271 mg, 6.77 mmol) and DMF (6.5 ml). At 0°C, 4-pentyn-1-ol (0.6 ml, 6.45 mmol) was added dropwise. It was then allowed to stir at 0°C for 30 mins. Then, benzyl bromide (800 µl, 6.77 mmol) was added dropwise. Allowed to stir for 2 hours at rt. Quenched with solution of aqueous $NH_4Cl$ and $Et_2O$ was added. Washed three timed with water, a saturated solution of brine, dried over $Na_2SO_4$, filtered and concentrated. Purification by flash chromatography (PE/$Et_2O$: 100/1→80/1) afforded alkyne **S32** as a colourless oil (552 mg, 49%). At -78°C, 1.7M of *n*BuLi (0.8 ml, 1.38 mmol) was added to a solution of **S32** (200 mg, 1.15 mmol) in THF (1.2 ml). After 15 mins of stirring at -78°C, iodomethane (107 µl, 1.72 mmol) was added. The solution was allowed to stir for 15 mins at -78°C. Then the ice-bath was removed and allowed to stir at rt for 30 mins. Afterwards, the reaction was quenched with a saturated solution of $NH_4Cl$. $Et_2O$ was added and the aqueous layer was extracted two times with $Et_2O$. The organic layer was washed with water and a saturated solution of brine. Dried over $Na_2SO_4$, filtered and concentrated. Purification by flash column chromatography (PE/$Et_2O$, 50/1) gave **5z** as a colourless oil (187 mg, 87%).; $^1$H NMR (500 MHz, $CDCl_3$): $\delta$ = 7.36 – 7.25 (m, 5H), 4.50 (s, 2H), 3.54 (t, *J* = 6.2 Hz, 2H), 2.28 – 2.20 (m, 2H), 1.81 – 1.72 (m, 5H); IR (neat): $\tilde{\nu}$ = 3064 (w), 3030 (w), 2946 (w), 2919 (w), 2856 (m), 1496 (w), 1454 (m), 1364 (m), 1204 (w), 1102 (s), 1079 (s), 1028 (w), 909 (w), 735 (s), 697 (s) $cm^{-1}$; HRMS (CI): calcd for $(C_{13}H_{16}O + H)^+$: 189.1274; found: 189.1274

**Compound 5aa**

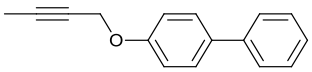


This compound was prepared by Jet-Sing Lee. Under $N_2$, a solution of biphenyl-4-methanol (400 mg, 2.17 mmol) in DMF (5.5 mL) was added NaH (60 wt%, 130 mg, 3.26 mmol) at 0˚C. The

mixture was left to stir at r.t. for 1 hour. To this mixture was then added dropwise 1-bromo-2-butyne (300 µL, 3.26 mmol) at 0˚C. The mixture was left to stir at r.t. overnight. The golden coloured mixture was quenched with a saturated solution of $NH_4Cl$ at 0˚C, diluted with $Et_2O$ and washed with brine. The organic phase was dried over $Na_2SO_4$, filtered and concentrated *in vacuo*. The residue was purified by column chromatography (PE/EtOAc, 50:1) to yield **5aa** as a white solid (452 mg, 89%). $^1$H NMR (500Mz, $CDCl_3$): 7.64-7.59 (m, 4H), 7.50-7.44 (m, 4H), 7.40-7.35 (m, 1H), 4.66 (s, 2H), 4.21-4.18 (d, *J* = 2.3 Hz, 2H), 1.92 (t, *J* = 2.3 Hz, 3H).

**Compound 43**

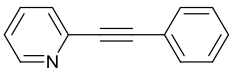

This compound was prepared from commercially available phenylacetylene (153 µl, 1.39 mmol) and 2-iodopyridine (115 µl, 1.07 mmol) according to the procedure described for the preparation of **5h**. White solid (100 mg, 58%). This is a known compound.[42]; $^1$H NMR (500 MHz, $CDCl_3$): $\delta$ = 8.60 (d, *J* = 4.6Hz, 1H), 7.65 (apt dt, *J* = 7.7, 1.3 Hz,1H), 7.61 – 7.55 (m, 2H), 7.50 (d, *J* = 7.8 Hz, 1H), 7.37 – 7.31 (m, 3H), 7.23 – 7.18 (m, 1H)

**Compound 44**

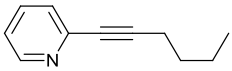

This compound was prepared from commercially available 1-hexyne (160 µl, 1.39 mmol) and 2-iodopyridine (115 µl, 1.07 mmol) according to the procedure described for the preparation of **5h**. Colourless oil (142 mg, 73%).This is a known compound.[43]; $^1$H NMR (500 MHz, $CDCl_3$): $\delta$ = 8.51 (d, *J* = 4.4 Hz, 1H), 7.57 (apt dt, *J* = 7.7, 1. 50 Hz, 1H), 7.34 (d, *J* = 7.9 Hz, 1H), 7.14 (dd, *J* = 7.0, 5.4 Hz, 1H), 2.42 (t, *J* = 7.1 Hz, 2H), 1.59 (pent, *J* = 7.4 Hz, 2H), 1.47 (sext, *J* = 7.3 Hz, 2H), 0.92 (t, *J* = 7.3 Hz, 3H)

**Compound 56**

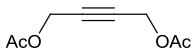


In a flame-dried schlenk, 2-butyne-1,4-diol (200 mg, 2.3 mmol), $Et_3N$ (1 ml, 6.97 mmol) and DCM (4.7 ml) were added. At 0°C, acetyl chloride (0.5 ml, 6.97 mmol) was added dropwise over 5 mins. Then allowed to stir overnight at rt. Afterwards, the reaction was quenched with $H_2O$ and EtOAc was added. The organic layer was washed with a saturated solution of $NaHCO_3$, water and a saturated solution of brine. Dried over $Na_2SO_4$, filtered and concentrated. Purification by flash column chromatography (PE/$Et_2O$, 7/1) gave **56** as a colourless oil (328 mg, 83%). This is a known compound. [44]; $^1$H NMR (500 MHz, $CDCl_3$): $\delta$ = 4.68 (s, 4H), 2.07 (s, 6H)

**Compound 57**

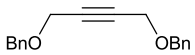


This compound was prepared from commercially available 2-butyne-1,4-diol (200 mg, 2.3 mmol), benzyl bromide (608 µl, 5.1 mmol) and 60% NaH (205 mg, 5.1 mmol) according to the procedure described for the preparation of **5v**. Colourless Oil (401 mg, 65%): $^1$H NMR (500 MHz, $CDCl_3$): $\delta$ = 7.42 – 7.28 (m, 10H), 4.62 (s, 4H), 4.25 (s, 4H); $^{13}$C NMR (125 MHz, $CDCl_3$): $\delta$ = 137.3, 128.4, 128.1, 127.9, 82.5, 71.6, 57.4; IR (neat): $\tilde{\nu}$ = 3064 (w), 3031 (w), 2860 (w), 1717 (w), 1603 (w), 1454 (m), 1349 (m), 1264 (w), 1119 (m), 1069 (s), 1026 (m), 908 (w), 739 (s), 698 (s) cm$^{-1}$; HRMS (CI): calcd for $(C_{18}H_{18}O_2 + NH_4)^+$: 284.1645; found: 284.1643

**Compound 58**

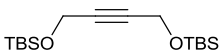


This compound was prepared from commercially available 2-butyne-1,4-diol (200 mg, 2.3 mmol), TBSCl (840 mg, 5.6 mmol) and imidazole (840 mg, 10.2 mmol) in DMF (2ml) according

to the procedure described for the preparation of **5x**. Colourless oil (768 mg, quantitative). This a known compound.[45]; $^1$H NMR (500 MHz, $CDCl_3$): $\delta$ = 4.32 (s, 4H), 0.88 (s, 18H), 0.09 (s, 12H)

**Compound 59**

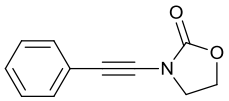


Compound **59** was obtained using a procedure described by Liu and is fully described within.[29a] White solid (109 mg, 53%).; $^1$H NMR (500 MHz, $CDCl_3$): $\delta$ = 7.45 – 7.39 (m, 2H), 7.31 – 7.26 (m, 3H), 4.48 (apt t, *J* = 8.0 Hz, 2H), 4.00 (apt t, *J* = 8.0 Hz, 2H)

**Compound 60**

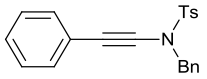


Compound **59** was obtained using a modified procedure described by Liu.[29a] This compound is known.[46] Purple solid (356 mg, 89%).; $^1$H NMR (500 MHz, $CDCl_3$): $\delta$ = 7.77 (d, *J* = 8.2 Hz, 2H), 7.35 – 7.26 (m, 7H), 7.24 – 7.19 (m, 5H), 4.56 (s, 2H), 2.43 (s, 3H)

**Compound 61**

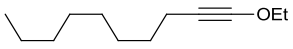


At -78°C, 1.8M *n*Buli (0.4 ml, 0.7 mmol) was added to a yellow solution of ethoxyacetylene solution (~40 wt. % in hexanes) **S7** (150 µl, 0.61 mmol) in THF (0.7 ml). The solution was stirred for 15 mins at -78°C. Afterwards, HMPA (212 µl, 1.22 mmol) was added and the solution was stirred for a further ten minutes. Then, 1-bromooctane (84 µl, 0.49 mmol) was added. The solution was allowed to stir for 15 mins at -78°C. Then the ice-bath was removed and allowed to stir at rt for 90 mins. Afterwards, the reaction was quenched with a saturated solution of

$NH_4Cl$. $Et_2O$ was added and extracted two times with $Et_2O$. The organic layer was washed with water and a saturated solution of brine. Dried over $Na_2SO_4$, filtered and concentrated. Purification by flash column chromatography (PE) gave **61** as a colourless oil (55 mg, 65%).; $^1H$ NMR (500 MHz, $CDCl_3$): $\delta$ = 4.00 (q, *J* = 7.0 Hz, 2H), 2.08 (t, *J* = 6.9 Hz, 2H), 1.46 – 1.38 (m, 2H), 1.37 – 1.16 (m, 13H), 0.89 – 0.83 (m, 3H); $^{13}C$ NMR (125 MHz, $CDCl_3$): $\delta$ = 89.3, 73.8, 37.4, 31.8, 29.7,29.2, 29.1,28.8, 22.7, 17.2, 14.4, 14.1; IR (neat): $\tilde{\nu}$ = 2952 (w), 2926 (m), 2854 (m), 2271 (m), 1466 (w), 1439 (w), 1379 (w), 1289 (w), 1222 (s), 1089 (w), 1010 (m), 924 (w), 864 (w), 723 (w) $cm^{-1}$

**Compound 62**

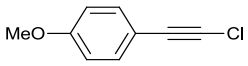


This compound was prepared from 4-ethynylanisole (300 µl, 2.3 mmol) and NCS (402mg, 3.0 mmol) according to the procedure described for the preparation of **5d** except at -78°C. Yellow Oil (294 mg, 76%).; $^1H$ NMR (500 MHz, $CDCl_3$): $\delta$ = 7.38 – 7.33 (m, 2H), 6.84 – 6.79 (m, 2H), 3.79 (s, 3H); $^{13}C$ NMR (125 MHz, $CDCl_3$): $\delta$ = 159.8, 133.4, 114.2, 114.0, 69.3, 66.4, 55.3; IR (neat): $\tilde{\nu}$ = 3005 (w), 2934 (w), 2838 (w), 2220 (w), 1606 (m), 1507 (s), 1291 (m), 1248 (s), 1172 (m), 1034 (m), 888 (w), 830 (m) $cm^{-1}$; HRMS (CI): calcd for $(C_9H_7ClO + NH_4)^+$: 184.0524; found: 184.0528

**Compound 63**

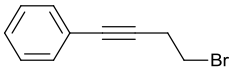


This compound was prepared from commercially available iodobenzene (120 µl, 1.07 mmol) and 4-bromo-1-butyne (130 µl, 1.39 mmol) according to the procedure described for the preparation of **5h**. Colourless oil (192 mg, 86%). This is a known compound.[47]; $^1H$ NMR (500

MHz, $CDCl_3$): $\delta$ = 7.45 – 7.37 (m, 2H), 7.31 – 7.26 (m, 2H), 3.51 (t, *J* = 7.4 Hz, 2H), 2.96 (t, *J* = 7.3 Hz, 2H)

**Compound 100**

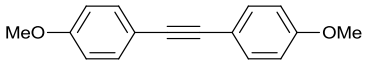


This compound was prepared from commercially available 4-iodoanisole (250 mg, 1.07 mmol) and 4-ethynylanisole (180 µl, 1.39 mmol) according to the procedure described for the preparation of **5h**. Yellow solid (176 mg, 70%). This is a known compound.[48]; $^1$H NMR (500 MHz, $CDCl_3$): $\delta$ = 7.45 – 7.40 (m, 2H), 6.87 – 6.82 (m, 2H), 3.81 (s, 3H)

### 2.7.4 Nickel(0): Synthesis of pyridinones and pyranones

**Procedures**

Method **I**. Inside a glovebox, a Teflon-screw flame-dried Schlenk flask equipped with a small stirrer bar was charged with $Ni(cod)_2$ (8 mg, 0.03 mmol) and taken out of the glovebox. Under $N_2$, $PPh_3$ (23 mg, 0.09 mmol) and dioxane (1.3 ml) were added. The suspension was stirred for 5 minutes and then commercially available azetidinone **7** (49 mg, 0.29 mmol) was added as solid in one portion. After stirring for 5 more minutes, bis-phenylacetylene **5a** (57 mg, 0.32 mmol) was added and the flask was sealed and immersed into an oil bath pre-heated at 90 oC. After stirring for 17 hours at that temperature, the mixture was allowed to cool and filtered through a silica plug before evaporation. Purification by flash chromatography (PE/Et2O, 10/1 → 1/1) afforded **6a** as white solid (91 mg, 90%).

Method **II**. Used for alkynes which are oils or liquids, the procedure is identical to method **I** except that $Ni(cod)_2$ and $PPh_3$ were diluted in 1 ml dioxane and that the alkyne was added as a dioxane solution (0.3 ml) under $N_2$.

Method **III**. Identical to method **I** except that $Ni(cod)_2$ and $PPh_3$ were diluted in 0.3 mL of dioxane before azetidinone and alkyne were added via canula as a premixed dioxane solution (1 mL).

The NMR spectra of some compounds were recorded at the different temperatures and using a modified delay (d given in s) for the $^{13}C$ spectra in order to obtain optimum resolution, which was poor at room temperature due to slow conformer equilibration. Details mentioned after description of the compound.

**Compound 6a**

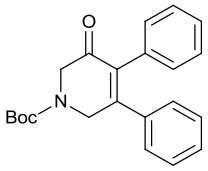


White solid. (91 mg, 90% using method **I**): m.p. 127–129°C; $^1H$ NMR (500 MHz, $CDCl_3$): $\delta$ = 7.21–7.13 (m, 6H), 7.12–7.06 (m, *2*H), 7.00–6.94 (m, 2H), 4.61 (br s, *2H*), 4.31 (s, 2H), 1.51 (s, 9H); $^{13}C$ NMR (100 MHz, $CDCl_3$): $\delta$ = 192.3, 154.9 (br),^ 154.3, 137.0, 135.9, 133.6, 130.8 (2C), 128.7, 128.5 (2C), 128.2 (2C), 127.7 (2C), 127.3, 81.2, 51.8 (br), 48.0 (br), 28.4 (3C); IR (neat): $\tilde{\nu}$ = 3057 (w), 3007 (w), 2974 (w), 2929 (w), 1682 (s), 1619 (w), 1596 (w), 1574 (w), 1492 (w), 1479 (w), 1443 (m), 1421 (s), 1366 (m), 1326 (m), 1250 (m), 1232 (m), 1155 (s), 1194 (s), 1104 (s), 1083 (w), 994 (w), 936 (w), 924 (w), 904 (w), 858 (m), 768 (m), 757 (s), 694 (s) $cm^{-1}$; HRMS (ESI): calcd for ($C_{22}H_{23}NO_3$ + Na): 372.1576; found: 372.1589; elemental analysis (%) calcd for $C_{22}H_{23}NO_3$: C 75.62, H 6.63, N 4.01; found: C 75.03, H 6.50, N 3.75.

^ Carbon appears as a very broad peak in $^{13}C$ CPD NMR spectrum and is not visible in the $^{13}C$ APT NMR spectrum. Similar observation was made on related Boc-protected compounds.[49]

($^{13}C$ APT NMR (d = 2) and $^{13}C$ CPD NMR (d = 4): 40°C)

**Compound 8**

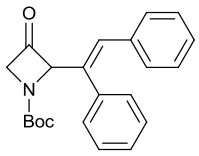


Colourless oil isolated in 30% yield following conditions of table 1, entry 1. $^{1}$H NMR (400 MHz, $CDCl_3$): $\delta$ = 7.95–7.51 (br s, 1H), 7.39 (d, *J* = 7.7 Hz, 2H), 7.32 (t, *J* = 7.5 Hz, 2H), 7.29–7.14 (m, 6H), 4.57 (d, *J* = 1.6 Hz, 1H), 4.20 (d, *J* = 18.9 Hz, 1H), 3.95 (dd, *J* = 18.8 Hz, 2.1 Hz, 1H), 1.53 (s, 9H); $^{13}$C NMR (100 MHz, $CDCl_3$): $\delta$ = 201.7, 151.9 (br), 137.7, 135.7, 129.3 (2C), 128.6 (2C), 127.9, 127.7 (2C), 127.0, 125.3 (2C + 1C), 116.0, 82.5, 56.0 (br), 50.2 (br), 28.3 (3C); IR (neat): $\tilde{\nu}$ = 3058 (w), 2978 (w), 2930 (w), 1759 (m), 1702 (s), 1599 (w), 1492 (w), 1448 (w), 1394 (w), 1369 (m), 1316 (w), 1239 (s), 1149 (s), 1117 (m), 1072 (w), 1026 (w), 852 (w), 764 (m), 698 (s) $cm^{-1}$; HRMS (ESI): calcd for ($C_{22}H_{23}NO_3$ + Na): 372.1576; found: 372.1581.

($^{13}$C APT NMR (d = 2): 50°C, $^{13}$C CPD NMR (d = 4): 50°C)

**Compound 6b**

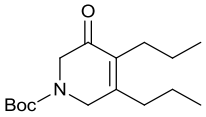


Colourless oil (65 mg, 88% using method **I**); $^{1}$H NMR (500 MHz, $CDCl_3$): δ = 4.09 (br s, 2H), 4.00 (s, 2H), 2.22 (dt, *J* = 7.2 Hz, 4H), 1.52 (sext, *J* = 7.6 Hz, 2H), 1.43 (s, 9H), 1.32 (sext, *J* = 7.6Hz, 2H), 0.95 (t, J = 7.3 Hz, 3H), 0.88 (t, J = 7.3Hz, 3H); $^{13}$C NMR (100 MHz, $CDCl_3$): δ = 193.1, 154.2, 155.8,^ 134.3, 80.6, 51.4, 46.1, 34.2, 28.3, 26.6, 22.4, 21.4, 14.1, 14.1; IR (neat): $\tilde{\nu}$ = 2962 (m), 2032 (w), 2873 (w), 1700 (s), 1672 (s), 1633 (m), 1417 (m), 1366 (s), 1281 (m), 1240 (m), 1164 (s), 1130 (s), 1095 (m), 1032 (w), 978 (w), 904 (m), 861 (w), 766 (m), 737 (w) $cm^{-1}$; MS (ESI): calcd for ($C_{16}H_{27}NO_3$ + Na): 304.1889; found: 304.1895; elemental analysis (%) calcd for $C_{16}H_{27}NO_3$: C 68.29, H 9.67, N 4.98; found: C 66.50, H 9.53, N 4.98.

^ Carbon is not visible in the $^{13}C$ APT NMR spectrum but its chemical shift could be determined by HMBC correlation

**Compound 6c**

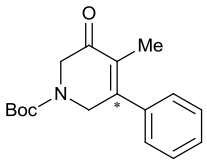


Colourless oil (64 mg, 80% from 48 mg of **7** using method **II**): $^{1}H$ NMR (500 MHz, $CDCl_3$): $\delta$ = 7.46–7.33 (m, 3H), 7.29–7.22 (m, 2H), 4.39 (br s, 2H), 4.17 (s, 2H), 1.75 (s, 3H), 1.46 (s, 9H); $^{13}C$ NMR (100 MHz, $CDCl_3$): $\delta$ = 193.9, 154.1, 153.6 (br),^ 137.3, 130.6, 128.8, 128.6 (2C), 127.6 (2C), 80.8, 51.2 (br), 47.8 (br), 28.3 (3C), 11.9; IR (neat): $\tilde{\nu}$ = 3053 (w), 2977 (w), 2929 (w), 1694 (s), 1675 (s), 1632 (w), 1575 (w), 1476 (w), 1416 (m), 1383 (m), 1381 (m), 1364 (s), 1326 (m), 1281 (m), 1244 (s), 1230 (s), 1163 (s), 1116 (s), 1068 (w), 1032 (w), 1003 (w), 994 (w), 896 (w), 861 (w), 763 (m), 701 (s) $cm^{-1}$; HRMS (ESI): calcd for ($C_{17}H_{21}NO_3$ + Na): 310.1419; found: 310.1432; elemental analysis (%) calcd for $C_{17}H_{21}NO_3$: C 71.06, H 7.37, N 4.87; found: C 70.74, H 7.51, N 4.92.

^ Carbon appears as a very broad peak in $^{13}C$ CPD NMR spectrum and is not visible in the $^{13}C$ APT NMR spectrum.

($^{13}C$ APT NMR (d = 2): 40°C)

**Compound 11c**

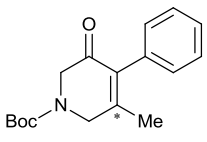


White solid (10 mg, 12% from 48 mg of **7** using method **II**): m.p.: 104–106°C; $^{1}H$ NMR (500 MHz, $CDCl_3$): $\delta$ = 7.37 (t, $J$ = 7.3 Hz, 2H), 7.33–7.28 (m, 1H), 7.07 (d, $J$ = 7.4 Hz, 2H), 4.28 (br s, 2H), 4.20 (s, 2H), 1.84 (s, 3H), 1.48 (s, 9H); $^{13}C$ NMR (100 MHz, $CDCl_3$): $\delta$ = 191.6, {154.6},^

154.2, 136.3, 133.8, 129.9 (2C), 128.2 (2C), 127.7, 81.0, 51.4 (br), 47.7 (br), 28.4 (3C), 19.5; IR (neat): $\tilde{\nu}$ = 2977 (w), 2931 (w), 1695 (s), 1677 (s), 1636 (w), 1600 (w), 1495 (w), 1479 (w), 1417 (m), 1393 (w), 1365 (m), 1323 (w), 1285 (w), 1243 (s), 1217 (w), 1157 (s), 1107 (m), 1075 (w), 1047 (w), 977 (w), 946 (w), 895 (m), 857 (w), 763 (m), 701 (w); HRMS (ESI): calcd for ($C_{17}H_{21}NO_3$ + Na): 310.1419; found: 310.1422.

($^{13}$C APT NMR (d = 2): 45°C)

^ Carbon marked with an asterisk is not visible in the $^{13}$C APT NMR spectrum but its chemical shift could be determined by HMBC correlation and is indicated in brackets.

**Compound 6c**

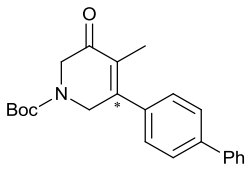


White foam (86 mg, 83% from 49 mg of **7** using method **I**): $^1$H NMR (500 MHz, $CDCl_3$): $\delta$ = 7.64 (d, $J$ = 8.2 Hz, 2H), 7.62–7.57 (m, 2H), 7.47–7.41 (m, 2H), 7.38–7.32 (m, 3H), 4.43 (br s, 2H), 4.19 (s, 2H), 1.82 (t, $J$ = 1.8 Hz, 3H), 1.49 (s, 9H); $^{13}$C NMR (100 MHz, $CDCl_3$): $\delta$ = 193.9, 154.2, {153.8},^ 141.9, 140.2, 136.1, 130.8, 128.9 (2C), 128.2 (2C), 127.8, 127.3 (2C), 127.1 (2C), 80.9, 51.4, 47.8, 28.4 (3C), 12.1; IR (neat): $\tilde{\nu}$ = 2975 (w), 2926 (w), 1698 (s), 1676 (s), 1629 (w), 1488 (w), 1419 (m), 1401 (m), 1380 (m), 1364 (m), 1283 (w), 1240 (m), 1232 (m), 1165 (s), 1119 (m), 1071 (w), 1007 (w), 898 (w), 861 (w), 841 (w), 766 (m), 735 (w), 698 (w) cm$^{-1}$; MS (ESI): calcd for ($C_{23}H_{25}NO_3$ + Na): 386.1732; found: 386.1745; elemental analysis (%) calcd for $C_{23}H_{25}NO_3$: C 76.01, H 6.93, N 3.85; found: C 75.08, H 7.04, N 3.71.

($^{13}$C APT NMR (d = 2): 40°C)

^ Carbon marked with an asterisk is not visible in the $^{13}$C APT NMR spectrum but its chemical shift could be determined by HMBC correlation and is indicated in brackets.

**Compound 11d**

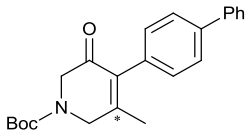


Colourless oil (8 mg, 8% from 49 mg of **7** using method **I**): $^{1}$H NMR (500 MHz, $CDCl_3$): $\delta$ = 7.63–7.56 (m, 4H), 7.45–7.39 (m, 2H), 7.36–7.29 (m, 1H), 7.15 (d, *J* = 8.1 Hz, 2H), 4.30 (br s, 2H), 4.20 (s, 2H), 1.90 (s, 3H), 1.50 (s, 9H); $^{13}$C NMR (100 MHz, $CDCl_3$): $\delta$ = 191.6, {155.2},^ 154.1, 140.9, 140.6, 136.0, 132.7, 130.3 (2C), 128.7 (2C), 127.3, 127.1 (2C), 126.9 (2C), 81.0, 51.5, 47.7, 28.4 (2C), 19.6; IR (neat): $\tilde{\nu}$ = 3029 (w), 2977 (w), 2933 (w), 1696 (s), 1678 (s), 1636 (w), 1601 (w), 1487 (w), 1417 (w), 1366 (m), 1325 (w), 1284 (w), 1243 (m), 1220 (w), 1157 (s), 1108 (w), 1040 (w), 1008 (w), 977 (w), 938 (w), 895 (w), 837 (w), 766 (m), 732 (m), 698 (m) cm$^{-1}$; HRMS (ESI): calcd for ($C_{23}H_{25}NO_3$ + Na): 386.1732; found: 386.1733.

($^{13}$C APT NMR (d = 2): 40°C)

^ Carbon marked with an asterisk is not visible in the $^{13}$C APT NMR spectrum but its chemical shift could be determined by HMBC correlation and is indicated in brackets.

**Compound 6e**

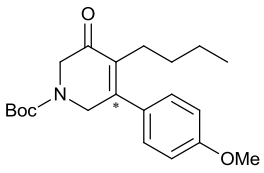


Yellow oil (80 mg, 79% from 48 mg of **7** using method **II**): $^{1}$H NMR (500 MHz, $CDCl_3$): $\delta$ = 7.18 (d, *J* = 8.4 Hz, 2H), 6.92 (d, *J* = 8.6 Hz, 2H), 4.32 (br s, 2H), 4.12 (s, 2H), 3.82 (s, 3H), 2.24–2.14 (m, 2H), 1.46 (s, 9H), 1.30–1.20 (m, 2H), 1.14 (sext, *J* = 7.3 Hz, 2H), 0.74 (t, *J* = 7.2 Hz, 3H); $^{13}$C NMR (100 MHz, $CDCl_3$): $\delta$ = 193.7, 160.0, 154.3, 153.7 (br),^ 135.2, 129.7, 128.8 (2C), 114.1 (2C), 80.8, 55.3, 51.7 (br), 48.3 (br), 31.4, 28.3 (2C), 25.6, 22.6, 13.6; IR (neat): $\tilde{\nu}$ = 2960 (w),

2931 (w), 2861 (w), 1699 (m), 1675 (s), 1607 (m), 1510 (m), 1412 (m), 1366 (m), 1287 (w), 1246 (s), 1163 (s), 1124 (s), 1040 (m), 1028 (m), 945 (w), 900 (w), 861 (w), 732 (s), 767 (m), 731 (m) $cm^{-1}$; HRMS (ESI): calcd for ($C_{21}H_{29}NO_4$ + Na): 382.1994; found: 382.1985; elemental analysis (%) calcd for $C_{21}H_{29}NO_4$: C 70.17, H 8.13, N 3.90; found: C 69.19, H 8.41, N 3.64.

($^{13}C$ APT NMR (d = 2): 40°C and $^{13}C$ CPD NMR (d = 4): 45°C)

^ Carbon marked with an asterisk appears as a very broad peak in $^{13}C$ CPD NMR spectrum and is not visible in the $^{13}C$ APT NMR spectrum. However, HMBC correlations are visible which confirms the $^{13}C$ CPD NMR.

**Compound 11e**

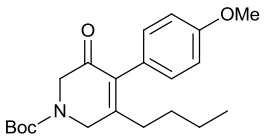


Colourless oil (10 mg, 10% from 48 mg of **7** using method **II**): $^1H$ NMR (500 MHz, $CDCl_3$): $\delta$ = 6.97 (d, *J* = 8.5 Hz, 2H), 6.89 (d, *J* = 8.7 Hz, 2H), 4.28 (br s, 2H), 4.17 (s, 2H), 3.80 (s, 3H), 2.19–2.11 (m, 2H), 1.48 (s, 9H), 1.46–1.36 (m, 2H), 1.25–1.14 (m, 2H), 0.79 (t, *J* = 7.3 Hz, 3H); $^{13}C$ NMR (100 MHz, $CDCl_3$): $\delta$ = 192.5, 159.1, 158.1 (br),^ 154.3, 135.9, 131.0 (2C), 126.0, 113.8 (2C), 80.9, 55.2, 51.7 (br), 46.1 (br), 33.0, 30.2, 28.4 (3C), 22.7, 13.6; IR (neat): $\tilde{\nu}$ = 2959 (w), 2930 (w), 2862 (m), 1698 (m), 1676 (s), 1606 (m), 1510 (m), 1416 (m), 1366 (m), 1329 (w), 1287 (m), 1243 (s), 1154 (s), 1107 (m), 1033 (m), 989 (w), 927 (w), 896 (w), 858 (w), 828 (m), 798 (w), 766 (w) $cm^{-1}$; HRMS (ESI): calcd for ($C_{21}H_{29}NO_4$ + Na): 382.1994; found: 382.1996.

($^{13}C$ APT NMR (d = 2) and $^{13}C$ CPD NMR (d = 4): 45°C)

^ Carbon marked with an asterisk appears as a very broad peak in $^{13}C$ CPD NMR spectrum and is not visible in the $^{13}C$ APT NMR spectrum. However, HMBC correlations are visible which confirms the $^{13}C$ CPD NMR.

**Compound 6f**

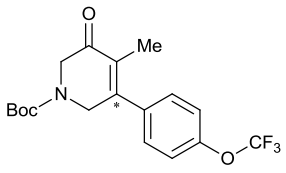


Colourless oil (72 mg, 69% from 48 mg of **7** using method **II**): $^{1}$H NMR (500 MHz, $CDCl_3$): $\delta$ = 7.33 – 7.24 (m, 4H), 4.35 (br s, 2H), 4.16 (s, 2H), 1.77 – 1.71 (m, 3H), 1.46 (s, 9H); $^{13}$C NMR (100 MHz, $CDCl_3$): $\delta$ = 193.6, 154.1, 152.0,^ 149.5 (m), 135.9, 131.3, 129.3, 120.5 (q, 257.9 Hz), 121.0, 81.1, 51.4, 47.8, 28.3, 12.0; IR (neat): $\tilde{\nu}$ = 2984 (w), 2922 (w), 1692 (m), 1677 (m), 1625 (w), 1507 (w), 1420 (w), 1363 (w), 1244 (s), 1209 (s), 1152 (s), 1114 (s), 1016 (w), 1001 (w), 897 (w), 834 (m), 762 (w), 685 (w) $cm^{-1}$; HRMS (ESI): calcd for ($C_{18}H_{20}NO_4F_3$ + Na): 394.1242; found: 394.1258

($^{13}$C APT NMR (d = 2) and $^{13}$C CPD NMR (d = 4): 45°C)

^ Carbon marked with an asterisk appears as a very broad peak in $^{13}$C CPD NMR spectrum and is not visible in the $^{13}$C APT NMR spectrum. However, HMBC correlations are visible which confirms the $^{13}$C CPD NMR.

**Compound 6g**

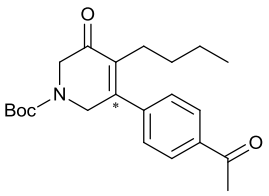


Yellow oil (91 mg, 88% from 48 mg of **7** using method **II**): $^{1}$H NMR (500 MHz, $CDCl_3$): $\delta$ = 7.98 (d, *J* = 7.4 Hz, 2H), 7.32 (d, *J* = 7.4 Hz, 2H), 4.32 (br s, *2*H), 4.14 (s, 2H), 2.60 (s, 3H), 2.20–2.05 (m, 2H), 1.44 (s, 9H), 1.28–1.18 (m, 2H), 1.15–1.03 (m, 2H), 0.70 (t, *J* = 7.2 Hz, 3H); $^{13}$C NMR (100 MHz, $CDCl_3$): $\delta$ = 197.1, 193.2, 154.2, {152.8},^ 146.6, 142.1, 137.2, 135.9, 128.6 (2C), 127.6 (2C), 82.1, 51.6 (br), 48.0 (br), 31.3, 28.3 (2C), 26.4, 25.6, 22.5, 13.6; IR (neat): $\tilde{\nu}$ = 2960 (w), 2931 (w), 2872 (w), 1680 (s), 1604 (m), 1560 (w), 1401 (m), 1365 (s), 1264 (s), 1162 (s),

1128 (s), 1076 (w), 1037 (w), 1015 (w), 958 (m), 910 (w), 835 (m), 769 (w), 732 (m) $cm^{-1}$; HRMS (ESI): calcd for ($C_{22}H_{29}NO_4$ + Na): 394.1994; found: 394.2001.

(13C APT NMR (d = 2): 40°C)

^ Carbon marked with an asterisk is not visible in the $^{13}C$ APT NMR spectrum but its chemical shift could be determined by HMBC correlation and is indicated in brackets

**Compound 11g**

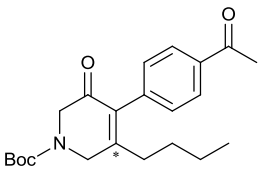


Colourless oil (12 mg, 11% from 48 mg of **7** using method **II**): $^1H$ NMR (400 MHz, $CDCl_3$): $\delta$ = 7.95 (d, *J* = 8.1 Hz, 2H), 7.16 (d, *J* = 8.2 Hz, 2H), 4.31 (br s, 2H), 4.18 (s, 2H), 2.59 (s, 3H), 2.19–2.09 (m, 2H), 1.49 (s, 9H), 1.47–1.36 (m, 2H), 1.26–1.14 (m, 2H), 0.78 (t, *J* = 7.4 Hz, 3H); $^{13}C$ NMR (100 MHz, $CDCl_3$): $\delta$ = 197.6, 191.8, {158.8},^ 154.2, 139.2, 136.6, 135.6, 130.2 (2C), 128.2 (2C), 81.2, 51.7 (br), 46.1 (br), 33.0, 30.2, 28.4 (3C), 26.5, 22.7, 13.6; IR (neat): $\tilde{\nu}$ = 2961 (w), 2932 (w), 2872 (w), 1683 (s), 1628 (w), 1604 (w), 1430 (w), 1403 (w), 1366 (w), 1324 (w), 1265 (w), 1244 (w), 1159 (m), 1110 (w), 958 (w), 897 (w), 830 (w) $cm^{-1}$; MS (ESI): calcd for ($C_{22}H_{29}NO_4$ + Na): 394.1994; found: 394.2000.

($^1H$ NMR: 45°C, $^{13}C$ APT NMR (d = 2): 45°C)

^ Carbon marked with an asterisk is not visible in the $^{13}C$ APT NMR spectrum but its chemical shift could be determined by HMBC correlation and is indicated in brackets

**Compound 6h**

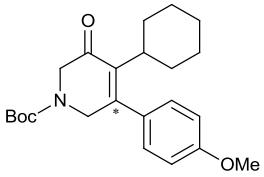


Colorless oil (88 mg, 76% from 51 mg of **7** using method **III**); $^{1}$H NMR (500 MHz, $CDCl_3$): $\delta$ = 7.20–7.11 (m, 2H), 6.92 (d, *J* = 8.0 Hz, 2H), 4.27 (br s, 2H), 4.05 (s, 2H), 3.83 (s, 3H), 2.25 (t, *J* = 11.3 Hz, 1H), 1.90 (qd, *J* = 12.6 Hz, 2.8 Hz, 2H), 1.63 (d, *J* = 12.7 Hz, 2H), 1.55–1.48 (m, 1H), 1.46 (s, 9H), 1.38 (d, *J* = 12.4 Hz, 2H), 1.26–1.11 (m, 2H), 1.06–0.93 (m, 2H); $^{13}$C NMR (100 MHz, $CDCl_3$): $\delta$ = 193.8, 160.0, 154.3, 154.0 (br), 138.7, 130.1, 128.8 (2C), 114.1 (2C), 80.7, 55.3, 52.5 (br), 48.9 (br), 40.1, 30.6, 28.4 (3C), 26.9, 25.8; IR (neat): $\tilde{\nu}$ = 2972 (w), 2926 (m), 2852 (w), 1698 (s), 1674 (s), 1608 (m), 1572 (w), 1509 (m), 1442 (w), 1413 (w), 1393 (w), 1366 (s), 1328 (w), 1307 (m), 1287 (m), 1244 (s), 1166 (s), 1129 (s), 1088 (w), 1031 (w), 996 (w), 926 (w), 890 (w), 870 (w), 832 (m), 791 (w), 772 (m), 741 (w) cm$^{-1}$; HRMS (ESI): calcd for ($C_{23}H_{31}NO_4$ + Na): 408.2151; found: 408.2145; elemental analysis (%) calcd for $C_{23}H_{31}NO_4$: C 71.66, H 8.11, N 3.63; found: C 70.08, H 8.18, N 3.39.

($^{13}$C APT NMR (d = 2) and $^{13}$C CPD NMR (d = 4): 45°C)

^ Carbon appears as a very broad peak in $^{13}$C CPD NMR spectrum and is not visible in the $^{13}$C APT NMR spectrum.

**Compound 11h**

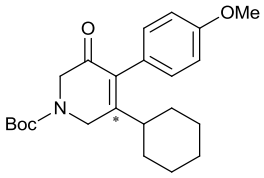


Colourless oil (14 mg, 12% from 51 mg of **7** using method **III**); $^{1}$H NMR (500 MHz, $CDCl_3$): $\delta$ = 6.95 (d, *J* = 8.8 Hz, 2H), 6.89 (d, *J* = 8.7 Hz, 2H), 4.28 (br s, 2H), 4.14 (s, 2H), 3.81 (s, 3H), 2.40 (tt, *J* = 12.1 Hz, 3.1 Hz, 1H), 1.77–1.67 (m, 2H), 1.66–1.55 (m, 3H), 1.49 (s, 9H), 1.46–1.32 (m, 3H),

1.18–0.99 (m, 3H); $^{13}$C NMR (100 MHz, $CDCl_3$): $\delta$ = 193.0, 162.1 (br),^ 159.1, 154.3, 134.9, 130.7 (2C), 126.2, 113.8 (2C), 80.9, 55.2, 52.0 (br), 43.1 (br), 42.4, 30.7, 28.4 (3C), 25.9, 25.7; IR (neat): ṽ = 2967 (w), 2929 (m), 2854 (w), 1698 (s), 1678 (s), 1605 (m), 1510 (s), 1445 (m), 1422 (m), 1393 (w), 1366 (m), 1324 (w), 1286 (m), 1243 (s), 1158 (s), 1107 (w), 1034 (w), 1002 (w), 903 (w), 858 (w), 828 (m), 801 (w), 766 (w), 731 (w) cm$^{-1}$; HRMS (ESI): calcd for ($C_{23}H_{31}NO_4$ + Na): 408.2151; found: 408.2157.

($^{13}$C APT NMR (d = 2) and $^{13}$C CPD NMR (d = 4): 45°C)

^ Carbon appears as a very broad peak in $^{13}$C CPD NMR spectrum and is not visible in the $^{13}$C APT NMR spectrum.

**Compound 6i**

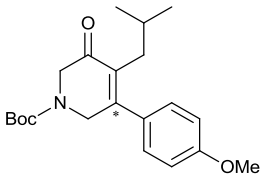


Colourless oil (76 mg, 76% from 47 mg of **7** using method **III**): $^1$H NMR (500 MHz, $CDCl_3$): $\delta$ = 7.19–7.13 (m, 2H), 6.91 (d, *J* = 8.6 Hz, 2H), 4.32 (br s, 2H), 4.13 (s, 2H), 3.82 (s, 3H), 2.17 (d, *J* = 7.4 Hz, 2H), 1.65– 1.56 (m, 1H), 1.47 (s, 9H), 0.64 (d, *J* = 6.7, 6H); $^{13}$C NMR (100 MHz, $CDCl_3$): $\delta$ = 194.0, 159.9, {155.8},^ 154.4, 134.4, 129.7, 129.1 (2C), 114.1 (2C), 80.8, 55.2, 51.8 (br), 48.8 (br), 34.1, 28.3 (3C), 27.6, 22.2; IR (neat): ṽ = 2957 (m), 2932 (w), 2869 (w), 1698 (s), 1674 (s), 1608 (m), 1573 (w), 1510 (m), 1464 (m), 1440 (m), 1412 (m), 1394 (m), 1365 (s), 1323 (m), 1306 (w), 1282 (m), 1242 (s), 1162 (s), 1124 (s), 1070 (m), 1042 (m), 1027 (m), 981 (w), 917 (w), 880 (m), 858 (w), 832 (s), 769 (m), 733 (w) cm$^{-1}$; HRMS (ESI): calcd for ($C_{21}H_{29}NO_4$ + Na): 382.1994; found: 382.2002; elemental analysis (%) calcd for $C_{23}H_{29}NO_4$: C 70.17, H 8.13, N 3.90; found: C 69.56, H 8.22, N 3.84.

($^{13}$C APT NMR (d = 2): 45°C);

^ Carbon marked with an asterisk is not visible in the $^{13}C$ APT NMR spectrum but its chemical shift could be determined by HMBC correlation and is indicated in brackets

**Compound 11i**

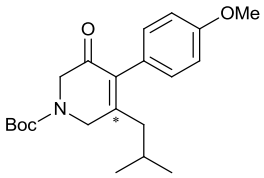


Colourless oil (15 mg, 15% from 47 mg of **7** using method **III**): $^1H$ NMR (500 MHz, $CDCl_3$): $\delta$ = 6.95 (d, *J* = 8.6 Hz, 2H), 6.88 (d, *J* = 8.6 Hz, 2H), 4.25 (br s, 2H), 4.17 (s, 2H), 3.80 (s, 3H), 2.10 (d, *J* = 7.4 Hz, 2H), 1.87–1.75 (m, 1H), 1.47 (s, 9H), 0.78 (d, *J* = 6.1 Hz, 6H); $^{13}C$ NMR (100 MHz, $CDCl_3$): $\delta$ = 192.6, 159.1, {157.7},^ 154.2, 136.8, 131.2 (2C), 126.1, 113.8 (2C), 81.0, 55.2, 51.8 (br), 46.4 (br), 42.2, 28.4 (3C), 27.2, 22.5; IR (neat): $\tilde{\nu}$ = 2958 (m), 2932 (w), 2870 (w), 2837 (w), 1697 (s), 1677 (s), 1606 (m), 1577 (w), 1510 (s), 1420 (m), 1393 (m), 1366 (s), 1322 (w), 1287 (m), 1241 (s), 1154 (s), 1106 (m), 1034 (m), 990 (w), 926 (w), 900 (w), 856 (w), 828 (m), 810 (w), 797 (w), 766 (w), 730 (w), 675 (w) $cm^{-1}$; HRMS (ESI): calcd for ($C_{21}H_{29}NO_4$ + Na): 382.1994; found: 382.2000.

($^{13}C$ APT NMR (d = 4): 45°C);

^ Carbon marked with an asterisk is not visible in the $^{13}C$ APT NMR spectrum but its chemical shift could be determined by HMBC correlation and is indicated in brackets

**Compound 6j and 11j**

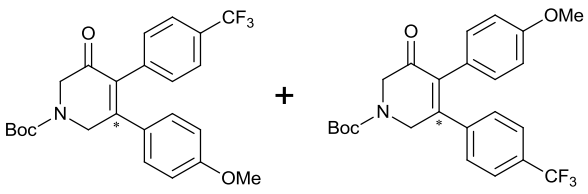


After purification by flash chromatography, a 55:45 mixture of regioisomers was obtained as white solid (102 mg, 82% from 47 mg of **7** using method **I**). However, solubilisation of this

material in 1 mL $CH_2Cl_2$ and adding a layer of PE (3 mL) induced precipitation of a solid which was filtered and washed with PE and dried. This solid was an enriched mixture (**6j**/**11j** = 6:1) and evaporation of the filtrate gave a mixture enriched in the other regioisomer (**6j**/**11j** = 1:4). This facilitated the interpretation of the NMR spectra. $^1$H NMR (400 MHz, $CDCl_3$): (**6j**) $\delta$ = 7.44 (d, *J* = 8.0 Hz, 2H), 7.13 (d, *J* = 8.0 Hz, 2H), 7.01 (d, *J* = 8.0 Hz, 2H), 6.71 (d, *J* = 8.0 Hz, 2H), 4.62 (br s, 2H), 4.29 (s, 2H), 3.74 (s, 3H), 1.51 (s, 9H); (**11j**) $\delta$ = 7.46 (d, *J* = 8.0 Hz, 2H), 7.22 (d, *J* = 8.0 Hz, 2H), 6.87 (d, *J* = 8.5 Hz, 2H), 6.71 (d, *J* = 8.4 Hz, 2H), 4.58 (br s, 2H), 4.30 (s, 2H), 3.73 (s, 3H), 1.51 (s, 9H); $^{13}$C NMR (100 MHz, $CDCl_3$): (**6j**) $\delta$ = 191.9, 159.2, {156.4},^ 154.2, 138.1, 134.0, 131.4 (2C), 130.3 (2C), 129.3 (q, *J* = 32.7 Hz), 124.7 (q, *J* = 3.7 Hz, 2C), 124.2 (q, *J* = 272.2 Hz), 114.0 (2C), 81.3, 55.2, 51.9, 47.8, 28.4 (3C); (**11j**) $\delta$ = 192.4, 160.5, 154.2, {153.1},^ 141.0, 136.3, 132.0 (2C), 130.6, (q, *J* = 32.7 Hz), 128.9 (2C), 125.3 (q, *J* = 3.7 Hz, 2C), 123.7 (q, *J* = 272.3 Hz), 113.6 (2C), 81.4, 55.1, 51.9, 47.8, 28.4 (3C); IR (neat): $\tilde{\nu}$ = 2978 (w), 2935 (w), 2840 (w), 1677 (s), 1605 (m), 1571 (w), 1509 (m), 1408 (m), 1366 (m), 1322 (s), 1293 (m), 1247 (s), 1156 (s), 1122 (s), 1109 (s), 1066 (s), 1029 (m), 1019 (m), 991 (w), 909 (m), 868 (w), 828 (s), 766 (w), 729 (s), 692 (w) cm$^{-1}$; HRMS (ESI): calcd for ($C_{24}H_{24}NO_4F_3$ + Na): 470.1555; found: 470.1574.

($^1$H NMR: 45°C, $^{13}$C APT NMR (d = 2): 45°C);

^ Carbon marked with an asterisk is not visible in the $^{13}$C APT NMR spectrum but its chemical shift could be determined by HMBC correlation and is indicated in brackets

**Compound 6k and 11k**

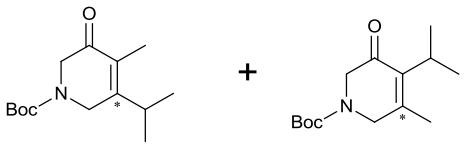


Colourless oil (67 mg, 90% from 50 mg of **1** using method **II**), mixture of regioisomers (**6k**/**11k** = 60:40): $^1$H NMR (500 MHz, $CDCl_3$): (**6k**) $\delta$ = 4.09 (br s, 2H), 3.98 (s, 2H), 2.95 (sept, *J* = 7.0 Hz, 1H), 1.76 (t, *J* = 1.7 Hz, 3H), 1.41 (s, 9H), 1.08 (d, *J* = 7.0 Hz, 6H); (**11k**) $\delta$ = 4.01 (br s, 2H), 3.91

(s, 2H), 2.90 (sept, *J* = 7.1 Hz, 1H), 1.90 (s, 3H), 1.41 (s, 9H), 1.13 (d, *J* = 7.3 Hz, 6H); $^{13}$C NMR (100 MHz, $CDCl_3$): (**6k**) $\delta$ = 193.7, 160.9 (br),^ 154.2, 128.4, 80.6, 51.3 (br), 42.0 (br), 30.6, 28.3 (3C), 19.7 (2C), 9.4; (**11k**) $\delta$ = 192.5, 154.0, 151.7 (br),^ 138.8, 80.6, 51.8 (br), 48.0 (br), 28.3 (3C), 27.0, 20.2 (2C), 17.8; IR (neat): $\tilde{\nu}$ = 2971 (m), 2932 (w), 2874 (w), 1697 (s), 1671 (s), 1628 (m), 1419 (m), 1392 (m), 1382 (m), 1364 (s), 1318 (m), 1281 (m), 1242 (s), 1205 (w), 1159 (s), 1125 (s), 1061 (w), 970 (w), 926 (w), 899 (m), 859 (w), 766 (m), 684 (w) $cm^{-1}$; HRMS (ESI): calcd for ($C_{14}H_{23}NO_3$ + Na): 276.1576; found: 276.1575.

($^1$H NMR: 47°C; $^{13}$C APT NMR (d = 2) and $^{13}$C CPD NMR (d = 4): 45°C);

^ Carbon marked with an asterisk appears as a very broad peak in $^{13}$C CPD NMR spectrum and is not visible in the $^{13}$C APT NMR spectrum. However, HMBC correlations are visible which confirms the $^{13}$C CPD NMR.

**Compound 6l**

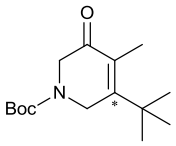


Colourless oil (64 mg, 87% from 47 mg of **7** using method **II**): $^1$H NMR (500 MHz, $CDCl_3$): $\delta$ = 4.20 (br s, 2H), 4.00 (s, 2H), 1.95 (t, *J* = 1.7 Hz, 3H), 1.44 (s, 9H), 1.26 (s, 9H); $^{13}$C NMR (100 MHz, $CDCl_3$): $\delta$ = 194.9, {162.4},^ 154.2, 130.4, 80.7, 50.9 (br), 44.9 (br), 36.9, 29.1 (3C), 28.3 (3C), 13.2; IR (neat): $\tilde{\nu}$ = 2974 (w), 1698 (s), 1676 (s), 1606 (w), 1477 (w), 1421 (m), 1367 (m), 1288 (w), 1249 (m), 1234 (w), 1167 (s), 1124 (m), 1072 (w), 1039 (w), 1020 (w), 972 (w), 901 (w), 858 (w), 766 (w) $cm^{-1}$; HRMS (ESI): calcd for ($C_{15}H_{25}NO_3$ + Na): 290.1732; found: 290.1740; elemental analysis (%) calcd for $C_{15}H_{25}NO_3$: C 67.38, H 9.42, N 5.24; found: C 66.86, H 9.70, N 4.78.

($^{13}$C APT NMR (d = 10): 32°C)

^ Carbon marked with an asterisk is not visible in the $^{13}C$ APT NMR spectrum but its chemical shift could be determined by HMBC correlation and is indicated in brackets.

**Compound 6m**

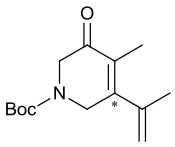


Colourless oil (56 mg, 77% from 47 mg of **7** using method **II**): $^{1}H$ NMR (500 MHz, $CDCl_3$): $\delta$ = 5.10 (s, 1H), 4.84 (br s, 1H), 4.12 (s, 2H), 4.02 (s, 2H), 2.26 (q, *J* = 7.4 Hz, 2H), 1.91 (s, 3H), 1.44 (s, 9H), 0.95 (t, *J* = 7.4 Hz, 3H); $^{13}C$ NMR (100 MHz, $CDCl_3$): $\delta$ = 193.4, 156.5 (br),^ 154.2, 141.4, 134.7, 115.2, 80.8, 51.5 (br), 46.1 (br), 28.3 (3C), 21.8, 19.4, 14.2; IR (neat): $\tilde{\nu}$ = 2976 (w), 2935 (w), 2876 (w), 1699 (s), 1679 (s), 1620 (w), 1477 (w), 1416 (m), 1394 (m), 1366 (s), 1336 (w), 1276 (w), 1237 (s), 1166 (s), 1132 (s), 1085 (w), 1056 (w), 1011 (w), 981 (w), 905 (m), 865 (w), 768 (w) $cm^{-1}$; HRMS (ESI): calcd for ($C_{15}H_{23}NO_3$ + Na): 288.1576; found: 288.1582; elemental analysis (%) calcd for $C_{15}H_{23}NO_3$: C 67.90, H 8.74, N 5.28; found: C 67.66, H 8.83, N 5.27.

($^{1}H$ NMR: 45°C, $^{13}C$ APT NMR (d = 2): 45°C)

^ Carbon marked with an asterisk appears as a very broad peak in $^{13}C$ CPD NMR spectrum and is not visible in the $^{13}C$ APT NMR spectrum. However, HMBC correlations are visible which confirms the $^{13}C$ CPD NMR.

**Compound 11m**

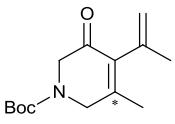


Colourless oil (8 mg, 11% from 50 mg of **7** using method **II**): $^{1}H$ NMR (500 MHz, $CDCl_3$): $\delta$ = 5.19 (s, 1H), 4.72 (s, 1H), 4.18 (br s, 2H), 4.05 (s, 2H), 2.31 (q, *J* = 7.6 Hz, 2H), 1.84 (s, 3H), 1.47 (s, 9H), 1.12 (t, *J* = 7.6 Hz, 3H); $^{13}C$ NMR (100 MHz, $CDCl_3$): $\delta$ = 192.1, {157.9},^ 154.2, 139.4, 137.5,

116.6, 80.9, 51.5 (br), 45.3 (br), 28.4 (3C), 26.1, 23.3, 13.0; IR (neat): ṽ = 2976 (w), 1699 (s), 1678 (s), 1622 (w), 1419 (m), 1367 (m), 1326 (w), 1244 (m), 1163 (s), 1115 (w), 1018 (w), 888 (w), 768 (w) $cm^{-1}$; HRMS (ESI): calcd for ($C_{15}H_{23}NO_3$ + Na): 288.1576; found: 288.1584.

($^1$H NMR: 45°C, $^{13}$C APT NMR (d = 2): 45°C)

^ Carbon marked with an asterisk is not visible in the $^{13}$C APT NMR spectrum but its chemical shift could be determined by HMBC correlation and is indicated in brackets.

**Compound 6n and 11n**

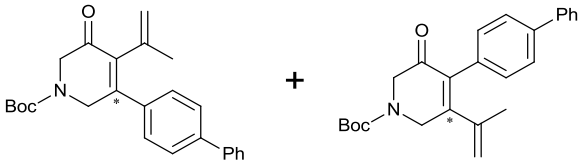


Yellow oil (69 mg, 86% from 35 mg of **7** using method **II**), inseparable mixture of regioisomers (**6n**/**11n** = 60:40): $^1$H NMR (500 MHz, $CDCl_3$): $\delta$ = 7.62 – 7.56 (m, 6H), 7.54 (d, *J* = 8.2 Hz, 2H), 7.46 – 7.28 (m, 8H), 7.23 (m, 1.5H), 5.12 – 5.07 (m, 1.7H), 5.05 (s, 0.7H), 4.71 (s, 1H), 4.49 (br s, 2H), 4.40 (br s, 1.3H), 4.23 (s, 1.3H), 4.20 (s, 2H), 1.77 (s, 3H), 1.62 (s, 2H), 1.53–1.48 (m, 17H); $^{13}$C NMR (100 MHz, $CDCl_3$):~ δ = *192.4*, 192.2, *157.0* (br),^ 154.2, 153.2 (br),^ 141.8, *141.7*, *140.8*, *140.6*, 140.1, 138.4, 138.0, 136.3, *134.2*, *133.0*, *130.4*, 128.8, *128.7*, 128.0, *127.7*, *127.3*, *127.04*, 127.01, *126.97*, 126.5, 119.2, *118.6*, 81.1, 51.7 (br) , 47.7 (br), *47.0* (br), 28.4 (3C), 23.3, *21.8*; IR (neat): ṽ = 3031 (w), 2977 (w), 2932 (w), 2251 (w), 1677 (s), 1601 (w), 1553 (w), 1519 (w), 1487 (w), 1393 (m), 1365 (s), 1323 (m), 1283 (w), 1240 (m), 1156 (s), 1113 (m), 1072 (w), 1029 (w), 1008 (w), 996 (w), 908 (m), 866 (w), 836 (m), 765 (s), 729 (s), 696 (s) $cm^{-1}$; HRMS (ESI): calcd for ($C_{25}H_{27}NO_3$ + Na): 412.1889; found: 412.1880.

(1H NMR: 47°C; $^{13}$C APT NMR (d = 2) and $^{13}$C CPD NMR (d = 4): 45°C)

~Peaks common to **6n** and **11n** are underlined, peaks attributed to **11n** are indicated in italic.

^ Carbon appears as a very broad peak in $^{13}$C CPD NMR spectrum and is not visible in the $^{13}$C APT NMR spectrum.

**Compound 6o**

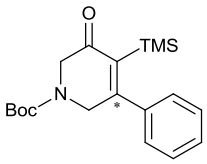


Colourless oil (183 mg, 91% from 100 mg of **7** using method **II**): $^{1}$H NMR (500 MHz, $CDCl_3$): $\delta$ = 7.42–7.34 (m, 3H), 7.27–7.20 (m, 2H), 4.29 (br s, 2H), 4.07 (s, 2H), 1.48 (s, 9H), -0.15 (s, 9H); $^{13}$C NMR (100 MHz, $CDCl_3$): $\delta$ = 197.7, 168.0 (br),^ 154.2, 139.3, 137.5, 129.3, 128.4 (2C), 127.8 (2C), 80.8, 51.3 (br), 49.3 (br), 28.3 (3C), 0.3; IR (neat): $\tilde{\nu}$ = 3053 (w), 2977 (w), 2897 (w), 1697 (s), 1665 (s), 1604 (w), 1582 (m), 1477 (w), 1408 (m), 1365 (m), 1242 (s), 1223 (m), 1160 (s), 1077 (w), 1024 (w), 999 (w), 940 (w), 927 (w), 905 (m), 842 (s), 759 (s), 700 (s) cm$^{-1}$; MS (ESI): calcd for ($C_{19}H_{27}NO_3Si$ + Na): 368.1658; found: 368.1662; elemental analysis (%) calcd for $C_{19}H_{27}NO_3Si$: C 66.05, H 7.88, N 4.05; found: C 65.82, H 7.96, N 3.86.

($^{13}$C APT NMR (d = 2): 40°C);

^ Carbon marked with an asterisk appears as a very broad peak in $^{13}$C CPD NMR spectrum and is not visible in the $^{13}$C APT NMR spectrum. However, HMBC correlations are visible which confirms the $^{13}$C CPD NMR.

**Compound 11o**

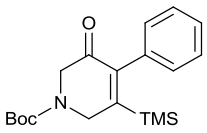


Colourless oil (5 mg, 3% using method **I**). $^{1}$H NMR (500 MHz, $CDCl_3$): δ = 7.35–7.31 (m, 3H), 7.08–7.04 (m, 2H), 4.35 (br s, 2H), 4.19 (s, 2H), 1.48 (s, 9H), -0.12 (s, 9H); IR (neat): $\tilde{\nu}$ = 2976 (w), 1686 (s), 1477 (w), 1412 (m), 1366 (m), 1307 (w), 1250 (m), 1160 (s), 1109 (w), 1062 (w), 927 (w), 841 (m), 759 (m), 701 (m) cm$^{-1}$; MS (ESI): calcd for ($C_{19}H_{27}NO_3Si$ + Na): 368.1658; found: 368.1660

**Compound 6p**

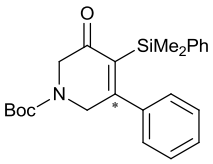


Colourless oil (108 mg, 91% from 48 mg of **7** using method **II**): $^{1}$H NMR (500 MHz, $CDCl_3$): $\delta$ = 7.50 – 7.43 (m, 2H), 7.38 – 7.31 (m, 1H), 7.31 – 7.24 (m, 5H), 7.20 – 7.08 (m, 2H), 4.32 (br s, 2H), 4.09 (s, 2H), 1.49 (s, 9H), 0.04 (s, 6H); $^{13}$C NMR (100 MHz, $CDCl_3$): $\delta$ = 197.5, 169.0 (br),^ 154.3, 139.0, 138.9, 136.4, 133.9, 129.4, 128.6, 128.3, 128.0, 127.5, 80.9, 51.5, 49.5, 28.4, -1.0; IR (neat): $\tilde{\nu}$ = cm$^{-1}$; HRMS (ESI): calcd for $(C_{24}H_{29}NO_3Si + Na)^+$: 430.1814; found: 430.1813

^ Carbon marked with an asterisk appears as a very broad peak in $^{13}$C CPD NMR spectrum and is not visible in the $^{13}$C APT NMR spectrum. However, HMBC correlations are visible which confirms the $^{13}$C CPD NMR.

**Compound 11p**

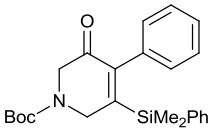


Colourless oil (6 mg, 5% from 48 mg of **7** using method **II**): $^{1}$H NMR (500 MHz, $CDCl_3$): $\delta$ = 7.40 – 7.20 (m, 8H), 6.97 (d, $J$ = 7.0 Hz, 2H), 4.28 (br s, 2H), 4.16 (s, 2H), 1.45 (s, 9H), 0.08 (s, 6H); IR (neat): $\tilde{\nu}$ = 2976 (w), 1685 (s), 1491 (w), 1477 (w), 1427 (m), 1365 (m), 1242 (m), 1157 (s), 1110 (m), 1061 (m), 925 (w), 846 (m), 831 (m), 808 (m), 779 (m), 736 (w), 699 (s) cm$^{-1}$; HRMS (ESI): calcd for $(C_{24}H_{29}NO_3Si + Na)^+$: 430.1814; found: 430.1808

**Compound 6q and 11q**

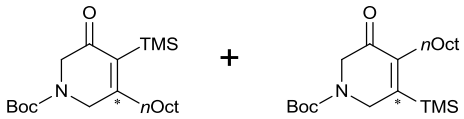

Colourless oil (55 mg, 80% from 30 mg of **7** following method **II** except that 1.5 equiv of alkyne was used), inseparable mixture of regioisomers (**6q**/**11q** = 80:20): $^{1}$H NMR (500 MHz, $CDCl_3$): $\delta$ = 4.16 (br s, 0.33H), 4.05 (br s, 1.6H), 4.00 (s, 0.33H), 3.92 (s, 1.6H), 2.35–2.27 (m, 2H), 1.54–1.41 (m, 1H), 1.45 (s, 9H), 1.39–1.19 (m, 11H), 0.90–0.82 (m, 3H), 0.24 (s, 1.6H), 0.21 (s, 7.4H); $^{13}$C NMR (100 MHz, $CDCl_3$):* $\delta$ = 197.5, *192.6*, *154.3*, {170.4},^ {*155.2*},^ 154.2, *146.0*, 135.1, 80.67, *80.65*, *51.9* (br), 51.3 (br), 47.1 (br), *46.5* (br), 35.6, *31.83*, 31.77, *30.1*, *30.0*, *29.9*, 29.8, 29.5, 29.4, *29.2*, 29.1, 28.4 (3C), 22.6, 14.0, *1.3* (3C), -0.5 (3C); IR (neat): $\tilde{\nu}$ = 2954 (m), 2928 (s), 2856 (m), 1702 (s), 1665 (m), 1590 (w), 1412 (w), 1368 (m), 1248 (s), 1159 (s), 904 (w), 844 (s), 768 (w) $cm^{-1}$; MS (ESI): calcd for ($C_{21}H_{39}NO_3Si$ + Na): 404.2597; found: 404.2601.

($^{1}$H NMR: 47°C; $^{13}$C APT NMR (d = 2) and $^{13}$C CPD NMR (d = 4): 45°C)

* Peaks common to **6q** and **11q** are underlined, peaks attributed to **6l** are indicated in italic.

^ Carbon marked with an asterisk is not visible in the $^{13}$C APT NMR spectrum but its chemical shift could be determined by HMBC correlation and is indicated in brackets.

**Compounds 6t**

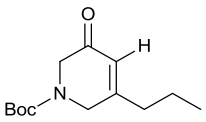

Colourless oil (21 mg, 44% from 49 mg of **7** using method **II**): This compound has not been fully characterised but the assignment of the isolated isomer is based on the proton of 2-cyclohexen-1-one.; $^{1}$H NMR (500 MHz, $CDCl_3$): $\delta$ = 5.97 (s, 1H), 4.09 (br s, 2H), 4.01 (s, 2H), 2.21 (t, $J$ = 7.4 Hz, 2H), 1.56 (sext, $J$ = 7.4 Hz, 2H), 1.44 (s, 9H), 0.94 (t, $J$ = 7.3 Hz, 3H)

**Compounds 6y and 11y**

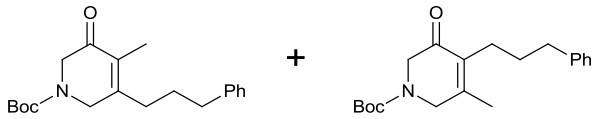

Colourless oil (43 mg, 75% from 30 mg of **7** following method **II**), inseparable mixture of regioisomers (**6y**/**11y** = 58:42), this compound has not been fully characterised but the assignment of the two isomers is based on the proton of **6k**/**11k**: $^{1}$H NMR (500 MHz, $CDCl_3$): (**6y**) $\delta$ = 7.35 – 7.16 (m, 5H), 4.15 (br s, 2H), 4.07 (s, 2H), 2.71 (t, *J* = 7.5 Hz, 2H), 2.34 – 2.27 (m, 2H), 1.87 (pent, *J* = 7.9 Hz, 2H), 1.78 (s, 3H), 1.49 (s, 9H); (**11y**) $\delta$ = 7.35 – 7.16 (m, 5H), 4.12 (br s, 2H), 4.06 (s, 2H), 2.66 (t, *J* = 7.8 Hz, 2H), 2.41 – 2.34 (m, 2H), 1.91 (s, 3H), 1.69 (pent, *J* = 7.9 Hz, 2H), 1.49 (s, 9H)

**Compounds 6z and 11z**

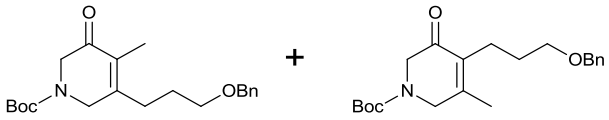

Colourless oil (57 mg, 91% from 30 mg of **7** following method **II**), inseparable mixture of regioisomers (**6z**/**11z** = 55:45): $^{1}$H NMR (500 MHz, $CDCl_3$): (**6z**) $\delta$ = 7.36 – 7.20 (m, 5H), 4.48 (s, 2H), 4.12 (br s, 2H), 4.01 (s, 2H), 3.48 (t, *J* = 6.0 Hz, 2H), 2.44 – 2.34 (m, 2H), 1.86 – 1.75 (m, 5H), 1.45 (s, 9H); (**11z**) $\delta$ = 7.36 – 7.20 (m, 5H), 4.46 (s, 2H), 4.08 (s, 2H), 3.44 (t, *J* = 6.2 Hz, 2H), 2.44 – 2.34 (m, 2H), 1.94 (s, 3H), 1.71 – 1.61 (m, 2H), 1.46 (s, 9H); $^{13}$C NMR (100 MHz, $CDCl_3$): $\delta$ = 193.3, 192.5, 154.1, 138.7, 138.3, 134.0, 130.1, 128.4, 128.3, 127.6, 127.6, 127.5, 127.4, 80.7, 80.7, 73.0, 72.8, 70.0, 69.4, 51.1, 47.7, 46.3, 29.3, 28.7, 28.3, 27.7, 21.5, 18.0, 9.9; IR (neat): $\tilde{\nu}$ = 2976 (w), 1930 (w), 2860 (w), 1698 (s), 1673 (s), 1641 (m), 1496 (w), 1454 (m), 1420 (s), 1365 (m), 1328 (w), 1282 (w), 1242 (m), 1168 (m), 1134 (m), 1102 (m), 1029 (w), 899 (w), 738 (m), 698 (m) cm$^{-1}$; MS (ESI): calcd for ($C_{21}H_{29}NO_4$ + Na): 382.1994; found: 382.2004.

($^{1}$H NMR and $^{13}$C APT NMR (d = 2): 40°C)

**Compound 6aa**

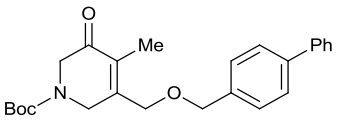


This product was made by Jet-Sing Lee: $^{1}$H NMR (400Mz, $CDCl_3$): $\delta$ = 7.60-7.54 (m, 5H), 7.45-7.37 (m, 5H), 7.36-7.31 (m, 1H), 4.58 (s, 2H), 4.33 (s, 2H), 4.29 (s, 2H), 4.08 (s, 2H), 1.79 (s, 3H), 1.47 (s, 9H); $^{13}$C NMR (100 MHz, $CDCl_3$): $\delta$ = 193.3, 154.1, 141.0, 140.7, 130.4, 128.7, 128.1, 127.3, 127.2, 127.0 80.7, 72.9, 68.2, 44.4, 28.3 (3C), 9.8; HRMS (ES+): calcd for ($C_{29}H_{25}NO_4$ + Na): 430.5; found: 430.2.

**Compound 11aa**

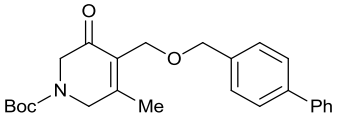


This product was made and characterised by Jet-Sing Lee. $^{1}$H NMR (400Mz, $CDCl_3$): $\delta$ = 7.63-7.58 (m, 4H), 7.48-7.42 (m, 4H), 7.38-7.33 (m, 1H), 4.60 (s, 2H), 4.35 (s, 2H), 4.20 (s, 2H), 4.11 (s, 2H), 2.10 (s, 3H), 1.50 (s, 9H); $^{13}$C NMR (100 MHz, $CDCl_3$): $\delta$ = 191.8, 140.9, 140.7, 137.2, 128.7 (2C), 128.4 (2C), 127.2, 127.1 (2C), 127.1 (2C), 81.0, 72.8, 61.5, 29.7, 28.3 (3C), 18.2; HRMS (ES+): calcd for ($C_{29}H_{25}NO_4$ + Na): 430.5; found: 430.2.

**Compound 54**

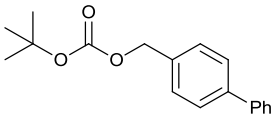


Colourless oil (6 mg, 49% from 10 mg of **7** using method **I** except with 30 mol% $Ni(cod)_2$ and 90 mol% $PPhCy_2$): $^{1}$H NMR (500 MHz, $CDCl_3$): $\delta$ = 7.60 – 7.54 (m, 4H), 7.46 – 7.39 (m, 4H), 7.36 – 7.31 (m, 1H), 5.12 (s, 2H), 1.49 (s, 9H); $^{13}$C NMR (100 MHz, $CDCl_3$): $\delta$ = 153.5, 141.3, 140.7,

134.6, 128.8, 128.7, 127.4, 127.3, 127.1, 82.3, 68.4, 27.8; HRMS (ESI): calcd for ($C_{18}H_{20}O_3$ + Na): 307.1310; found: 307.1305

**Compound 70b**

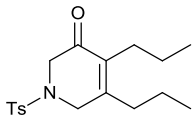


White solid (21 mg, 73% from **69** (19 mg, 0.09 mmol) using method **I**, except that 1.5 equiv of alkyne was used and that the oil bath temperature was set at 110 °C): m.p: 51–55 °C; $^1$H NMR (500 MHz, $CDCl_3$): $\delta$ = 7.62 (d, $J$ = 8.0 Hz, 2H), 7.30 (d, $J$ = 8.0 Hz, 2H), 3.83 (s, 2H), 3.70 (s, 2H), 2.40 (s, 3H), 2.19–2.13 (m, 2H), 2.12–2.07 (m, 2H), 1.51–1.40 (m, 2H), 1.20–1.08 (m, 2H), 0.94 (t, $J$ = 7.5 Hz, 3H), 0.82 (t, $J$ = 7.5 Hz, 3H); $^{13}$C NMR (125 MHz, $CDCl_3$): $\delta$ = 191.2, 153.8, 144.2, 134.7, 132.8, 130.0 (2C), 129.7 (2C), 52.5, 47.8, 34.4, 26.5, 22.4, 21.5, 21.3, 14.3, 14.2; IR (neat): $\tilde{\nu}$ = 2961 (m), 2872 (w), 1675 (s), 1630 (w), 1598 (w), 1447 (w), 1350 (s), 1244 (w), 1165 (s), 1138 (w), 1090 (m), 1038 (w), 1010 (w), 964 (m), 815 (w), 672 (m) cm$^{-1}$; HRMS (ESI): calcd for ($C_{18}H_{25}NO_3S$ + Na): 358.1453; found: 358.1456; elemental analysis (%) calcd for $C_{18}H_{25}NO_3S$: C 64.45, H 7.51, N 4.18; found: C 64.02, H 7.60, N 3.93.

**Compound 70c**

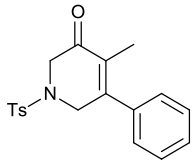


Colourless oil (23 mg, 62% from **69** (25 mg, 0.11 mmol) using method **I**, except that 1.5 equiv of alkyne was used and that the oil bath temperature was set at 100 °C); $^1$H NMR (500 MHz, $CDCl_3$): $\delta$ = 7.65 (d, $J$ = 8.0 Hz, 2H), 7.44 – 7.36 (m, 3H), 7.31 (d, $J$ = 8.1 Hz, 2H), 7.19 – 7.15 (m, 2H), 4.12 (s, 2H), 3.86 (s, 2H), 2.40 (s, 3H), 1.60 (s, 3H); $^{13}$C NMR (125 MHz, $CDCl_3$): $\delta$ = 192.1, 151.4, 144.3, 136.5, 132.7, 131.1, 130.0 (2C), 129.2, 128.7 (2C), 127.7 (2C), 127.6 (2C), 52.5,

49.5, 21.5, 11.9; IR (neat): ṽ = 3058 (w), 2925 (w), 1679 (s), 1633 (w), 1598 (w), 1493 (w), 1443 (w), 1350 (s), 1327 (m), 1252 (w), 1165 (s), 1118 (w), 1089 (w), 1023 (w), 988 (w), 951 (w), 917 (w), 867 (w), 816 (w), 804 (w), 793 (w), 765 (w), 702 (m), 669 (s) $cm^{-1}$; MS (ESI): calcd for ($C_{19}H_{19}NO_3S$ + Na): 364.0983; found: 364.0992.

**Compound 71c**

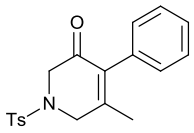


Colourless oil (5 mg, 13% from **69** (25 mg, 0.11 mmol) using method **I**, except that 1.5 equiv of alkyne was used and that the oil bath temperature was set at 100 °C); $^1$H NMR (500 MHz, $CDCl_3$): $\delta$ = 7.69 (d, *J* = 8.0 Hz, 2H), 7.35 (d, *J* = 8.0 Hz, 2H), 7.34–7.26 (m, 3H), 6.85–6.77 (m, 2H), 4.05 (s, 2H), 3.93 (s, 2H), 2.44 (s, 3H), 1.77 (s, 3H);$^{13}$C NMR (125 MHz, $CDCl_3$): $\delta$ = 189.8, 152.0, 144.4, 136.6, 133.3, 132.8, 130.1 (2C), 129.6 (2C), 128.1 (2C), 127.8, 127.7 (2C), 52.7, 49.4, 21.5, 19.7; IR (neat): ṽ = 2924 (w), 1677 (m), 1634 (w), 1598 (w), 1495 (w), 1443 (w), 1380 (w), 1349 (m), 1307 (w), 1187 (w), 1162 (s), 1092 (w), 1030 (w), 954 (w), 933 (w), 836 (w), 816 (w), 787 (w), 762 (w), 688 (w), 671 (w) $cm^{-1}$; HRMS (ESI): calcd for ($C_{19}H_{19}NO_3S$ + Na): 364.0983; found: 364.0986.

**Compound 73a**

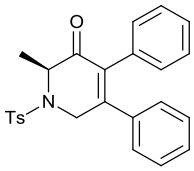


Colourless oil (32 mg, 92% from **72** (20 mg, 0.08 mmol) using method **I**, except that 1.5 equiv of alkyne was used and that the oil bath temperature was set at 110 °C); $^1$H NMR (500 MHz, $CDCl_3$): $\delta$ = 7.71 (d, *J* = 8.3 Hz, 2H), 7.28 (d, *J* = 8.2 Hz, 2H), 7.22 – 7.13 (m, 3H), 7.10 – 7.00 (m,

3H), 6.93 – 6.88 (m, 2H), 6.43 (d, *J* = 6.9 Hz, 2H), 4.87 (d, *J* = 20.4 Hz, 1H), 4.72 (q, *J* = 7.3 Hz, 1H), 4.40 (d, *J* = 20.4 Hz, 1H), 2.38 (s, 3H), 1.53 (d, *J* = 1.53 Hz, 3H); $^{13}$C NMR (125 MHz, $CDCl_3$): $\delta$ = 194.0, 150.9, 144.1, 136.5, 136.0, 134.5, 132.9, 130.4, 130.1, 129.0, 128.3, 128.2, 127.5, 127.3, 127.1, 57.0, 45.2, 21.4, 15.8; IR (neat): ṽ = 3057 (w), 2983 (w), 1673 (s), 1624 (w), 1597 (w), 1491 (w), 1375 (s), 1351 (m), 1335 (s), 1241 (w), 1157 (s), 1086 (m), 1043 (m), 985 (w), 921 (w), 867 (w), 819 (m), 769 (m), 757 (m), 738 (m) $cm^{-1}$

**Compound 73b**

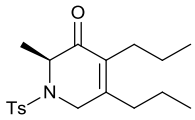


Colourless oil (32 mg, 91% from **72** (25mg, 0.10 mmol) using method **I**, except that 1.5 equiv of alkyne was used and that the oil bath temperature was set at 110°C); enantiomeric excess = 97%.[50] $[\alpha]_D^{20}$ = 59.1 (c = 2.7 in CHCl3); $^1$H NMR (500 MHz, $CDCl_3$): $\delta$ = 7.57 (d, *J* = 8.3 Hz, 2H), 7.20 (d, *J* = 8.0 Hz, 2H), 4.43 (q, *J* = 7.2Hz, 1H), 4.30 (d, *J* = 19.8 Hz, 1H), 3.94 (d, *J* = 19.8 Hz, 1H), 2.35 (s, 3H), 2.12 (ddd, *J* = 10.0 Hz, 9.3 Hz, 6.0 Hz, 1H), 2.07–2.01 (m, 1H), 2.00–1.88 (m, 2H), 1.51–1.40 (m, 1H), 1.39– 1.30 (m, 1H), 1.25 (d, *J* = 7.3 Hz, 3H), 1.03–0.92 (m, 1H), 0.91 (t, *J* = 7.4 Hz, 3H), 0.90–0.82 (m, 1H), 0.73 (t, *J* = 7.3 Hz, 3H); $^{13}$C NMR (125 MHz, $CDCl_3$): $\delta$ = 194.8, 152.2, 143.7, 136.5, 133.1, 129.8 (2C), 127.0 (2C), 56.5, 43.7, 33.9, 26.4, 22.4, 21.4, 21.4, 15.7, 14.3, 14.1; IR (neat): ṽ = 2961 (m), 2932 (w), 2872 (w), 1671 (s), 1630 (w), 1598 (w), 1457 (w), 1380 (w), 1350 (m), 1335 (m), 1240 (w), 1206 (w), 1161 (s), 1092 (m), 1037 (w), 1011 (w), 912 (m), 815 (w), 708 (w), 666 (m) $cm^{-1}$; HRMS (ESI): calcd for ($C_{19}H_{27}NO_3S$ + Na): 372.1609; found: 372.1618.

**Compound 73c**

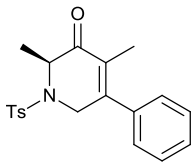


Colourless oil (27 mg, 93% from **72** (20 mg, 0.08 mmol) using method **I**, except that 1.5 equiv of alkyne was used and that the oil bath temperature was set at 100 °C); $^{1}$H NMR (400 MHz, $CDCl_3$): $\delta$ = 7.65 (d, $J$ = 8.2 Hz, 2H), 7.43 – 7.35 (m, 3H), 7.28 – 7.22 (m, 2H), 7.13 – 7.07 (m, 2H), 4.65 – 4.52 (m, 2H), 4.22 – 4.12 (m, 1H), 2.37 (s, 3H), 1.44 (s, 3H), 1.36 (d, $J$ =7.3 Hz, 3H); $^{13}$C NMR (100 MHz, $CDCl_3$): $\delta$ = 195.6, 150.1, 143.8, 136.4, 136.4, 129.8, 129.4, 129.1, 128.7, 127.4, 127.1, 56.7, 45.2, 21.5, 15.5, 11.9; IR (neat): $\tilde{\nu}$ = 3058 (w), 2926 (w), 1673 (s), 1597 (w), 1442 (m), 1351 (m), 1332 (s), 1187 (w), 1162 (s), 1091 (w), 1028 (m), 1002 (m), 906 (w), 815 (w), 764 (m), 702 (m) $cm^{-1}$

**Compound 74c**

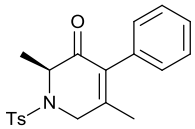


Colourless oil (1.9 mg, 7% from **72** (20 mg, 0.08 mmol) using method **I**, except that 1.5 equiv of alkyne was used and that the oil bath temperature was set at 100 °C); $^{1}$H NMR (400 MHz, $CDCl_3$): $\delta$ = 7.66 (d, $J$ = 8.2 Hz, 2H), 7.28 (d, $J$ = 8.1 Hz, 2H), 7.26 – 7.20 (m, 3H), 6.59 – 6.52 (m, 2H), 4.59 (q, $J$ = 7.3 Hz, 1H), 4.45 (d, $J$ = 20.0 Hz, 1H), 4.14 (d, $J$ = 20.1 Hz, 1H), 2.42 (s, 3H), 1.67 (s, 3H), 1.42 (d, $J$ = 7.3 Hz, 3H); $^{13}$C NMR (100 MHz, $CDCl_3$): $\delta$ = 193.2, 150.3, 144.0, 136.9, 135.2, 133.3, 130.1, 129.6, 128.0, 127.7, 127.1, 57.0, 45.4, 21.4, 19.1, 15.8; IR (neat): $\tilde{\nu}$ = 2984 (w), 2932 (w), 1675 (m), 1663 (w), 1597 (w), 1495 (w), 1443 (w), 1381 (w), 1353 (m), 1333 (m), 1160 (s), 1104 (m), 1059 (m), 1004 (m), 877 (w), 702 (w), 687 (w), 665 (m) $cm^{-1}$; HRMS (ESI): calcd for $(C_{20}H_{21}NO_3S + Na)^+$: 378.1140; found: 378.1154

**Compound 73o**

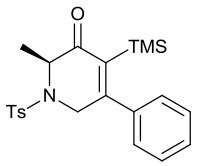


Colourless oil (25 mg, 71% from **72** (20 mg, 0.18 mmol) using method **I**, except that 1.5 equiv of alkyne was used and that the oil bath temperature was set at 110 °C); $^{1}$H NMR (500 MHz, $CDCl_3$): $\delta$ = 7.68 (d, *J* = 8.3 Hz, 2H), 7.42 – 7.34 (m, 3H), 7.26 (d, *J* = 8.1 Hz, 2H), 7.12 – 7.07 (m, 2H), 4.59 (d, *J* = 20.6 Hz, 1H), 4.46 (q, *J* = 7.2 Hz, 1H), 4.06 (d, *J* = 20.6 Hz, 1H), 2.36 (s, 3H), 1.36 (d, *J* = 7.3 Hz, 3H), -0.38 (s, 9H); $^{13}$C NMR (125 MHz, $CDCl_3$): $\delta$ = 198.8, 164.4, 143.9, 138.4, 136.5, 136.4, 130.0, 129.5, 128.5, 127.6, 127.1, 56.5, 46.7, 21.4, 15.8, 0.1; IR (neat): $\tilde{\nu}$ = 3060 (w), 2954 (w), 2897 (w), 1662 (m), 1581 (w), 1490 (w), 1429 (w), 1351 (m), 1325 (w), 1247 (m), 1161 (s), 1105 (w), 1042 (w), 990 (w), 902 (w), 838 (s), 773 (m), 700 (m), 667 (s) $cm^{-1}$; MS (ESI): calcd for ($C_{22}H_{27}NO_3SiS$ + Na): 436.1379; found: 436.1378.

**Compound 88a**

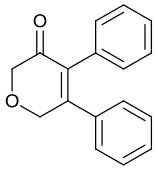


White solid (64 mg, 82% from commercially available **87** (20 µL, 0.31 mmol) using method **I**); m.p. 100–103 °C; $^{1}$H NMR (500 MHz, $CDCl_3$): $\delta$ = 7.22–7.15 (m, 6H), 7.09–6.99 (m, 4H), 4.76 (s, 2H), 4.38 (s, 2H); $^{13}$C NMR (125 MHz, $CDCl_3$): $\delta$ = 193.3, 155.3, 135.4, 134.6, 132.7, 130.7 (2C), 128.9, 128.4 (2C), 128.3 (2C), 127.8 (2C), 127.4, 71.2, 69.5; IR (neat): $\tilde{\nu}$ = 3056 (w), 3023 (w), 2969 (w), 2853 (w), 2816 (w), 1678 (s), 1613 (w), 1596 (w), 1573 (w), 1491 (w), 1443 (w), 1380 (w), 1327 (m), 1280 (w), 1250 (w), 1195 (w), 1141 (m), 1080 (w), 1052 (w), 1038 (w), 1027 (w), 1001 (w), 967 (w), 932 (w), 912 (w), 868 (w), 755 (m), 720 (w), 696 (s) $cm^{-1}$; HRMS (ESI): calcd

for ($C_{17}H_{14}O_2$ + Na): 273.0891; found: 273.0890; elemental analysis (%) calcd for $C_{17}H_{14}O_2$: C 81.58, H 5.64; found: C 80.98, H 5.73.

**Compound 88g**

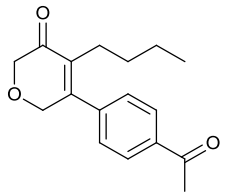

Colourless oil (93 mg, 73% from commercially available **87** (20 µL, 0.47 mmol) using method **II**); $^1$H NMR (500 MHz, $CDCl_3$): $\delta$ = 7.98 (d, *J* = 8.4 Hz, 2H), 7.30 (d, *J* = 8.4 Hz, 2H), 4.47 (s, 2H), 4.20 (s, 2H), 2.59 (s, 3H), 2.22–2.13 (m, 2H), 1.34 – 1.21 (m, 2H), 1.13 (sext, *J* = 7.3 Hz, 2H), 0.71 (t, *J* = 7.2 Hz, 3H); $^{13}$C NMR (125 MHz, $CDCl_3$): $\delta$ = 197.3, 194.3, 153.3, 140.5, 137.0, 135.0, 128.6 (2C), 127.6 (2C), 71.9, 69.3, 31.3, 26.6, 24.9, 22.5, 13.6; IR (neat): $\tilde{\nu}$ = 2958 (w), 2932 (w), 2860 (w), 1683 (s), 1604 (w), 1440 (w), 1403 (w), 1380 (w), 1359 (w), 1338 (w), 1266 (w), 1206 (w), 1151 (w), 1119 (w), 1014 (w), 960 (w), 922 (w), 833 (w) cm$^{-1}$; HRMS (ESI): calcd for ($C_{17}H_{20}O_3$ + Na): 295.1310; found: 295.1311; elemental analysis (%) calcd for $C_{17}H_{20}O_3$: C 74.97, H 7.40; found: C 74.95, H 7.75.

**Compound 89g**

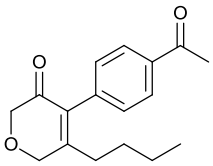

Colourless oil (25 mg, 19% from commercially available **87** (30 µL, 0.47 mmol) using method **II**); $^1$H NMR (500 MHz, $CDCl_3$): $\delta$ = 7.96 (d, *J* = 8.2 Hz, 2H), 7.20 (d, *J* = 8.2 Hz, 2H), 4.46 (s, 2H), 4.24 (s, 2H), 2.59 (s, 3H), 2.14–2.07 (m, 2H), 1.41–1.32 (m, 2H), 1.19 (sext, *J* = 7.4 Hz, 2H), 0.77 (t, *J* = 7.3 Hz, 3H); $^{13}$C NMR (125 MHz, $CDCl_3$): $\delta$ = 197.8, 192.7, 159.7, 138.1, 136.3, 134.4, 130.0 (2C), 128.2 (2C), 72.0, 68.1, 31.5, 30.0, 26.6, 22.6, 13.6; IR (neat): $\tilde{\nu}$ = 2958 (w), 2931 (w),

2862 (w), 2819 (w), 1678 (s), 1626 (w), 1603 (m), 1560 (w), 1466 (w), 1438 (w), 1403 (w), 1384 (w), 1358 (w), 1330 (w), 1265 (s), 1184 (w), 1126 (m), 1088 (w), 1017 (w), 960 (m), 830 (w), 762 (w), 701 (w) $cm^{-1}$; HRMS (ESI): calcd for ($C_{17}H_{20}O_3$ + Na): 295.1310; found: 295.1313; elemental analysis (%) calcd for $C_{17}H_{20}O_3$: C 74.97, H 7.40; found: C 74.74, H 7.42.

**Compound 88o**

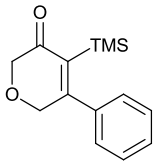


White solid (73 mg, 95% from commercially available **87** (20 µL, 0.31 mmol) using method **II**); m.p. 39–41 °C; $^1$H NMR (500 MHz, $CDCl_3$): $\delta$ = 7.43–7.34 (m, 3H), 7.24–7.18 (m, 2H), 4.41 (s, 2H), 4.13 (s, 2H), -0.13 (s, 9H); $^{13}$C NMR (125 MHz, $CDCl_3$): $\delta$ = 198.1, 169.0, 137.8, 136.2, 129.4, 128.4 (2C), 127.9 (2C), 71.4, 70.3, 0.2 (3C); IR (neat): $\tilde{\nu}$ = 3059 (w), 2952 (w), 2897 (w), 2850 (w), 2812 (w), 1665 (s), 1603 (w), 1581 (w), 1567 (w), 1490 (w), 1443 (w), 1433 (w), 1372 (w), 1288 (m), 1275 (m), 1244 (s), 1216 (w), 1137 (m), 1077 (w), 1053 (w), 1033 (w), 1016 (w), 969 (w), 937 (m), 835 (s), 756 (s), 699 (s), 682 (m) $cm^{-1}$; HRMS (ESI): calcd for ($C_{14}H_{18}O_2Si$+ Na): 269.0974; found: 269.0975; elemental analysis (%) calcd for $C_{14}H_{18}O_2Si$: C 68.25, H 7.36; found: C 68.10, H 7.42.

**Compound 89o**

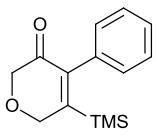


Yellow oil (3 mg, 4% from commercially available **87** using method **II**); $^1$H NMR (500 MHz, $CDCl_3$): $\delta$ = 7.35–7.29 (m, 3H), 7.15–7.05 (m, 2H), 4.53 (s, 2H), 4.25 (s, 2H), -0.13 (s, 9H); $^{13}$C NMR (100 MHz, $CDCl_3$): $\delta$ = 192.4, 159.9, 145.2, 135.7, 130.0 (2C), 128.2, 127.9 (2C), 72.4, 69.1, -1.2 (3C); IR (neat): $\tilde{\nu}$ = 3048 (w), 3028 (w), 2956 (w), 2896 (w), 2851 (w), 2810 (w), 1685 (s),

1492 (w), 1444 (w), 1374 (w), 1312 (w), 1251 (m), 1192 (w), 1138 (m), 1033 (w), 952 (w), 869 (s), 840 (s), 755 (w), 701 (w) $cm^{-1}$; MS (CI): *m*/*z* (rel. intensity): 264 (100) $[M+NH_4]^+$, 247 (55) $[M+H]^+$; HRMS (ESI): calcd for ($C_{14}H_{18}O_2Si$ + Na): 269.0974; found: 269.0967.

**Compound 91**

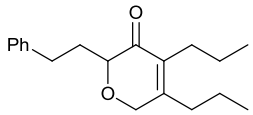


Colourless oil (14 mg, 44% from **90** (20 mg, 0.11 mmol) using method **I**); $^1$H NMR (500 MHz, $CDCl_3$): $\delta$ = 7.29 – 7.23 (m, 2H), 7.22 – 7.13 (m, 3H), 4.30 (apt q, *J* = 17.5 Hz, 2H), 3.85 – 3.79 (m, 1H), 2.82 – 2.64 (m, 2H), 2.30 – 2.08 (m, 5H), 2.01 – 1.91 (m, 1H), 1.49 (sext, *J* = 7.5 Hz, 2H), 1.33 (sext, *J* = 7.4 Hz, 2H), 0.97 (t, *J* = 7.3 Hz, 3H), 0.89 (t, *J* = 7.3 Hz, 3H); $^{13}$C NMR (125 MHz, $CDCl_3$): $\delta$ = 196.0, 155.9, 141.6, 133.2, 128.6, 128.3, 125.8, 78.9, 66.9, 32.6, 31.7, 31.3, 26.3, 22.5, 21.4, 14.3, 14.2; MS (ESI): calcd for ($C_{19}H_{26}O_2$ + Na): 309.1831; found: 309.1827.

**Compound 92**

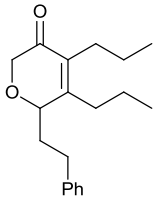


Colourless oil (4 mg, 11% from **90** (20 mg, 0.11 mmol) using method **I**); $^1$H NMR (500 MHz, $CDCl_3$): $\delta$ = 7.31 – 7.26 (m, 2H), 7.22 – 7.16 (m, 3H), 4.26 (d, *J* = 16.6 Hz, 1H), 4.21 (d, *J* = 10.0 Hz, 1H), 4.05 (d, *J* = 17.0 Hz, 1H), 2.90 – 2.81 (m, 1H), 2.81 – 2.68 (m, 1H), 2.35 – 2.27 (m, 1H), 2.27 – 2.16 (m, 2H), 2.09 – 1.86 (m, 3H), 1.52 – 1.42 (m, 1H), 1.40 – 1.29 (m, 3H), 0.96 – 0.86 (m, 6H); $^{13}$C NMR (125 MHz, $CDCl_3$): $\delta$ = 194.5, 159.6, 141.4, 133.6, 128.5, 128.5, 126.1, 74.6, 67.8, 32.7, 32.5, 32.3, 26.4, 22.6, 21.8, 14.4, 14.2. Further analytical data was not obtained.

**Compound 93**

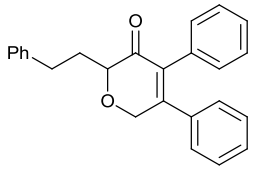


Colourless oil (17 mg, 42% from **90** (20 mg, 0.11 mmol) using method **I**); $^{1}$H NMR (500 MHz, $CDCl_3$): $\delta$ = 7.32 – 7.23 (m, 4H), 7.22 – 7.14 (m, 7H), 7.07 (m, 2H), 7.01 – 6.96 (m, 2H), 4.86 (d, *J* = 18.0 Hz, 1H), 4.70 (dd, *J* = 17.9, 1.3 Hz, 1H), 4.15 – 4.09 (m, 1H), 2.93 – 2.76 (m, 2H), 2.41 – 2.30 (m, 1H), 2.17 – 2.06 (m, 1H); $^{13}$C NMR (125 MHz, $CDCl_3$): $\delta$ = 195.0, 154.7, 141.4, 135.5, 134.4, 133.2, 130.8, 128.8, 128.7, 128.5, 128.4, 128.3, 127.8, 127.3, 126.0, 79.2, 68.4, 31.6, 31.2; IR (neat): $\tilde{\nu}$ = 3059 (w), 3026 (w), 2927 (w), 2861 (w), 2810 (w), 1677 (s), 1598 (w), 1494 (w), 1444 (w), 1327 (m), 1135 (m), 1030 (w), 1002 (w), 945 (w), 756 (m), 697 (s) cm$^{-1}$; MS (ESI): calcd for ($C_{25}H_{22}O_2$ + Na): 377.1517; found: 377.1521.

**Compound 101**

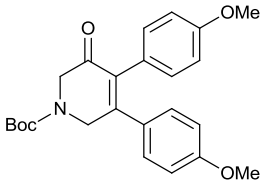


Colourless oil (48 mg, 41% from **7** (49 mg, 0.29 mmol) using method **I**, except that 1.5 equiv of alkyne and 20 mol% of $PhCy_2P$ were used. The reaction was also carried out in toluene and that the oil bath temperature was set at 100 °C)^; $^{1}$H NMR (400 MHz, $CDCl_3$): $\delta$ = 7.05 (d, *J* = 8.7 Hz, 2H), 6.92 (d, *J* = 8.7 Hz, 2H), 6.75 – 6.68 (m, 4H), 5.58 (s, 2H), 4.26 (s, 2H), 3.75 – 3.72 (m, 6H), 1.51 (s, 9H); $^{13}$C NMR (125 MHz, $CDCl_3$): $\delta$ = 192.7, 160.0, 158.8, 154.3,^ 153.9, 132.1, 130.3, 134.6, 129.3, 126.3, 113.8, 113.5, 82.1, 55.2, 55.1, 51.9, 47.8, 28.4; IR (neat): $\tilde{\nu}$ = 2975 (w), 2935 (w), 2837 (w), 1694 (m), 1675 (s), 1605 (m), 1508 (s), 1440 (w), 1366 (m), 1289 (m),

1245 (s), 1157 (s), 1110 (w), 1031 (m), 938 (w), 827 (m) $cm^{-1}$; MS (ESI): calcd for ($C_{xx}H_{xx}NO_xS$ + Na): 432.1787; found: 432.1778.

^ Carbon marked with an asterisk appears as a very broad peak in $^{13}C$ CPD NMR spectrum and is not visible in the $^{13}C$ APT NMR spectrum. However, HMBC correlations are visible which confirms the $^{13}C$ CPD NMR.

($^{13}C$ APT NMR (d = 2): 40°C, $^{13}C$ CPD NMR (d = 4): 40°C)

**Compound 102**

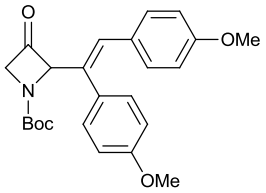


Orange oil (57 mg, 49% from **7** (49 mg, 0.29 mmol) using method **I**, except that 1.5 equiv of alkyne and 20 mol% of $PhCy_2P$ were used. The reaction was also carried out in toluene and that the oil bath temperature was set at 100 °C)^; $^1H$ NMR (500 MHz, $CDCl_3$): $\delta$ = 7.77 – 7.33 (br m, 1H), 7.27 (d, *J* = 8.6 Hz, 2H), 7.18 (d, *J* = 8.7 Hz, 2H), 6.87 – 6.81 (m, 2H), 6.78 (d, *J* = 8.7 Hz, 2H), 4.44 (d, *J* = 1.8 Hz, 1H), 4.18 (br d, *J* = 18.2 Hz, 1H), 3.91 (dd, *J* = 18.8, 2.0 Hz, 1H), 3.76 (s, 3H), 3.74 (s, 3H), 1.52 (s, 9H); $^{13}C$ NMR (125 MHz, $CDCl_3$): $\delta$ = 202.1, 159.5, 159.0, 152.0, 130.2, 128.8, 127.6, 126.4, 123.7, 114.7, 114.2, 82.2, 77.3, 55.5, 55.3, 50.3, 49.6, 28.3; IR (neat): $\tilde{\nu}$ = 2976 (w), 2933 (w), 2837 (w), 1702 (s), 1647 (m), 1607 (m), 1507 (s), 1441 (m), 1370 (s), 1294 (s), 1246 (s), 1152 (s), 1111 (m), 1034 (s), 946 (w), 827 (m), 765 (w) $cm^{-1}$; MS (ESI): calcd for $(C_{24}H_{27}NO_5 + Na)^+$: 432.1787; found: 432.1779.

($^{13}C$ APT NMR (d = 2): 40°C, $^{13}C$ CPD NMR (d = 2): 40°C)

### 2.7.5 Nickel(II): Synthesis of pyridinones

Method **I**. Inside a glovebox, a Teflon-screw flame-dried Schlenk flask equipped with a small stirrer bar was charged with $NiCl_2(PCy_3)_2$ (8.1 mg, 0.0.1 mmol) and zinc (16 mg, 0.58 mmol) and taken out of the glovebox. Under $N_2$, azetidinone **7** (20 mg, 0.12 mmol) and alkyne **5b** (19 µl, 0.73 mmol) were then added. Afterwards, *i*PrOH (0.6 ml) was then added and the flask was sealed and immersed into an oil bath pre-heated at 60°C. After stirring for 17 hours at that temperature, the mixture was allowed to cool and filtered through a silica plug before evaporation. Purification by flash chromatography (PE/EtOAc, 9/1) gave **6b** as colourless oil (23 mg, 72%).

Method **II**. On the bench top, under $N_2$, a flame-dried Schlenk flask equipped with a small stirrer bar was charged with $NiBr_2 \bullet xH_2O$ (38.8 mg, 0.18 mmol) and $PPh_3$ (93 mg, 0.36 mmol) and *iPrOH* (3.6 ml). The suspension was stirred at 60°C for 10 minutes and was then cooled back down to rt. Afterwards, zinc (58 mg, 0.89 mmol), azetidinone **69** (200 mg, 0.89 mmol) and alkyne **5m** (121 µl, 0.98 mmol) were then added. Afterwards, the schlenk was immersed into an oil bath pre-heated at 60°C. After stirring for 17 hours at that temperature, the mixture was allowed to cool and filtered through a silica plug before evaporation. The crude ratio of **120**:**121** is 86:14 as judged by $^1$H NMR analysis. Purification by flash chromatography (PE/EtOAc, 8/1 → 4/1) afforded **120** as a white solid (196 mg, 69%) and **121** as white solid (36 mg, 13%).

**Compound 6b**

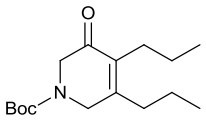


Colourless oil (23 mg, 72%) using method **I**; Full characterisation reported earlier.

**Compound 6c**

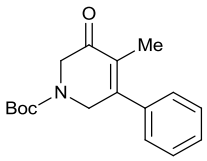


Colourless oil (696 mg, 83% from 500 mg of **6c** using method **I**), except 5 mol% $NiBr_2(PPh_3)_2$ and 50 mol% zinc were used and the oil bath was set at 40°C: Full characterisation reported earlier.

**Compound 121**

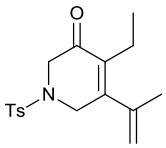


White solid (196 mg, 69%) from **69** (200 mg, 0.89 mmol) using method **II**; $^1$H NMR (500 MHz, $CDCl_3$): $\delta$ = 7.63 (d, *J* = 8.3 Hz, 2H), 7.32 – 7.28 (m, 2H), 5.10 – 5.08 (m, 1H), 4.76 – 4.73 (m, 1H), 3.92 (s, 2H), 3.80 (s, 2H), 2.40 (s, 3H), 2.11 (q, *J* = 7.5 Hz, 2H), 1.87 – 1.85 (m, 3H), 0.75 (t, *J* = 7.5 Hz, 3H); $^{13}$C NMR (125 MHz, $CDCl_3$): $\delta$ = 191.5, 153.8, 144.3, 140.7, 135.2, 133.3, 130.0, 127.7, 115.7, 52.6, 47.6, 21.8, 21.5, 19.2, 14.0; IR (neat): $\tilde{\nu}$ = 2969 (w), 2928 (w), 2871 (w), 1679 (s), 1618 (w), 1598 (w), 1494 (w), 1444 (w), 1350 (s), 1253 (w), 1163 (s), 1121 (w), 1090 (w), 1029 (w), 960 (w), 910 (w), 815 (w) 785 (w), 768 (w), 662 (w) $cm^{-1}$; MS (ESI): calcd for ($C_{17}H_{21}NO_3S$ + Na): 342.1140; found: 342.1135.

**Compound 122**

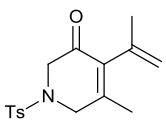


Colourless oil (36 mg, 13% from **69** (200 mg, 0.89 mmol) using method **II**); $^1$H NMR (500 MHz, $CDCl_3$): $\delta$ = 7.64 (d, *J* = 8.3 Hz, 2H), 7.31 (d, *J* = 8.0 Hz, 2H), 5.10 – 5.06 (m, 1H), 4.45 – 4.41 (m,

1H), 3.95 (s, 2H), 3.81 (s, 2H), 2.40 (s, 3H), 2.20 (q, *J* = 7.6 Hz, 2H), 1.66 (s, 3H), 1.04 (t, *J* = 7.6 Hz, 3H); $^{13}$C NMR (125 MHz, $CDCl_3$): $\delta$ = 190.2, 155.4, 144.3, 138.6, 137.7, 133.3, 130.0, 127.6, 113.7, 52.7, 47.0, 26.0, 23.0, 21.4, 12.8; IR (neat): $\tilde{\nu}$ = 2974 (w), 2937 (w), 2923 (w), 2878 (w), 1677 (m), 1620 (w), 1598 (w), 1444 (w), 1350 (m), 1308 (w), 1241 (w), 1185 (w), 1163 (s), 1089 (w), 1046 (w), 998 (w), 957 (w), 906 (w), 830 (w), 816 (w), 707 (w), 681 (w) $cm^{-1}$; HRMS (ESI): calcd for $(C_{17}H_{21}NO_3S + Na)^+$: 342.1140; found: 342.1129

### 2.7.6 Hydrogenation and Aromatisation

**Compound 85a**

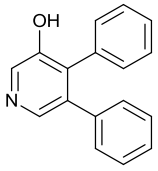


Under air, a suspension of **6a** (50 mg, 0.14 mmol), $SiO_2$ (50 mg) and TFA (0.15 ml) in dichloromethane (0.5 ml) was stirred at room temperature for 10 minutes. $NaNO_2$ (15 mg, 0.21 mmol) was then added and the suspension was stirred at room temperature for 30 minutes. Afterwards, $Et_3N$ (0.5 ml) was added and the suspension was stirred for another 30 minutes. Afterwards, $SiO_2$ was added and all volatiles were removed *in vacuo*. The residue was loaded on a column and purified by flash chromatography (PE/EtAOc, 3/1 → 2/3) to give **85a** as a white solid (33 mg, 83%): $^1$H NMR (500 MHz, $CDCl_3$): $\delta$ = 8.44 (s, 1H), 8.21 (s, 1H), 8.06 (br s, OH), 7.35 – 7.25 (m, 3H), 7.21 – 7.13 (m, 5H), 7.09 – 7.03 (m, 2H); $^{13}$C NMR (125 MHz, $CDCl_3$): $\delta$ = 150.6, 141.9, 137.2, 137.1, 136.6, 134.8, 133.0, 129.7, 128.8, 128.0, 127.3; IR (neat): $\tilde{\nu}$ = 3028 (w), 2590 (br w), 1696 (w), 1578 w)1543 (w), 1491 (w), 1443 (w), 1415 (s), 1319 (w), 1287 (m), 1195 (w), 1117 (m), 1073 (w), 999 (w), 910 (w), 763 (s), 696 (s) $cm^{-1}$; HRMS (ESI): calcd for ($C_{17}H_{14}NO$ + Na): 248.1075; found: 248.1071; elemental analysis (%) calcd for $C_{17}H_{14}NO$: C 82.56, H 5.30, N 5.67; found: C 82.27, H 5.31, N 5.63.

**Compound 85d**

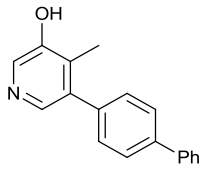


Under air, a suspension of **6d** (30 mg, 0.08 mmol), $SiO_2$ (25 mg) and TFA (0.1 ml) in dichloromethane (0.25 ml) was stirred at room temperature for 1 hour. $NaNO_2$ (8.5 mg, 0.12 mmol) was then added and the suspension was stirred at room temperature for 1 hour before adding another batch of $NaNO_2$ (8.5mg, 0.12 mmol). After 1 hour stirring for 1 hour, $Et_3N$ (0.25 ml) was added and the suspension was stirred for another 30 minutes. Afterwards, $SiO_2$ was added and all volatiles were removed *in vacuo*. The residue was loaded on a column and purified by flash chromatography (PE/EtAOc, 2/1 → 1/9) to give **85d** as a white solid (13mg, 68%): m.p. 158–163 °C (decomposition); $^1$H NMR (500 MHz, $CDCl_3$): $\delta$ = 8.37 (s, 1H), 8.06 (s, 1H), 7.68 (d, *J* = 8.1 Hz, 2H), 7.64 (d, *J* = 7.5 Hz, 2H), 7.46 (t, *J* = 7.6 Hz, 2H), 7.42 (d, *J* = 8.1 Hz, 2H), 7.37 (t, *J* = 7.3 Hz, 1H), 2.31 (s, 3H); $^{13}$C NMR (125 MHz, $CDCl_3$): $\delta$ = 154.4, 140.7, 140.5, 139.3, 138.8, 136.1, 134.9, 132.8, 129.8 (2C), 128.9 (2C), 127.5, 127.2 (2C), 127.1 (2C), 13.3; IR (neat): $\tilde{\nu}$ = 3030 (m), 2962 (w), 2916 (w), 2841 (w), 2618 (br and m), 1596 (w), 1569 (m), 1486 (s), 1422 (s), 1320 (m), 1293 (m), 1223 (w), 1142 (s), 1000 (m), 843 (m), 767 (s), 732 (w), 696 (m) cm$^{-1}$; HRMS (ESI): calcd for ($C_{18}H_{16}NO$ + Na): 262.1232; found: 262.1236.

**Compound 85f**

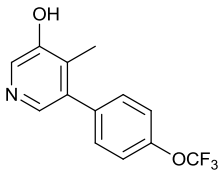


Under air, a suspension of **6f** (24 mg, 0.07 mmol) in dichloromethane (0.2 ml) was added TFA (0.2 ml) and was then stirred at room temperature for 1 hour. $CH_3CN$ (0.6 ml) was then added

and then $NaNO_2$ (7 mg, 0.10 mmol) was added and the suspension was stirred at room temperature for 1 hour. Afterwards, $SiO_2$ was added and all volatiles were removed *in vacuo*. The residue was loaded on a column and purified by flash chromatography (PE/EtAOc, 1/2) to give **85f** as a white solid (14 mg, 81%): $^1$H NMR (500 MHz, $CD_3COCD_3$): $\delta$ = 8.68 (s, 1H), 8.35 (s, 1H), 7.70 (d, *J* = 8.6 Hz, 2H), 7.56 (d, *J* = 8.1 Hz, 2H), 2.36 (s, 3H); $^{13}$C NMR (125 MHz, $CD_3COCD_3$): $\delta$ = 155.2, 149.3, 141.2, 139.6, 134.6, 133.7, 131.4, 128.1, 121.3, 120.5 (q, *J* = 255.6 Hz), 13.2; HRMS (ESI): calcd for ($C_{13}H_{11}NO_2F_3$ + Na): 270.0742; found: 270.0752

**Compound 85h**

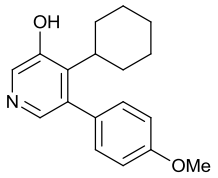


This compound was prepared from **6h** (50 mg, 0.14 mmol) according to the procedure described for the preparation of **85a**, except a second batch of $NaNO_2$ (1.5 equiv.) was added and allowed to stir for 1 hour before quenching with $Et_3N$. Yellow solid (25 mg, 66%): $^1$H NMR (500 MHz, $CDCl_3$): $\delta$ = 8.31 (s, 1H), 7.91 (s, 1H), 7.18 (d, *J* = 8.4 Hz, 2H), 6.95 (d, *J* = 8.4 Hz, 2H), 3.86 (s, 3H), 2.71 (t, *J* = 11.9 Hz, 1H), 2.31 – 2.16 (m, 2H), 1.69 (d, *J* = 12.6 Hz, 2H), 1.63 – 1.47 (m, 3H), 1.25 -1.03 (m, 3H). Further analytical data was not obtained.

**Compound 85o**

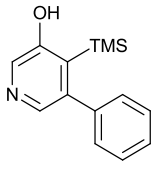


This compound was prepared from **6o** (70 mg, 0.20 mmol) according to the procedure described for the preparation of **85a**. White solid (27 mg, 53%); $^1$H NMR (500 MHz, $CDCl_3$): $\delta$ = 8.28 (s, 1H), 7.95 (s, 1H), 7.40 – 7.34 (m, 3H), 7.28 – 7.22 (m, 2H), 0.00 (s, 9H); $^{13}$C NMR (125

MHz, $CD_3COCD_3$): $\delta$ = 158.1, 144.3, 141.5, 141.2, 135.4, 131.2, 129.5, 127.9, 127.5, -0.1; IR (neat): $\tilde{\nu}$ = $cm^{-1}$; elemental analysis (%) calcd for $C_{14}H_{17}NOSi$: C 69.09, H 7.04, N 5.76; found: C 67.65, H 6.79, N 5.56.

**Compound 124**

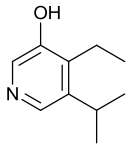


A vial was charged with **121** (63 mg, 0.20 ml), Pd/C (6 mg) and suspended in EtOAC (2 ml). The vial was quickly evacuated and backfilled with $H_2$. Kept under 1 atm of $H_2$ with a $H_2$ balloon and stirred vigorously for 4 hours. Afterwards, the Pd/C was filtered off and concentrated. The residue was re-dissolved in THF (2 ml) and KO*t*Bu (66 mg, 0.59 mmol) was added. After completion within 30 mins as judged by TLC, all volatiles were removed and the residue was loaded on top of a silica column. Purification by flash chromatography (PE/EtAOc, 1/1 → 1/5) afforded **124** as a white solid (14 mg, 43%): $^1$H NMR (500 MHz, $CDCl_3$): $\delta$ = 8.16 (s, 1H), 8.00 (s, 1H), 3.16 (sept, *J* = 6.9 Hz, 1H), 2.77 (q, *J* = 7.5 Hz, 2H), 1.27 (d, *J* = 6.9 Hz, 6H), 1.18 (t, *J* =7.5 Hz, 3H); $^{13}$C NMR (125 MHz, $CDCl_3$): $\delta$ = 153.2, 143.3, 139.1, 137.1, 132.9, 27.6, 23.8, 18.6, 13.8; IR (neat): $\tilde{\nu}$ = 2965 (w), 2933 (w), 2873 (w), 2596 (w), 1727 (w), 1678 (w), 1596 (w), 1569 (w), 1511 (w), 1464 (w), 1429 (s), 1389 (w), 1301 (s), 1194 (w), 1168 (w), 1154 (w), 1084 (w), 1052 (w), 953 (w), 869 (w) $cm^{-1}$; HRMS (CI): calcd for $(C_{10}H_{15}NO + H)^+$: 166.1226; found: 166.1233

**Compound 125**

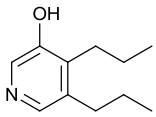


Compound **70b** (40mg, 0.12 mmol) was dissolved in THF (1.2 ml) and KO*t*Bu (67 mg, 0.60 mmol) was added. After allowing it to stir at rt overnight, all volatiles were removed and the

residue was loaded on top of a silica column. Purification by flash chromatography (PE/EtAOc, 1/1 → 1/5) afforded **125** as a white solid (10 mg, 92%). $^{1}$H NMR (500 MHz, $CDCl_3$): $\delta$ = 8.68 (s, 1H), 7.77 (s, 1H), 2.82-2.75 (m, 2H), 2.72 – 2.65 (m, 2H), 1.70 – 1.54 (m, 4H), 1.06 – 0.97 (m, 6H). Further analytical data was not obtained.

## 2.8 References


1.) D. Crépin, J. Dawick, C. Aïssa, *Angew. Chem. Int. Ed.* **2010**, *49*, 620–623.

2.) M. Murakami, S. Ashida, T. Matsuda, *J. Am. Chem. Soc.* **2005**, *127*, 6932–6933.

3.) M. Ackermann, A. Pascariu, T. Höcher, H.-U. Siehl, S. Berger, *J. Am. Chem. Soc.* **2006**, *128*, 8434–8440.

4.) C. A. Tolman, *Chem. Rev.* **1977**, *77*, 313–348.

5a.) T. Tsuda, T. Kiyoi, T. Saegusa, *J. Org. Chem.* **1990**, *55*, 2554–2558; (b) W.-S. Huang, J. Chan, T. F. Jamison, *Org. Lett.* **2000**, *2*, 4221–4223; (c) E. A. Colby, T. F. Jamison, *J. Org. Chem.* **2003**, *68*, 156–166; (d) K. M. Miller, W.-S. Huang, T. F. Jamison, *J. Am. Chem. Soc.* **2003**, *125*, 3442–3443; (e) G. M. Mahandru, G. Liu, J. Montgomery, *J. Am. Chem. Soc.* **2004**, *126*, 3698–3699; (f) T. Luanphaisarnnont, C. O. Ndubaku, T. F. Jamison, *Org. Lett.* **2005**, *7*, 2937–2940; (g) A. Herath, B. B. Thompson, J. Montgomery, *J. Am. Chem. Soc.* **2007**, *129*, 8712–8713; (h) M. R. Chaulagain, G. J. Sormunen, J. Montgomery, *J. Am. Chem. Soc.* **2007**, *129*, 9568–9569; (i) Y. Yang, S.-F. Zhu, C.-Y. Zhou, Q.-L. Zhou, *J. Am. Chem. Soc.* **2008**, *130*, 14052–14053.

6a.) P. R. McCarren, P. Liu, P. H.-Y. Cheong, T. F. Jamison, K. N. Houk, *J. Am. Chem. Soc.* **2009**, *131*, 6654–6655; (b) P. Liu, P. McCarren, P. H.-Y. Cheong, T. F. Jamison, K. N. Houk, *J. Am. Chem. Soc.* **2010**, *132*, 2050–2057.

7.) E. L. Eliel, S. H. Wilen, L. N. Mander in *Stereochemistry of Organic Compounds*, John Wiley & Sons, Inc: New York, **1994**, 696 – 697.

8a.) K. M. Miller, T. Luanphaisarnnont, C. Molinaro, T. F. Jamison, *J. Am. Chem. Soc.* **2004**, *126*, 4130–4131; (b) K. M. Miller, T. F. Jamison, *Org. Lett.* **2005**, *7*, 3077–3080.

9.) K. Sa-ei, J. Montgomery, *Org. Lett.* **2006**, *8*, 4441–4443.

10.) T. Bartik, B. Happ, M. Iglewsky, H. Bandmann, R. Boese, P. Heimbach, T. Hoffmann, E. Wenschuh, *Organometallics* **1992**, *11*, 1235–1241

11a.) S. Ikeda, Y. Sato, *J. Am. Chem. Soc.* **1994**, *116*, 5975–5976; (b) S. Ikeda, H. Yamamoto, K. Kondo, Y. Sato, *Organometallics* **1995**, *14*, 5015–5016; (c) S. Ikeda, K. Kondo, Y. Sato, *J. Org. Chem.* **1996**, *61*, 8248–8255; (d) E. Oblinger, J. Montgomery, *J. Am. Chem. Soc.* **1997**, *119*, 9065–9066; (e) S. J. Patel, T. F. Jamison, *Angew. Chem. Int. Ed.* **2003**, *42*, 1364–1367.

12.) P. Kumar, J. Louie, *Org. Lett.* **2012**, *14*, 2026–2029.

13a.) Y. Kajita, S. Matsubara, T. Kurahashi, *J. Am. Chem. Soc.* **2008**, *130*, 6058–6059; b) Compuational report: A. Poater, S. V. C. Vummaleti, L. Cavallo, *Organometallics* **2013**, *32*, 6330–6336.

14.) P.-H. Chen, T. Xu, G. Dong, *Angew. Chem. Int. Ed.* **2014**, *53*, 1674–1678.

15.) M. A. Huffman, L. S. Liebeskind, *J. Am. Chem. Soc.* **1991**, *113*, 2771–2772.

16.) N. Ishida, T. Yuhki, M. Murakami, *Org. Lett.* **2012**, *14*, 3898–3901.

17.) K. Niknam, B. Karami, M. A. Zolfigol, *Catal. Commun.* **2007**, *8*, 1427–1430.

18.) S.-S. Ng, C.-Y. Ho, T. F. Jamison, *J. Am. Chem. Soc.* **2006**, *128*, 11513–11528.

19a.) K. W. Quasdorf, X. Tian, N. K. Garg, *J. Am. Chem. Soc.* **2008**, *130*, 14422–14423; b) K. W. Quasdorf, M. Riener, K. V Petrova, N. K. Garg, *J. Am. Chem. Soc.* **2009**, *131*, 17748–17749.

20.) Y. Yoshino, T. Kurahashi, S. Matsubara, *J. Am. Chem. Soc.* **2009**, *131*, 7494–7495.

21.) D. R. Stuart, M. Bertrand-Laperle, K. M. N. Burgess, K. Fagnou, *J. Am. Chem. Soc.* **2008**, *130*, 16474–16475.

22.) M. P. Huestis, L. Chan, D. R. Stuart, K. Fagnou, *Angew. Chem. Int. Ed.* **2011**, *50*, 1338–1341.

23a.) T. J. Donohoe, J. F. Bower, J. A. Basutto, L. P. Fishlock, P. A. Procopiou, C. K. A. Callens, *Tetrahedron* **2009**, *65*, 8969–8980; b) T. J. Donohoe, L. P. Fishlock, J. A. Basutto, J. F. Bower, P. A. Procopiou, A. L. Thompson, *Chem. Commun.* **2009**, 3008–3010.

24.) K. Y. T. Ho, C. Aïssa, *Chem. Eur. J.* **2012**, *18*, 3486–3489.

25.) M. Gobbini, S. Armaroli, L. Banfi, A. Benicchio, G. Carzana, G. Fedrizzi, P. Ferrari, G. Giacalone, M. Giubileo, G. Marazzi, et al., *J. Med. Chem.* **2008**, *51*, 4601–4608.

26.) S. L. Huang, K. Omura, D. Swern, *J. Org. Chem.* **1976**, *41*, 3329–3331.

27.) L. Ye, W. He, L. Zhang, *J. Am. Chem. Soc.* **2010**, *132*, 8550–8551.

28.) A. Scarpaci, C. Cabanetos, E. Blart, Y. Pellegrin, V. Montembault, L. Fontaine, V. Rodriguez, F. Odobel, *Polym. Chem.* **2011**, *2*, 157–167.

29a.) A. Mukherjee, R. B. Dateer, R. Chaudhuri, S. Bhunia, S. N. Karad, R.-S. Liu, *J. Am. Chem. Soc.* **2011**, *133*, 15372–15375; Original article b) Y. Zhang, R. P. Hsung, M. R. Tracey, K. C. M. Kurtz, E. L. Vera, *Org. Lett.* **2004**, *6*, 1151–1154.

30.) T. Axenrod, C. Watnick, H. Yazdekhasti, *J. Org. Chem.* **1995**, *60* ,1959 13

31.) C. N. C. Drey, E. Mtetwa, *J. Chem. Soc. Perkin Trans. 1* **1982**, 1587

32.) A. C. B. Burtoloso, C. R. D. Correia, *Tetrahedron* **2008**, *64*, 9928–9936.

33.) J. Wang, Y. Hou, *J. Chem. Soc., Perkin Trans. 1* **1998**, 1919–1923.

34.) N. Mézailles, L. Ricard, F. Gagosz, *Org. Lett.* **2005**, *7*, 4133–4136.

35.) M. Chen, X. Zheng, W. Li, J. He, A. Lei, *J. Am. Chem. Soc.* **2010**, *132*, 4101

36.) L. Melzig, J. Stemper, P. Knochel, *Synthesis* **2010**, 2085

37.) J. Gil-Molto, C. Najera, *Eur. J. Org. Chem.* **2005**, 4073.

38.) V. Mouriès, R. Waschbüch, J. Carran, P. Savignac, *Synthesis* **1998**, 271.

39.) M. Kunishima, D. Nakata, S. Tanaka, K. Hioki, S. Tani, *Tetrahedron* **2000**, *56*, 9927.

40.) H. Zhang, X. Fu, J. Chen, E. Wang, Y. Liu, Y. Li, *J. Org. Chem.* **2009**, *74*, 9351–9358.

41.) M. Fischer, C. Schmölzer, C. Nowikow, W. Schmid, *Eur. J. Org. Chem.* **2011**, 1645–1651.

42.) H. Kim, P. H. Lee, *Adv. Synth. Catal.* **2009**, *351*, 2827–2832.

43.) M. Čížková, V. Kolivoška, I. Císařová, D. Šaman, L. Pospíšil, F. Teplý, *Org. Biomol. Chem.* **2011**, *9*, 450–462.

44.) P. J. Riss, R. Hummerich, P. Schloss, *Org. Biomol. Chem.* **2009**, *7*, 2688–2698.

45.) P. A. Wender, N. M. Deschamps, T. J. Williams, *Angew. Chem. Int. Ed. Engl.* **2004**, *43*, 3076–3079.

46.) S.Couty, M. Barbazanges, C. Meyer, J. Cossy, *Synlett* **2005**, 905–910.

47.) R. Shintani, S. Isobe, M. Takeda, T. Hayashi, *Angew. Chem. Int. Ed.* **2010**, *49*, 3795–3798.

48.) M. L. N. Rao, D. N. Jadhav, P. Dasgupta, *Org. Lett.* **2010**, *12*, 2048–2051.

49.) C. Taillier, T. Hameury, V. Bellosta, J. Cossy, *Tetrahedron* **2007**, *63*, 4472.

50.) Determined by chiral HPLC Chiralcel OJ - H Column, *i*PrOH:hexane = 5/95, 1 mL/min, 230 nm on a Agilent technologies 1200 apparatus

# Chapter 3 Mechanistic Investigations

## 3.1 Introduction

At the outset of this work, we postulated that the mechanism of the [4+2] cycloaddition would begin with the nickel-catalyst associating both azetidinone **1** and alkyne **2** to form intermediate **4** (Scheme 1). Afterwards, oxidative cyclisation would form oxanickelacyclopentene **5**. Ring enlargement by β-C elimination will form seven-membered nickelacycle intermediate **6**. Finally, reductive elimination would afford pyridinone **3**.

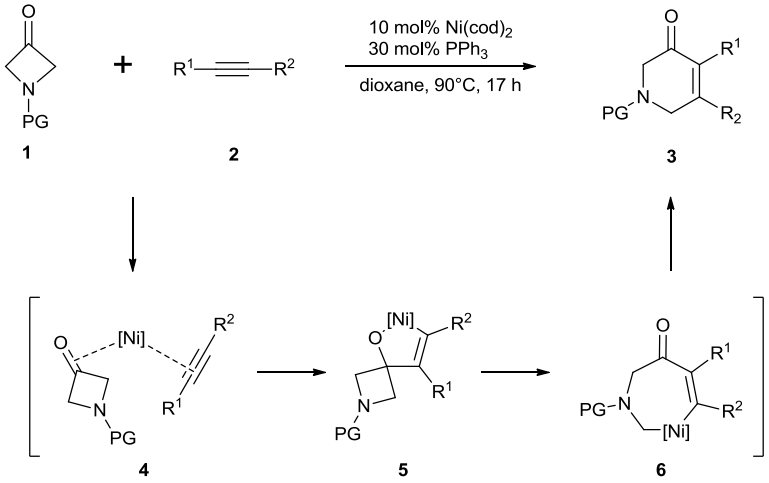


**Scheme 1** Original mechanistic proposal

In 1997, Oblinger and Montgomery reported a nickel-catalysed alkylative cyclisation of ynal **7** to form allylic alcohols **9** (Scheme 3).[1] The authors proposed the formation of oxanickelacyclopentene **8** as an intermediate of the reaction. If a $Ni(cod)_2/PtBu_3$ (1:4 ratio of Ni to phosphine) catalytic system was employed, a reductive cyclisation of ynals **10** will form

allylic alcohols **11** (Scheme 3). The formation of an oxanickelacyclopentene **8** is postulated to occur.

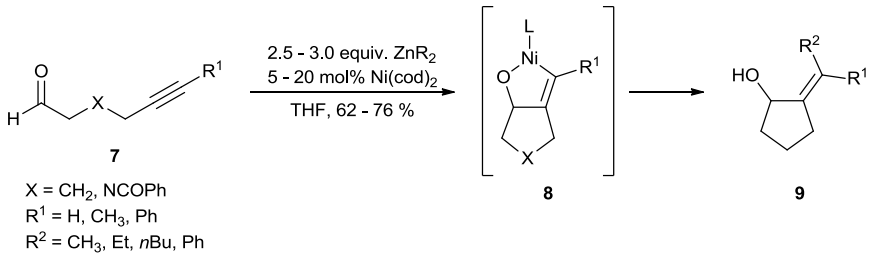


**Scheme 2** Alkylative cyclisation

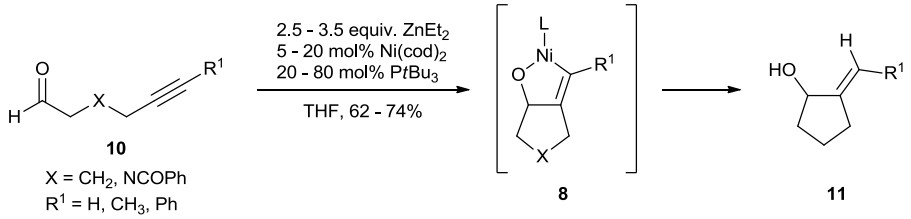


**Scheme 3** Reductive cyclisation

In the same paper, the authors reported a nickel-catalysed three-component coupling to form allyl alcohols **15** whereby the formation of oxanickelacyclopentene **14** is postulated to occur (Scheme 4). Jamison and co-workers reported a nickel-catalysed intermolecular reductive coupling of aldehydes **16** and alkynes **17** to form allylic alcohols **18** but no mechanism was proposed (Scheme 5). Regardless, oxanickelacyclopentene **14** can be invoked.[2] Furthermore, theoretical studies support the formation of **14**.[3]

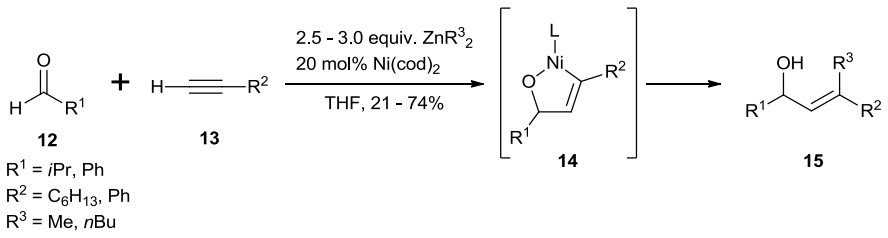


**Scheme 4** Nickel-catalysed three-component coupling

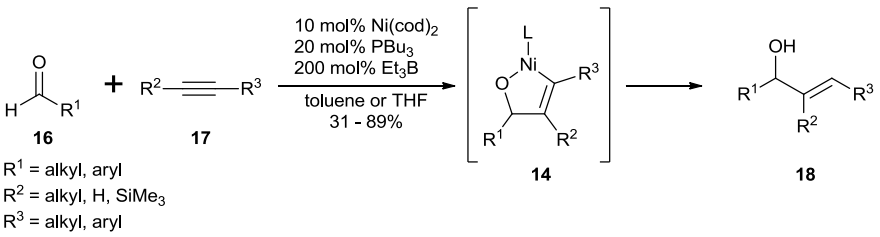


**Scheme 5** Nickel-catalysed intermolecular reductive coupling

Baxter and Montgomery carried out a mechanistic study of the nickel-catalysed intramolecular reductive cyclisation of ynal **19** to form silyl ether **20** (Scheme 6).[4] It is postulated that the formation of oxanickelacyclopentene **21** is most likely. However, intermediates **22** - **24** could lead to the formation of **20**. Therefore, a mechanistic study was commenced to gain mechanistic insight into the operative pathway.

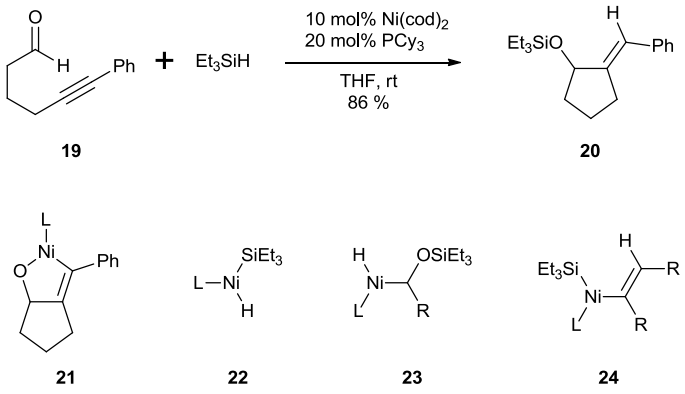


**Scheme 6** Nickel-catalysed reductive cyclisation

Kinetic studies by *in situ* IR monitoring allowed for real-time monitoring of the reaction. A first-order dependence of the reaction rate on ynal **19**, first-order dependence of the reaction rate on catalyst and zero-order dependence of the reaction rate on $Et_3SiH$ were observed. Kinetic isotopic effect studies revealed that $Et_3SiH$ and $Et_3SiD$ have no significant kinetic isotopic effect and crossover studies revealed little crossover (Scheme 7).

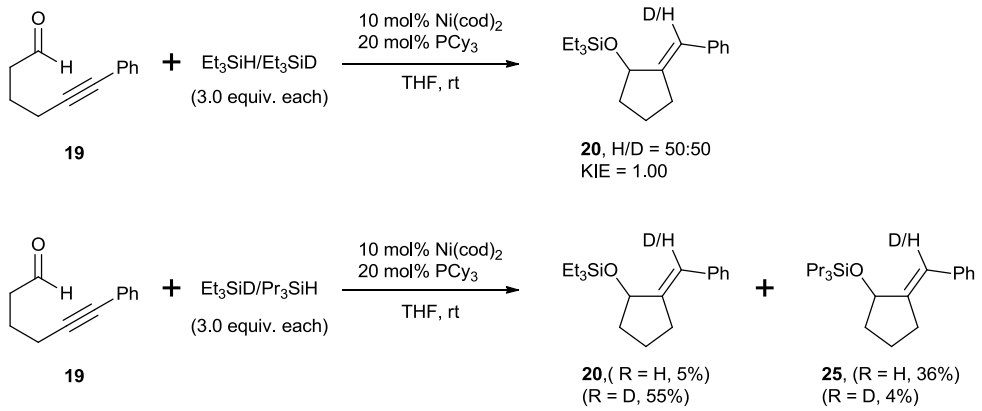


**Scheme 7** Kinetic isotopic effect study and crossover study

Afterwards, *in situ* IR monitoring of the addition of a solution of 1.0 equiv of the catalyst derived from $Ni(cod)_2$ and $PCy_3$ to a solution of $Et_3SiH$ resulted in no change to the silicon hydride stretch (2100 $cm^{-1}$) which along with the other mechanistic data rules out intermediate **22**. Interestingly, the addition of a solution of 1.0 equiv of the same catalyst to a solution of $Et_3SiH$ and hydrocinnamaldehyde resulted in no change to the silicon hydride stretch which rules out intermediate **23**. Furthermore, the addition of a solution 1.0 equiv of the same catalyst to a solution of $Et_3SiH$ and phenyl propyne resulted in no change to the silicon hydride stretch which rules our intermediate **24**. Finally, the addition of a solution of 1.0 equiv of the same catalyst to a solution of $Et_3SiH$ and ynal **19** resulted in conversion to **20**, which along with the previous mechanistic data support the intermediacy of **21**.

Ogoshi and co-workers reported a $AlMe_3$-promoted oxidative cyclisation between an alkene, a ketone and nickel(0) to give oxanickelacyclopentene **28** (Scheme 8).[5] The reaction of $Ni(cod)_2$ and $PCy_3$ with ketone **26** gave complex **27**. Complex **27** was isolated in a 86% and the X-ray structure confirmed that C=O and C=C bonds both coordinate to the nickel centre in $\eta^2$-fashion. After the formation of **27**, heating to 60°C or the addition of $Me_3SiOTf$ did not induce the transformation to oxanickelacyclopentene **28**. Reaction of **27** with $AlMe_3$ in $C_6D_6$ then afforded **28** in a quantitative yield. The structure of **28** was confirmed by X-ray diffraction analysis. However, no further reaction was observed in $C_6D_6$.

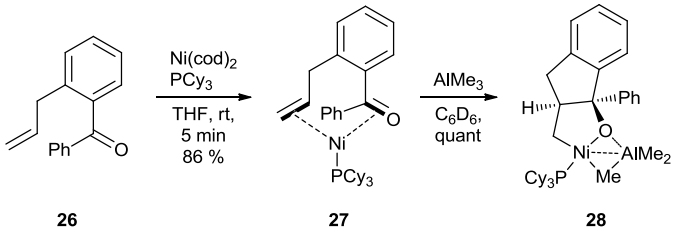


**Scheme 8** Oxidative cyclisation to form pentanickelacycle

The addition of THF to oxanickelacyclopentene **28** generated complex **31** (Scheme 9). The authors proposed the initial transmetallation was followed by methane elimination to afford intermediate **29**. Oxidation addition into the C–O bond would afford intermediate **30**. Finally, transmetallation would afford complex **31** in a 56% yield. Interestingly, when catalytic amount of $Ni(cod)_2$ and $PCy_3$ were employed, rapid cycloisomerisation of ketone **26** formed allylic alcohol **32** after protonation in a 86% yield (Scheme 10).

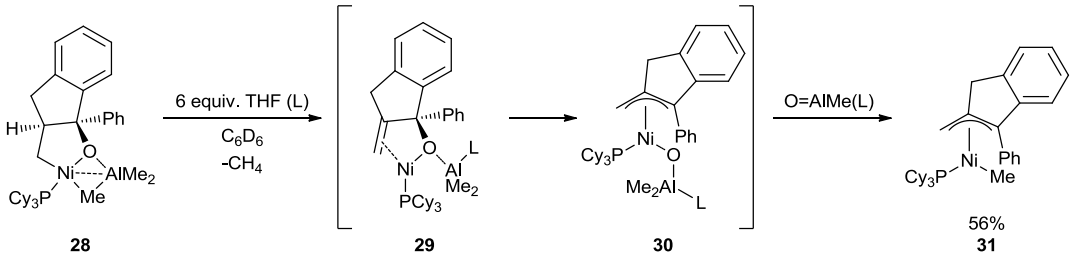


**Scheme 9** Generation of complex **31**

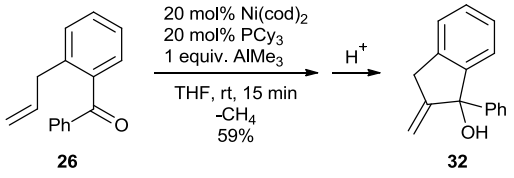


**Scheme 10** Cycloisomerisation of ketone **26** to form allylic alcohol **32**

Ogoshi and co-workers reported a nickel-catalysed transformation of aldehyde **33** to form ketone **34** (Scheme 11).[6] Stoichiometric reactions were then carried out to gain insight into the mechanism. The treatment of **34** with $Ni(cod)_2$ and I*t*Bu resulted in the quick formation of

complex **35** and was isolated in a 83% yield. Complex **35** slowly dimerised to form a mixture of *syn*-**36** and *anti*-**36** over 33 days and the mixture was isolated together in a 84% yield. Furthermore, the structure of *anti*-**35** was confirmed by X-ray diffraction analysis. It is assumed the dimerisation goes through monomeric intermediate **37** but **37** is never observed over the course of the reaction as judged by NMR analysis. The conversion of **36** into **34** was very slow. When 2.5 mol% of **36** was used, the transformation of **33** into **34** took place within 5 hours and a yield of 101% (maximum 105%) was obtained. Therefore it is concluded that under the reaction conditions, monomeric **37** is part of the catalytic cycle and **37** is in equilibrium with **36**.

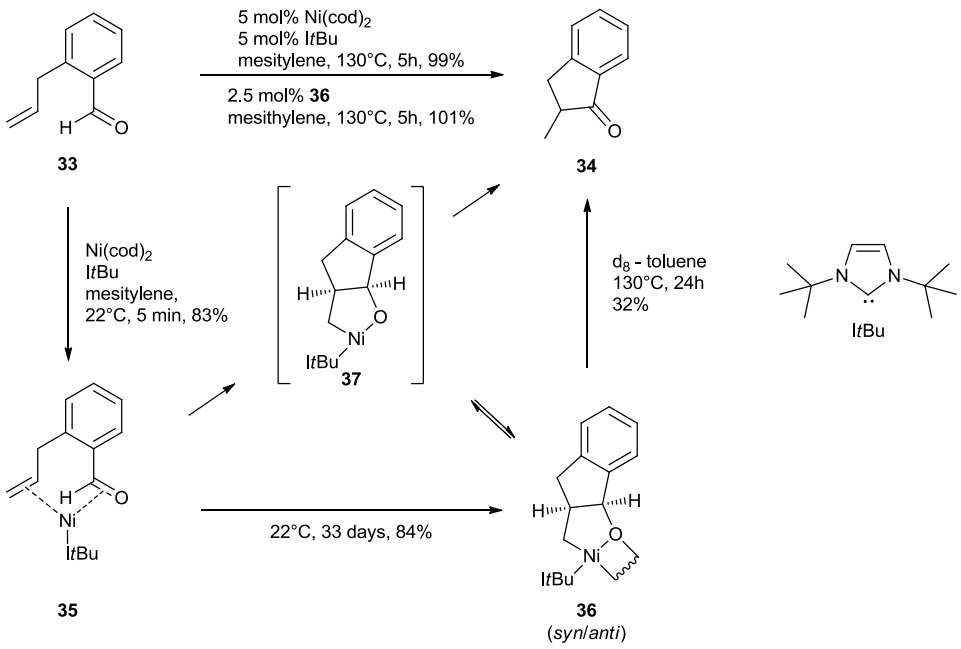


**Scheme 11** Mechanistic study on the nickel-catalysed transformation of **33** into **34**

Ogoshi and co-workers reported the formation of nickeladihydrofuran **40** from the reaction of benzaldehyde **38**, butyne **39**, $Ni(cod)_2$ and $PCy_3$ (Scheme 12).[7] Furthermore, **40** was isolated in a 40% yield and the structure was confirmed by X-ray diffraction analysis. Also, the nickel centre exhibits a square planar geometry. **40** decomposed in THF to form enone **42** and was

isolated in a 70% yield. It is postulated that β-H elimination from **40** would afford **41**. Subsequent reductive elimination would then afford **42**. This result demonstrates that **40** can be a key intermediate in a nickel-catalysed reaction.

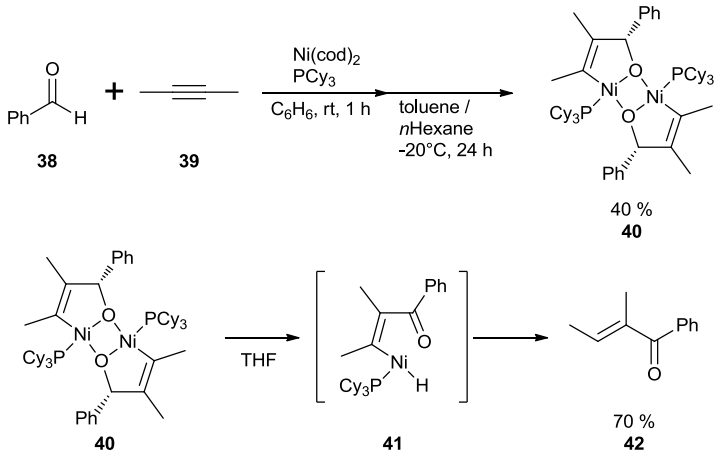


**Scheme 12** Formation of nickeladihydrofuran **40** and its decomposition

The postulated mechanism for the [4+2] cycloaddition relied on the formation of an oxanickelacyclopentene via oxidative cyclisation. Overall, all experimental and theoretical studies discussed above are in support of this mechanistic proposal.

In contrast, Li and Lin recently reported a theoretical study on the nickel-catalysed cycloaddition of 3-azetidinones with alkynes.[8] After modelling the insertion of 2-butyne with the proposed model (Scheme 1),[9] the barrier calculated for the β-C elimination step from oxanickelacyclopentene **43** was calculated to be 46.7 kcal/mol and is therefore inaccessible. Alternatively, a ligand could ligate to form oxanickelacyclopentene **45** but the barrier calculated for the subsequent β-C elimation step is still inaccessible (46.5 kcal/mal). Therefore, these calculations rule out the initial formation of oxanickelacyclopentene **43** or **45** (Scheme 13).

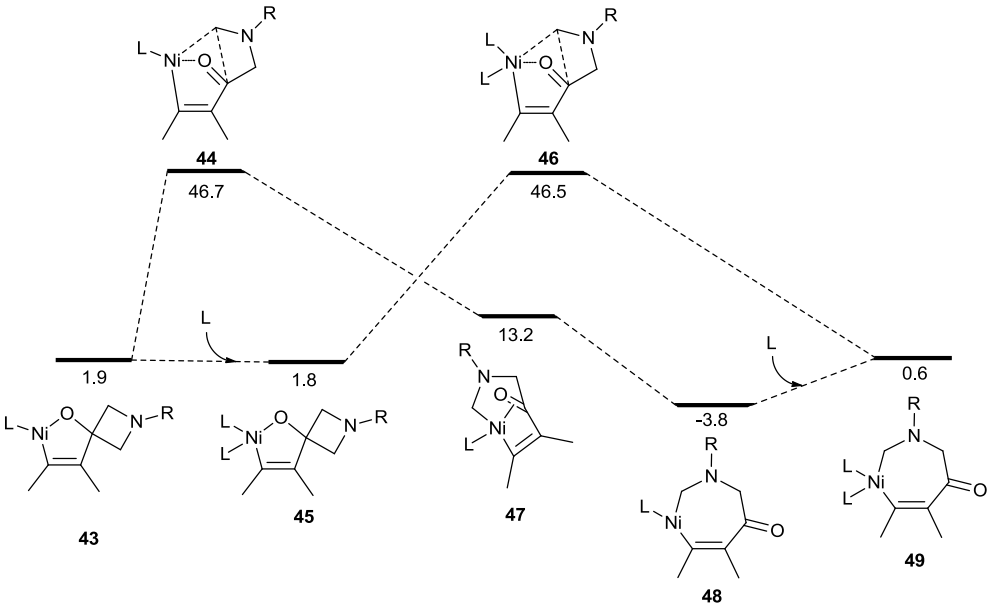


**Scheme 13** The β-C elimination pathway, L = $PMe_3$ and R = Boc

As a result, the authors proposed that the oxidative insertion of the nickel complex **50** into azetidinone **51** will occur instead (Scheme 14). The oxidative insertion of **50** into **51** is calculated to be the rate determining step with a barrier of 26.8 kcal/mol. Furthermore, this energy barrier is far lower than the energy barrier calculated for the β-C elimination step. Importantly, the authors' new mechanistic proposal is very different from the mechanism proposed for the [4+2] cycloaddition.[9]

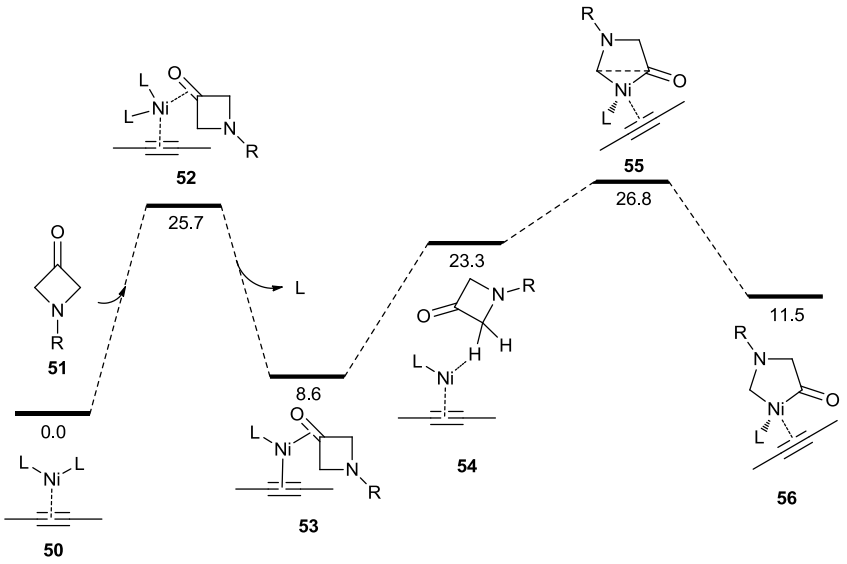


**Scheme 14** Oxidative insertion pathway, L = $PMe_3$ and R = Boc

Furthermore, the theoretical study also looked at the nature of the insertion of 1-(trimethylsilyl)propyne (Scheme 15). The oxidative insertion of the nickel-complex **57** into **51** has the same energy barrier regardless of the orientation of the alkyne. The TMS group is a strong π acceptor and will decrease the electron density at the carbon atom of the alkyne which is substituted with the methyl group. This therefore makes it more difficult for the carbon atom of the alkyne which is substituted with the methyl group to attack the metal bonded C=O carbon centre. This is reflected in the higher energy requirements to reach transition states **61** and **66**. Therefore, the authors proposed the insertion of the silylated alkyne into the Ni–C bond occurs instead. Furthermore, the calculations revealed that the orientation of the alkyne have a significant effect on the transition state. The authors proposed that since the carbon atom of the alkyne which is substituted with the methyl group is π electron poor, it will couple with the Ni-bonded carbon better. Also, the carbon atom of the alkyne which is substituted with the methyl group is less sterically hindered than the carbon atom of the alkyne which is substituted with the TMS group. This is reflected in the lower energy requirements to reach transition state **67** when compared to **60**. Interestingly,

the predicted regioselectivity of the insertion is in good agreement with the experimental observation.[9]

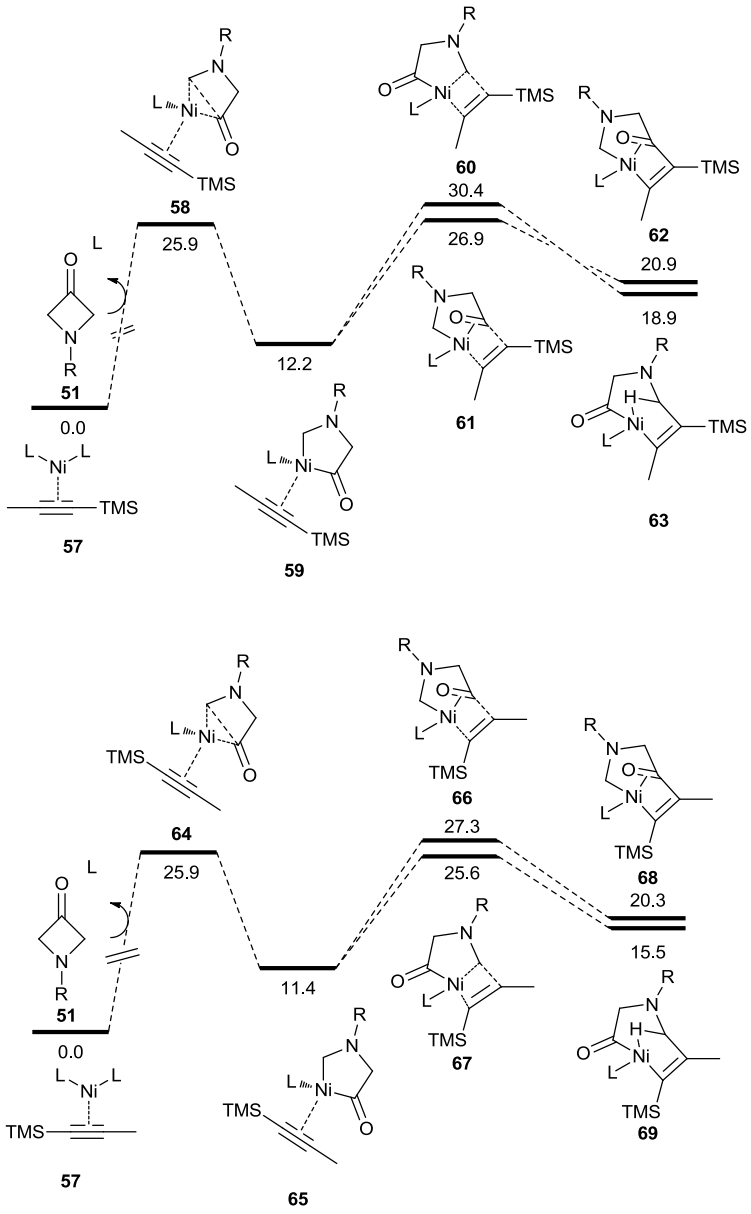


**Scheme 15** Insertion of 1-(trimethylsilyl)propyne

The mechanism of the nickel-catalysed cycloaddition of 3-azetidinones with alkynes has yet to be studied experimentally. From the theoretical work of Li and Lin, the β-C elimination step is not a feasible step due to the high energy barrier but proposed the insertion of nickel into the acyl–carbon bond of azetidinone to account for the C–C bond cleavage step. On the other

hand, experimental work by Ogoshi and co-workers demonstrated that oxanickelacyclopentene are real intermediates which could be potentially present in the nickel-catalysed [4+2] cycloaddition. Therefore, our efforts towards the understanding of the mechanism of the nickel-catalysed cycloaddition of 3-azetidinones with alkynes are described.

## 3.2 Results and Discussion

### 3.2.1 Re-optimisation of the reaction conditions

Before commencing the kinetic study, it was of interest to re-optimise the reaction conditions in light of different conditions reported by Louie and Murakami (Table 1).[10] Furthermore, the reaction had to be sufficiently slow for meaningful kinetic data to be obtained. Moreover, it was of interest to see if the kinetic study can be carried out in toluene. This will allow the possibility of NMR experiments to be carried out in $d_8$-toluene which will be far more economical than using $d_8$-dioxane. It was found that the reaction is complete in 10 minutes when carried out at 90°C in toluene (Table 1, entry 1). Lowering the temperature of the reaction to 70°C and 60°C resulted in the reaction being over within 30 minutes (Table 1, entry 2 and 3). Lowering the temperature of the reaction to 40°C resulted in 50% conversion after 30 minutes (Table 1, entry 4). However, the rate of the reaction became too slow when the reaction was carried out at rt (Table 1, entry 5).

**Table 1** Re-optimisation of the reaction conditions in toluene

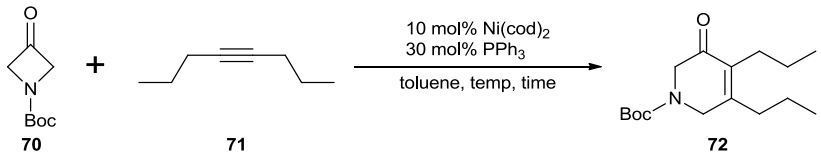


| Entry | Temp (°C) | Time (mins) | Conversion[a] |
|---|---|---|---|
| 1 | 90 | 10 | Full |
| 2 | 70 | 60 | Full |
| 3 | 60 | 30 | Full |
| 4 | 40 | 30 | ~50% |
| 5 | rt | 30 | ~10% |

[a] Conversion determined from the ratio of **70** and **72** by $^{1}$H NMR

The progress of the reaction for the kinetic study is monitored by the appearance of product by taking aliquots from the reaction vessel at specific times. However, there was an issue with the mass balance and it was found that either **70** could azeotrope with the solvent during evaporation or decompose over silica. However, when the reaction of 1 equiv. of **70** and 1.1 equiv. of **71** is monitored until >95% conversion as judged by integration of **72** against 1 equiv. of triphenylethylene as an internal standard, no unexpected disappearance of **72** was observed (Scheme 16). This therefore validates the initial rate method used in the subsequent kinetic study.

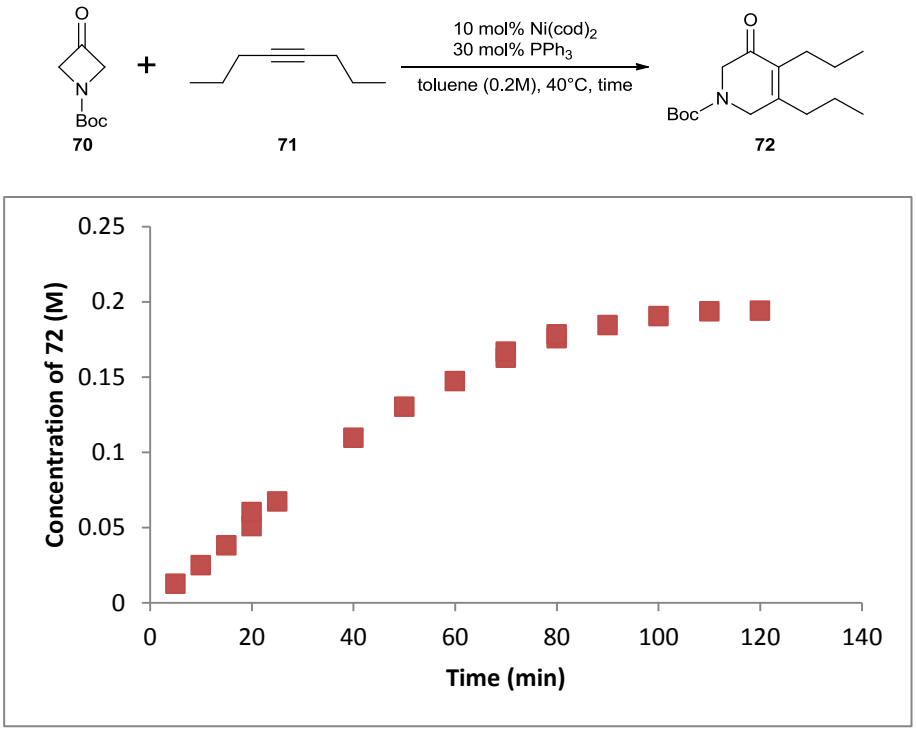


**Scheme 16** Until full conversion, 0.2M scale

### 3.2.2 Rate law with silylated alkyne 74

#### 3.2.2.1 "Initial Burst" Phase

A systematic study was then commenced to determine the rate law to gain insight into the mechanism. Initial rates were monitored by taking aliquots from the reaction mixture periodically and analysed by $^{1}$H NMR. It was of interest to carry out a kinetic study of the cycloaddition of azetidinone **70** with silylated alkyne **74** using the re-optimised conditions (Scheme 17).

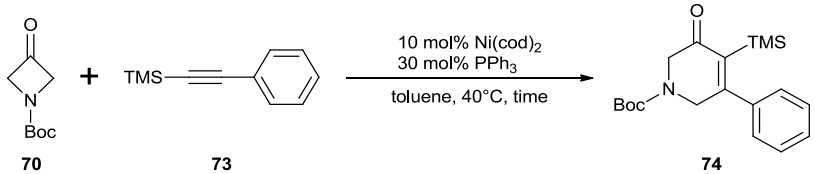


**Scheme 17** Kinetic study

On the initial attempt with 10 mol% $Ni(cod)_2$, 30 mol% $PPh_3$ in toluene at 40°C with 1 equivalent of **70** and 1.1 equivalents of **73**, it was discovered the trend line would not give a good fit if passed through the intercept at 0 (Scheme 18). Therefore, this initial burst phase in the reaction was looked into with more detail. Attempts to maintain the "initial burst" phase by slow dropwise addition of either the alkyne or a solution of alkyne and azetidinone at 40°C proved to be unfruitful. Therefore, a more detailed study of the "initial burst" phase was carried out.

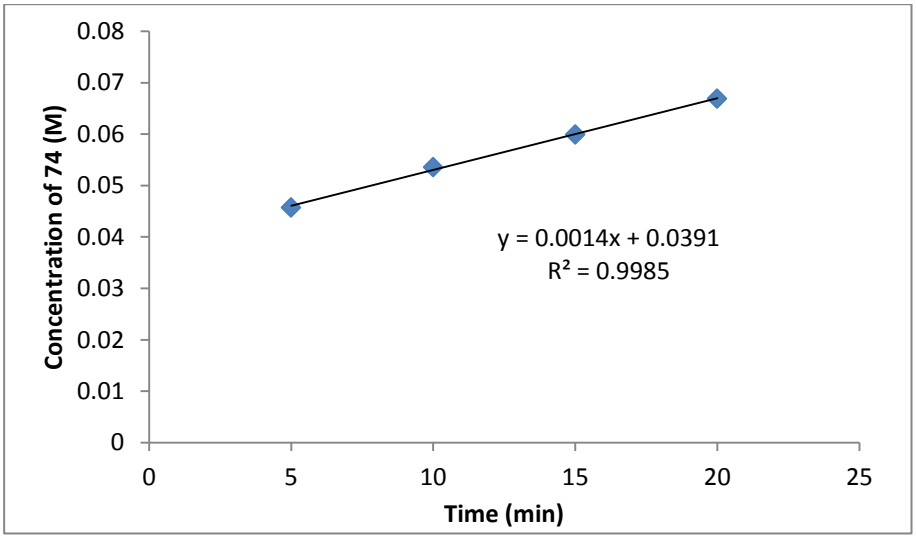


**Scheme 18** Initial discovery of the initial "burst" phase

Temperature effects on the initial "burst" phase were then studied (Table 2). When the first point was taken at 10 minutes at 40°C, there was 32% conversion to **74** (Table 2, entry 1). On prolonging the reaction to 60 minutes, the conversion to **74** was at 54% (Table 2, entry 2). Interestingly, upon lowering the reaction temperature to rt, there was 21% conversion (Table 2, entry 3). At the 30 minute mark, the conversion increased slightly to 23 % (Table 2, entry 4). Analysis of the aliquot taken at the 60 minute mark revealed only 30% conversion to **74** and some decomposition of the starting material was observed (Table 2, entry 5). These results tell us that they are two phases in the reaction; an initial "burst" phase at the start of the reaction and the steady state phase. The steady state phase appears to be the more energetically

demanding of the two phases of the reaction as a high temperature was required for a reasonable rate.

**Table 2** Temperature effects on the "initial burst"

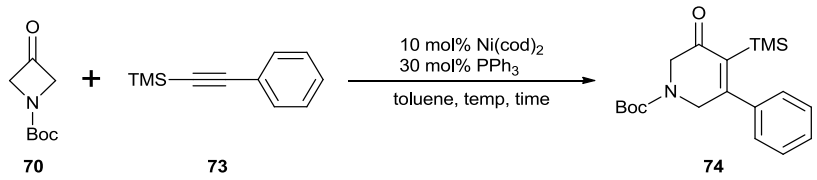


| Entry | Temp (°C) | Time (mins) | Conv. (%)[a] |
|---|---|---|---|
| 1 | 40 | 10 | 32 |
| 2 | 40 | 60 | 54 |
| 3 | r.t. | 10 | 21 |
| 4 | r.t. | 30 | 23 |
| 5 | r.t. | 60 | 30 |

[a] Conversion against triphenylethylene as internal standard

However, there were some issues, as different batches of commercially available azetidinone **70** gave slightly different results despite being from the same supplier but the conclusions remain the same (Table 3). The first batch of azetidinone was purified by flash column chromatography and stored inside the glove box. Furthermore, this batch was used in the examples of the previous table. The second batch of azetidinone was a separate purification by flash column chromatography and also stored inside the glove box. As azetidinone **70** is known to be hygroscopic, the varying time required for the solvent evaporation might have influenced how much water was absorbed by the azetidinone. Regardless, both $^{1}$H NMRs of the purified material were identical.

The conversion after 10 minutes under the standard conditions with batch 1 is 32% (Table 3, entry 1). Interestingly, the conversion after 10 seconds was 17% (Table 3, entry 2). A 20 mol%

$PPh_3$ resulted in 14% conversion to **74** at 10 seconds (Table 3, entry 3). Interestingly, when the experiment was repeated with batch 2 of azetidinone, the conversion at 10 minutes with 30% $PPh_3$ averaged out at 23% over two runs (22% and 24%) (Table 3, entry 4). Furthermore, the conversion at 10 minutes is lower with batch 2 when compared with batch 1 (Table 3, entry 4 vs 1). The conversion at 10 seconds with 30 mol% $PPh_3$ averaged out at 13% over two runs (12% and 13%) (Table 3, entry 5). These results confirmed the reproducibility of the reaction when **70** is stored correctly. The conversion at 10 seconds with 20 mol% $PPh_3$ is 11% (Table 3, entry 6). On the other hand, with 10 mol% $PPh_3$, the conversion at 10 seconds is 5% and 12% at 10 minutes (Table 3, entry 7 and 8). Regardless of the two batches, the results reveal the initial "burst" phase is extremely fast and does not appear to go much past the 10% conversion mark which suggests the initial "burst" phase is stoichiometric in the active metal complex which promotes it. The little difference in the conversion in the initial "burst" phase between 20 and 30 mol% $PPh_3$ suggests 20 mol% $PPh_3$ is sufficient for the reaction. The big difference in the conversion between the two batches suggests trace water could indeed have a negative impact on the reaction. Then it was of interest to see if the initial "burst" was indeed promoted by a nickel-phosphine complex. Elimination of either or both $Ni(cod)_2$ and $PPh_3$ resulted in no reaction (Table 3, entry 9- 11).

**Table 3** A study on the initial burst

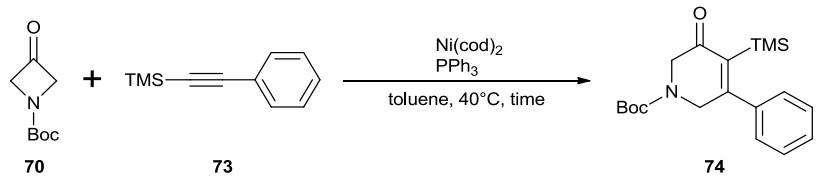


| Entry | $Ni(cod)_2$ (mol %) | $PPh_3$ (mol %) | Azetidinone | Time | Conv (%) |
|---|---|---|---|---|---|
| 1 | 10 | 30 | Batch 1 | 10 min | 32 |
| 2 | 10 | 30 | Batch 1 | 10 sec | 17 |
| 3 | 10 | 20 | Batch 1 | 10 sec | 14 |
| 4 | 10 | 30 | Batch 2 | 10 min | 23[a] |
| 5 | 10 | 30 | Batch 2 | 10 sec | 13[a] |
| 6 | 10 | 20 | Batch 2 | 10 sec | 11 |
| 7 | 10 | 10 | Batch 2 | 10 sec | 5 |
| 8 | 10 | 10 | Batch 2 | 10 min | 12 |
| 9 | 0 | 0 | Batch 2 | 10 min | 0 |
| 10 | 0 | 30 | Batch 2 | 10 min | 0 |
| 11 | 10 | 0 | Batch 2 | 10 min | 0 |

[a] average of two runs

It was then proposed that the formation of the nickel-alkyne complex was responsible for the suppression of the initial "burst" phase. Therefore, a study on the effect of the alkyne loading on the initial "burst" phase was then commenced (Table 4). After the generation of the nickel-phosphine catalyst, a precise amount of alkyne was then added and after another 5 minutes, azetidinone and the remaining alkyne (to make it a total of 1.1 equiv.) were then added.

An initial addition of 5 mol% of alkyne gave a 13% conversion after 10 seconds (Table 4, entry 1) and 25% conversion at 10 minutes (Table 4, entry 2). On increasing the loading of initial alkyne to 10 mol%, the conversion was reduced to 9% at 10 seconds (Table 4, entry 3) and 15%

at 10 minutes (Table 4, entry 4). When 20 mol% $PPh_3$ was used, the conversion at 10 seconds was worst with 5% (Table 4, entry 5). On increasing the alkyne loading further to 20 mol%, the conversion was reduced further to 5% at 10 seconds and 13% at 10 minutes (Table 4, entry 6 and 7). The conversion with 20 mol% $PPh_3$ at 10 seconds is now minimal (Table 4, entry 8). If all of the alkyne was added first before the azetidinone, the conversion at 10 seconds is barely noticeable (Table 4, entry 9) and the conversion at 10 minutes stands at 10% (Table 4, entry 10). This result is reproducible (Table 4, entry 11). Furthermore, carrying out the same reaction with 20 mol% $PPh_3$ gave 15% conversion at 10 minutes (Table 4, entry 12).

As noted, there is a trend linking increased initial alkyne loading with decreased levels of conversion. Furthermore, these results confirmed the nickel-alkyne complex is not the active catalyst for the initial burst. It does appear that the higher loading of phosphine gave better conversion for the burst phase (Table 4, entry 3 vs 5). Perhaps, the extra phosphine prevents the formation of a less active Ni-alkyne complex. Furthermore, after the formation of the nickel-alkyne complex, the lower loading of phosphine is more effective as it displayed a higher reactivity (Table 4, entry 12 vs 10). Also, in the steady state, the extra phosphine will compete for binding with the reactants and the binding is reversible. However, the role of the extra phosphine in the initial “burst” phase remains speculative.

**Table 4** Effects on the concentration of alkyne on the initial "burst" phase.

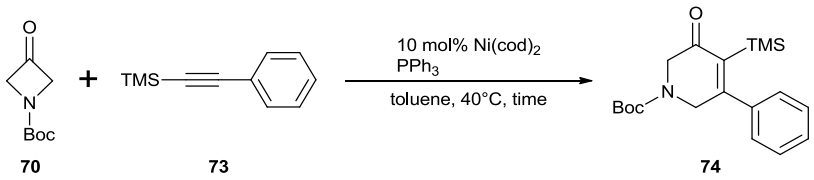


70 73 74

| Entry | $PPh_3$ (mol %) | Initial alkyne (mol %) | Time | Conv (%) |
|---|---|---|---|---|
| 1 | 30 | 5 | 10 sec | 13 |
| 2 | 30 | 5 | 10 min | 25 |
| 3 | 30 | 10 | 10 sec | 9 |
| 4 | 30 | 10 | 10 min | 15 |
| 5 | 20 | 10 | 10 sec | trace |
| 6 | 30 | 20 | 10 sec | 5 |
| 7 | 30 | 20 | 10 min | 13 |
| 8 | 20 | 20 | 10 sec | trace |
| 11 | 30 | 110 | 10 sec | trace |
| 9 | 30 | 110 | 10 min | 10 |
| 10 | 30 | 110 | 10 min | 8 |
| 12 | 20 | 110 | 10 min | 15 |

Afterwards, a study on the stoichiometry and ratio of $Ni(cod)_2$ and $PPh_3$ were carried out in anhydrous toluene. The conversion at 10 seconds was then analysed in all cases. As mentioned earlier, with 10 mol% $Ni(cod)_2$, the conversion was 12% when 30 mol% $PPh_3$ was used (Table 5, entry 1) and 11% when 20 mol% $PPh_3$ was used (Table 5, entry 2). On reducing the loading of $Ni(cod)_2$ to 7.5 mol%, the conversion was reduced to 8 % with 22.5 mol% $PPh_3$ (Table 5, entry 3) and 7% with 15 mol% $PPh_3$ (Table 5, entry 4). On reducing the loading of $Ni(cod)_2$ further to 5 mol%, the conversion was reduced more to 6% with 15 mol% $PPh_3$ (Table 5, entry 5) and 4% with 10 mol% $PPh_3$ (Table 5, entry 6).

**Table 5** A study on the stoichiometry and ratio of $Ni(cod)_2$ and $PPh_3$

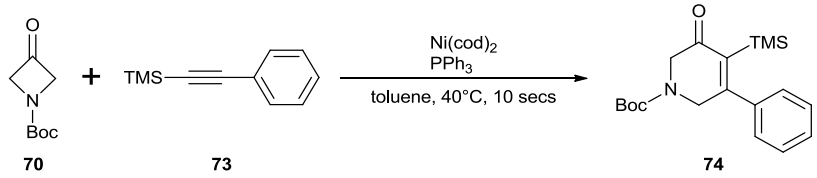


| Entry | $Ni(cod)_2$ (mol %) | $PPh_3$ (mol %) | Conversion (%) |
|---|---|---|---|
| 1 | 10 | 30 | 12 |
| 2 | 10 | 20 | 11 |
| 3 | 7.5 | 22.5 | 8 |
| 4 | 7.5 | 15 | 7 |
| 5 | 5 | 15 | 6 |
| 6 | 5 | 10 | 4 |

Then it was of interest to see if the initial burst was suppressed by the product when 30 mol% $PPh_3$ was used (Table 6). Therefore, the reaction was carried out whereby a known amount of pyridinone **74** is added after the formation of the active catalyst. Then after five minutes, the remaining reactants were then added. If the reaction was started with 20 mol% **74**, the conversion at 10 minutes is 22% (Table 6, entry 1) which is the virtually the same as the reaction that was carried out without 20 mol% **74** (Table 3, entry 4). Even with a lower loading of 10 mol% **74**, the conversion at 10 minutes remained unaffected (Table 6, entry 2). Even the initial "burst" phase is not affected by **74** as the conversion is 12% (Table 6, entry 3) which is virtually the same as the reaction that was carried without the inclusion of the product (Table 3, entry 5). Therefore, it can be concluded that the product does not inhibit the catalyst that allows for the initial "burst" phase.

**Table 6** A study on the effect of product on the initial burst

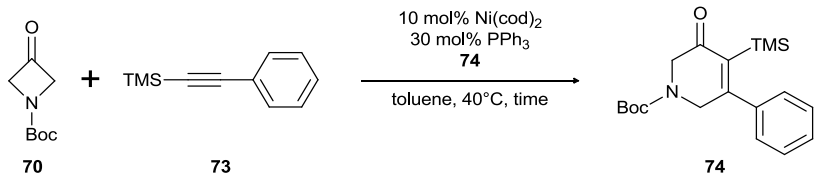


70 73 74

| Entry | **74** (mol %) | Time | Conv. (%) |
|---|---|---|---|
| 1 | 20 | 10 mins | 22 |
| 2 | 10 | 10 mins | 22 |
| 3 | 10 | 10 secs | 12 |

### 3.2.2.2 Kinetic study with silylated alkyne 73

The kinetic study was carried out with the method of initial rate. The kinetic study was carried out in a round-bottom flask under an atmosphere of Argon with triphenylethylene as an internal standard. Aliquots were taken from the reaction vessel at specific times, filtered over a plug of silica, rinsed, all volatiles removed and analysed by $^{1}$H NMR to allow the monitoring of the reaction. To gain the order dependence in each reactant, the appearance of product is plotted vs the time as the concentration of each reactant is varied. The kinetic study was first carried out with a $Ni(cod)_2$ and $PPh_3$ ratio of 1:3 (Scheme 19).

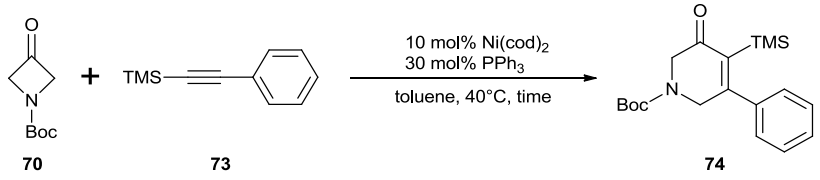


70 73 74

**Scheme 19** The reaction to be studied

Firstly, the concentration of the azetidinone was varied while the concentration of the other reactants remains constant. The concentration of azetidinone varied from 0.12 – 0.24 M. After obtaining the rate with each concentration of azetidinone, by plotting the log(initial rate) against log(M), first order dependence on the azetidinone was found (Figure 1).

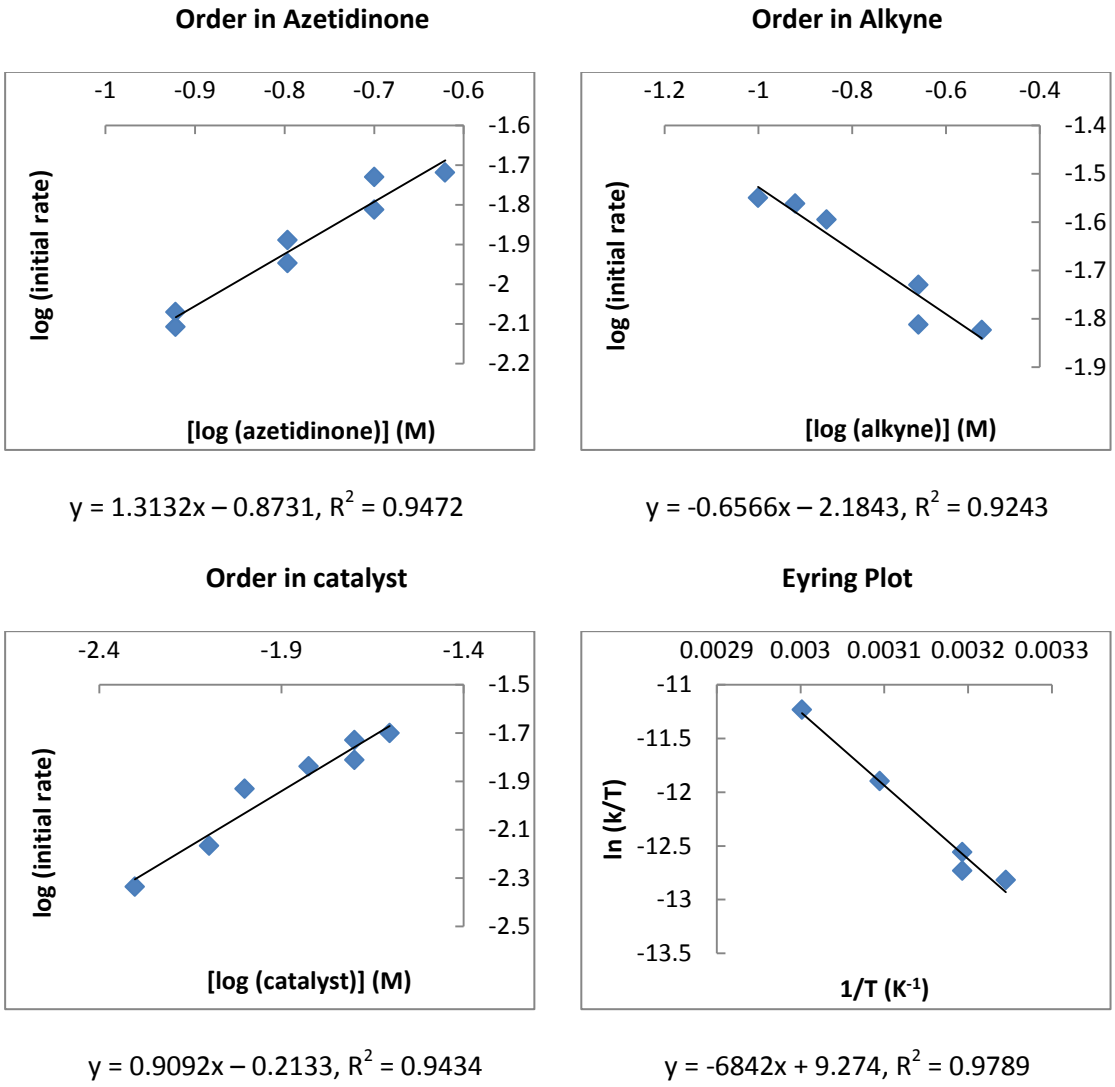


**Figure 1** $Ni(cod)_2$ and $PPh_3$ ratio of 1:3

Secondly, the concentration of the alkyne was varied while the concentration of the other reactants remains constant. The concentration of alkyne was varied from 0.10 – 0.30 M. After obtaining the rate with each concentration of alkyne, by plotting the log(initial rate) against

log(M), negative first order dependence on the alkyne was found. Finally, the concentration of the $Ni(cod)_2$ and $PPh_3$ were varied but the ratio of 1:3 was kept while the concentration of the other reactants remains constant. The concentration of $Ni(cod)_2$ was varied from 0.005 – 0.025M. The concentration of $PPh_3$ was varied from 0.015 – 0.075M. After obtaining the rate with each concentration of the catalyst, by plotting the log(initial rate) against log(M), first order dependence in the catalyst was found. As a result, the rate law can be formulated by the following:

$$\text{Rate} = k_{obs}[\text{Azetidinone}]^{1.3}[\text{Alkyne}]^{-0.7}[\text{Catalyst}]^{0.9}$$

An Eyring plot was then plotted to elucidate the nature of the transition state of the rate determining step. From the Eyring plot an equation of y = -6842x + 9.274 was obtained. ΔH is obtained from the following equation whereby R is gas constant (8.314 J $K^{-1}$ $mol^{-1}$):

$$\Delta H = mR$$

As a result, ΔH is calculated to be 56.9 kJ $mol^{-1}$. ΔS is obtained from the following equation whereby h is the Planck constant (6.626 x $10^{-34}$ J•s) and $k_B$ is the Boltzmann's constant (1.38 x $10^{-23}$ J $K^{-1}$):

$$y(x = 0) = \ln\frac{h}{k_b} + \frac{\Delta S}{R}$$

As a result, ΔS is calculated to be -120.4 J mol $K^{-1}$. Finally, the ΔG is obtained from the following equation:

$$\Delta G = \Delta H - T\Delta S$$

As a result, ΔG is calculated to be 94.6 kJ $mol^{-1}$ at 40°C. These data demonstrate the high pre-organisation that exists in the transition state. From the experimental rate law, both the azetidinone and the catalyst are present at the rate determining step. However, a negative order dependence on the alkyne revealed the alkyne competes for binding to the catalyst with the azetidinone.

Before postulating a mechanism, the role of the extra phosphine was studied. The cycloaddition of azetidinone **70** with silylated alkyne **73** was studied using the modified optimised conditions of 10 mol% $Ni(cod)_2$ and 20 mol% $PPh_3$.

Firstly, the concentration of the azetidinone was varied while the concentration of the other reactants remains constant. The concentration of azetidinone varied from 0.12 – 3.0M. After obtaining the rate with each concentration of azetidinone, by plotting the log(initial rate) against log(M), first order dependence on the azetidinone was found (Figure 2).

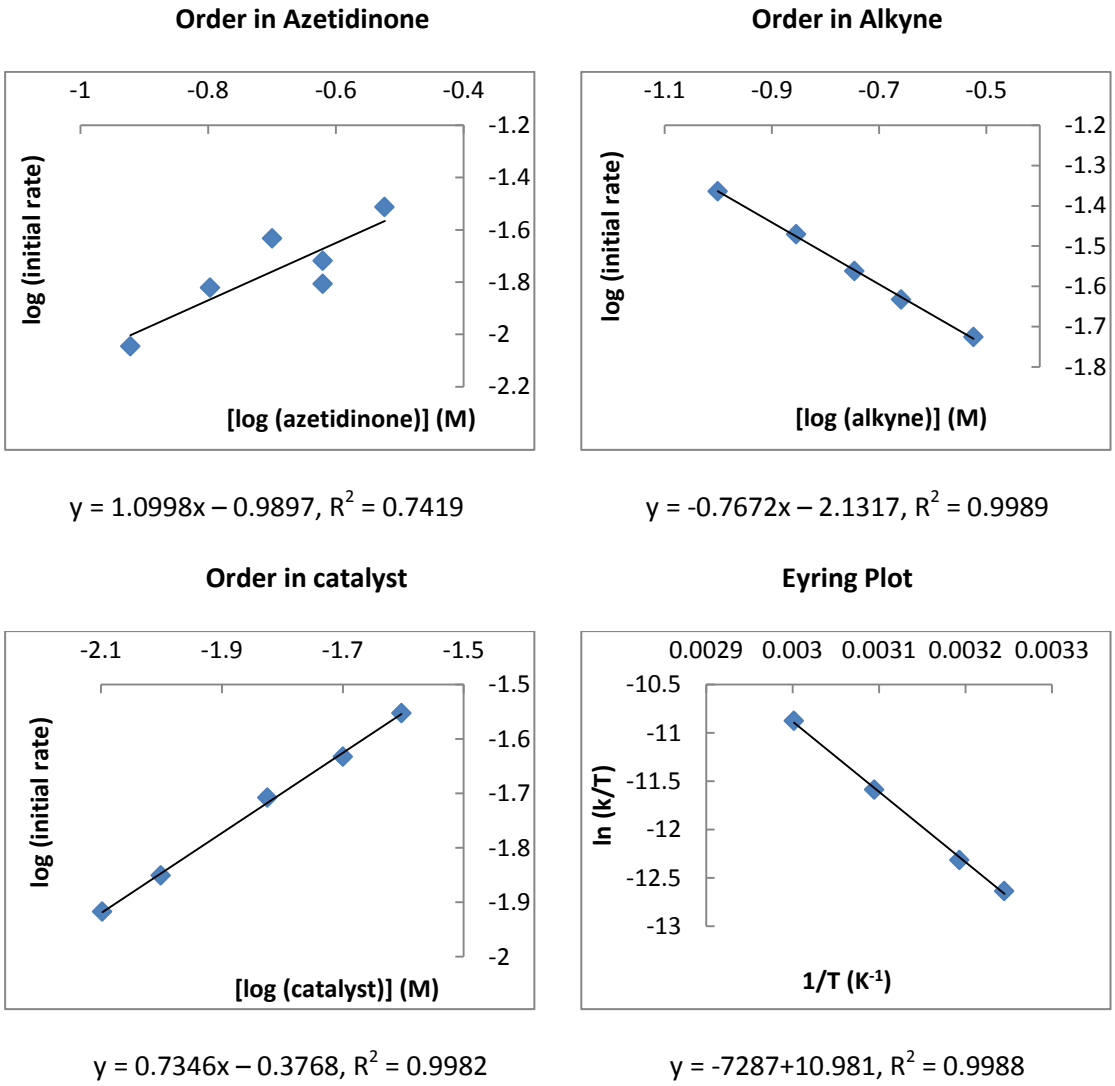


**Figure 2** $Ni(cod)_2$ and $PPh_3$ ratio of 1:2

Secondly, the concentration of the alkyne was varied while the concentration of the other reactants remain constant. The concentration of alkyne varied from 0.10 – 0.30M. After obtaining the rate with each concentration of alkyne, by plotting the log(initial rate) against log(M), negative first order dependence on the alkyne was found. Finally, the concentration of the $Ni(cod)_2$ and $PPh_3$ were varied but the ratio of 1:2 was kept while the concentration of the other reactants remained constant. The concentration of $Ni(cod)_2$ was varied from 0.008 – 0.025M. The concentration of $PPh_3$ was varied from 0.016 – 0.050M. After obtaining the rate with each concentration of catalyst, by plotting the log(initial rate) against log(M), first order dependence on the catalyst was found. As a result, the rate law can be formulated by the following:

$$\text{Rate} = k_{obs}[\text{Azetidinone}]^{1.1}[\text{Alkyne}]^{-0.8}[\text{Catalyst}]^{0.7}$$

An Eyring plot was then plotted to elucidate the nature of the transition state of the rate determining step. A $\Delta H$ of 60.6 kJ $mol^{-1}$, $\Delta S$ -106.3 J mol $K^{-1}$ and $\Delta G$ 93.8 kJ $mol^{-1}$ at 40°C were obtained.

### 3.2.2.3 NMR studies

A NMR study in a J-Young NMR tube was then carried out to determine if there was any complexation of pyridinone **74** to the catalyst (Scheme 20). Treatment of 1 equiv of $Ni(cod)_2$ and 3 equiv of $PPh_3$ in $d_8$-toluene resulted in the rapid formation of a dark-red solution assumed to be $PPh_3$-nickel-complex **75**. Afterwards, **74** was added and then NMR measurements were taken. Analysis of the $^1H$ and $^{31}P$ NMR spectra showed peaks which are characteristic of **74** and **75**. **75** has two $PPh_3$ and a cod ligand attached to the nickel centre which is formed from the displacement of the first cod ligand. In the spectra, there is a second peak which is assumed to be either $Ni(PPh_3)_3$ or $O{=}PPh_3$. However, no formation of nickel-product complex **76** was observed as confirmed by analysis of the $^1H$ NMR spectra which

suggests that the remaining cod ligand is not readily displaced by **74**. Furthermore, this reveals that inhibition of the catalyst by **74** is unlikely as there is no complexation of **74** to the catalyst.

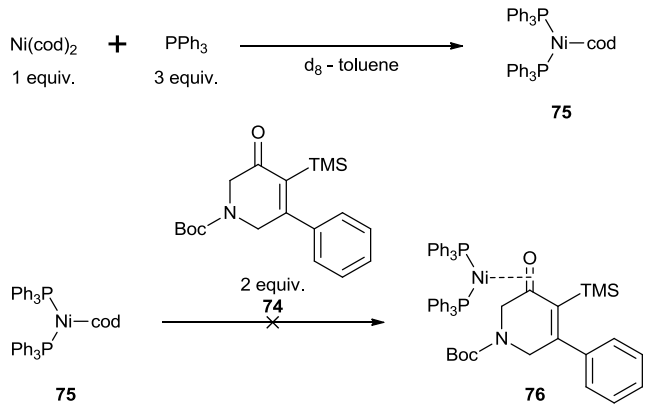


**Scheme 20** Attempted study on the complexation of **74** to the catalyst

A competition study between alkyne **73** and product **74** was then carried out (Scheme 21). After 5 minutes of stirring to form phosphine-nickel complex **75** in $d_8$-toluene, **74** and then **73** were added. Observation by $^{31}P$ NMR showed new peaks. The peak attributed to **75** was completely consumed and two new peaks (40.5 ppm, d, *J* = 31.7 Hz and 37.9 ppm, d, *J* = 31.7Hz) were there instead. Since the nickel-alkyne complex **77** is described,[11] we are confident complex **77** is indeed formed and the product remains uncoordinated. Furthermore, $^1H$ NMR peaks of **74** matched with the example given above which indicates that **74** is likely to be uncoordinated. Furthermore, this study revealed that the displacement of the alkyne with **74** is a very difficult process.


**Scheme 21** Competition study between product and alkyne

The synthesis of complex **77** began with the addition of **73** to a pre-mixed solution of $Ni(cod)_2$ in $PPh_3$ in toluene (Scheme 22). After stirring for 1 hour, the suspension was filtered and all the volatiles were removed and washed with hexane to give **77** in a yield of 97%. **77** is also catalytically competent as full conversion to **74** was observed under the modified standard reaction conditions (Scheme 23).

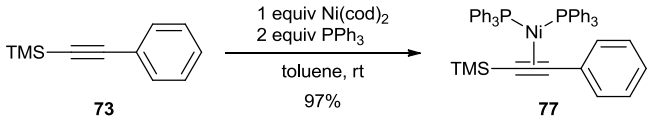


**Scheme 22** Synthesis of complex **77**

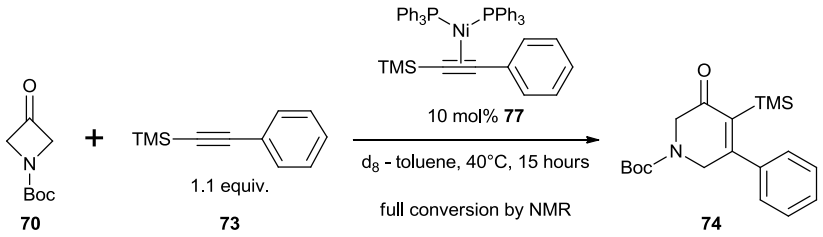


**Scheme 23** Catalysis with 10 mol% of complex **77** as catalyst

A NMR study was then commenced to see if complex **77** is the active catalyst. In the kinetic study, a negative first order dependence in alkyne **73** was found. Therefore, **77** could lose an alkyne to give the active catalyst or **77** is the active catalyst which came from bis-alkyne nickel-complex **78**. To test which of the two pathways were most plausible, an attempt to force the formation of the *bis*-alkyne complex **78** by addition of 5 equivalents of **73** was made (Scheme 24)**.** However, no new peaks were observed in either the $^{31}P$ or $^{1}H$ spectra. As a result of the difficulty in forcing the formation of **78**, the active catalyst is most likely formed by the loss of alkyne **73** at the rate determining step.

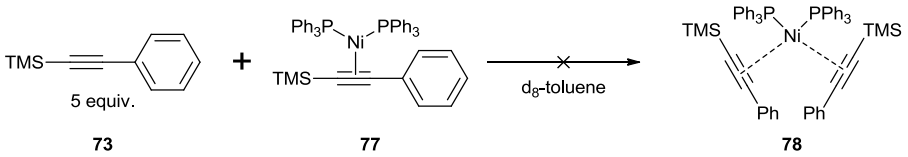


**Scheme 24** Forcing the formation of complex **78**

Furthermore, mixing complex **78** and alkyne **79** in $d_8$-toluene resulted in the formation of complex **80** and **73** as determined by $^{31}P$ NMR (Scheme 25). It is likely there is an equilibration between **77** and **80**. However, no other peaks were observed in the $^{31}P$ or $^{1}H$ HNMR spectra. Therefore, this shows the exchange of alkyne occurs faster than the "NMR timescale".

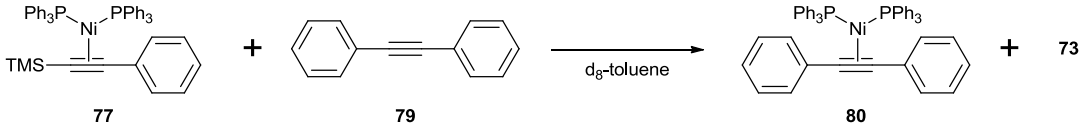


**Scheme 25** Alkyne equilibration

The formation of the oxanickelacyclopentene **81** was attempted by mixing complex **77** with 1 equiv. of azetidinone **70** in $d_8$-toluene (Scheme 26). However, no formation of **81** was detected by $^{1}H$ or $^{31}P$ NMR. On the other hand, there was a slow appearance of product **74**. Heating the solution to 40°C did not significantly improve the conversion to **74**.

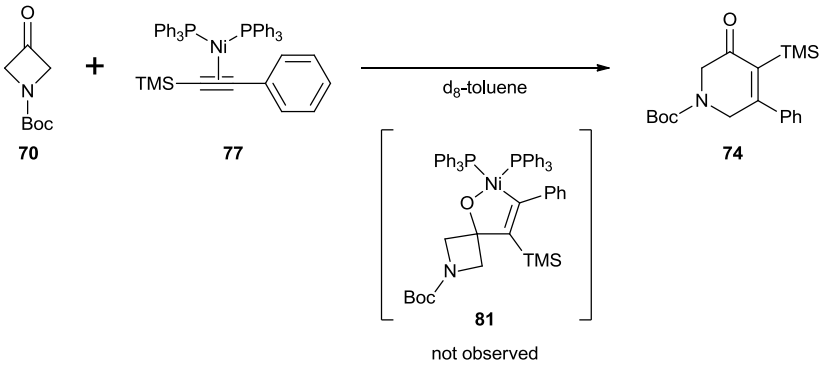


**Scheme 26** Attempted to force the formation of oxanickelacyclopentene

## 3.3 Revised Mechanism and Conclusion

In light of the kinetic study and various NMR investigations, a mechanism is proposed (Scheme 27). Nickel-complex **77** is a resting state of the reaction and is observed experimentally. From the kinetic study, a negative first order dependence on the alkyne, a first order dependence on the azetidinone and a first order dependence on the catalyst were observed. Furthermore, the formation of oxanickelacyclopentene **81** and *bis*-alkyne complex **78** were not possible. Therefore, a revised mechanism was hypothesised (Scheme 26). This revealed that **77** is an inactive resting state and is therefore off cycle because an alkyne has to be lost. Therefore, complex **83** is the active catalyst which will participate in the oxidative addition in the RDS which will account for the first order dependence on catalyst. The addition of azetidinone at the RDS will account for the first order dependence on azetidinone. Finally, the loss of an alkyne will account for the negative first order dependence on alkyne.

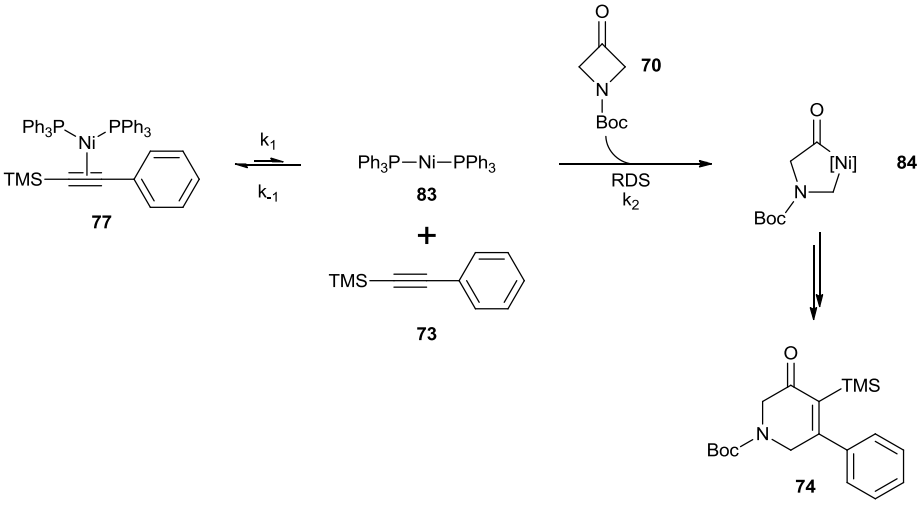


**Scheme 27** Revised mechanism

Based on the revised mechanism, the following equation gives the rate of the reaction which depends on the concentration of intermediate **83** and azetidinone **70**:

$$\frac{d[\mathbf{84}]}{dt} = k_2[\mathbf{83}][\mathbf{70}]$$

Equation 1

Intermediate **83** is formed by the loss of an alkyne **73** from complex **77.** However, **83** is depleted by the reverse reaction with **83** and **73**. Also, **83** is depleted in the reaction with **70**. Therefore, the concentration of **83** will change as a function of time:

$$\frac{d[\mathbf{83}]}{dt} = k_1[\mathbf{77}] - k_{-1}[\mathbf{73}][\mathbf{83}] - k_2[\mathbf{83}][\mathbf{70}] = 0$$

Equation 2

By carrying out a steady state approximation whereby the concentration of **83** does not change with time, upon rearrangement of the previous equation, the following equation is attained:

$$[\mathbf{83}] = \frac{k_1[\mathbf{77}]}{k_{-1}[\mathbf{73}] + k_2[\mathbf{70}]}$$

Equation 3

Substitution of the expression for [**83**] into equation 1 will arrive at the following equation:

$$\frac{d[\mathbf{84}]}{dt} = \frac{k_1 k_2[\mathbf{77}][\mathbf{70}]}{k_{-1}[\mathbf{73}] + k_2[\mathbf{70}]}$$

Equation 4

To fit the observed order dependence of each reactant, $k_2$[Azetidinone]<<$k_{-1}$[Alkyne]. This isn't surprising as **77** is observed as a resting state by NMR. As a result, the kinetic expression is simplified to:

$$\frac{d[\mathbf{84}]}{dt} = \frac{k_1 k_2[\mathbf{77}][\mathbf{70}]}{k_{-1}[\mathbf{70}]}$$

Equation 5

Therefore the $k_{obs}$ is:

$$k_{obs} = \frac{k_1 k_2}{k_{-1}}$$

From the kinetic studies, an alkyne is lost at the rate determining step which is different from what is predicted theoretically by Li and Lin.[8] Furthermore, the original proposed mechanism is now in doubt.[9] As judged by NMR studies, a nickel-complex **77** is the resting state in the catalytic cycle and no other intermediates are observed over the course of the reaction. Also, the **77** is catalytically competent. However, further tests will be necessary to determine if the insertion of the catalyst into the azetidinone to form **84** is a reality.

## 3.4 Experimental data

### 3.4.1 Kinetic study

General procedure for all kinetic studies: Kinetic experiments were run inside an argon filled glovebox. Reactions were run up to about 6 – 63% conversion and the data (% product versus time) was analysed using the initial rates method.

#### 3.4.1.1 Kinetic study: Ni(cod)2/PPh3 (1:3)

Order in azetidinone **70**: The order in **70** was determined by studying the initial rate of reactions with different [**70**]: Inside a glovebox, a round bottom flask was charged with the $Ni(cod)_2$ (6.4 mg, 0.02 mmol) and $PPh_3$ (18.4 mg, 0.07 mmol). A rubber septa was used to seal the round bottom flask and taken out of the glovebox. Immediately, an argon balloon was used to keep the round bottom flask under inert atmosphere. Toluene (0.37 ml) was then added *via* syringe. After 5 mins of stirring at rt, a solution of azetidinone (0.14 – 0.28 mmol), alkyne (51 µl, 0.26 mmol) and triphenylethylene (59.9 mg, 0.24 mmol) in toluene (0.80 ml) was added *via* syringe. Immediately, the round bottom flask was transferred to a pre-heated oil bath set at 40°C. Aliquots were taken out with a syringe from the reaction vessel at specific

times and immediately filtered through a plug of $SiO_2$ and washing with $Et_2O$. After all the volatiles were removed, product yield from the corresponding reaction was monitored by $^1H$ NMR analysis using triphenylethylene as internal standard.

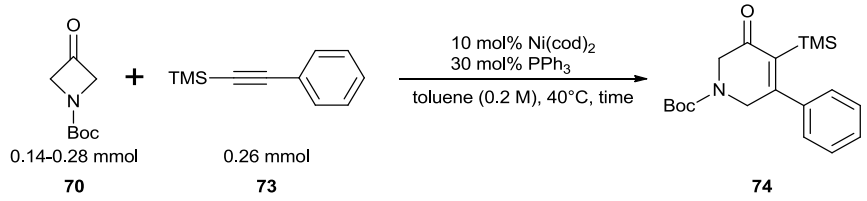


0.14 mmol of **70**

| Time (min) | Int Std[a] | **74**[a] | **74** (M) |
|---|---|---|---|
| 15 | 1 | 1.0562 | 0.052718 |
| 30 | 1 | 1.3201 | 0.065889 |
| 46 | 1 | 1.417 | 0.070726 |
| 61 | 1 | 1.55 | 0.077364 |

[a] Integration of $^1H$ NMR

0.14 mmol of **70**

| Time (min) | Int Std[a] | **74**[a] | **74** (M) |
|---|---|---|---|
| 10 | 1 | 1.1063 | 0.055218 |
| 20 | 1 | 1.2086 | 0.060324 |
| 30 | 1 | 1.2972 | 0.064746 |
| 40 | 1 | 1.3877 | 0.069264 |

[a] Integration of $^1H$ NMR

0.19 mmol of **70**

| Time (min) | Int Std[a] | **74**[a] | **74** (M) |
|---|---|---|---|
| 10 | 1 | 1.1291 | 0.056356 |
| 20 | 1 | 1.2909 | 0.064432 |
| 30 | 1 | 1.4321 | 0.07148 |
| 40 | 1 | 1.5346 | 0.076596 |

[a] Integration of $^{1}$H NMR

0.19 mmol of **70**

| Time (min) | Int Std[a] | **74**[a] | **74** (M) |
|---|---|---|---|
| 10 | 1 | 1.2184 | 0.060813 |
| 20 | 1 | 1.393 | 0.069528 |
| 30 | 1 | 1.54 | 0.076865 |
| 40 | 1 | 1.6863 | 0.084167 |

[a] Integration of $^{1}$H NMR

0.24 mmol of **70**

| Time (min) | Int Std[a] | **74**[a] | **74** (M) |
|---|---|---|---|
| 5 | 1 | 0.9558 | 0.047706 |
| 10 | 1 | 1.0802 | 0.053915 |
| 15 | 1 | 1.1888 | 0.059336 |
| 20 | 1 | 1.2925 | 0.064512 |

[a] Integration of $^{1}$H NMR

0.24 mmol of **70**

| Time (min) | Int Std[a] | **74**[a] | **74** (M) |
|---|---|---|---|
| 10 | 1 | 1.1691 | 0.058353 |
| 20 | 1 | 1.3459 | 0.067177 |
| 30 | 1 | 1.5452 | 0.077125 |
| 40 | 1 | 1.7202 | 0.085859 |

[a] Integration of $^1$H NMR

0.28 mmol of **70**

| Time (min) | Int Std[a] | **74**[a] | **74** (M) |
|---|---|---|---|
| 10 | 1 | 1.2562 | 0.0627 |
| 20 | 1 | 1.4971 | 0.074724 |
| 30 | 1 | 1.7257 | 0.086134 |
| 40 | 1 | 1.9437 | 0.097015 |

[a] Integration of $^1$H NMR

Order in alkyne **73**: The order in **73** was determined by studying the initial rate of reactions with different [**73**]: Inside a glovebox, a round bottom flask was charged with the $Ni(cod)_2$ (6.4 mg, 0.02 mmol) and $PPh_3$ (18.4 mg, 0.07 mmol). A rubber septa was used to seal the round bottom flask and taken out of the glovebox. Immediately, an argon balloon was used to keep the round bottom flask under inert atmosphere. Toluene (0.37 ml) was then added *via* syringe. After 5 mins of stirring at rt, a solution of azetidinone (40 mg, 0.23 mmol), alkyne (0.12 – 0.35 mmol) and triphenylethylene (59.9 mg, 0.13 mmol) in toluene (0.80 ml) was added *via* syringe. Immediately, the round bottom flask was transferred to a pre-heated oil bath set at 40°C. Aliquots were taken out with a syringe from the reaction vessel at specific times and immediately filtered through a plug of $SiO_2$ and washing with $Et_2O$. After all the volatiles were

removed, product yield from the corresponding reaction was monitored by $^1$H NMR analysis using triphenylethylene as internal standard.

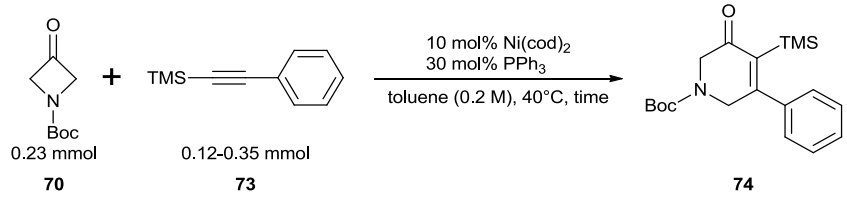


0.12 mmol of **73**

| Time (min) | Int Std[a] | **74**[a] | **74** (M) |
|---|---|---|---|
| 3 | 1 | 0.699 | 0.034889 |
| 6 | 1 | 0.8453 | 0.042191 |
| 9 | 1 | 0.9328 | 0.046558 |
| 12 | 1 | 1.0085 | 0.050337 |

[a] Integration of $^1$H NMR

0.14 mmol of **73**

| Time (min) | Int Std[a] | **74**[a] | **74** (M) |
|---|---|---|---|
| 5 | 1 | 1.0399 | 0.051904 |
| 10 | 1 | 1.2625 | 0.063014 |
| 15 | 1 | 1.4081 | 0.070282 |
| 20 | 1 | 1.5401 | 0.07687 |

[a] Integration of $^1$H NMR

0.16 mmol of **73**

| Time (min) | Int Std[a] | **74**[a] | **74** (M) |
|---|---|---|---|
| 5 | 1 | 0.9538 | 0.047606 |
| 10 | 1 | 1.1166 | 0.055732 |
| 15 | 1 | 1.2583 | 0.062805 |
| 20 | 1 | 1.416 | 0.070676 |

[a] Integration of $^{1}$H NMR

0.26 mmol of **73**

| Time (min) | Int Std[a] | **74**[a] | **74** (M) |
|---|---|---|---|
| 5 | 1 | 0.9558 | 0.047706 |
| 10 | 1 | 1.0802 | 0.053915 |
| 15 | 1 | 1.1888 | 0.059336 |
| 20 | 1 | 1.2925 | 0.064512 |

[a] Integration of $^{1}$H NMR

0.26 mmol of **73**

| Time (min) | Int Std[a] | **74**[a] | **74** (M) |
|---|---|---|---|
| 10 | 1 | 1.1691 | 0.058353 |
| 20 | 1 | 1.3459 | 0.067177 |
| 30 | 1 | 1.5452 | 0.077125 |
| 40 | 1 | 1.7202 | 0.085859 |

[a] Integration of $^{1}$H NMR

0.35 mmol of **73**

| Time (min) | Int Std[a] | **74**[a] | **74** (M) |
|---|---|---|---|
| 10 | 1 | 0.7665 | 0.038258 |
| 20 | 1 | 0.9586 | 0.047846 |
| 30 | 1 | 1.1214 | 0.055972 |
| 40 | 1 | 1.315 | 0.065635 |

[a] Integration of $^{1}$H NMR

Order in catalyst: The order in catalyst was determined by studying the initial rate of reactions with different loadings of catalyst: Inside a glovebox, a round bottom flask was charged with the $Ni(cod)_2$ (0.006 – 0.029 mmol) and $PPh_3$ (0.018 – 0.088 mmol). A rubber septa was used to seal the round bottom flask and taken out of the glovebox. Immediately, an argon balloon was used to keep the round bottom flask under inert atmosphere. Toluene (0.37 ml) was then added *via* syringe. After 5 mins of stirring at rt, a solution of azetidinone (40 mg, 0.23 mmol), alkyne (51 µl, 0.26 mmol) and triphenylethylene (59.9 mg, 0.23 mmol) in toluene (0.80 ml) was added *via* syringe. Immediately, the round bottom flask was transferred to a pre-heated oil bath set at 40°C. Aliquots were taken out with a syringe from the reaction vessel at specific times and immediately filtered through a plug of $SiO_2$ and washing with $Et_2O$. After all the volatiles were removed, product yield from the corresponding reaction was monitored by $^{1}$H NMR analysis using triphenylethylene as internal standard.

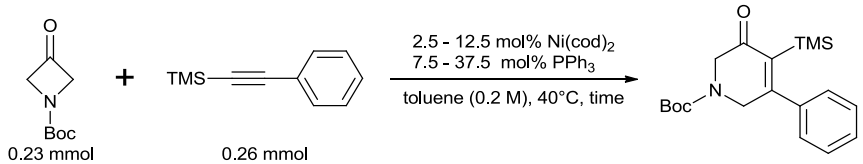


0.006 mmol of $Ni(cod)_2$ and 0.018 mmol of $PPh_3$

| Time (min) | Int Std[a] | **74**[a] | **74** (M) |
|---|---|---|---|
| 15 | 1 | 0.241 | 0.012029 |
| 30 | 1 | 0.3172 | 0.015832 |
| 45 | 1 | 0.4066 | 0.020294 |
| 60 | 1 | 0.4864 | 0.024277 |

[a] Integration of $^1H$ NMR

0.009 mmol of $Ni(cod)_2$ and 0.028 mmol of $PPh_3$

| Time (min) | Int Std[a] | **74**[a] | **74** (M) |
|---|---|---|---|
| 10 | 1 | 0.482 | 0.024058 |
| 20 | 1 | 0.5865 | 0.029274 |
| 30 | 1 | 0.6644 | 0.033162 |
| 40 | 1 | 0.7298 | 0.036426 |

[a] Integration of $^1H$ NMR

0.012 mmol of $Ni(cod)_2$ and 0.035 mmol of $PPh_3$

| Time (min) | Int Std[a] | **74**[a] | **74** (M) |
|---|---|---|---|
| 10 | 1 | 0.6853 | 0.034205 |
| 20 | 1 | 0.8329 | 0.041572 |
| 30 | 1 | 0.9799 | 0.048909 |
| 40 | 1 | 1.1045 | 0.055128 |

[a] Integration of $^1H$ NMR

0.018 mmol of $Ni(cod)_2$ and 0.053 mmol of $PPh_3$

| Time (min) | Int Std[a] | **74**[a] | **74** (M) |
|---|---|---|---|
| 5 | 1 | 0.7479 | 0.03733 |
| 10 | 1 | 0.8333 | 0.041592 |
| 15 | 1 | 0.9345 | 0.046643 |
| 20 | 1 | 1.0044 | 0.050132 |

[a] Integration of $^1H$ NMR

0.023 mmol of $Ni(cod)_2$ and 0.070 mmol of $PPh_3$

| Time (min) | Int Std[a] | **74**[a] | **74** (M) |
|---|---|---|---|
| 5 | 1 | 0.9558 | 0.047706 |
| 10 | 1 | 1.0802 | 0.053915 |
| 15 | 1 | 1.1888 | 0.059336 |
| 20 | 1 | 1.2925 | 0.064512 |

[a] Integration of $^1H$ NMR

0.023 mmol of $Ni(cod)_2$ and 0.070 mmol of $PPh_3$

| Time (min) | Int Std[a] | **74**[a] | **74** (M) |
|---|---|---|---|
| 10 | 1 | 1.1691 | 0.058353 |
| 20 | 1 | 1.3459 | 0.067177 |
| 30 | 1 | 1.5452 | 0.077125 |
| 40 | 1 | 1.7202 | 0.085859 |

[a] Integration of $^1H$ NMR

0.029 mmol of $Ni(cod)_2$ and 0.088 mmol of $PPh_3$

| Time (min) | Int Std[a] | **74**[a] | **74** (M) |
|---|---|---|---|
| 5 | 1 | 1.0452 | 0.052168 |
| 10 | 1 | 1.1927 | 0.059531 |
| 15 | 1 | 1.2836 | 0.064068 |
| 20 | 1 | 1.4143 | 0.070591 |

[a] Integration of $^1H$ NMR

Eyring plot: The Eyring plot was determined by studying the initial rate of reactions at different temperatures: Inside a glovebox, a round bottom flask was charged with the $Ni(cod)_2$ (6.4 mg, 0.02 mmol) and $PPh_3$ (18.4 mg, 0.07 mmol). A rubber septa was used to seal the round bottom flask and taken out of the glovebox. Immediately, an argon balloon was used to keep the round bottom flask under inert atmosphere. Toluene (0.37 ml) was then added *via* syringe. After 5 mins of stirring at rt, a solution of azetidinone (40 mg, 0.23 mmol), alkyne (51 µl, 0.26 mmol) and triphenylethylene (59.8 mg, 0.23 mmol) in toluene (0.80 ml) was added *via* syringe. Immediately, the round bottom flask was transferred to a pre-heated oil bath (35 – 60°C). Aliquots were taken out with a syringe from the reaction vessel at specific times and immediately filtered through a plug of $SiO_2$ and washing with $Et_2O$. After all the volatiles were

removed, product yield from the corresponding reaction was monitored by $^1$H NMR analysis using triphenylethylene as internal standard.

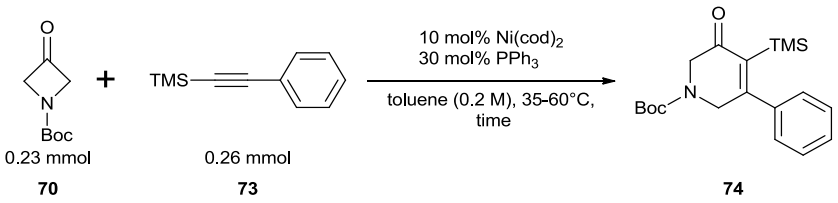


At 35°C

| Time (min) | Int Std[a] | **74**[a] | **74** (M) |
|---|---|---|---|
| 10 | 1 | 0.8106 | 0.040459 |
| 20 | 1 | 1.007 | 0.050262 |
| 30 | 1 | 1.1739 | 0.058592 |
| 40 | 1 | 1.3122 | 0.065495 |

[a] Integration of $^1$H NMR

At 40°C

| Time (min) | Int Std[a] | **74**[a] | **74** (M) |
|---|---|---|---|
| 5 | 1 | 0.9558 | 0.047706 |
| 10 | 1 | 1.0802 | 0.053915 |
| 15 | 1 | 1.1888 | 0.059336 |
| 20 | 1 | 1.2925 | 0.064512 |

[a] Integration of $^1$H NMR

At 40°C

| Time (min) | Int Std[a] | **74**[a] | **74** (M) |
|---|---|---|---|
| 10 | 1 | 1.1691 | 0.058353 |
| 20 | 1 | 1.3459 | 0.067177 |
| 30 | 1 | 1.5452 | 0.077125 |
| 40 | 1 | 1.7202 | 0.085859 |

[a] Integration of $^{1}$H NMR

At 50°C

| Time (min) | Int Std[a] | **74**[a] | **74** (M) |
|---|---|---|---|
| 10 | 1 | 1.2286 | 0.061322 |
| 15 | 1 | 1.4619 | 0.072967 |
| 20 | 1 | 1.7046 | 0.085081 |
| 25 | 1 | 1.8754 | 0.093606 |

[a] Integration of $^{1}$H NMR

At 60°C

| Time (min) | Int Std[a] | **74**[a] | **74** (M) |
|---|---|---|---|
| 4 | 1 | 1.0826 | 0.054035 |
| 8 | 1 | 1.4499 | 0.072368 |
| 12 | 1 | 1.8064 | 0.090162 |
| 16 | 1 | 2.1283 | 0.106229 |

[a] Integration of $^{1}$H NMR

### 3.4.1.2 Kinetic Study: Ni(cod)2/PPh3 (1:2)

Order in azetidinone **70**: The order in **70** was determined by studying the initial rate of reactions with different [**70**]: Inside a glovebox, a round bottom flask was charged with the $Ni(cod)_2$ (6.4 mg, 0.02 mmol) and $PPh_3$ (12.3 mg, 0.05 mmol). A rubber septa was used to seal the round bottom flask and taken out of the glovebox. Immediately, an argon balloon was used to keep the round bottom flask under inert atmosphere. Toluene (0.37 ml) was then added *via* syringe. After 5 mins of stirring at rt, a solution of azetidinone (0.14 – 0.35 mmol), alkyne (51 µl, 0.26 mmol) and triphenylethylene (59.8 mg, 0.23 mmol) in toluene (0.80 ml) was added *via* syringe. Immediately, the round bottom flask was transferred to a pre-heated oil bath set at 40°C. Aliquots were taken out with a syringe from the reaction vessel at specific times and immediately filtered through a plug of $SiO_2$ and washing with $Et_2O$. After all the volatiles were removed, product yield from the corresponding reaction was monitored by $^1H$ NMR analysis using triphenylethylene as internal standard.

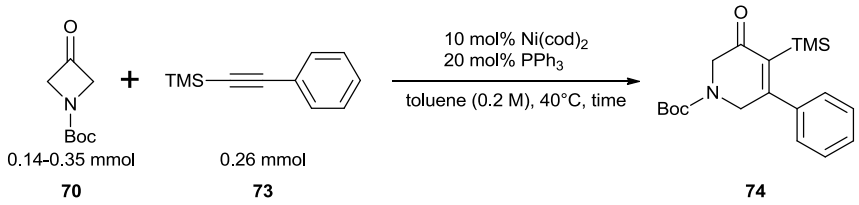


0.14 mmol of **70**

| Time (min) | Int Std[a] | **74**[a] | **74** (M) |
|---|---|---|---|
| 15 | 1 | 0.9236 | 0.046099 |
| 30 | 1 | 1.1116 | 0.055483 |
| 45 | 1 | 1.2627 | 0.063024 |
| 60 | 1 | 1.4134 | 0.070546 |

[a] Integration of $^1H$ NMR

0.19 mmol of **70**

| Time (min) | Int Std[a] | **74**[a] | **74** (M) |
|---|---|---|---|
| 10 | 1 | 1.0423 | 0.052024 |
| 20 | 1 | 1.239 | 0.061842 |
| 30 | 1 | 1.4324 | 0.071495 |
| 40 | 1 | 1.5839 | 0.079056 |

[a] Integration of $^{1}$H NMR

0.24 mmol of **70**

| Time (min) | Int Std[a] | **74**[a] | **74** (M) |
|---|---|---|---|
| 5 | 1 | 0.9166 | 0.04575 |
| 10 | 1 | 1.0727 | 0.053541 |
| 15 | 1 | 1.201 | 0.059945 |
| 20 | 1 | 1.3401 | 0.066888 |

[a] Integration of $^{1}$H NMR

0.28 mmol of **70**

| Time (min) | Int Std[a] | **74**[a] | **74** (M) |
|---|---|---|---|
| 5 | 1 | 0.9595 | 0.047891 |
| 10 | 1 | 1.081 | 0.053955 |
| 15 | 1 | 1.1918 | 0.059486 |
| 20 | 1 | 1.3045 | 0.065111 |

[a] Integration of $^{1}$H NMR

0.28 mmol of **70**

| Time (min) | Int Std[a] | **74**[a] | **74** (M) |
|---|---|---|---|
| 10 | 1 | 1.054 | 0.052608 |
| 15 | 1 | 1.1658 | 0.058188 |
| 20 | 1 | 1.2516 | 0.06247 |
| 25 | 1 | 1.3379 | 0.066778 |

[a] Integration of $^1$H NMR

0.35 mmol of **70**

| Time (min) | Int Std[a] | **74**[a] | **74** (M) |
|---|---|---|---|
| 5 | 1 | 1.0044 | 0.050132 |
| 10 | 1 | 1.1932 | 0.059556 |
| 15 | 1 | 1.3883 | 0.069293 |
| 20 | 1 | 1.5537 | 0.077549 |

[a] Integration of $^1$H NMR

Order in alkyne **73**: The order in **73** was determined by studying the initial rate of reactions with different [**73**]: Inside a glovebox, a round bottom flask was charged with the $Ni(cod)_2$ (6.4 mg, 0.02 mmol) and $PPh_3$ (12.3 mg, 0.05 mmol). A rubber septa was used to seal the round bottom flask and taken out of the glovebox. Immediately, an argon balloon was used to keep the round bottom flask under inert atmosphere. Toluene (0.37 ml) was then added *via* syringe. After 5 mins of stirring at rt, a solution of azetidinone (40 mg, 0.23 mmol), alkyne (0.12 – 0.35 mmol) and triphenylethylene (59.8 mg, 0.23 mmol) in toluene (0.80 ml) was added *via* syringe. Immediately, the round bottom flask was transferred to a pre-heated oil bath set at 40°C. Aliquots were taken out with a syringe from the reaction vessel at specific times and immediately filtered through a plug of $SiO_2$ and washing with $Et_2O$. After all the volatiles were

removed, product yield from the corresponding reaction was monitored by $^1$H NMR analysis using triphenylethylene as internal standard.

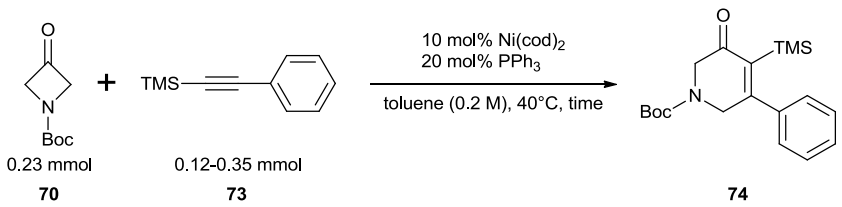


0.12 mmol of **73**

| Time (min) | Int Std[a] | **74**[a] | **74** (M) |
|---|---|---|---|
| 3 | 1 | 0.737 | 0.036785 |
| 6 | 1 | 0.8968 | 0.044761 |
| 9 | 1 | 1.0595 | 0.052882 |
| 12 | 1 | 1.2026 | 0.060025 |

[a] Integration of $^1$H NMR

0.16 mmol of **73**

| Time (min) | Int Std[a] | **74**[a] | **74** (M) |
|---|---|---|---|
| 10 | 1 | 1.3263 | 0.066199 |
| 15 | 1 | 1.5382 | 0.076775 |
| 20 | 1 | 1.7489 | 0.087292 |
| 25 | 1 | 1.9338 | 0.096521 |

[a] Integration of $^1$H NMR

0.21 mmol of **73**

| Time (min) | Int Std[a] | **74**[a] | **74** (M) |
|---|---|---|---|
| 10 | 1 | 1.1339 | 0.056596 |
| 20 | 1 | 1.4984 | 0.074789 |
| 30 | 1 | 1.8289 | 0.091285 |
| 40 | 1 | 2.1232 | 0.105974 |

[a] Integration of $^{1}$H NMR

0.26 mmol of **73**

| Time (min) | Int Std[a] | **74**[a] | **74** (M) |
|---|---|---|---|
| 5 | 1 | 0.9166 | 0.04575 |
| 10 | 1 | 1.0727 | 0.053541 |
| 15 | 1 | 1.201 | 0.059945 |
| 20 | 1 | 1.3401 | 0.066888 |

[a] Integration of $^{1}$H NMR

0.35 mmol of **73**

| Time (min) | Int Std[a] | **74**[a] | **74** (M) |
|---|---|---|---|
| 10 | 1 | 0.9663 | 0.04823 |
| 20 | 1 | 1.2041 | 0.0601 |
| 30 | 1 | 1.4113 | 0.070441 |
| 40 | 1 | 1.6508 | 0.082395 |

[a] Integration of $^{1}$H NMR

Order in catalyst: The order in catalyst was determined by studying the initial rate of reactions with different loadings of catalyst: Inside a glovebox, a round bottom flask was charged with

the $Ni(cod)_2$ (0.009 – 0.29 mmol) and $PPh_3$ (0.018 – 0.58 mmol). A rubber septa was used to seal the round bottom flask and taken out of the glovebox. Immediately, an argon balloon was used to keep the round bottom flask under inert atmosphere. Toluene (0.37 ml) was then added *via* syringe. After 5 mins of stirring at rt, a solution of azetidinone (40 mg, 0.23 mmol), alkyne (51 µl, 0.26 mmol) and triphenylethylene (59.8 mg, 0.23 mmol) in toluene (0.80 ml) was added *via* syringe. Immediately, the round bottom flask was transferred to a pre-heated oil bath set at 40°C. Aliquots were taken out with a syringe from the reaction vessel at specific times and immediately filtered through a plug of $SiO_2$ and washing with $Et_2O$. After all the volatiles were removed, product yield from the corresponding reaction was monitored by $^1H$ NMR analysis using triphenylethylene as internal standard.

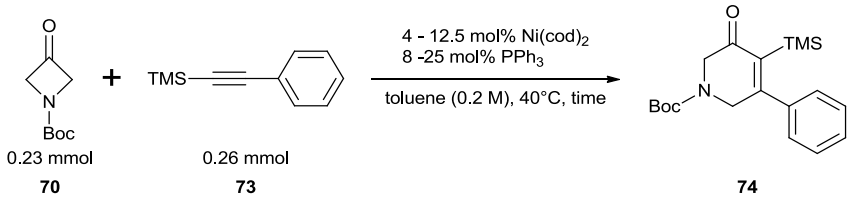


0.009 mmol of $Ni(cod)_2$ and 0.018 mmol of $PPh_3$

| Time (min) | Int Std[a] | **74**[a] | **74** (M) |
|---|---|---|---|
| 10 | 1 | 0.5215 | 0.026029 |
| 20 | 1 | 0.6776 | 0.033821 |
| 30 | 1 | 0.8197 | 0.040913 |
| 40 | 1 | 0.9608 | 0.047956 |

[a] Integration of $^1H$ NMR

0.012 mmol of $Ni(cod)_2$ and 0.023 mmol of $PPh_3$

| Time (min) | Int Std[a] | **74**[a] | **74** (M) |
|---|---|---|---|
| 10 | 1 | 0.5424 | 0.027073 |
| 20 | 1 | 0.73 | 0.036436 |
| 30 | 1 | 0.8913 | 0.044487 |
| 40 | 1 | 1.0524 | 0.052528 |

[a] Integration of $^1H$ NMR

0.018 mmol of $Ni(cod)_2$ and 0.036 mmol of $PPh_3$

| Time (min) | Int Std[a] | **74**[a] | **74** (M) |
|---|---|---|---|
| 5 | 1 | 0.66 | 0.032942 |
| 10 | 1 | 0.7648 | 0.038173 |
| 15 | 1 | 0.8989 | 0.044866 |
| 20 | 1 | 1.007 | 0.050262 |

[a] Integration of $^1H$ NMR

0.023 mmol of $Ni(cod)_2$ and 0.047 mmol of $PPh_3$

| Time (min) | Int Std[a] | **74**[a] | **74** (M) |
|---|---|---|---|
| 5 | 1 | 0.9166 | 0.04575 |
| 10 | 1 | 1.0727 | 0.053541 |
| 15 | 1 | 1.201 | 0.059945 |
| 20 | 1 | 1.3401 | 0.066888 |

[a] Integration of $^1H$ NMR

0.029 mmol of $Ni(cod)_2$ and 0.058 mmol of $PPh_3$

| Time (min) | Int Std[a] | **74**[a] | **74** (M) |
|---|---|---|---|
| 5 | 1 | 1.2178 | 0.060783 |
| 10 | 1 | 1.3697 | 0.068365 |
| 15 | 1 | 1.5592 | 0.077823 |
| 20 | 1 | 1.7157 | 0.085635 |

[a] Integration of $^1H$ NMR

Eyring plot: The Eyring plot was determined by studying the initial rate of reactions at different temperatures: Inside a glovebox, a round bottom flask was charged with the $Ni(cod)_2$ (6.4 mg, 0.02 mmol) and $PPh_3$ (12.3 mg, 0.05 mmol). A rubber septa was used to seal the round bottom flask and taken out of the glovebox. Immediately, an argon balloon was used to keep the round bottom flask under inert atmosphere. Toluene (0.37 ml) was then added *via* syringe. After 5 mins of stirring at rt, a solution of azetidinone (40 mg, 0.23 mmol), alkyne (51 µl, 0.26 mmol) and triphenylethylene (59.8 mg, 0.23 mmol) in toluene (0.80 ml) was added *via* syringe. Immediately, the round bottom flask was transferred to a pre-heated oil bath (35 – 60°C). Aliquots were taken out with a syringe from the reaction vessel at specific times and immediately filtered through a plug of $SiO_2$ and washing with $Et_2O$. After all the volatiles were removed, product yield from the corresponding reaction was monitored by $^1H$ NMR analysis using triphenylethylene as internal standard.

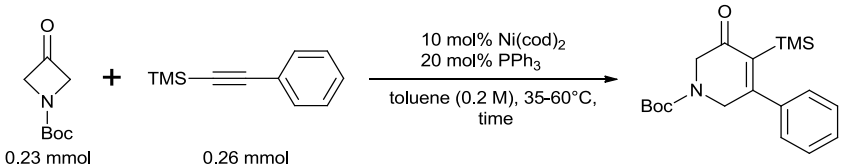


At 35°C

| Time (min) | Int Std[a] | **74**[a] | **74** (M) |
|---|---|---|---|
| 10 | 1 | 0.8565 | 0.04275 |
| 20 | 1 | 1.0764 | 0.053726 |
| 30 | 1 | 1.2736 | 0.063569 |
| 40 | 1 | 1.4459 | 0.072168 |

[a] Integration of $^{1}$H NMR

At 40°C

| Time (min) | Int Std[a] | **74**[a] | **74** (M) |
|---|---|---|---|
| 5 | 1 | 0.9166 | 0.04575 |
| 10 | 1 | 1.0727 | 0.053541 |
| 15 | 1 | 1.201 | 0.059945 |
| 20 | 1 | 1.3401 | 0.066888 |

[a] Integration of $^{1}$H NMR

At 50°C

| Time (min) | Int Std[a] | **74**[a] | **74** (M) |
|---|---|---|---|
| 5 | 1 | 0.7997 | 0.039915 |
| 10 | 1 | 1.0986 | 0.054834 |
| 15 | 1 | 1.3971 | 0.069733 |
| 20 | 1 | 1.7018 | 0.084941 |

[a] Integration of $^{1}$H NMR

At 60°C

| Time (min) | Int Std[a] | **74**[a] | **74** (M) |
|---|---|---|---|
| 4 | 1 | 1.022 | 0.051011 |
| 8 | 1 | 1.5725 | 0.078487 |
| 12 | 1 | 2.0797 | 0.103803 |
| 16 | 1 | 2.5262 | 0.126089 |

[a] Integration of $^{1}$H NMR

### 3.4.2 NMR studies

All solvents used were stored in a schlenk or in a glovebox. All solvents were degasses prior to use by standard techniques.

#### 3.4.2.1 Product Inhibition

Procedure: In the glovebox, a J-Young NMR tube is charged with $Ni(cod)_2$ (3.2mg, 0.01 mmol) and taken out. Under Ar, dissolved in $d_8$-toluene (0.1 ml) and a solution of $PPh_3$ (9.2 mg, 0.04 mmol) in $d_8$-toluene (0.15 ml) was added. Afterwards, the contents were mixed gently. Finally, under Ar, a solution of **74** (8 mg, 0.2 mmol) in $d_8$-toluene (0.3 ml) was added. Again, the contents were mixed gently and the NMR study was carried out at rt and 40°C. At rt: Complex **75**; $^{31}$P NMR (162 MHz, $d_8$-tol): $\delta$ = 39.4. $Ni(PPh_3)_3$ or $O{=}PPh_3$; $^{31}$P NMR (162 MHz, $d_8$-tol): $\delta$ =

24.4. At 40°C: Complex **75**; $^{31}P$ NMR (162 MHz, $d_8$-tol): $\delta$ = 39.1. $Ni(PPh_3)_3$ or $O{=}PPh_3$; $^{31}P$ NMR (162 MHz, $d_8$-tol): $\delta$ = 24.2

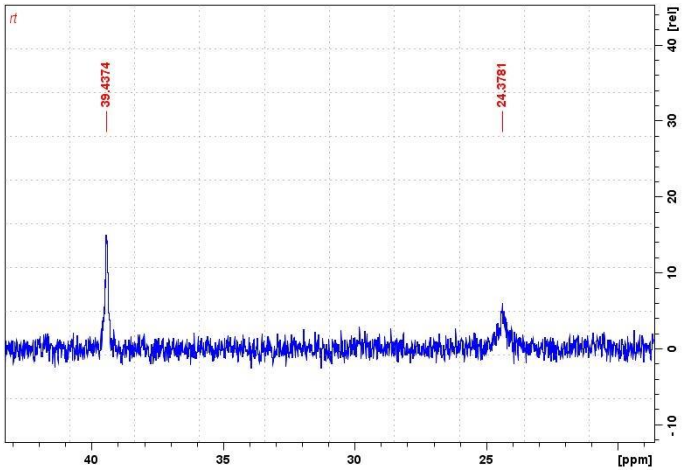


$^{31}P$ at rt

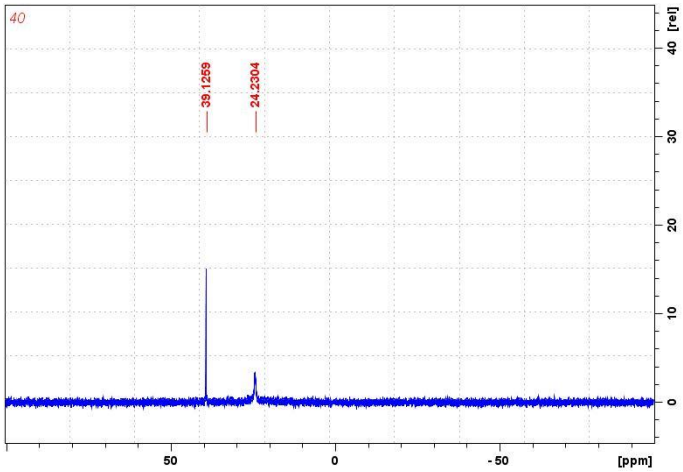


$^{31}P$ at 40°C

### 3.4.2.2 Competition Experiment

Procedure: In the glovebox, a J-Young NMR tube is charged with $Ni(cod)_2$ (3.2mg, 0.01 mmol) and taken out. Under Ar, dissolved in $d_8$-toluene (0.1 ml) and a solution of $PPh_3$ (9.2 mg, 0.04 mmol) in $d_8$-toluene (0.15 ml) was added. Afterwards, the contents were mixed gently. Finally, under Ar, a solution of **74** (8 mg, 0.2 mmol) in $d_8$-toluene (0.3 ml) was added. Then, alkyne **73** (25µl, 0.13 mmol) was added. Again, the contents were mixed gently and the NMR study was

carried out at rt and 40°C. At rt: Complex **77**; $^{31}$P NMR (162 MHz, $d_8$-tol): $\delta$ = 40.5 (d, $J$ = 31.4 Hz), 37.9 (d, $J$ = 31.3 Hz). $Ni(PPh_3)_3$ or $O{=}PPh_3$; $^{31}$P NMR (162 MHz, $d_8$-tol): $\delta$ = 24.4. At 40°C: Complex **77**; $^{31}$P NMR (162 MHz, $d_8$-tol): $\delta$ = 40.5 (d, $J$ = 31.3 Hz), 37.9 (d, $J$ = 31.2 Hz). $Ni(PPh_3)_3$ or $O{=}PPh_3$; $^{31}$P NMR (162 MHz, $d_8$-tol): $\delta$ = 24.2.

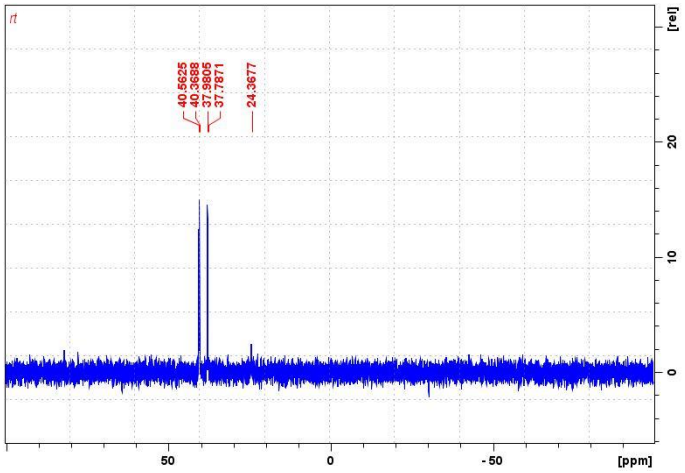


$^{31}$P at rt

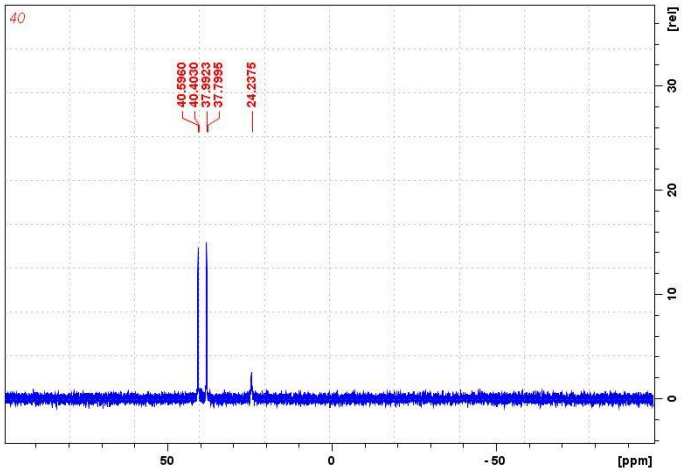


$^{31}$P at 40°C

### 3.4.2.3 Synthesis of 77

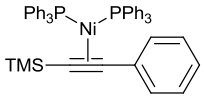


Inside a glovebox, toluene (2.4 ml) was added to a flask containing $Ni(cod)_2$ (100 mg, 0.36 mmol) and $PPh_3$ (191 mg, 0.73 mmol). After allowing the deep red solution to stir for 10 minutes, **73** (72 µl, 0.36 mmol) was added dropwise. Allowed to stir at rt for 1 hour whereupon the solution became dark brown. Afterwards, all volatiles were removed. The orange solid was washed with hexanes (3 x 5 ml) to give a golden yellow solid (269 mg, 97%). This is a known compound.[11]; $^1$H NMR (500 MHz, $C_7C_8$): $\delta$ = 7.64 – 7.55 (m, 6H), 7.39 (apt t, $J$ = 8.5 Hz, 6H), 7.04 – 6.90 (m, 11H), 6.90 – 6.83 (m, 3H), 6.82 – 6.74 (m, 9H), -0.04 (s, 9H); $^{31}$P NMR (202 MHz, $C_7D_8$): $\delta$ = 40.5 (d, $J$ = 31.5 Hz), 37.9 (d, $J$ = 30.6 Hz)

### 3.4.2.4 Catalytic competency of 77

Inside a glovebox, **77** (8.8 mg, 0.01 mmol) was dissolved in $d_8$-toluene (0.58 ml). After 5 minutes, **70** (20 mg, 0.12 mmol), **73** (25 µl, 0.13 mmol) and 3,5-dimethoxytoluene (19.6 mg, 0.12 mmol) were added. After 5 minutes of stirring, the contents were transferred to a J-Young NMR tube. Taken out of the glovebox and heated at 40°C for 15 hours. NMR integration of the product against 3,5-dimethoxytoluene as an internal standard revealed full conversion.

### 3.4.2.5 Reaction of 77 with excess 73

Inside a glovebox, **77** (8.8 mg, 0.01 mmol) was dissolved in $d_8$-toluene (0.58 ml). Afterwards, **73** (11.5 µl, 0.06 mmol) was added. After 5 minutes of stirring, the contents were transferred to a J-Young NMR tube. No change in the $^1$H and $^{31}$P NMR spectra was observed between rt and 40°C.

### 3.4.2.6 Reaction of 77 with excess 79

Inside a glovebox, **77** (8.8 mg, 0.01 mmol) was dissolved in $d_8$-toluene (0.58 ml). Afterwards, **73** (10.4 mg, 0.06 mmol) was added. After 5 minutes of stirring, the contents were transferred to a J-Young NMR tube. From the $^{31}$P NMR spectra, the appearance of **80** is found at rt and at 40°C. Complex **80** is a known compound.[11] At rt: Complex **77**; $^{31}$P NMR (202 MHz, $d_8$-tol): $\delta$ = 40.5 (d, $J$ = 30.9 Hz), 37.9 (d, $J$ = 30.4 Hz). Complex **80**; $^{31}$P NMR (202 MHz, $d_8$-tol): $\delta$ = 39.8. At 40°C: Complex **77**; $^{31}$P NMR (202 MHz, $d_8$-tol): $\delta$ = 40.5 (d, $J$ = 31.1 Hz), 37.9 (d, $J$ = 31.6 Hz). Complex **80**; $^{31}$P NMR (202 MHz, $d_8$-tol): $\delta$ = 39.8.

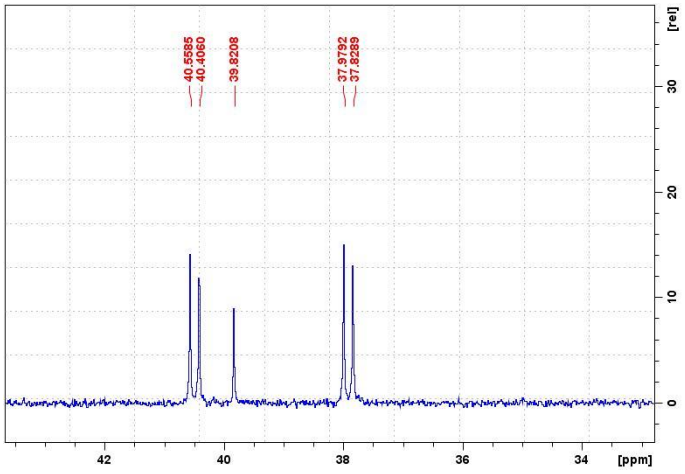


$^{31}$P at rt

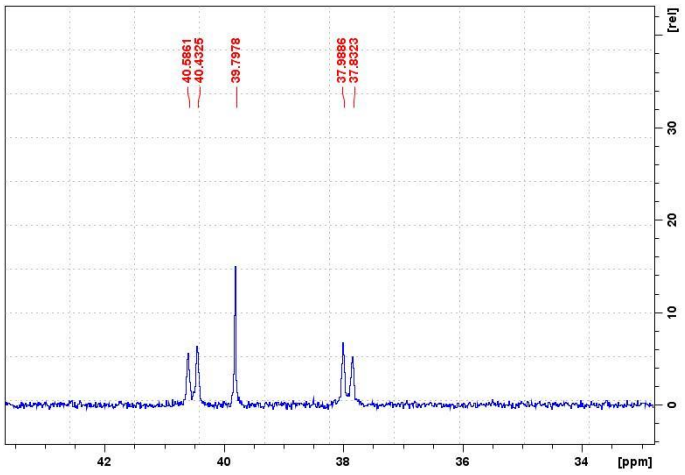


$^{31}$P at 40°C

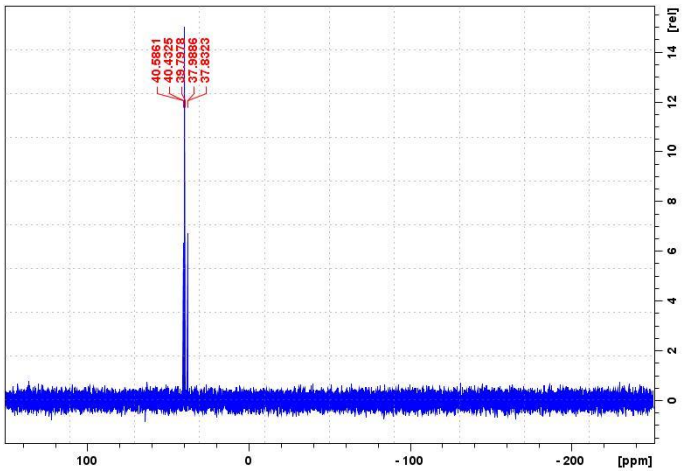


$^{31}$P at 40°C - zoomed out

#### 3.4.2.7 Reaction of 77 with 70

Inside a glovebox, **77** (8.8 mg, 0.01 mmol) was dissolved in $d_8$-toluene (0.58 ml). Afterwards, **70** (4.5 mg, 0.03 mmol) was added. After 5 minutes of stirring, the contents were transferred to a J-Young NMR tube. No change was observed in the $^{31}$P NMR. By $^{1}$H NMR spectra, the appearance of **74** is found at rt and at 40°C but trace conversion was found after 1 hour at 40°C.

## 3.5 References

1.) E. Oblinger, J. Montgomery, *J. Am. Chem. Soc.* **1997**, *119*, 9065–9066.

2.) W.-S. Huang, J. Chan, T. F. Jamison, *Org. Lett.* **2000**, *2*, 4221–4223.

3a.) P. R. McCarren, P. Liu, P. H.-Y. Cheong, T. F. Jamison, K. N. Houk, *J. Am. Chem. Soc.* **2009**, *131*, 6654–6655; b.) P. Liu, P. McCarren, P. H.-Y. Cheong, T. F. Jamison, K. N. Houk, *J. Am. Chem. Soc.* **2010**, *132*, 2050–2057.

4.) R. D. Baxter, J. Montgomery, *J. Am. Chem. Soc.* **2011**, *133*, 5728–5731.

5.) S. Ogoshi, M. Ueta, T. Arai, H. Kurosawa, *J. Am. Chem. Soc.* **2005**, *127*, 12810–12811.

6.) Y. Hoshimoto, Y. Hayashi, H. Suzuki, M. Ohashi, S. Ogoshi, *Angew. Chem. Int. Ed.* **2012**, *51*, 10812–10815

7.) S. Ogoshi, T. Arai, M. Ohashi, H. Kurosawa, *Chem. Commun.* **2008**, 1347–1349.

8.) Y. Li, Z. Lin, *Organometallics* **2013**, *32*, 3003–3011.

9.) K. Y. T. Ho, C. Aïssa, *Chem. Eur. J.* **2012**, *18*, 3486–3489.

10a.) P. Kumar, J. Louie, *Org. Lett.* **2012**, *14*, 2026–2029; b) N. Ishida, T. Yuhki, M. Murakami, *Org. Lett.* **2012**, *14*, 3898–3901.

11.) T. Bartik, B. Happ, M. Iglewsky, H. Bandmann, R. Boese, P. Heimbach, T. Hoffmann, E. Wenschuh, *Organometallics* **1992**, *11*, 1235–1241

# Chapter 4 Transition Metal-Catalysed Functionalisation of an Alkene C–H Bond with another Alkene

## 4.1 Introduction

Transition metal-catalysed activation and subsequent transformation of aromatic C–H bonds is an area of research which has experienced a rapid rate of growth.[1] Hydrovinylation reactions using ethylene to functionalised alkene C–H bonds have been well documented and won't be covered in this review.[2] Furthermore, homo co-dimerisation of alkenes will not be covered.[3] However, transition metal-catalysed C–H functionalisation of an alkene with another different alkene has been less studied. Regardless, several modes of C–H functionalisation of an alkene with another different alkene by a transition metal have been postulated to occur to account for the products observed. Oxidative cyclisation, *in situ* generation of the metal hydride and C–H bond activation are three modes of C–H functionalisation commonly postulated.

For example, Mitsudo and co-workers reported a ruthenium-catalysed codimerisation of norbornenes **1** with various Michael acceptors **2** to give products **3** and **4**.[4] The reaction generally proceeded in a *trans*-selective manner. The authors then proposed three pathways to account for the results of the reaction. Path A is the oxidative cyclisation which would form ruthenacycle **5**. Then β-H elimination would form intermediate **6**. Afterwards, reductive elimination would give mainly **3**.

Path B is the addition of the *in situ* generated ruthenium hydride across the alkene of norbornene **1** which would form intermediate **7**. Insertion of alkene **2** would form intermediate **8**. Finally reductive elimination would afford product **3**.

Lastly, path C is the carbonyl-directed C–H activation pathway which would form intermediate **9**. Hydrometallation across the alkene of norbornene **1** would afford intermediate **10**. Finally, reductive elimination would afford product **4**. However, path C was postulated to be unlikely as products of the C–H activation pathway would have been predominantly *cis*-products **4**. This methodology allowed the codimerisation of various norbornenes with various Michael acceptors to proceed in good to high yields with good to excellent *trans*-selectivity.

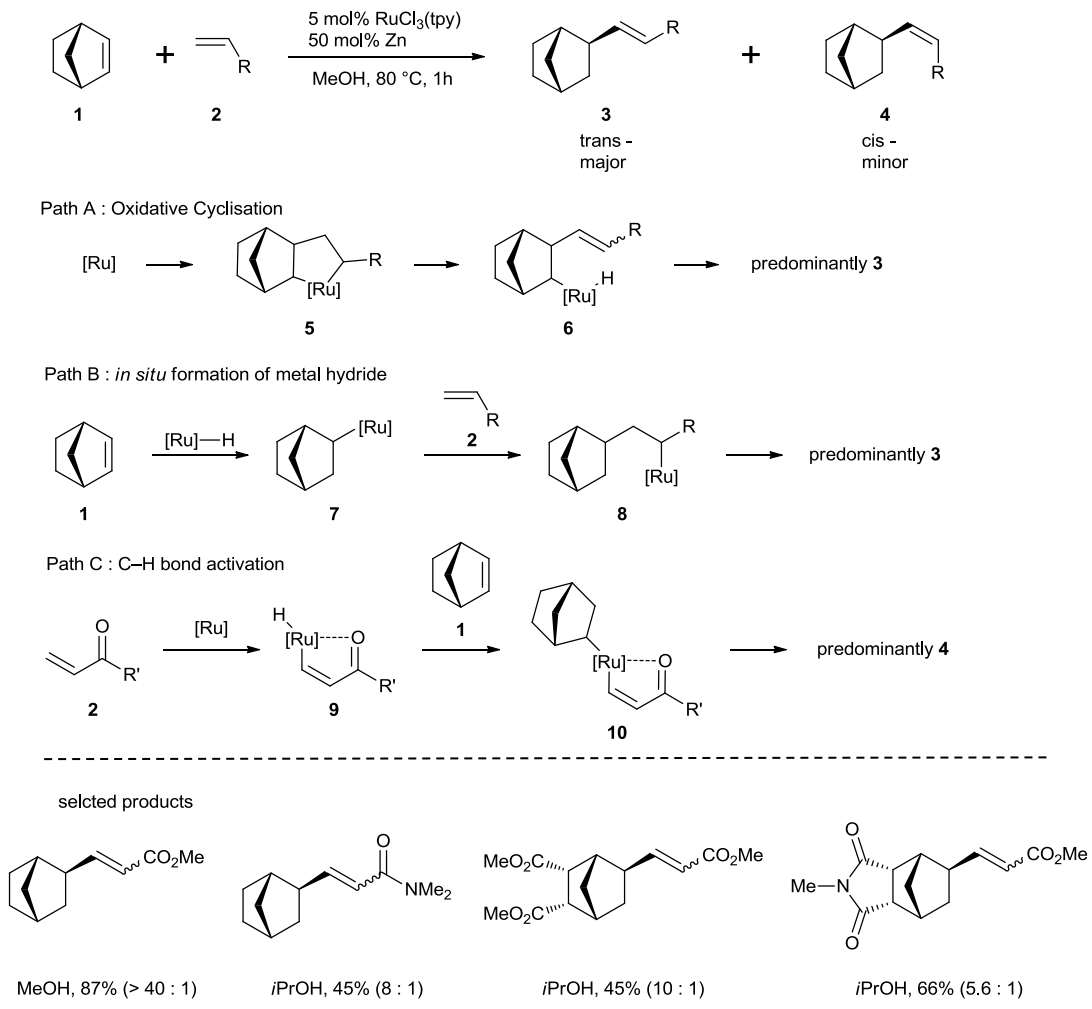


**Scheme 1** Ruthenium catalysed codimerisation of norbornenes with various Michael acceptors

### 4.1.1 Formation of a metallacycle intermediate via oxidative cyclisation

Hirano and co-workers reported a ruthenium-catalysed asymmetric codimerisation of methyl methacrylate **11** with various alkenes.[5] It was observed that the codimerisation of methyl methacrylate **11** with alkene **12** proceeded to give **13** in high yields and with high enantioselectivity (Scheme 2). Furthermore, three other products **14**-**16** were also identified. To account for the formation of the four products, the authors proposed that the initial oxidative cyclisation would form intermediate **17**. Then the major product **13** would then come about from the *endo* β-H elimination which would form intermediate **18**. Reductive elimination would then afford product **13**. However, *exo* β-H elimination from the methyl group would form intermediate **19**. Reductive elimination would then afford product **14**. Alternatively, β-H elimination from the tetrahydrofuran core would result in the formation of intermediate **20**. Finally, reductive elimination would then afford product **15**. However, the formation of **16** is currently speculative.

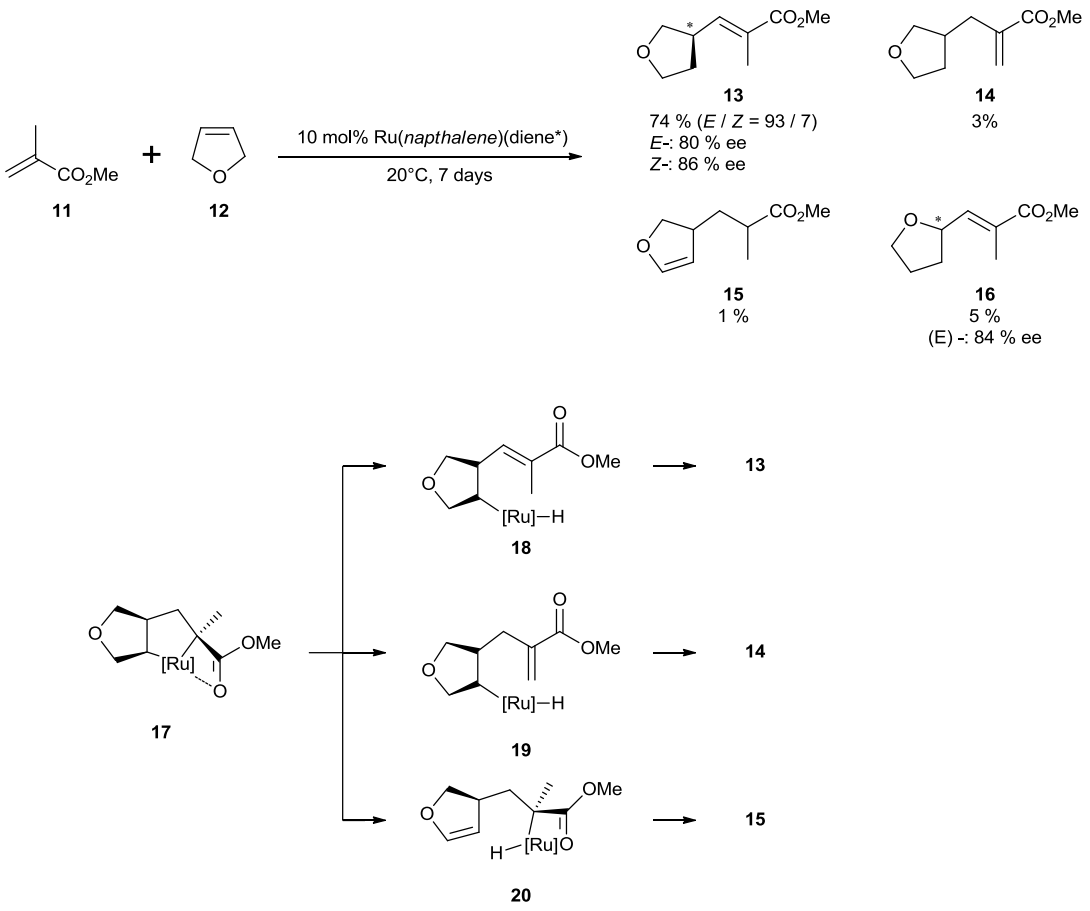


**Scheme 2** Ruthenium catalysed asymmetric codimerisation of methyl methacrylate with various alkenes

Ogoshi and co-workers reported a nickel-catalysed direct conjugate addition of simple alkenes **22** to enones **21** to form product **23** (Scheme 3).[6] The nickel catalyst would pre-organise alkene **22** and enone **21** to form intermediate **24**. Afterwards, oxidative cyclisation would afford intermediate **25**. β-H elimination would afford intermediate **26**. Finally, reductive elimination would then afford product **23**. This methodology allowed the synthesis of various conjugate addition products in good to high yields. Furthermore, potentially isomerisable alkenes were employed successfully.

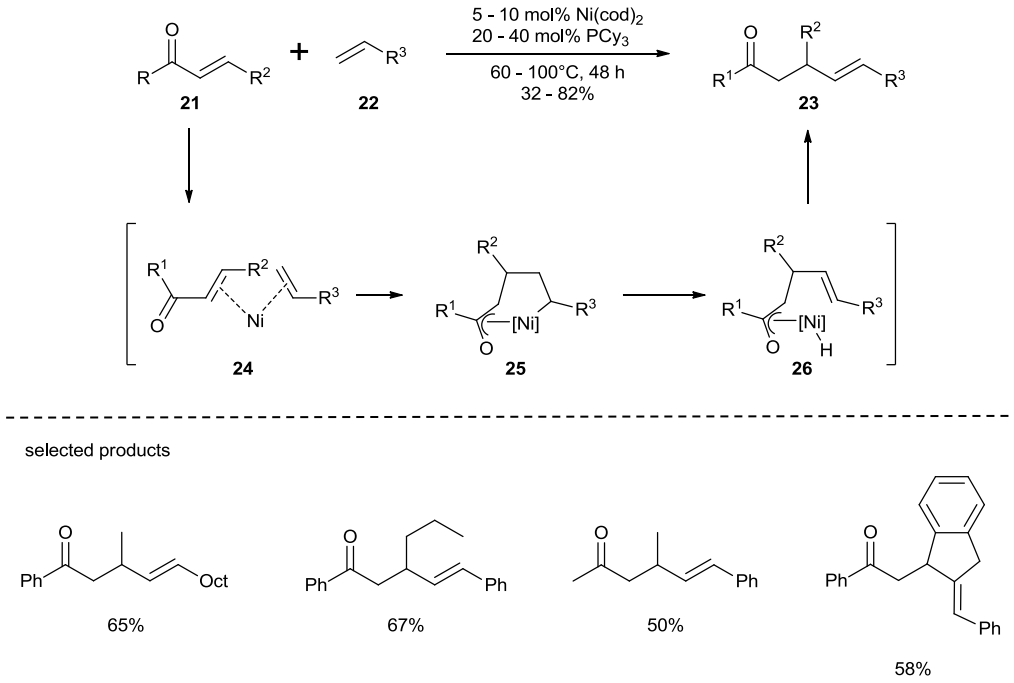


**Scheme 3** Nickel-catalysed direct conjugate addition of simple alkenes to enones

### 4.1.2 *In situ* formation of metal hydride

Kondo and co-workers reported a ruthenium-catalysed codimerisation reaction of alkenes **28** with *N*-vinylamides **27** (Scheme 4).[7] After the *in situ* formation of the putative ruthenium hydride, it would then add across alkene **28** to form intermediate **30**. The chelation assisted insertion of *N*-vinylamide **27** would form intermediate **31**. Then β-H elimination would proceed to give product **29**. Electron deficient alkenes dimerised with *N*-vinylamide in good to high yields with excellent *E*-selectivity. However, norbornene or ethene dimerised with *N*-vinylamide in poor yields (33% and 16% respectively) but with excellent *E*-selectivity.

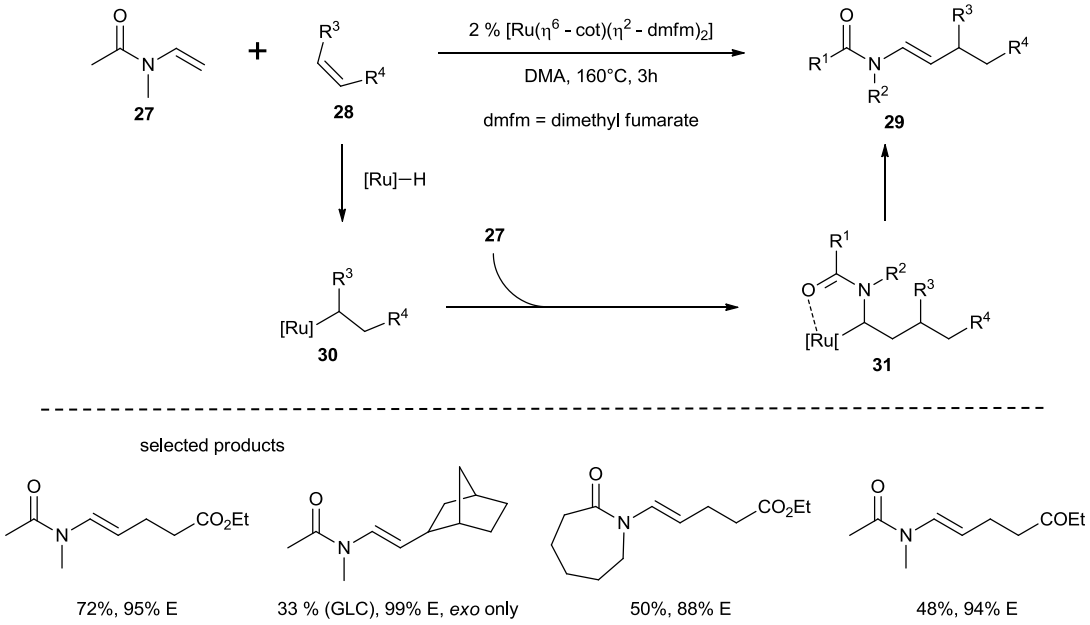


**Scheme 4** Ruthenium-catalysed codimerisation reaction of alkenes with *N*-vinylamides

Zhou and co-workers reported a ruthenium-catalysed dimerisation of *N*-acetyl α-arylenamines **32** with acrylates **33** to form product **34** (Scheme 5).[8] Though there was no mechanistic proposal by the authors, *N*-acetyl α-arylenamine **32** could direct the ruthenium hydride in a regioselective manner to form intermediate **35**. The coordination of alkene **33** to the metal centre would then form intermediate **36**. Afterwards, migratory insertion would form intermediate **37**. Finally, reductive elimination would occur to give product **34**. Various *N*-acetyl α-arylenamines with different functional groups on the phenyl ring dimerised with various acrylates in usually high yields with excellent *E*-selectivity.

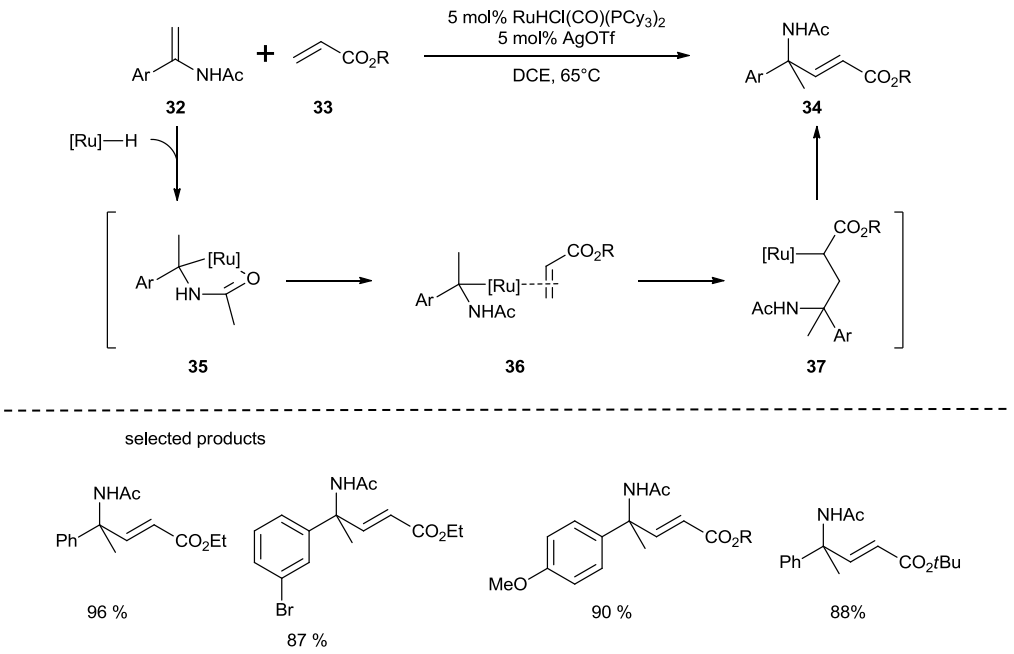


**Scheme 5** Ruthenium catalysed dimerisation of *N*-acetyl α-arylenamines with acrylates

### 4.1.3 C–H bond activation

#### 4.1.3.1 Oxidative cross coupling

Ishii and co-workers reported a palladium-catalysed oxidative cross coupling of acrylates **38** with enol acetate **39** to form diene **40**.[9] It is postulated the palladium catalyst would react with enol acetate **39** to form intermediate **41** with concomitant loss of acetic acid. As a comparison, C–H bond activation with a Pd(0) catalyst would form a palladium hydride complex. Acrylate **38** would then insert itself into the Pd–C bond of intermediate **41** to give intermediate **42**. Finally, β-H elimination would afford product **40**. The oxidative cross coupling between a variety of acrylates and a variety of enol acetates proceeded in good yields but usually with poor *E*/*Z* selectivity.

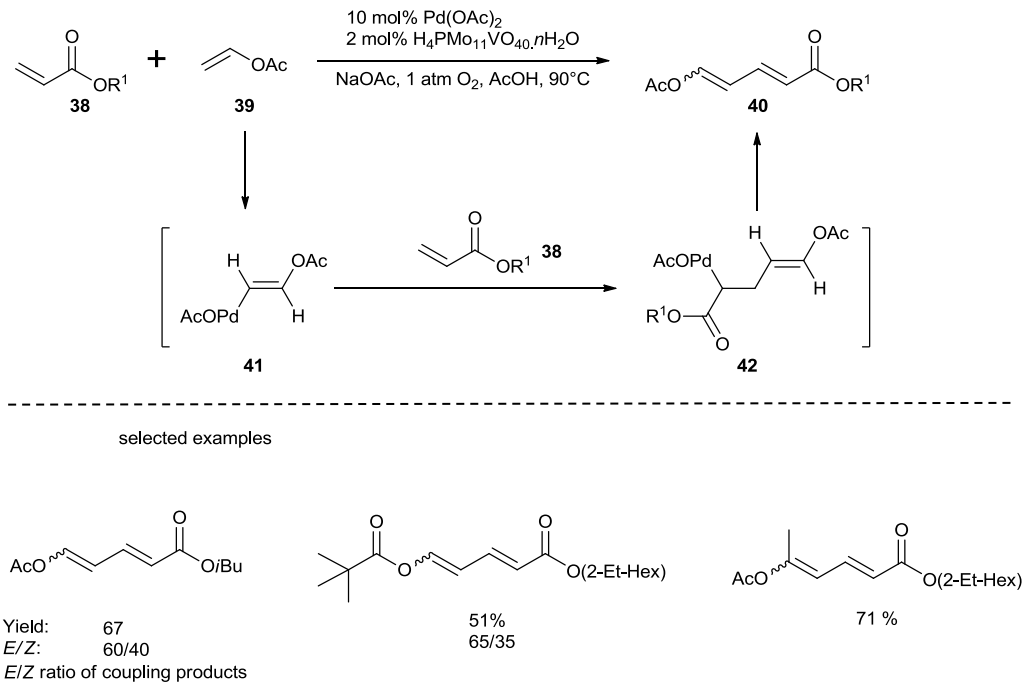


**Scheme 6** Palladium catalysed oxidative cross coupling of acrylates with enol acetate

Loh and co-workers demonstrated the first example of a direct cross coupling reaction between simple alkenes **43** and acrylates **44** (Scheme 7).[10] Palladium-catalysed C–H activation of simple alkene **43** would form intermediate **46**. Acrylate **44** would then insert itself into the Pd–C bond of intermediate **46** to give intermediate **47**. Finally, β-H elimination would afford product **45**. A wide range of 2-substituted alkenes **43** were compatible. Generally, the reaction was selective for the *E*-isomer but non-styrene type alkenes were not as stereoselective. Later, the same group expanded the scope of the palladium catalysed direct cross coupling of indenes with various electron deficient alkenes.[11]

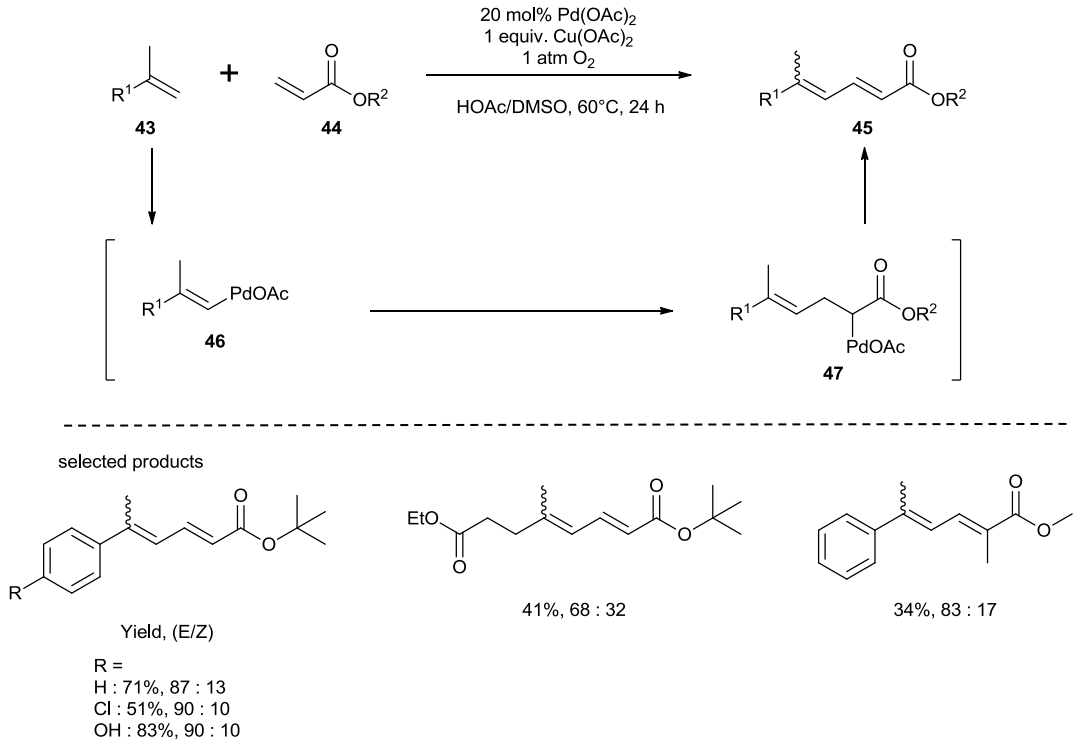


**Scheme 7** Palladium catalysed cross coupling between simple alkenes and acrylates

Miura and co-workers reported a rhodium-catalysed oxidative cross-dimerisation of acrylic acids **48** with acrylates **49** to form butenolide **50** (Scheme 8).[12] It was proposed the carboxylic acid of **48** would direct the rhodium catalyst for β C–H activation to form rhodacycle **51**. Subsequent alkene insertion would form intermediate **52**. This would then be followed by β-H elimination to give intermediate **53**. This intermediate would then undergo nucleophilic cyclisation to afford butenolide **50**. A variety of butenolides **50** were synthesised in generally good yields. However, in certain cases a slight modification of reaction conditions was required for higher yields.

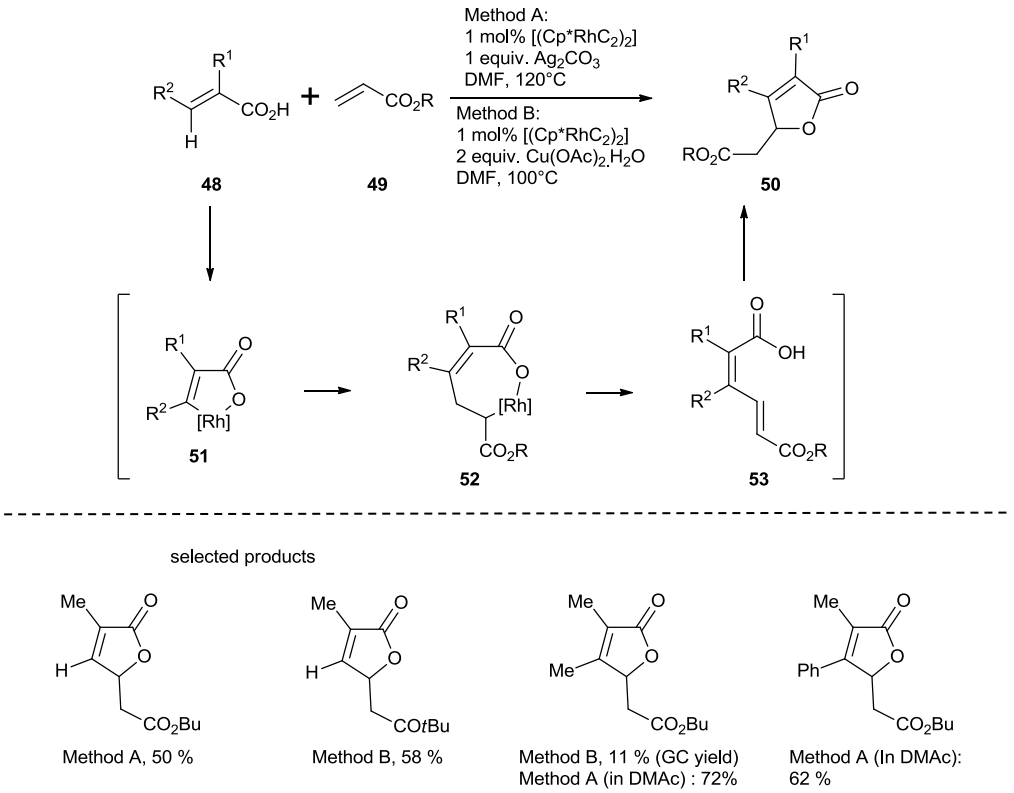


**Scheme 8** Rhodium catalysed oxidative cross-dimerisation of acrylic acids with acrylates

### 4.1.3.2 Group directed C–H activation

In the 1970s, Yamamoto and co-workers reported the first experimental evidence of an oxidative addition of ruthenium complex **54** into the C–H of alkene **55** to generate ruthenium complex **56** (Scheme 9).[13] Complex **56** was fully characterised and an X-Ray crystal structure was obtained. The X-Ray revealed the coordination of the carbonyl moiety to the ruthenium complex which could suggest that the carbonyl moiety directed ruthenium complex **63** into the *cis*-C–H alkene bond.

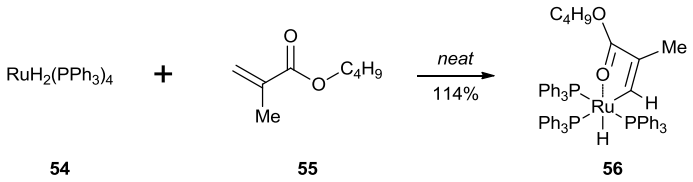


**Scheme 9** Experimental evidence of group-directed C–H activation

In 1995, Trost and co-workers reported the first catalytic functionalisation of an alkene C–H bond with another alkene *via* group directed C–H bond activation (Scheme 10).[14] It is remarkable that methyl benzoate failed to couple with an alkene under the optimised reaction condition. In an attempt to elucidate the mechanism, the resting state of the catalyst was found to have no hydrogen as deduced by NMR. Furthermore, carrying the reaction under an atmosphere of CO inhibited the reaction which suggests no CO is likely to be ligated onto the active catalyst. Furthermore, if the β-C-H bond is *trans* to the carbonyl group, no reaction was observed.

Therefore, it was proposed that the conjugated carbonyl moiety of **57** would direct the catalyst into the *syn*-C–H alkene bond to give intermediate **60**. Afterwards, **60** would coordinate to alkene **58** to form intermediate **61**. Migratory insertion of the alkene would form intermediate **62**. Finally, reductive elimination would afford product **59**. It was demonstrated that the ester functional group is a better directing group than a ketone. Furthermore, various functional groups on the ester were tolerated under the reaction conditions. Independently, Murai and co-workers reported similar observations[15] and later demonstrated that an aldehyde can behave as a directing group[16].

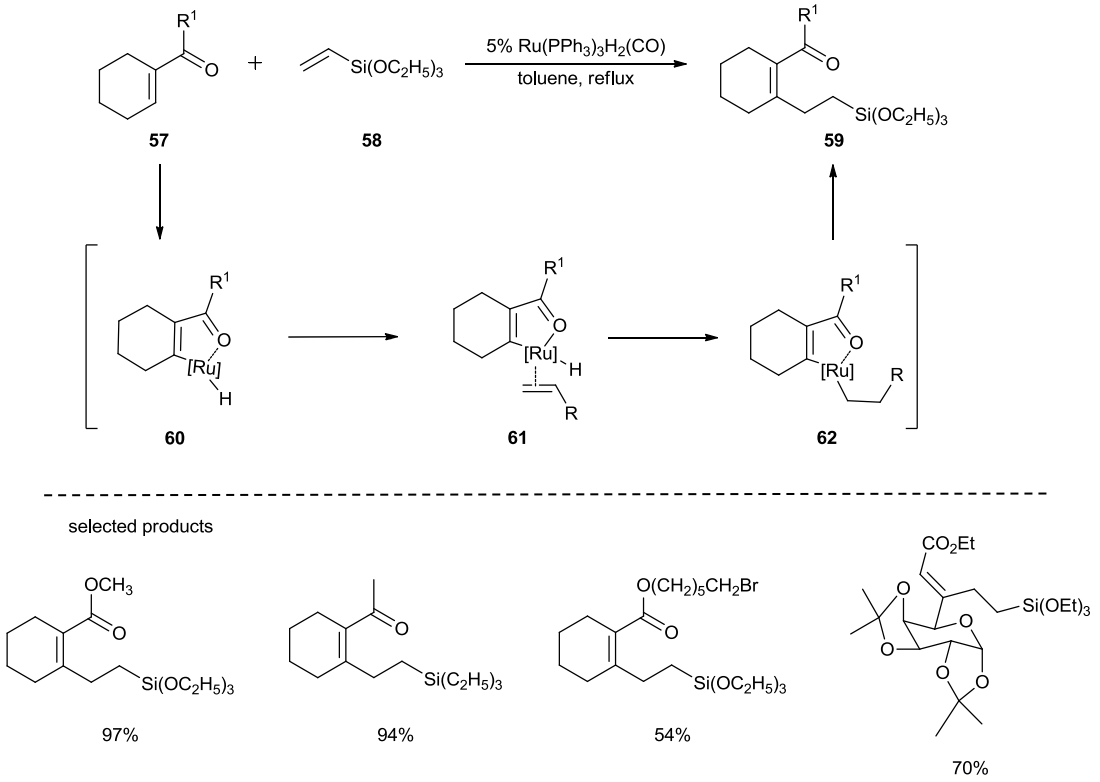


**Scheme 10** Ruthenium catalysed functionalisation of an alkene C–H bond with another alkene

Since then, several groups have reported examples whereby group directed C–H bond activation is postulated to occur. For example, Darses and co-workers reported a ruthenium-catalysed functionalisation of the *syn* C–H bond of Michael acceptors **63** with vinyl silanes **64** to form either **65** or **66** (Scheme 11).[17] For the synthesis of **65**, it was proposed that the carbonyl moiety of **63** would direct the ruthenium catalyst into the *cis*-C–H alkene bond to give intermediate **67**. Afterwards, **67** would hydrometallate onto alkene **64** to form intermediate **68**. Finally, reductive elimination and dissociation of the ruthenium catalyst would occur to afford product **65**. For the synthesis of **66**, after the formation of putative intermediate **68**, conjugate addition of the alkyl silane moiety would form intermediate **69**. Then β-H elimination would happen to form intermediate **70**. Afterwards, reductive elimination and keto-enol tautomerism would then occur to afford product **66**. While most substrates couple in a similar manner to the examples observed by Trost[14] and Murai[15] to form silane **65**, crotyl

substrates **63** would couple with vinyl silanes **64** to give rise to products **66** with a stereodefined trisubstituted allyl silanes (*E*/*Z* > 97 : 3 in all examples).

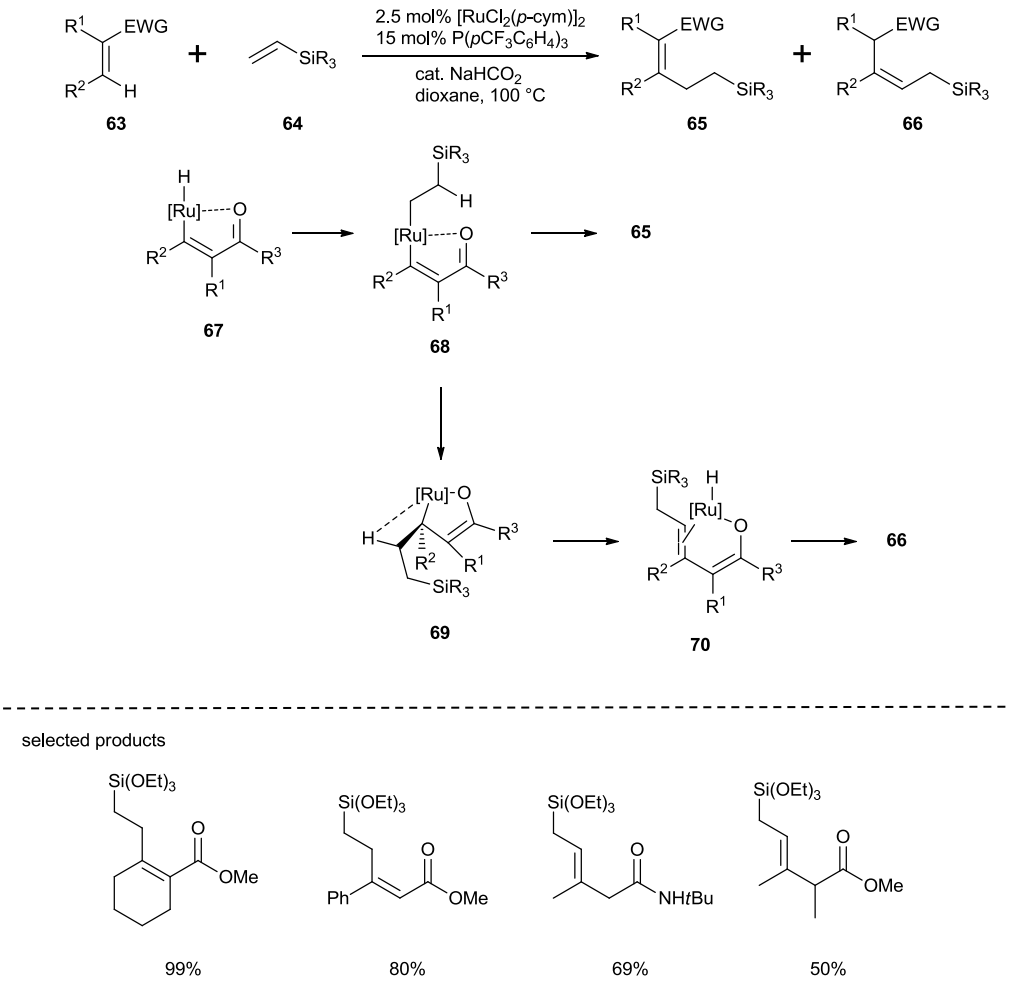


**Scheme 11** Ruthenium catalysed functionalisation of an alkene C–H bond with another alkene with differing reactivity

Another way to direct the functionalisation of the *cis*-C–H bond of Michael acceptors is through temporary chelation assistance. Jun and co-workers reported a rhodium-catalysed chelation assisted C–H bond activation of Michael acceptors **71** for β-alkylation (Scheme 12).[18] Control experiments supported the presence of dienamine **75** for the chelation assisted C–H bond activation. Therefore it is proposed that after the formation of the putative dienamine **75**, the nitrogen would direct the rhodium catalyst for C–H bond activation to form

intermediate **76**. Afterwards, migratory insertion of the alkene would form intermediate **77**. Finally reductive elimination would afford intermediate **78** which would equilibrate with intermediate **79**. Finally, acid hydrolysis would afford a mixture of products **73** and **74**. Furthermore, the deconjugation likely happened during the rhodium catalysis step rather than at the hydrolysis step. Various β alkylation products were synthesised in good to high yields with moderate to high selectivity for the deconjugated product.

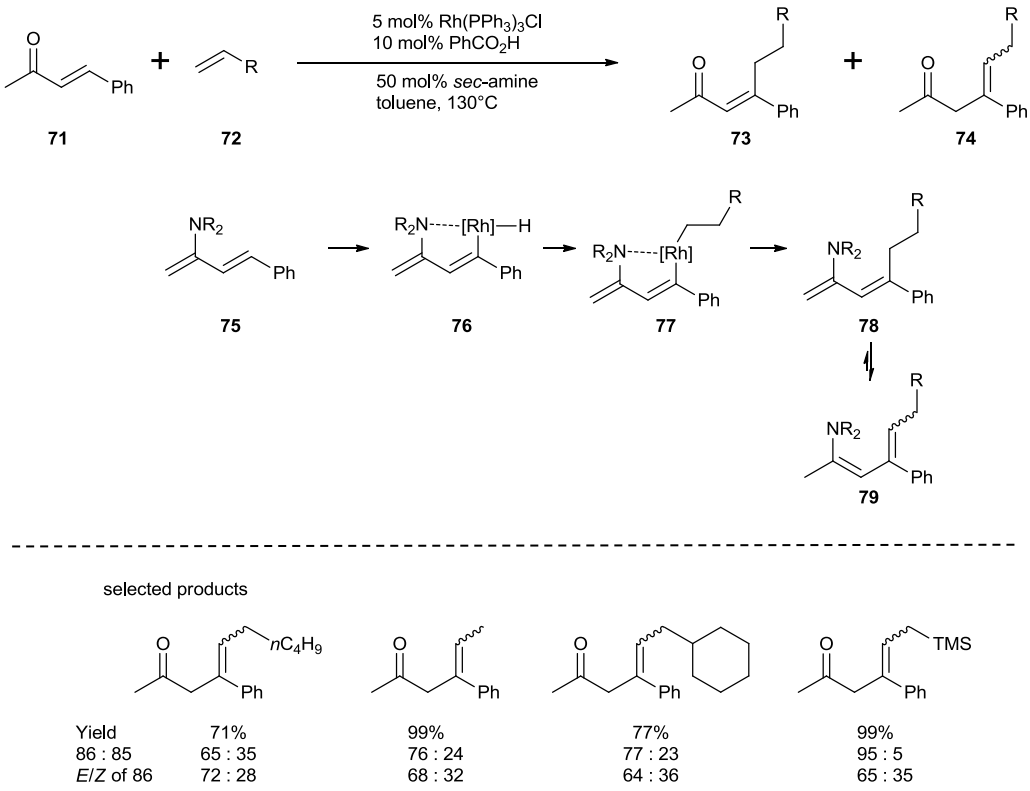


**Scheme 12** Rhodium catalysed chelation assisted C–H bond activation

Bergman and co-workers reported a rhodium-catalysed reaction whereby an imine can behave as a directing group (Scheme 13).[19] It was found that α,β-unsaturated imines **80** can be alkylated with simple alkenes **81** via C–H activation in a highly stereoselective manner when both a rhodium catalyst and an electron-donating ligand were used. Therefore, it is proposed that the imine would direct the rhodium catalyst into the alkene C–H bond to form

intermediate **84**. Afterwards, migratory insertion of the alkene would form intermediate **85**. Finally, reductive elimination and hydrolysis would afford products **82** and **83**. While the β-alkylation is initially *Z*-selective, the hydrolysis resulted in some isomerisation of the double bond. Nonetheless, the process is generally high yielding whereby even alkenes with β-Hs can be incorporated successfully. Furthermore, the same group later applied the methodology as a key step in the total synthesis of (-)-Incarvillateine **89**.[20]

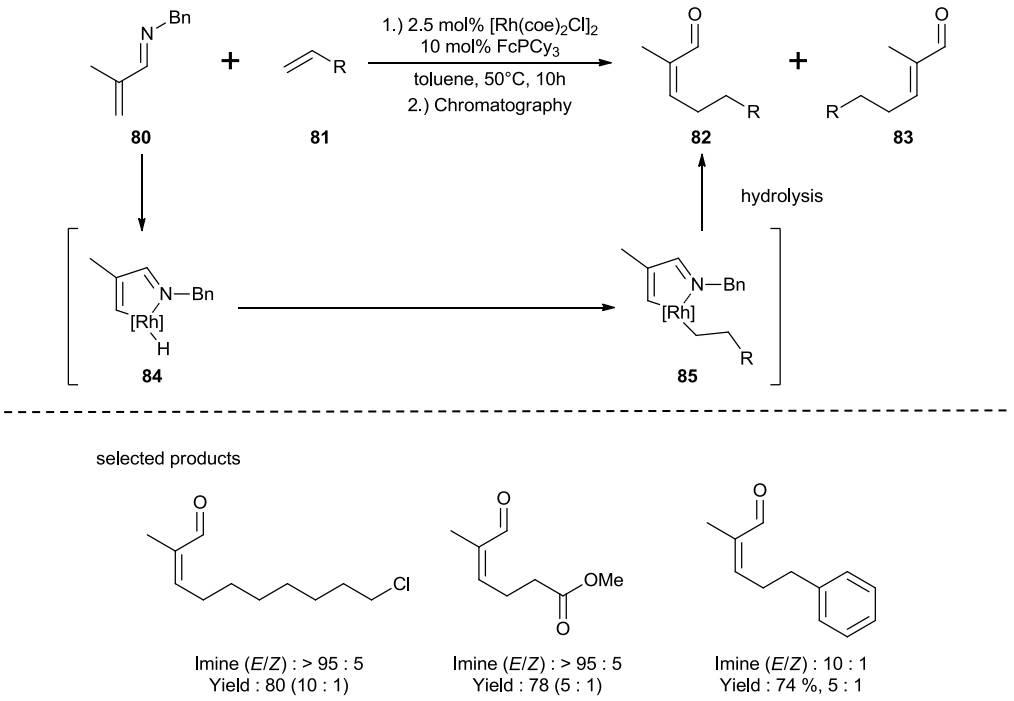


**Scheme 13** Rhodium catalysed β alkylation

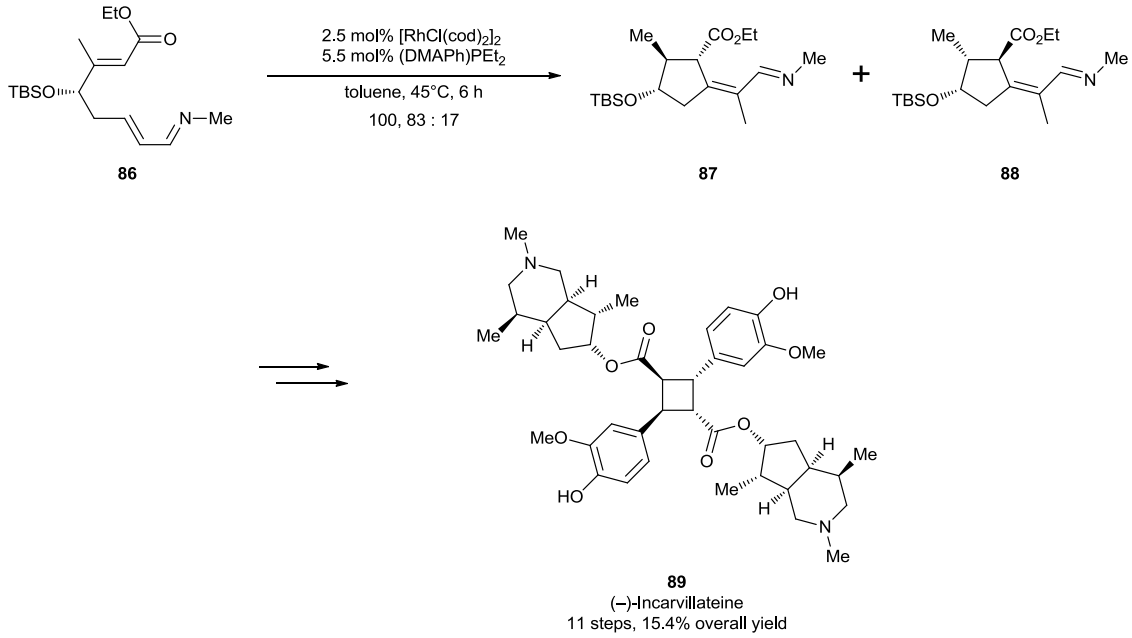


**Scheme 14** Synthesis of (-)-Incarvillateine with C–H bond as the key step

In contrast to chelation assisted C–H bond activation for β-alkylation as mentioned previously, Dong and Mo reported a rhodium-catalysed chelation assisted C–H bond activation for α-alkylation (Scheme 15).[21] After the formation of the putative enamine, group directed C–H activation would afford intermediate **92**. Afterwards, the coordination of an alkene would form intermediate **93**. Next, migratory insertion of the alkene would afford intermediate **94**. Reductive elimination and hydrolysis would afford product **91**. The α-alkylation proceeded in good yields and a wide range of functional groups substituted on the cyclopentanone were tolerated.

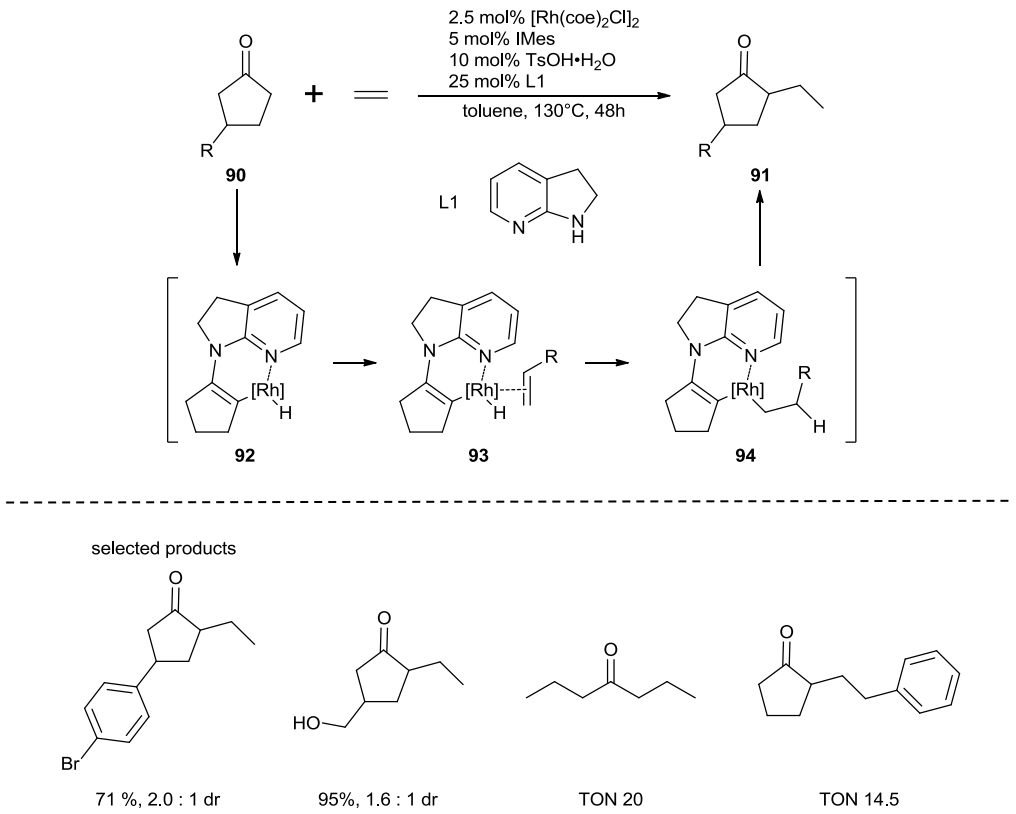


**Scheme 15** Rhodium catalysed chelation assisted C–H bond activation for α alkylation.

Another directing group used to direct the transition metal into the *cis*-C–H bond of the alkene is pyridine. Kim and co-workers reported a rhodium-catalysed pyridine directed C–H activation.[22] Alkylation of vinyl pyridines **95** is believed to be *Z*-selective but under the reaction conditions, some isomerisation took place which suggests another reaction pathway could be taking place (Scheme 16). Pyridine directed C–H activation would afford intermediate **98**. After the initial alkene coordination which would form intermediate **99**, migratory insertion would form intermediate **100**. Finally, reductive elimination would afford product **97**. The alkylation proceeded with a variety of alkenes in generally excellent yields and with moderate to good *trans*-selectivity. Furthermore, this methodology was extended to functionalisation of the vinyl pyridine with norbornene[23] and allyl ethers.[24]

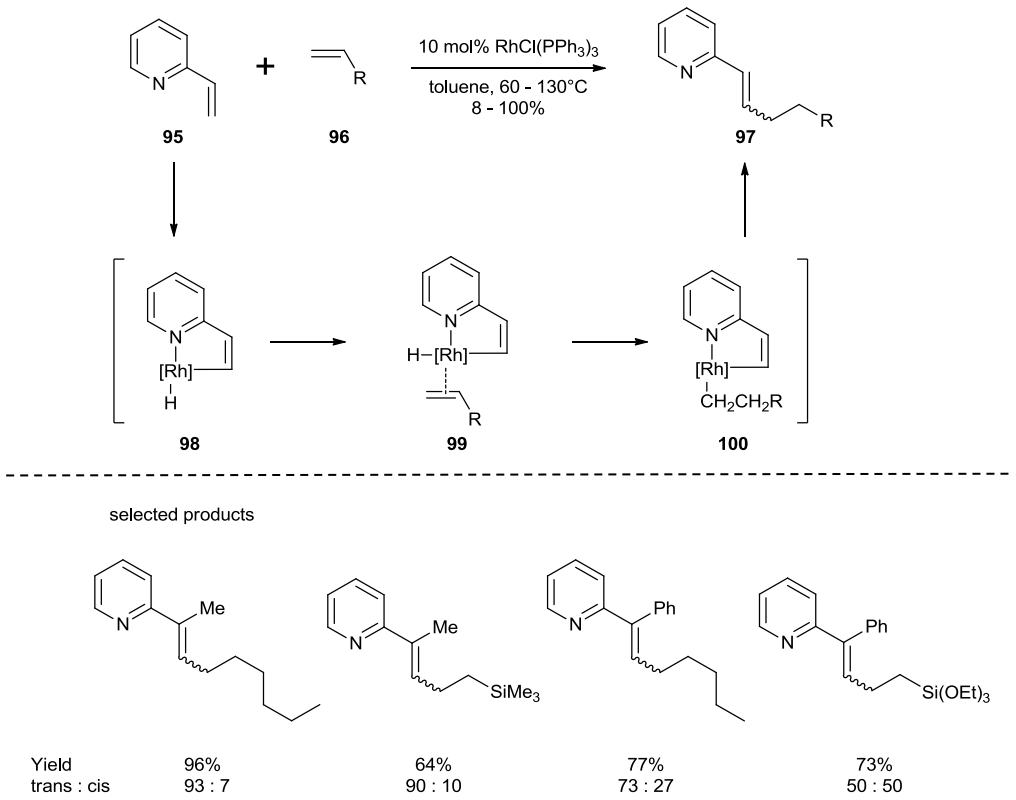


**Scheme 16** Rhodium catalysed pyridine directed C–H activation

Lim and co-workers reported striking ligand effects in the rhodium-catalysed reaction of 2-vinylpyridines **101** with 1,5-hexadiene **102** (Scheme 17).[25] Carrying out the reaction with the Wilkinson's catalyst gave a mixture of three products. Switching the catalyst source to $[Rh(coe)_2Cl]_2$ and 20 mol% $PPh_3$ did not alter the selectivity of the reaction. On exchanging the ligand to 20 mol% $PCy_3$, selective formation of functionalised alkene **105** was observed. Furthermore, it was found that other ligands altered the selectivity of the reaction. The small electron poor phosphine, $P(OMe)_3$, gave mostly product **106** whereby the alkylation occurs on the same side as the pyridine (Scheme 18). Furthermore, $P(n\text{Bu})_3$ gave mostly product **107** whereby the alkylation occurs predominantly on the same side as the pyridine (Scheme 19).

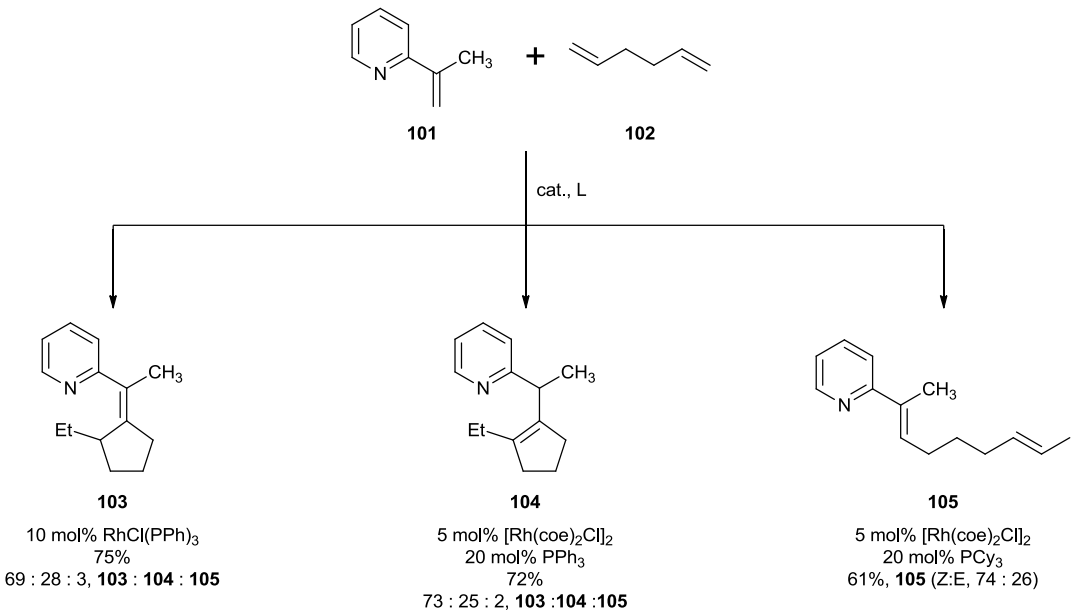


**Scheme 17** Rhodium catalysed reaction of 2-vinylpyridine with 1,5-hexadiene

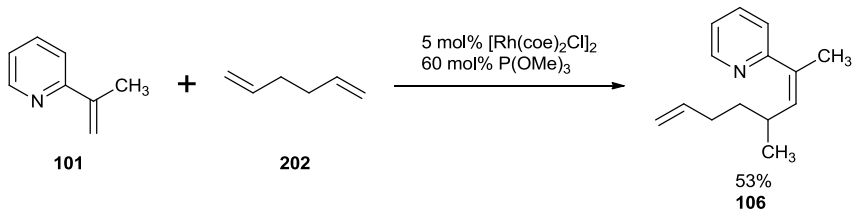


**Scheme 18** Rhodium catalysed reaction of 2-vinylpyridine with 1,5-hexadiene

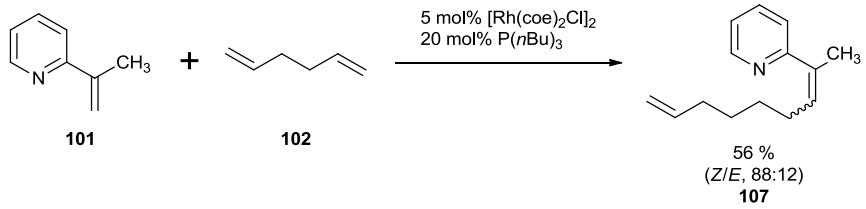


**Scheme 19** Rhodium catalysed reaction of 2-vinylpyridine with 1,5-hexadiene

Murai and co-workers reported a rhodium-catalysed intramolecular pyridine directed C–H activation with concomitant alkene insertion to form cyclic structures.[26] A three carbon unit tether **108** resulted in the non-selective formation of six-membered ring **109** and five-membered ring **110** (Scheme 20). It was postulated that the pyridine directed C–H bond activation would form intermediate **111** and then the insertion of the alkene could then proceed to give heptarhodacycle **112**. Then reductive elimination would give product **109**.

Alternatively, the insertion of the alkene could proceed to give hexarhodacycle **113** which would then undergo reductive elimination to give product **110**.

A two carbon tether **114** resulted in the selective formation of five-membered ring **115** (Scheme 21). It was proposed that the pyridine directed C–H bond activation would occur to form intermediate **116**. Afterwards, the insertion of the alkene would then proceed to give hexarhodacycle **117**. Subsequently, reductive elimination would then occur to give product **115**. The formation of various five-membered rings were synthesised in good to high yields. Furthermore, various substitutions on the alkene were tolerated.

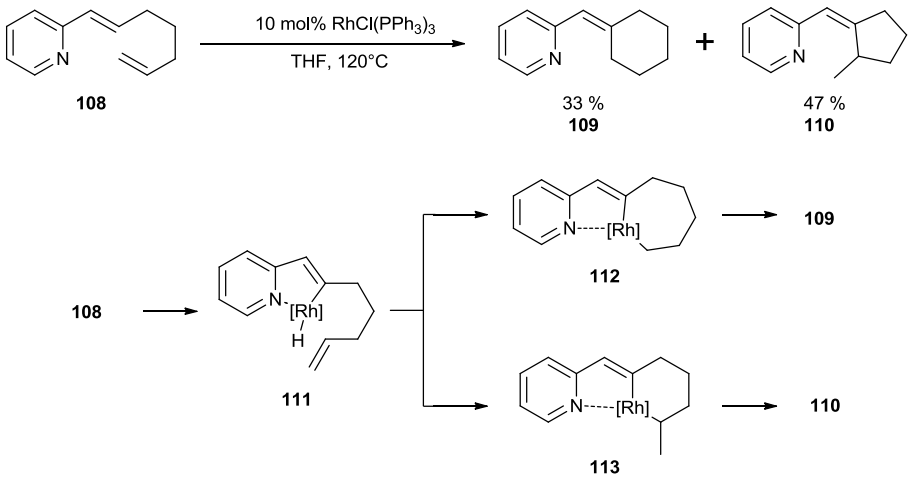


**Scheme 20** Rhodium catalysed intramolecular C–H activation with concomitant alkene insertion

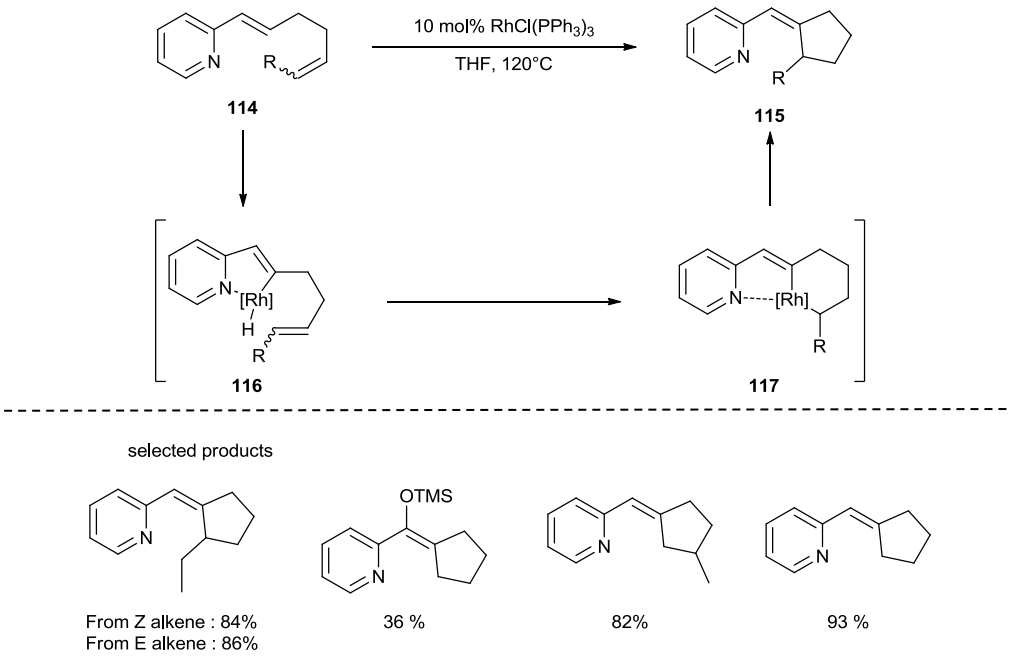


**Scheme 21** Rhodium catalysed intramolecular C–H activation with concomitant alkene insertion

Aïssa and Fürstner reported a rhodium-catalysed C–H / C–C bond activation sequence to form seven-membered rings **119** (Scheme 22).[27] Initial C–H activation with a neutral rhodium catalyst would form intermediate **120**. Hydrometalation onto an ACP would form pentarhodacycle **121**. Subsequently, the C–C bond cleavage of the cyclopropane would result in a ring enlarged metallacycle **122**. Finally, reductive elimination would furnish product **119**. While the yields were generally moderate to good, it offered a proof of concept of a tandem catalytic C–H / C–C bond activation sequence.

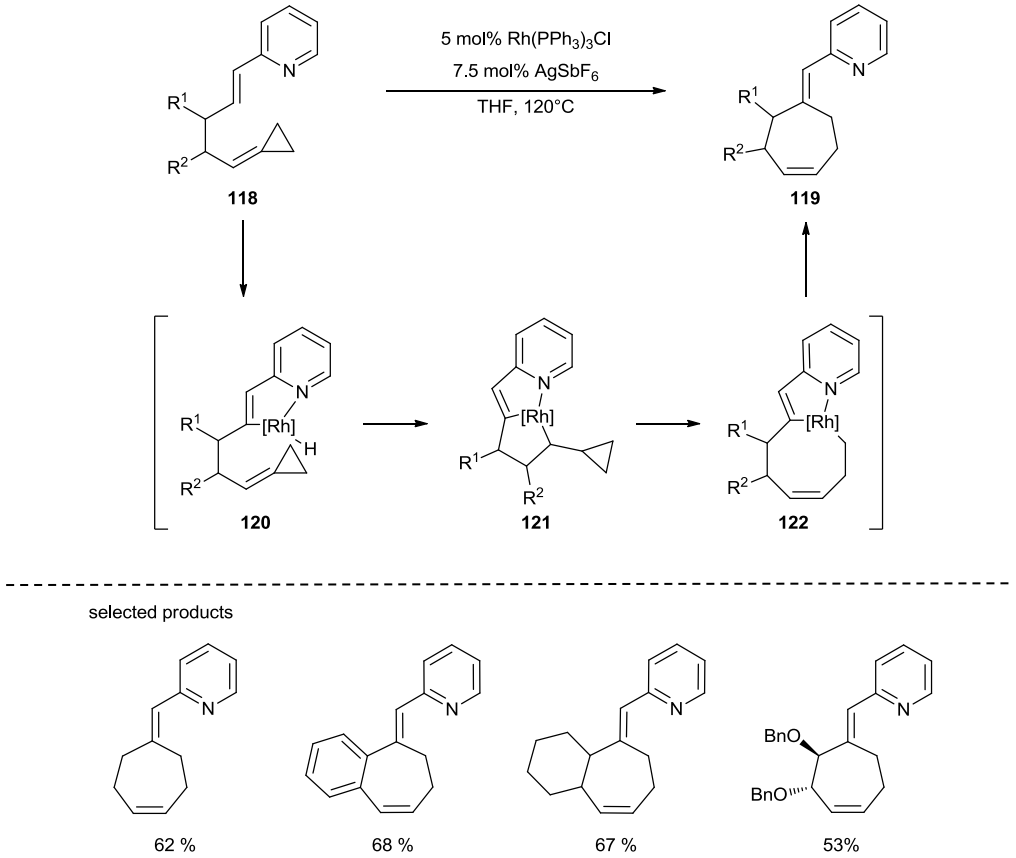


**Scheme 22** Rhodium-catalysed C–H / C–C bond activation sequence to form seven-membered rings

## 4.2 Aims and Hypothesis

Transition metal-catalysed C–H functionalisation of an alkene with another alkene is an area of increasing research. This had to lead to the discovery of various modes of activation. Though C–H activation by a directing group has been studied extensively, oxidative cyclisation and exploitation of *in situ* generated metal hydrides have contributed to the diversity of products generated.

As mentioned earlier, Aïssa and Fürstner reported a rhodium-catalysed C–H / C–C bond activation sequence to form seven-membered rings whereby C–C bond activation is used to trap the intermediate formed by the reversible hydrometalation (Scheme 22).[27]

Therefore, it was of interest to determine if there was another way to trap the intermediate formed by the reversible hydrometalation. With that in mind, it was postulated a tethered alkene could trap the proposed intermediate and to form bicyclo[2.2.1]heptane **125** (Scheme 23).

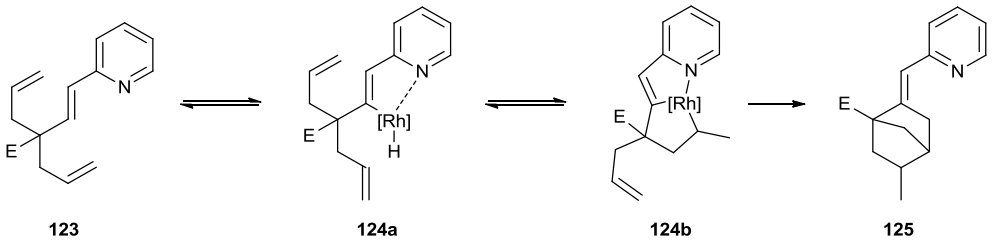


**123** **124a** **124b** **125**

**Scheme 23** Hypothesis

In this context, the aim of the work presented herein is to:

a.) Synthesise a substrate of type **123**

b.) Optimise the reaction and determine the scope

c.) Investigate the mechanism of the reaction

## 4.3 Optimisation of the reaction

Vinyl pyridine **126** was used as a model substrate to test the hypothesis (Table 1). Treating **126** with 5 mol% $[Rh(cod)_2Cl]_2$ in THF at 90°C for 17 hours did not proceed to give the desired product **127** but with 33% conversion to the five-membered ring **128**. However, when 10 mol% P(*p*OMePh)$_3$ was used as a ligand, the formation of **127** was observed despite incomplete conversion. When the loading of ligand was increased to 20 mol%, full consumption of the **126** was observed with improved selectivity towards **127**. However, the two products were not separable by standard flash column chromatography. This necessitated a need to optimise the reaction to achieve a selectivity to **127** of >95:5.

The alkene geometry of starting material **127** was discovered to affect product selectivity. When **126** was synthesised by the Wittig method, a variable *cis*/*trans* mixture of **126** was observed (91:9). Using the *cis*/*trans* mixture of **126** resulted in the formation of **127** and **128** in ratio of 83:17 under the rhodium catalysis. On the other hand, when **126** was synthesised by another method (see synthesis of precursor) to give selectively the *E*-isomer, improved selectivity towards **127** was observed. However, the increase in phosphine loading did not improve the selectivity towards **127**. Therefore, the method that gave pure *E*-**126** was used in the subsequent screenings.

**Table 1** Initial optimisation

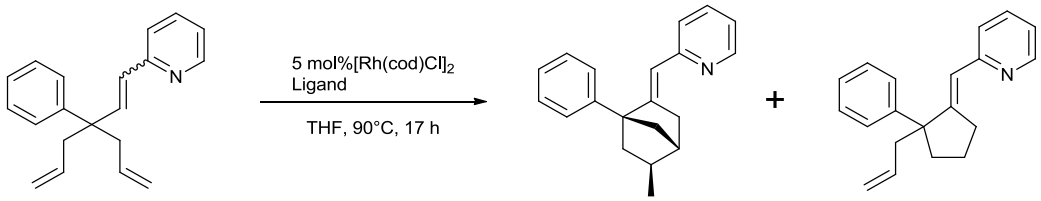


126 127 128

| Entry | E:Z ratio of **126** | Ligand | mol % | Conv.[a] | Ratio (**127**:**128**)[b] |
|---|---|---|---|---|---|
| 1 | >95:5 | No | | 33% | 5:>95 |
| 2 | 91:9 | P(*p*OMePh)$_3$ | 10 | 70% | 58:42 |
| 3 | 91:9 | P(*p*OMePh)$_3$ | 20 | >95% | 83:17 |
| 4 | >95:5 | P(*p*OMePh)$_3$ | 20 | >95% | 92:8 |
| 5 | >95:5 | P(*p*OMePh)$_3$ | 30 | >95% | 90:10 |

[a] Conversion based on ratio of **126** against the combined ratio of **127**:**128** as determined by $^1$H NMR spectroscopy. [b] Ratio determined by $^1$H NMR spectroscopy

Afterwards, it was of interest to see if other rhodium catalysts could provide better selectivity towards **126** (Table 2). With 10 mol% [Rh(cod)$_2$)BF$_4$ and 10 mol% P(*p*MeOC$_6$H$_4$)$_3$ (Table 2, Entry 1), the starting material was completely consumed but the selectivity between the **127** and

**128** was the same as with 5 mol% $[Rh(cod)Cl]_2$ and 20 mol% P(*p*$MeOC_6H_4)_3$. Increasing the phosphine loading to 20 mol% (Table 2, entry 2) improved the selectivity towards **127** slightly but the overall conversion was reduced. Increasing the phosphine loading to 30 mol% (Table 2, entry 3) eroded the selectivity when compared to with 20 mol% phosphine and the overall conversion was barely improved. Furthermore, the catalytic system of 5 mol% $[Rh(CO)_2Cl]_2$ and 10 mol% P(*p*$MeOC_6H_4)_3$ (Table 2, Entry 4) was completely ineffective and no conversion was observed. Carrying out the reaction with an increased phosphine loading of 20 mol% P(*p*$MeOC_6H_4)_3$ (Table 2, entry 5) or 30 mol% P(*p*$MeOC_6H_4)_3$ (Table 2, entry 6) were equally ineffective as both conditions resulted in no conversion of the starting material.

**Table 2** Rhodium catalyst

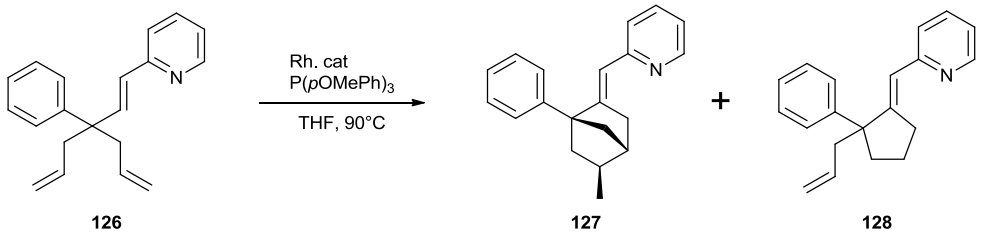


**126** **127** **128**

| Entry | Rh. cat. | mol % | Ligand (mol %) | Conv.[a] | Ratio (**127**:**128**)[b] |
|---|---|---|---|---|---|
| 1 | $[Rh(cod)_2]BF_4$ | 10 | 10 | >95% | 88:12 |
| 2 | $[Rh(cod)_2]BF_4$ | 10 | 20 | 88% | 91:9 |
| 3 | $[Rh(cod)_2]BF_4$ | 10 | 30 | 91% | 88:12 |
| 4 | $[Rh(CO)_2Cl]_2$ | 5 | 10 | 0 | N/A |
| 5 | $[Rh(CO)_2Cl]_2$ | 5 | 20 | 0 | N/A |
| 6 | $[Rh(CO)_2Cl]_2$ | 5 | 30 | 0 | N/A |

[a] Conversion based on ratio of **126** against the combined ratio of **127**:**128** as determined by $^1$H NMR spectroscopy. [b] Ratio determined by $^1$H NMR spectroscopy

A study on the temperature effects on the selectivity of **127** and **128** with 5 mol% $[Rh(cod)Cl]_2$ and varying mol% of $P(pMeOC_6H_4)_3$ was then commenced (Table 3). When the reaction was carried out with 10 mol% $P(pMeOC_6H_4)_3$ at 110°C (Table 3, entry 1), the selectivity towards **127** is significantly eroded. This erosion was remedied by increasing the phosphine loading to 20 mol% $P(pMeOC_6H_4)_3$ (Table 3, entry 2) which improved the selectivity towards **127**, albeit the selectivity remained slightly poorer than in the case of the reaction carried out at 90°C (Table 1, entry 4). However, when the temperature of the reaction was reduced to 70°C (Table 3, entry 3), the conversion dropped significantly and the five-membered ring **128** is formed with high selectivity.

**Table 3** Temperature effects

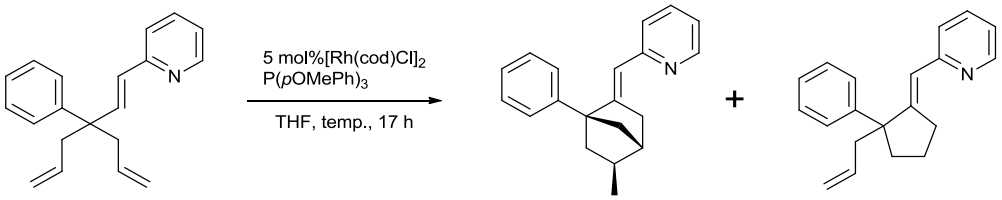


**126** **127** **128**

| Entry | Ligand (mol %) | Temp (°C) | Conv.[a] | Ratio (**127**:**128**)[b] |
|---|---|---|---|---|
| 1 | 10 | 110 | >95% | 65:35 |
| 2 | 20 | 110 | >95% | 87:13 |
| 3 | 20 | 70 | 18% | 5:>95 |

[a] Conversion based on ratio of **126** against the combined ratio of **127**:**128** as determined by $^1$H NMR spectroscopy. [b] Ratio determined by $^1$H NMR spectroscopy

Intrigued by the sudden drop of reactivity when the reaction was carried out at 70°C, it was assumed the rhodium concentration was simply too low. Therefore, the concentration of the reaction was increased to 100mM from 50mM and a screening of different temperatures was carried out (Table 4). Carrying the reaction out at 90°C gave complete conversion with good

selectivity of 89:11 for **127** (Table 4, entry 1). When the temperature was reduced to 70°C, the conversion vastly improved from 18% to 91% (Table 3, entry 3 vs Table 4, entry 2 and the selectivity towards **127** improved to 92:8. Lowering the temperature further to 60°C lowered the conversion but the selectivity towards **127** is fractionally better (Table 4, entry 3).

**Table 4** Temperature effects at 100mM

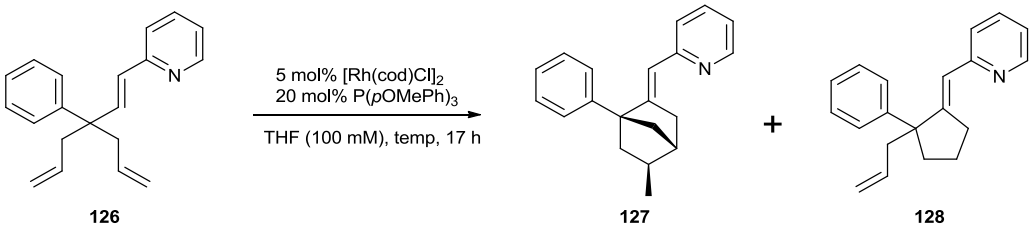


**126** **127** **128**

| Entry | Temp (°C) | Conv.[a] | Ratio (**127**:**128**)[b] |
|---|---|---|---|
| 1 | 90 | >95% | 89:11 |
| 2 | 70 | 91% | 92:8 |
| 3 | 60 | 55% | 93:7 |

[a] Conversion based on ratio of **126** against the combined ratio of **127**:**128** as determined by $^{1}$H NMR spectroscopy. [b] Ratio determined by $^{1}$H NMR spectroscopy

A screen of different ligands was then carried out to see if the selectivity towards **127** could be increased further (Table 5). Furthermore, as the conversion at 60°C was very low, the screen was carried out at 70°C. When the reaction was carried out with 20 mol% $PPh_3$, there was full conversion and the selectivity was found to be 90:10. Modifications of the phenyl ring which made the phosphine more electron deficient resulted in the reaction to proceed with lower conversion but the selectivity remained unaffected (Table 5, entry 2 and 3). However, electron deficient P(2-furyl)$_3$ (Table 5, Entry 4) proved to be an exception with full conversion and slightly improved selectivity towards **127** of 91:9. On the other hand, modification of the phenyl ring which made the phosphine more electron rich resulted in the reaction to proceed

with excellent to full conversion and with a selectivity of 91:9 (Table 5, entry 5 and 6). It was noted that a phosphine with a large cone angle is an ineffective ligand (Table 5, entry 7). Substitution of a phenyl ring with a cyclohexyl group gave poor conversion and reduced the selectivity towards **127** (Table 5, entry 8). Replacement of another phenyl ring with a cyclohexyl group gave poor conversion and the reaction is now more or less non-selective (Table 5, entry 9). These last two results suggest that incremental increase in the cone angle is detrimental to the rate of reaction and selectivity for **127**. Electron poor triphenyl phosphite is an ineffective ligand (Table 5, entry 10). Furthermore, hemi-lable ligand JohnPhos is also an ineffective ligand (Table 5, entry 11).

**Table 5** Ligand Screen

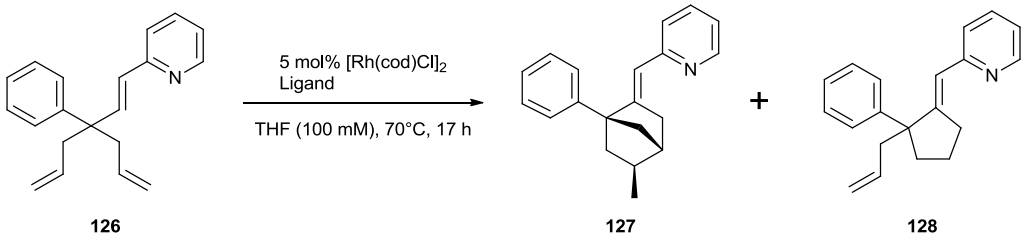


126 127 128

| Entry | Ligand | mol % | Conv.[a] | Ratio (**127**:**128**)[b] |
|---|---|---|---|---|
| 1 | $PPh_3$ | 20 | >95% | 90:10 |
| 2 | $P(pCF_3Ph)_3$ | 20 | 80% | 90:10 |
| 3 | $P(pClPh)_3$ | 20 | 68% | 91:9 |
| 4 | $P(2\text{-furyl})_3$ | 20 | >95% | 91:9 |
| 5 | $P(3, 5\text{-xylyl})_3$ | 20 | >95% | 91:9 |
| 6 | $P(p\text{-tol})_3$ | 20 | 93% | 91:9 |
| 7 | $P(o\text{-tol})_3$ | 20 | 0 | n/a |
| 8 | $PPh_2Cy$ | 20 | 32% | 68:32 |
| 9 | $PPhCy_2$ | 20 | 40% | 55:45 |
| 10 | $P(OPh)_3$ | 20 | 0 | n/a |
| 11 | JohnPhos | 10 | 0 | n/a |

[a] Conversion based on ratio of **126** against the combined ratio of **127**:**128** as determined by $^1$H NMR spectroscopy. [b] Ratio determined by $^1$H NMR spectroscopy

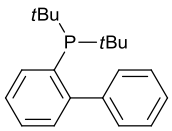


JohnPhos

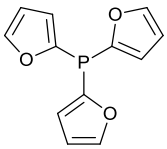


$P(2\text{-furyl})_3$

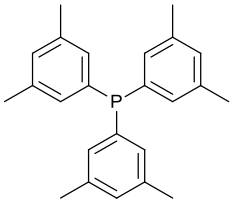


$P(3, 5\text{-xylyl})_3$

After the identification of ligands which displayed excellent conversion and selectivity, they were then tested with the temperature of the reaction reduced to 60°C (Table 6). It was previously found that 20 mol% P(*p*MeOC$_6$H$_4$)$_3$ at 60°C resulted in a conversion of 55% and with a selectivity of 93:7. Interestingly, carrying out the reaction with $PPh_3$ gave 87% conversion and a selectivity of 91:9 (Table 6, Entry 1). P(3, 5-xylyl)$_3$ is an effective ligand with excellent conversion and with an even better selectivity of 93:7 (Table 6, Entry 2). The electron poor P(2-fur)$_2$ also proved to be an effective ligand with excellent conversion and with a selectivity of 92:8 (Table 6, Entry 3). However, P(*p*tol)$_3$ proved to be ineffective at 60°C as the conversion was reduced from 93% at 70°C to 29%. Furthermore, the selectivity dropped from 91:9 to 65:35 (Table 6, Entry 4). This result appears to indicate if the rate of formation of **127** is slowed down, then the formation of five-membered ring **128** becomes more noticeable.

**Table 6** Selected ligands at 60°C

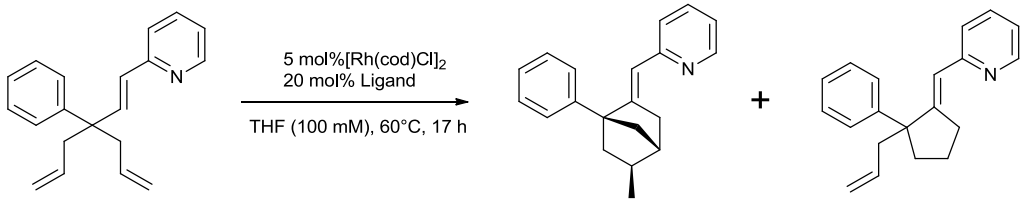


126 127 128

| Entry | Ligand | Conv.[a] | Ratio (**127**:**128**)[b] |
|---|---|---|---|
| 1 | $PPh_3$ | 87% | 91:9 |
| 2 | P(3, 5-xylyl)$_3$ | 92% | 93:7 |
| 3 | P(2-furyl)$_3$ | 91% | 92:8 |
| 4 | P(*p*tol)$_3$ | 29% | 65:35 |

[a] Conversion based on ratio of **126** against the combined ratio of **127**:**128** as determined by $^1$H NMR spectroscopy. [b] Ratio determined by $^1$H NMR spectroscopy

A change of model substrate to **129** was then decided and was used to continue the optimisation as we became interested if **126** was the optimal substrate for the methodology. Phosphines P(3, 5-xylyl)$_3$ and P(2-furyl)$_3$ were chosen because both ligands gave excellent conversion and good selectivity for **127** at 60°C (Table 7). However, carrying out the reaction with 5 mol% [Rh(cod)Cl]$_2$ and 20 mol% P(3, 5-xylyl)$_3$ gave poor conversion and poor selectivity which appears to confirm that the new substrate might be more challenging than the original substrate (Table 7, entry 1). Using 20 mol% P(2-furyl)$_3$ gave even worst conversion and the selectivity of the reaction becomes in favour of **130** (Table 7, entry 2). On changing the source of rhodium catalyst to 5 mol% [Rh(coe)$_2$Cl]$_2$ and with 20 mol% P(3, 5-xylyl)$_3$ gave a much improved conversion of 86% but the selectivity remains poor (Table 7, entry 3). Using 20 mol% P(2-furyl)$_3$ did not improve the conversion and the reaction becomes non-selective (Table 7, entry 4).

**Table 7** Rhodium and Phosphine screen

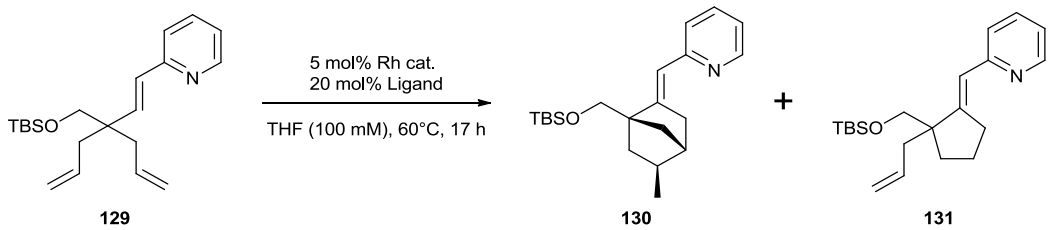


**129** **130** **131**

| Entry | Rh cat. | Ligand | Conv.[a] | Ratio (**130**:**131**)[b] |
|---|---|---|---|---|
| 1 | [Rh(cod)Cl]$_2$ | P(3, 5-xylyl)$_3$ | 35% | 56:44 |
| 2 | [Rh(cod)Cl]$_2$ | P(2-furyl)$_3$ | 16% | 37:63 |
| 3 | [Rh(coe)$_2$Cl]$_2$ | P(3, 5-xylyl)$_3$ | 86% | 56:44 |
| 4 | [Rh(coe)$_2$Cl]$_2$ | P(2-furyl)$_3$ | 64% | 48:52 |

[a] Conversion based on ratio of **129** against the combined ratio of **130**:**131** as determined by $^1$H NMR spectroscopy. [b] Ratio determined by $^1$H NMR spectroscopy

After the identification of P(3, 5-xylyl)$_3$ as the ideal ligand, a screen of different solvents was carried out to determine if the selectivity towards **130** could be improved further (Table 8). Non-polar toluene gave a conversion of 82% but there was almost no selectivity (Table 8, entry 1). Polar acetone gave a conversion of 79% but, there was no selectivity (Table 8, entry 2). The more polar MeCN gave no conversion which could be because of the increased coordinating capability of MeCN which could render the catalyst inactive (Table 8, entry 3). The polar and protic *i*PrOH gave full conversion and with a selectivity for **130** of 75:25 (Table 8, entry 4). Interestingly, if HPLC grade *i*PrOH was used, full conversion was observed and the selectivity towards **130** improved slightly to 78:22 (Table 8, Entry 5). Using EtOH which came from a bottle exposed to air and moisture gave a conversion of 85% but the selectivity towards **130** improved further to 82:18 (Table 8, Entry 6). Using MeOH which came from a bottle exposed to air and moisture gave only a conversion of 52% but the selectivity towards **130** increased to 84:16 (Table 8, Entry 7). Interestingly, when dry methanol was used instead, the conversion lowered to 29% and the selectivity towards **130** dropped to 73:27 (Table 8, Entry 8). This suggests that trace water or air is actually beneficial to the selectivity towards **130**.

**Table 8** Solvent Screen

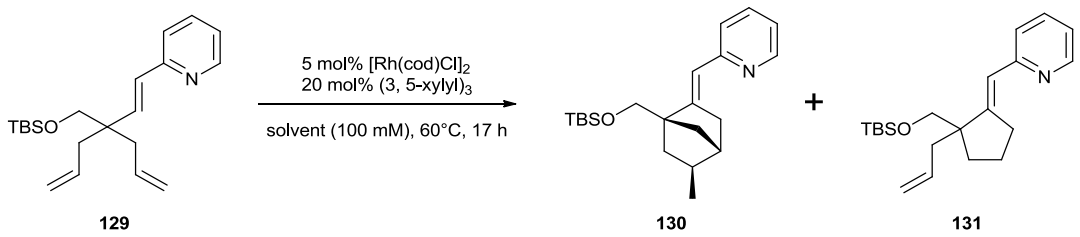


129 130 131

| Entry | Solvent | Conv.[a] | Ratio (**130**:**131**)[b] |
|---|---|---|---|
| 1 | Toluene | 82% | 45:55 |
| 2 | Acetone | 79% | 47:53 |
| 3 | MeCN | 0% | n/a |
| 4 | iPrOH | >95% | 75:25 |
| 5 | iPrOH (HPLC) | >95% | 78:22 |
| 6 | EtOH (GPR grade) | 85% | 82:18 |
| 7 | MeOH (GPR grade) | 52% | 84:16 |
| 8 | MeOH | 29% | 73:27 |

[a] Conversion based on ratio of **129** against the combined ratio of **130**:**131** as determined by $^1$H NMR spectroscopy. [b] Ratio determined by $^1$H NMR spectroscopy

Due to the lack of selectivity towards **130** with model substrate **129**, full characterisation of **130** was not carried out. Furthermore, **130** and **131** could not be separated by flash column chromatography. As a result, a screen of different solvents with the original substrate **126** was then investigated (Table 9). Therefore with 5 mol% $[Rh(coe)_2Cl]_2$ and 20 mol% P(3, 5-xylyl)$_3$ in dried methanol, the reaction proceeded with an improved conversion of 83% and a selectivity of 83:17 (Table 9, entry 1). As suspected earlier of the positive influence of water, doping the reaction with water resulted in an increase conversion from 83% to 88% and a slightly improved selectivity of 87:13 (Table 9, entry 2). However, when MeOH was used directly out of a bottle that has been exposed to air and moisture, the reaction proceeded with poorer

conversion of 68% and with an even poorer selectivity towards **127** of 67:33 (Table 9, entry 3). A mixed solvent system of MeOH and THF in a 1:1 ratio gave excellent conversion and selectivity towards **127** of 94:6 (Table 9, entry 4).

**Table 9** Solvent screen

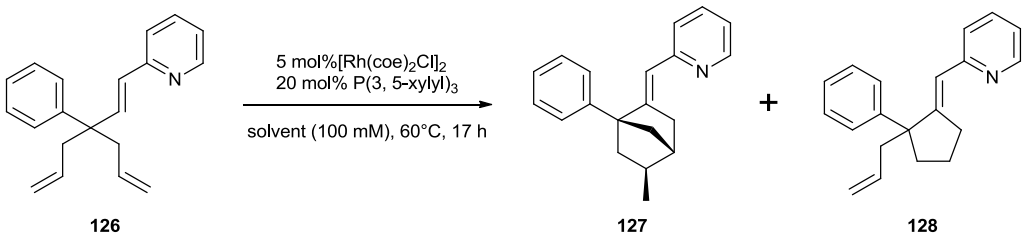


126 127 128

| Entry | Solvent | Conv.[a] | Ratio (**127**:**128**)[b] |
|---|---|---|---|
| 1 | MeOH | 83% | 83:17 |
| 2 | MeOH/$H_2O$ (5:1) | 88% | 87:13 |
| 3 | MeOH (bottle) | 69% | 67:33 |
| 4 | MeOH/THF (1:1) | 94% | 94:6 |

[a] Conversion based on ratio of **126** against the combined ratio of **127**:**128** as determined by $^1$H NMR spectroscopy. [b] Ratio determined by $^1$H NMR spectroscopy

Afterwards, a screening of other ligands and different solvent ratios was then commenced (Table 10). Sterically demanding NHC IPr is an ineffective ligand (Table 10, Entry 1). However, the electron poor P(2-furyl)$_3$ improved the selectivity towards **127** and gave full conversion (Table 10, Entry 2). Then it was decided to retest P(*p*MeOC$_6$H$_4$)$_3$ and the reaction proceeded with an excellent selectivity towards **127** of 97:3 and with full conversion (Table 10, Entry 3). Then the solvent ratio was modified but it was found that increasing the ratio in favour of THF had no effect on both the selectivity and conversion (Table 10, Entry 4-6). Except, the THF/MeOH solvent ratio of 9:1 reduced the conversion and decreased the selectivity towards **127** (Table 10, entry 6).

**Table 10** A screening of other ligands and different solvent ratios

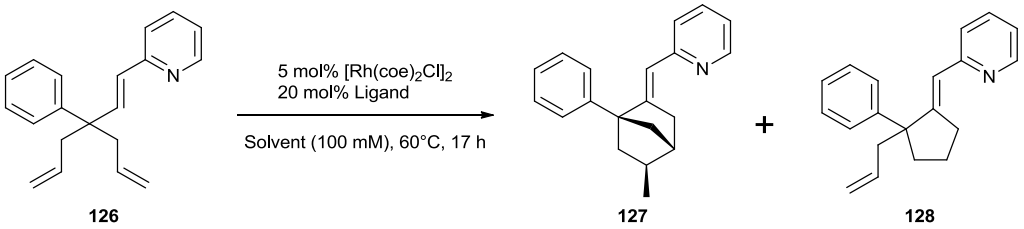


126 127 128

| Entry | Ligand | Solvent | Conv.[a] | Ratio (**127**:**128**)[b] |
|---|---|---|---|---|
| 1 | Ipr | MeOH/THF (1:1) | 0% | n/a |
| 2 | P(2-furyl)$_3$ | MeOH/THF (1:1) | >95% | 95:5 |
| 3 | P(*p*MeOC$_6$H$_4$)$_3$ | MeOH/THF (1:1) | >95% | 97:3 |
| 4 | P(*p*MeOC$_6$H$_4$)$_3$ | MeOH/THF (1:2) | >95% | 96:4 |
| 5 | P(*p*MeOC$_6$H$_4$)$_3$ | MeOH/THF (1:4) | >95% | 96:4 |
| 6 | P(*p*MeOC$_6$H$_4$)$_3$ | MeOH/THF (1:9) | 83% | 88:12 |

[a] Conversion based on ratio of **126** against the combined ratio of **127**:**128** as determined by $^1$H NMR spectroscopy. [b] Ratio determined by $^1$H NMR spectroscopy

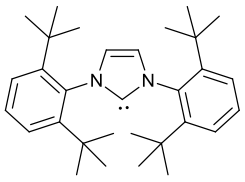


IPr

Then other bidentate ligands were tested to see if the selectivity towards **127** could be improved (Table 11). The solvent system of MeOH/THF in a 1:2 ratio was used as it was more practical than 1:4. However, all bidentate ligands that were examined led to no conversion (Table 11, entry 1-6).

**Table 11** Screening of other ligands

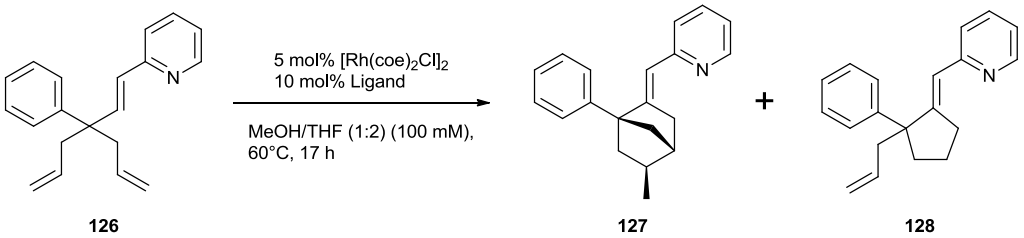


126 127 128

| Entry | Ligand | Conv.[a] | Ratio (**127**:**128**)[b] |
|---|---|---|---|
| 1 | DPePhos | 0% | n/a |
| 2 | DM-BINAP | 0% | n/a |
| 3 | R-Segphos | 0% | n/a |
| 4 | XantPhos | 0% | n/a |
| 5 | DPPF | 0% | n/a |
| 6 | XPhos | 0% | n/a |

[a] Conversion based on ratio of **126** against the combined ratio of **127**:**128** as determined by $^{1}$H NMR spectroscopy. [b] Ratio determined by $^{1}$H NMR spectroscopy

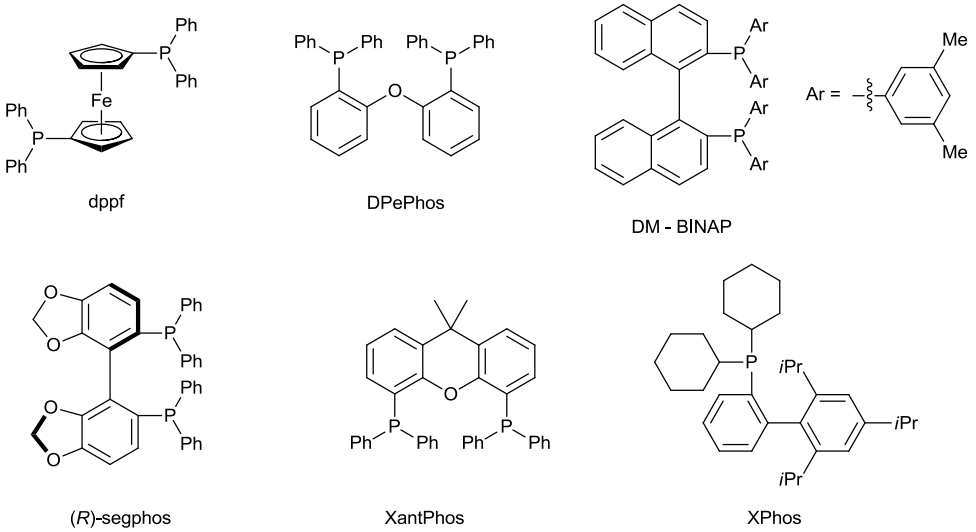


It was then thought that a cationic rhodium complex would be more active. Freeing up a coordination site on the rhodium centre might allow the second alkene to coordinate more readily to the rhodium centre and thus improve the selectivity towards **127**. A common

method used to make a neutral complex cationic is by halide abstraction with a silver salt (Table 12). Pleasingly, the halide abstraction with $AgBF_4$ gave complete conversion and with excellent selectivity towards **127** (Table 12, entry 1). A quick re-examination with different bidentate ligands gave no conversion despite the use of a silver salt (Table 12, entry 2 and 3). Abstraction of the halide with $AgSbF_6$ also proceeded with full conversion and with excellent selectivity towards **127** (Table 12, entry 4). However, halide abstraction with AgOBz or AgOTs proceeded with full conversion but the selectivity towards **127** was a little lower in both cases (Table 12, entry 5 and 6). The lower selectivity could be imputed to the greater coordinating ability of the OBz and OTs anion. It was assumed MeOH could complex to the cationic rhodium and as a result, diminished the selectivity towards **127**. Finally, carrying out the reaction in THF with $AgBF_4$ gave a selectivity of 98:2 with an isolated yield of 89% and further optimisation was halted (Table 12, entry 7). Therefore, the condition to be used for the subsequent screening is 5 mol% $[Rh(coe)_2Cl]_2$, 20 mol% P(*p*$MeOC_6H_4)_3$, 10 mol% $AgBF_4$ in 100mM THF at 60°C for 17 hours.

**Table 12** Screening of ligands and silver cation

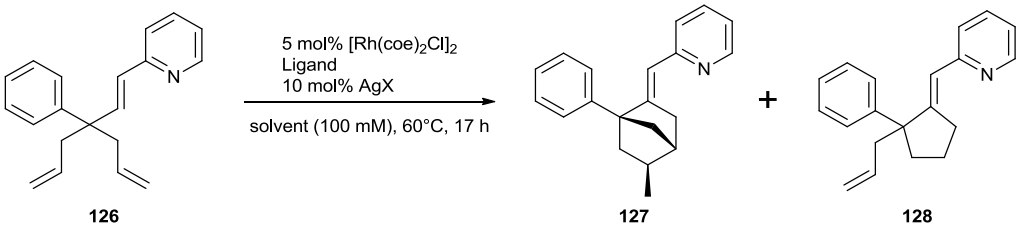


| Entry | Ligand | mol % | AgX | Solvent | Conv.[a] | Ratio (**127**:**128**)[b] |
|---|---|---|---|---|---|---|
| 1 | P(*p* $MeOC_6H_4)_3$ | 20 | $AgBF_4$ | THF/MeOH (2:1) | >95% | 97:3 |
| 2 | DM-BINAP (S) | 10 | $AgBF_4$ | THF/MeOH (2:1) | 0 | n/a |
| 3 | Segphos (R) | 10 | $AgBF_4$ | THF/MeOH (2:1) | 0 | n/a |
| 4 | P(*p* $MeOC_6H_4)_3$ | 20 | $AgSbF_6$ | THF/MeOH (2:1) | >95% | 97:3 |
| 5 | P(*p* $MeOC_6H_4)_3$ | 20 | AgOBz | THF/MeOH (2:1) | >95% | 95 |
| 6 | P(*p* $MeOC_6H_4)_3$ | 20 | AgOTs | THF/MeOH (2:1) | >95% | 93:7 |
| 7 | P(*p* $MeOC_6H_4)_3$ | 20 | AgBF4 | THF | >95% | 98:2[c] |

[a] Conversion based on ratio of **126** against the combined ratio of **127**:**128** as determined by $^1$H NMR spectroscopy. [b] Ratio determined by $^1$H NMR spectroscopy. [c] Isolated yield of 89%

**127** was fully characterised by $^1$H, $^{13}$C NMR, 2D NMR, IR and HRMS analysis. NOESY was used to ascertain the stereochemistry and revealed the bridgehead hydrogen **1** and one of the hydrogens of the *exo*-methyl **2** are *syn* in space (Scheme 24). Furthermore, *endo*-hydrogen **3** has a NOESY correlation with *endo*-hydrogen **4**. Furthermore, only one diastereoisomer is formed. It was then of interest to get an X-Ray to confirm the stereochemistry of **127**. As **127** is an oil, the hydrochloride salt was made which allowed crystals of sufficient X-ray quality to be grown (Scheme 25). The X-ray structure confirmed the stereochemistry of product **127** by analogy.

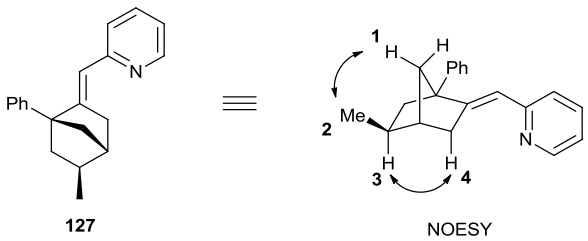


**Scheme 24** NOESY experiments

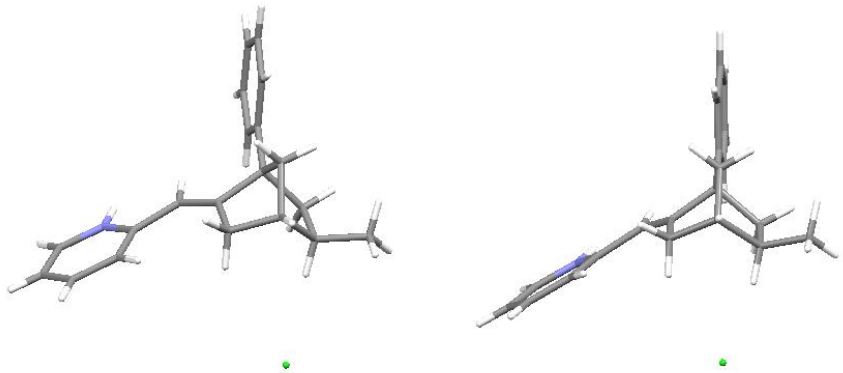

**Scheme 25** X-Ray of Pyridinium Salt of **127**

## 4.4 Scope of the reaction

With the optimised conditions in hand, the scope of the reaction was examined (Table 13). All products were fully characterised by $^{1}H$, $^{13}C$ NMR, 2D NMR, IR and HRMS analysis. In all cases whereby **133** is formed, **133** is isolated as a single diastereoisomer. Unfortunately in all cases, **133** and five-membered ring **134** were inseparable by flash column chromatography. As a result, the ratio described is the crude ratio of **133** and **134** as judged by $^{1}H$ NMR. Furthermore, the yield mentioned is the combined isolated yield of **133** and **134**.

The starting materials **132a-d, f** and **g** were prepared and subjected to the corresponding rhodium-catalysed reaction by Daniel J. Tetlow and are not described in this thesis. It is found that the selectivity for **133** over **134** is greater when R is large. Vinylpyridines **132a – c**, with R = aryl, gave high selectivity towards **133** in good to high yields (Table 13, Entry 1- 3). Modulation of the electronic properties of the aryl ring did not have a significant effect on the selectivity between the corresponding **133** and **134**. However, small erosion in selectivity is observed when a vinyl pyridine that contains an electron rich substituent was tested (Table 13, Entry 3). Interestingly, vinylpyridine **132d** with R = benzofuran gave poorer selectivity towards **133d** (Table 13, Entry 4). It was then of interest to determine what other functional groups are tolerated under the reaction conditions.

Vinylpyridines **132e-g** (Table 13, Entry 5-7), whereby R is a large group, gave excellent selectivity towards the corresponding **133e-g**. Vinylpyridine **132h** gave good selectivity towards **133h** when the loading of phosphine was reduced to 15 mol% (Table 13, Entry 8). Vinylpyridines **132i** and **132j** (Table 13, Entry 9 and 10), whereby R is a small group, gave moderate selectivity towards the **133i** and **133j** respectively.

**Table 13** Reaction scope

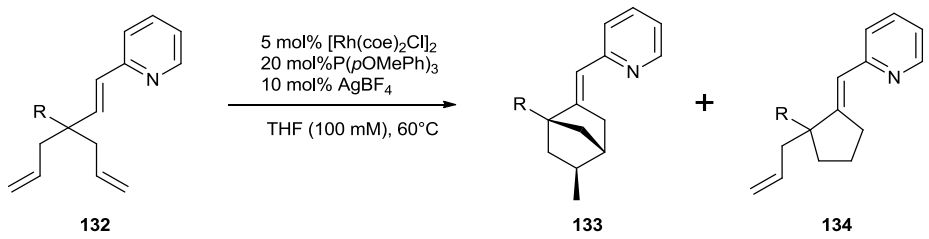


**132** **133** **134**

| Entry | Start Material **132** | Major Product | Ratio (**133**:**134**)[b] | Yield |
|---|---|---|---|---|
| 1[a] | 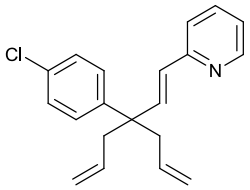 **132a** | 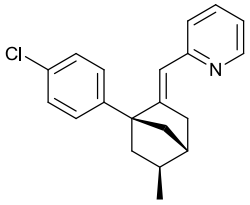 **133a** | 96 : 4 | 97% |
| 2[a] | 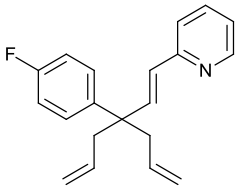 **132b** | 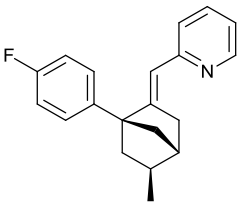 **133b** | 96 : 4 | 81% |
| 3[a] | 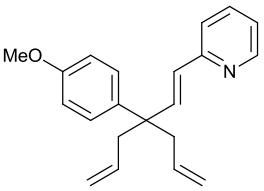 **132c** | 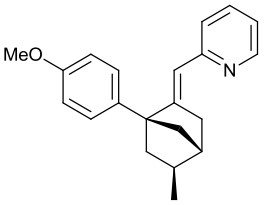 **133c** | 95 : 5 | 76% |
| 4[a] | 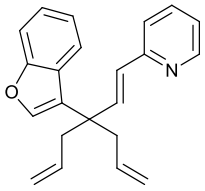 **132d** | 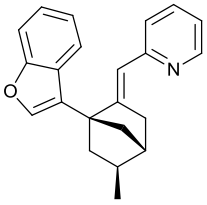 **133d** | 85 : 15 | 84% |

| | | | | |
|---|---|---|---|---|
| 5 | 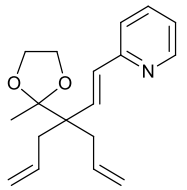 **132e** | 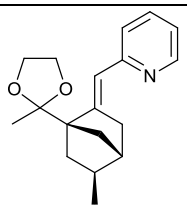 **133e** | 97 : 3 | 88% |
| 6[a] | 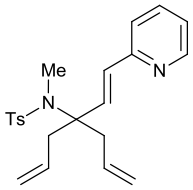 **132f** | 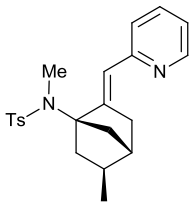 **133f** | 95 : 5 | 76% |
| 7[a] | 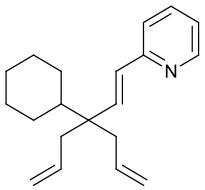 **132g** | 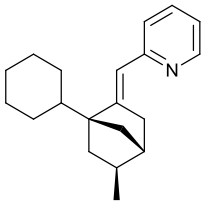 **133g** | 96 : 4 | 75% |
| 8 | 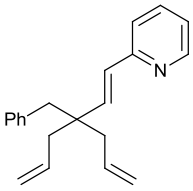 **132h** | 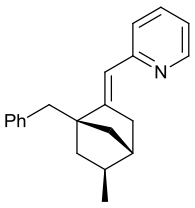 **133h** | 95 : 5[b] | 83% |
| 9 | 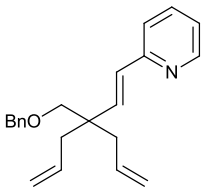 **132i** | 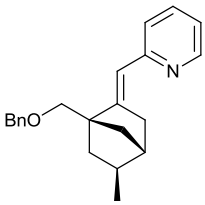 **133i** | 67 : 33 | 71% |
| 10 | 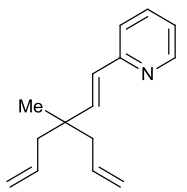 **132j** | 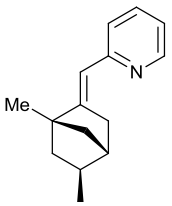 **133j** | 75 : 25 | 72 % |

[a] Syntheis of substrate and Rh-catalysed cyclisation were carried out by Daniel J. Tetlow. [b] Ratio determined by $^{1}$H NMR spectroscopy. [c] Rh : L (1:1.5)

### 4.4.1 Another directing group

Other directing groups have been successfully employed in C–H bond activation. It was of interest to see if the selectivity towards bicyclo[2.2.1]heptanes could be improved by a change in directing group. It was thought an imidazole directing group would be more effective as it is more basic. However, under the optimised conditions, no reaction was observed with vinyl imidazole **135** (Scheme 26).

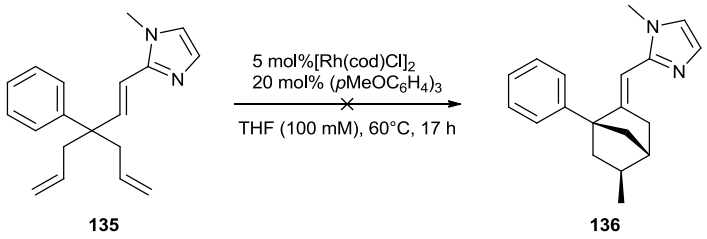


**Scheme 26** Imidazole directing group

## 4.5 Mechanistic studies

Daniel J. Tetlow then studied the conversion of **132f** by monitoring the reaction by $^{1}$H NMR. Over the course of the reaction, an extra set of signals were observed which would gradually build up and then disappear when the reaction was over. Monitoring the reaction by TLC revealed a new spot would form but would disappear by the end of the reaction. Therefore, the reaction was quenched after 30 mins and the intermediate **137** was isolated in a 33% yield (Scheme 27). Characterisation of the intermediate by 1H, $^{13}$C NMR, 2D NMR, IR and HRMS revealed the structure of the intermediate to be four-membered ring **137**. NOESY experiments allowed the assignment of the relative configuration at the stereocentres. Furthermore, the stereochemistry of **137** is inverted when compared to **133f**.

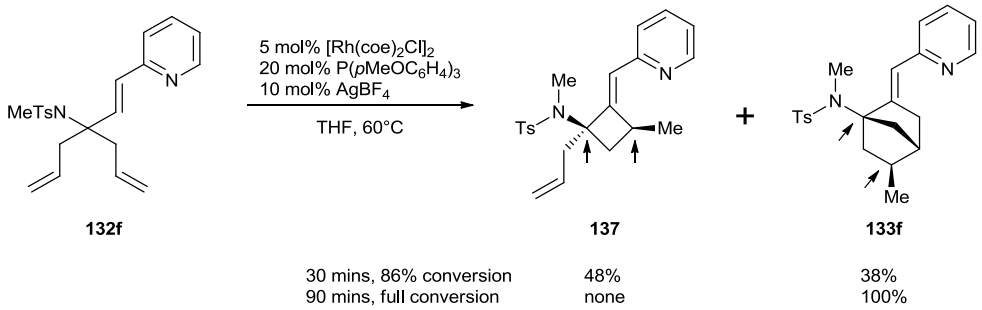


**Scheme 27** Formation of the four-membered ring as judged by $^{1}$H NMR

Therefore, it was then of interest to see if the four-membered ring intermediate could be isolated with substrate **126**. A kinetic profile using the standard reaction condition of the transformation of **126** was carried out by taking aliquots from the reaction and analysing the aliquot by $^{1}$H NMR (Scheme 28). As expected, an extra set of signals would gradually build up and would then disappear by the end of the reaction. These extra set of signals were assumed to the four-membered ring **138**. To confirm this, attempts were made to isolate **138** because isolation of **138** would allow the stereochemistry to be assigned. Furthermore, this would also allow the relative configuration of **138** and bicyclic **127** to be compared. However, **138** could not be separated from **127** by flash column chromatography as they co-elute together.

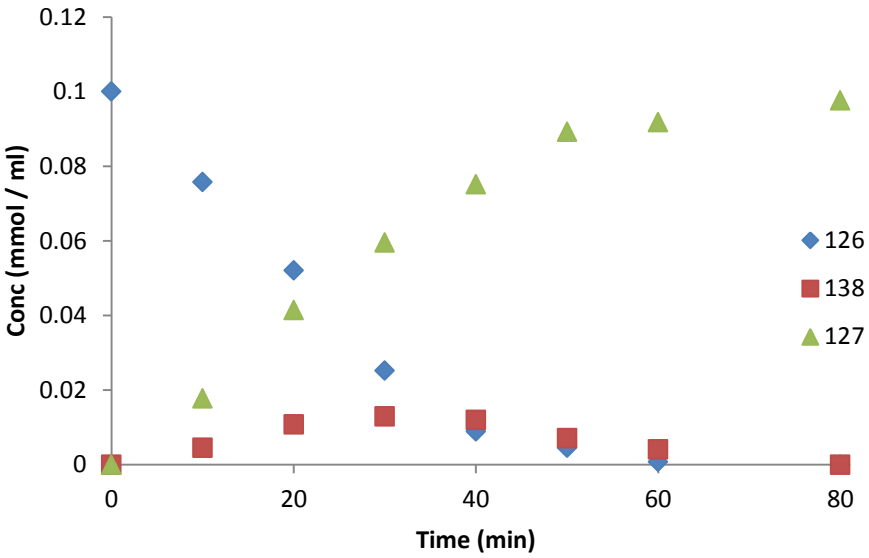


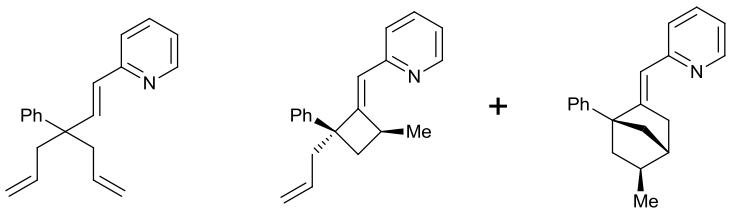


**126** **138** **127**

relative stereochemistry is assumed

**Scheme 28** Formation of the four-membered ring

### 4.5.1 Deuterium-labelling experiment

To obtain more mechanistic information, a deuterium labelling study of **139** was then carried out (Scheme 29). Subjecting a deuterium labelled **139** to the standard reaction conditions furnished bicyclic **140** and **141** in a combined 90% yield with a ratio of 60:40 as confirmed by $^{2}$H NMR (Scheme 30). Furthermore, there was complete transfer of the deuterium to the indicated positions. **140** has the deuterium on the *exo*-methyl carbon. **141** has the deuterium on the carbon α to the vinyl pyridine. Also, the deuterium on **141** is equally distributed on the *exo*- and *endo*- position.

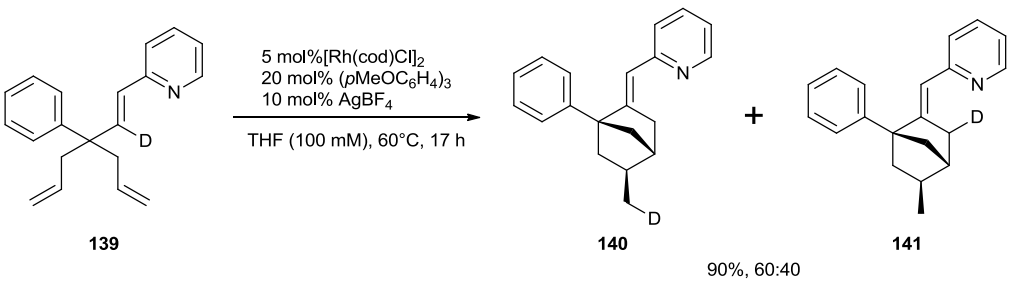


**Scheme 29** Deuterium Scrambling

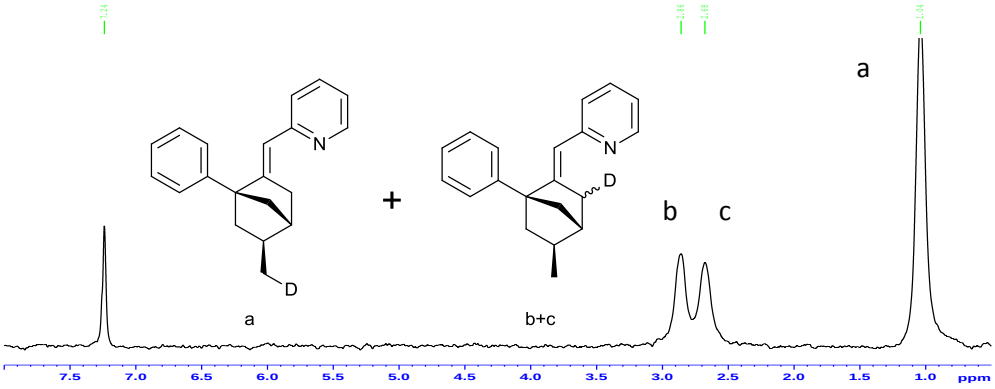


**Scheme 30** Deuterium NMR

Before determining the kinetic isotopic effect, it was of interest to understand a little bit more why the deuterium was scrambled over two carbons. In the study of the rhodium-catalysed intramolecular cyclisation of 1,5-diene **142**, Murai and co-workers reported the C–H activation and hydrometalation steps occur reversibly at room temperature with the deuterium atom scrambled over three positions (Scheme 31).[28] Furthermore, the hydrometalation of the alkene preferentially occurs in the 2,1-fashion.

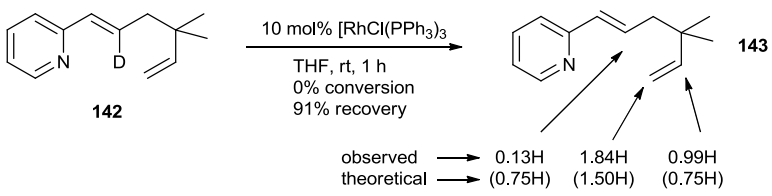


**Scheme 31** Kinetic experiment by Murai

To account for the non-statistical distribution of the deuterium atom, Murai and co-workers then subjected the labelled compound **142** to the standard reaction conditions (Scheme 32). Analysis of the product **144** revealed a near statistical distribution of the deuterium atom which suggests the equilibration is far faster than the alkene migratory insertion.

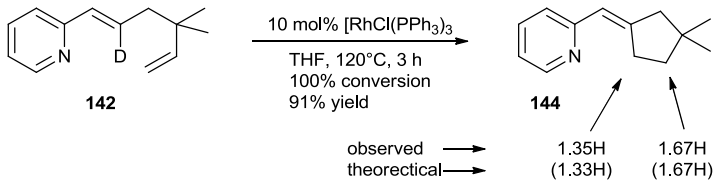


**Scheme 32** Labelled compound **142** to the standard reaction conditions

From these experiments, a mechanism was formulated by Murai and co-workers (Scheme 33). After the pyridine directed C–H bond activation to form intermediate **145**, hydrometalation of the alkene can occur in the 1,2- or 2,1-fashion. From the deuterium scrambling studies, the hydrometalation onto the alkene in the 2,1-fashion is fast and reversible. On the other hand, the hydrometalation onto the alkene in the 1,2- fashion is slow but, when it does occur, irreversible reductive elimination would furnish five membered ring **144**.

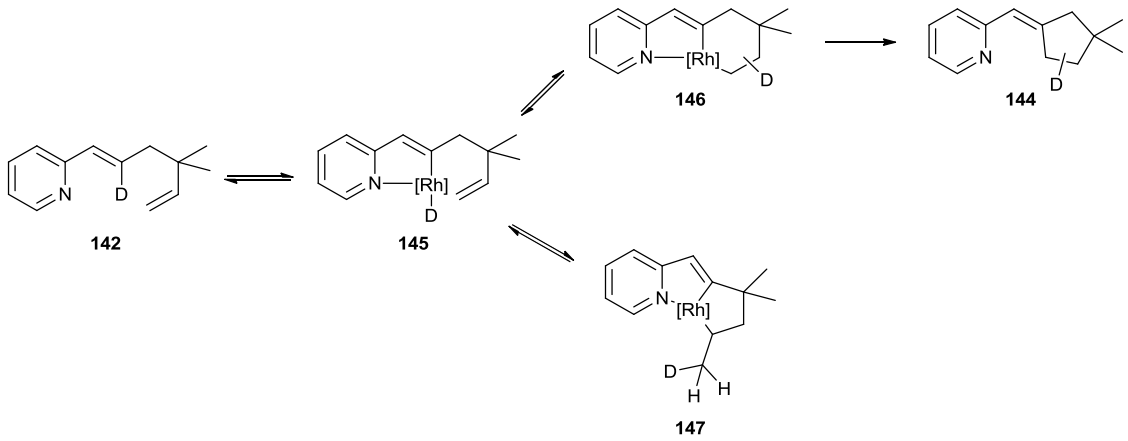


**Scheme 33** Proposed mechanism

Therefore, it was of interest to see if this phenomenon exists in our system. Subjecting deuterium labelled **139** to the standard reaction condition resulted in the deuterium remaining in the original position or being incorporated to the external alkene double bond **148** (Scheme 34). Interestingly, the alternative product **149** was not observed (Scheme 35). This is similar to the observations by Murai, whereby in our system, the deuterium atom is scrambled over two carbons. Like Murai's example, the 1,2-hydrometallation is a slow process and the deuterium incorporation at C2 is very small. On the other hand, the 2,1-hydrometallation is much faster as reflected in the deuterium incorporation into the alkene C1 being noticeably higher. No formation of the five-membered ring or **140** or **141** were observed after 1 hr. This therefore demonstrates that the C–H cleavage process is facile at room temperature. Also, the migratory insertion of the first alkene is reversible and happens much faster than the subsequent steps of the catalytic cycle.

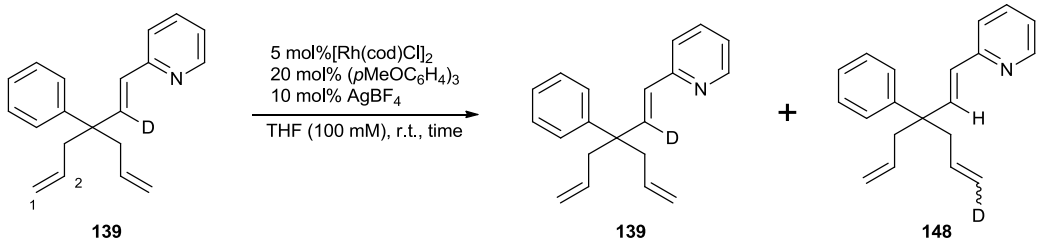


**139** **139** **148**

| Time | Ratio (**139:148)** |
|---|---|
| 10 min | 52 : 48 |
| 60 min | 26 : 74 |

**Scheme 34** Scrambling at r.t.

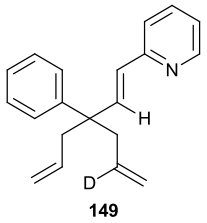


149

**Scheme 35** Deuterium-labelled product not observed

Then a study on the kinetic isotopic effect was commenced to gain insight into the mechanism. If the C–H activation step is indeed the rate determining step, this would be reflected in the rate of reaction between **126** and deuterated **139**. Therefore, parallel completion experiments of **126** and **139** were carried out (Scheme 36). By comparing the rate of the reaction between **126** and **139**, an average kinetic isotopic effect of $k_H$ / $k_D$ of 1.2 was obtained. Furthermore, the ratio of **126** and **139** does not change with time. This result demonstrated the C–H bond activation is not the rate determining step and a normal secondary kinetic isotopic effect is observed. Also, the formation of **127** is not reversible.

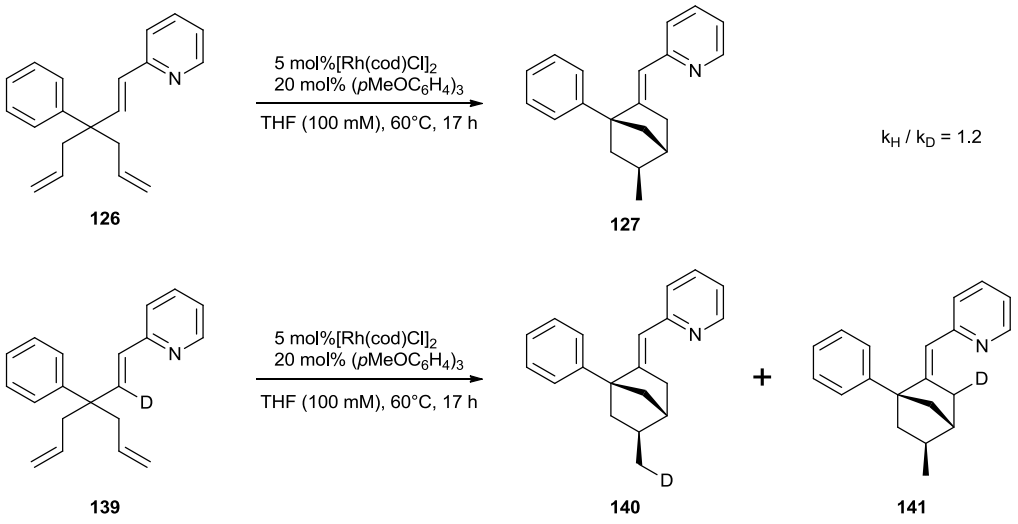


126 127

139 140 141

**Scheme 36** Study on the kinetic isotopic effect

Crossover experiment was then carried out to determine if the reaction is an intra- or inter-molecular process (Scheme 37). The rhodium-catalysed reaction was carried out with both substrate **139** and substrate **132f** in the same reaction vessel. However, at the end of the reaction substrate **132f** was isolated in 89% yield with no deuterium incorporation. Furthermore, product **140** and **141** were isolated in a combined 95% yield with a ratio of 64:36. Moreover, there was complete transfer of the deuterium to the indicated positions. **140** has the deuterium atom on the *exo*-methyl carbon. **141** has the deuterium atom on the carbon α to the vinyl pyridine. Also, the deuterium atom on **141** is equally distributed between the *exo*- and *endo*- position. The lack of crossover confirmed that the reaction is purely intramolecular.

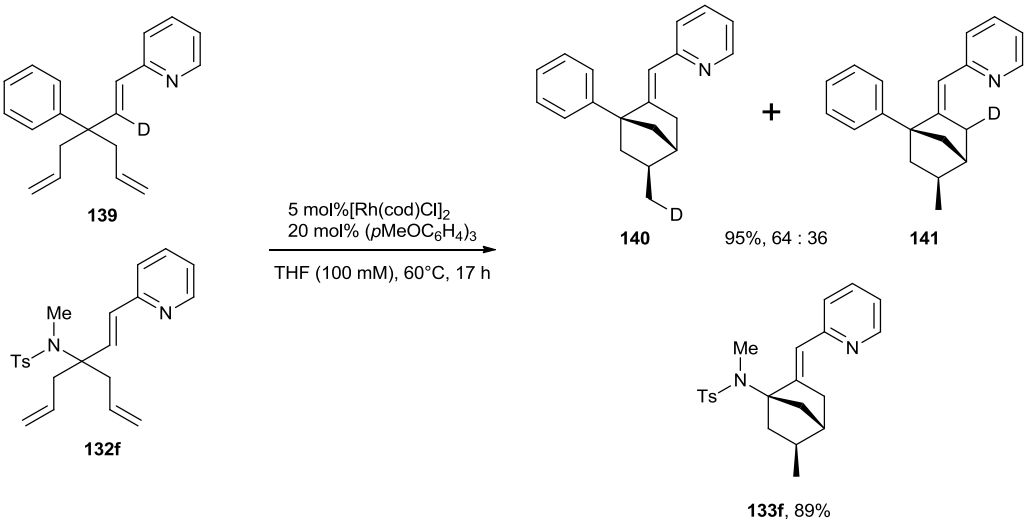


**Scheme 37** Crossover experiment

The deuterium scrambling studies revealed the C–H bond activation step and hydrometalation is reversible and both steps happen a lot faster than the subsequent steps. The crossover experiment confirms it is an intramolecular reaction. From the optimisation, the formation of five-membered ring **128** occurs faster at higher temperature than the formation of **127**. The stereocentres found in the four-membered ring side **137** is inverted when compared to

stereocenters of **133f**. Furthermore, the four-membered ring is not seen if the reaction is allowed to proceed to completion. The formation of the bicyclo[2.2.1]heptane is completely diastereoselective.

To account for all these observations, a potential mechanism have been postulated (Scheme 38). After the pyridine directed C–H bond activation to form intermediate **150**, hydrometalation onto the alkene can occur in the 1,2- or 2,1-fashion. The hydrometalation onto the alkene in the 1,2-fashion to form **152** is slow as determined by deuterium labelling studies. However, when it does occur, irreversible reductive elimination furnishes five-membered ring **134**.

From the deuterium-labelling studies, hydrometalation onto the alkene in the 2,1-fashion is considerably faster and reversible but it is also clear that the hydrometalation is not completely stereoselective. If the hydrometalation proceeds to give intermediate **153** whereby the *exo*-methyl group and the allyl group are *anti*, reductive elimination can occur to give four membered ring **154**. From the time profile studies, four membered ring **154** is not observed at the end of the reaction and therefore is reversibly formed.

The formation of **133** occurs when hydrometalation onto the alkene occurs in the 2,1-fashion to give intermediate **151** whereby the *exo*-methyl group and the allyl group are *syn*. After the formation of **151**, the migratory insertion of the pendant alkene occurs to furnish the seven-membered rhodacycle **155**. Finally, reductive elimination occurs to furnish **133**.

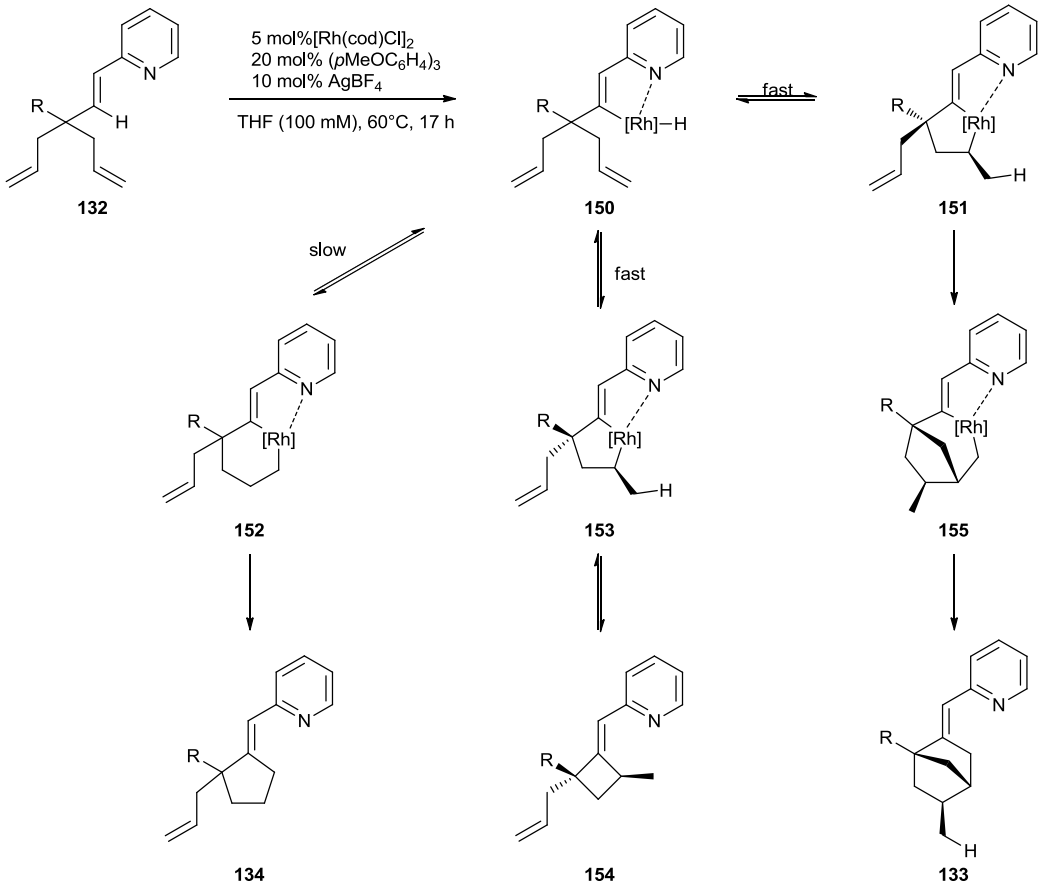


**Scheme 38** Postulated mechanism

## 4.6 Conclusion

The generation of bicyclo[2.2.1]heptane **133** from vinyl pyridines **132** by a rhodium catalyst have been accomplished (Scheme 39). Interestingly, **133** was formed as a single diastereoisomer in all cases whereby the bridgehead carbon and the *exo*-methyl carbon are *syn* in space. However, the **133** is always contaminated with **132** to varying degrees as neither could be separated by flash column chromatography. It has been noted that a large Thorpe-Ingold effect influences the selectivity in favour of **133**. Furthermore, this work could be further enhanced by carrying out the reaction enantioselectively.

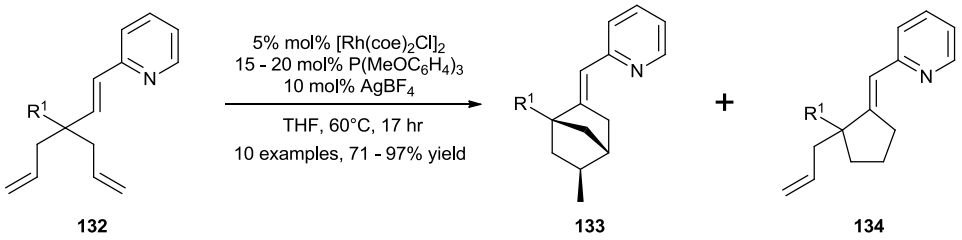


**Scheme 39** Summary

## 4.7 Future work

The generation of bicyclo[2.2.1]heptane **133** from vinyl pyridines **132** proceeded in a diastereoselective manner. Therefore, a further extension to this methodology would be an enantioselective synthesis of **133** (Scheme 40). This would make the methodology extremely attractive as there would be potentially complete stereocontrol on the formation of all 3 chiral centres of **133** despite starting from prochiral **132**.

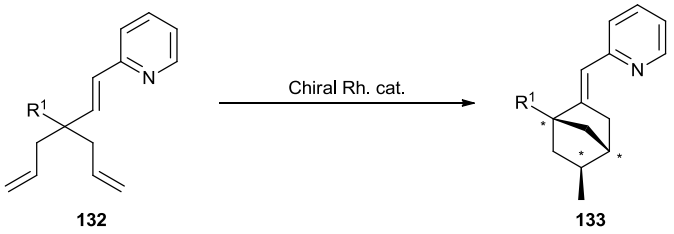


**Scheme 40** Possible enantioselective synthesis of **133**

Employing a chiral ligand should enable a catalytic enantioselective synthesis of **133**. As there is a large library of different chiral bidentate phosphine ligands available, chiral bidentate phosphines would be a good starting point to find conditions for the enantioselective synthesis of **133**. However, during the optimisation of this reaction, it became clear that bidentate ligands were ineffective.

On the other hand, chiral monodentate phosphine ligands have been recognised as effective ligands for many enantioselective transition-catalysed reactions.[29] Therefore, a suitable chiral monodentate phosphine ligand could potentially enable an enantioselective synthesis of **133**.

## 4.8 Synthesis of precursors

The synthesis of aldehyde **S5** started from commercially available ester **S1** (Scheme 41). The first allylation with allyl bromide afforded the mono-allylated ester **S2** in 97% yield. The allylation was then repeated with allyl bromide with TBAI to afford the *bis*-allylated ester **S3** in 97% yield. Reduction with $LiAlH_4$ gave alcohol **S4** in 97% yield. Finally, oxidation to aldehyde **S5** was achieved by Swern oxidation[30] which was then used directly in the next step.

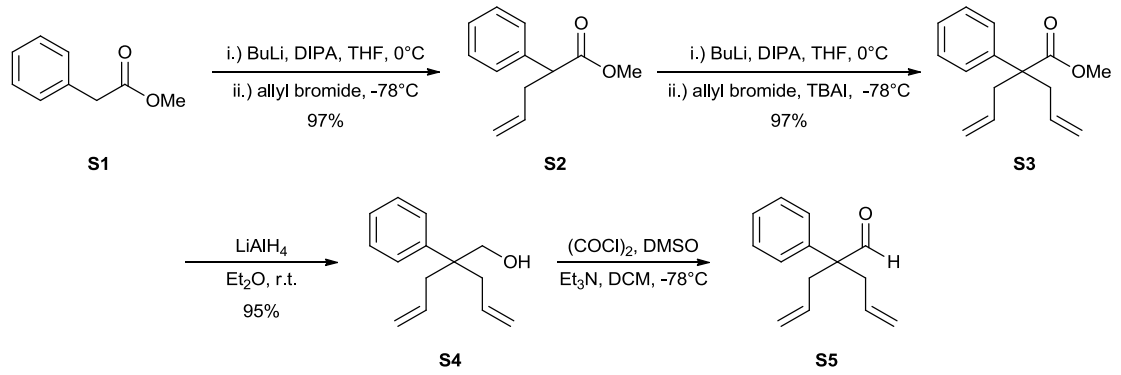


**Scheme 41** Synthesis of aldehyde **S5**

The synthesis of vinyl pyridine **126** via the Wittig olefination was achieved (Scheme 44). However, Wittig olefination with triphenyl(2-pyridylmethyl)phosphonium chloride hydrochloride generally proceeded with *E*-selectivities of roughly 91:9. Attempts to vary the reaction conditions did not drastically improve the selectivity for *E*-**126**. Therefore, a new method was devised which gave a *E*-selectivity of >95:5.

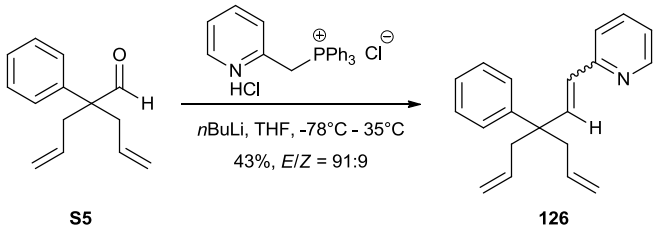


**Scheme 42** Synthesis of vinyl pyridine **126** via the Wittig method

The synthesis of vinyl pyridine **126** with an *E*-selectivity of >95:5 was achieved by E2 elimination with a strong base (Scheme 44). Aldehyde **S5** was added to the vinyl pyridine anion at -78°C. After purification by aqueous workup to form secondary alcohol **S7**, mesylation with mesyl chloride in DCM was then carried out. After purification by aqueous workup, the mesylated product was used directly in the next step. To the crude mesylate, E2 elimination was carried out with NaHMDS as base to afford vinyl pyridine **126** in 55% yield over four steps from **S4** with a *E*/*Z* ratio of >95:5.

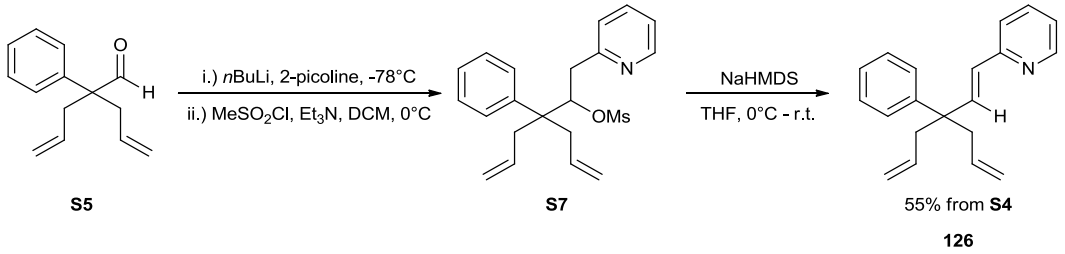


**Scheme 43** Synthesis of vinyl pyridine **126** via mesylation and E2 elimination

The synthesis of vinyl pyridine **132e** started from the commercially available β-ketoester **S8** (Scheme 44). One pot double allylation of β-ketoester **S8** with NaH as base afforded β-ketoester **S9** in 96% yield. The protection of ketone with ethylene glycol and then reduction with $LiAlH_4$ afforded **S10** in 52% over 2 steps. Afterwards, a Swern oxidation[30] was carried out. After a quick purification by filtration over a silica plug, the aldehyde was added to the vinyl

pyridine anion at -78°C to form the secondary alcohol. Finally, mesylation and E2 elimination with NaHMDS afforded vinyl pyridine **132e** in 52% yield over the four steps from **S10**.

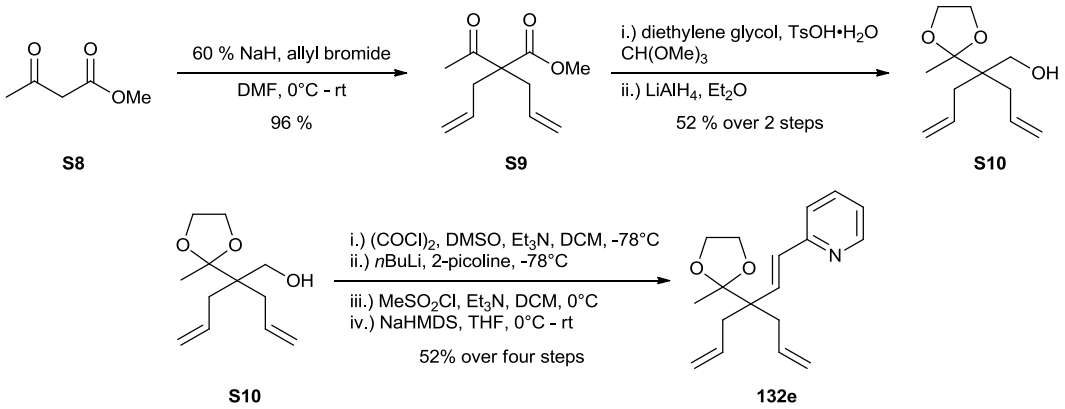


**Scheme 44** Synthesis of vinyl pyridine **132e**

The synthesis of vinyl pyridine **132h** started from the commercially available malonate **S11** (Scheme 45). Benzylation of malonate **S11** with NaH as base afforded malonate **S12**. Krapcho decarboxylation[31] using lithium chloride in DMSO under reflux gave monoester **S13**. Now, allyllation of malonate **S13** with LDA as base afforded malonate **S14** in quantitative yield. Afterwards, reduction with $LiAlH_4$ followed by the oxidation of the alcohol by the Swern oxidation[30] afforded the aldehyde. After a quick filtration over a silica plug, the crude material was of sufficient purity as judged by $^1$HMR to be used directly in the next step. Then, the aldehyde was added to the vinyl pyridine anion at -78°C to form the secondary alcohol. Finally, mesylation and E2 elimination with NaHMDS afforded vinyl pyridine **132h** in 64% yield over 4 steps.

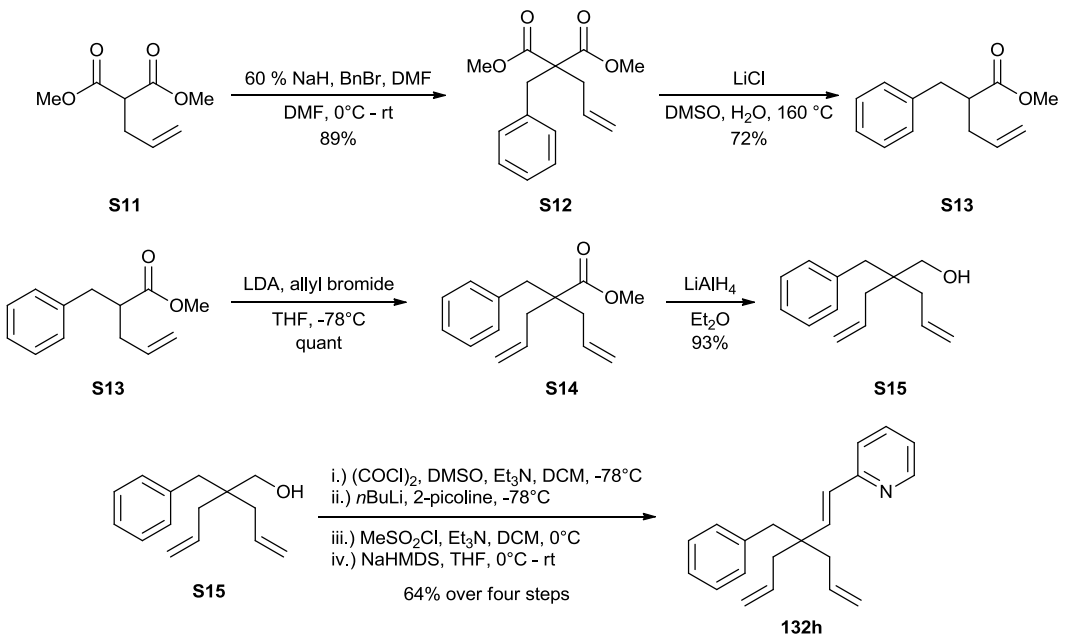


**Scheme 45** Synthesis of vinyl pyridine **132h**

The synthesis of diol **S17** started from the *bis*-allylation of the commercially available malonate **S17.** The synthesis of **129** and **132i** began with the mono-protection of diol **S17** using either *tert*-butyldimethylsilyl chloride or benzylbromide or as the electrophile which proceeded in a 84% and 69% yield respectively (Scheme 46). The resulting mono-protected alcohols were then subjected to Swern oxidation[30] to afford aldehydes. After a quick filtration over a silica plug, the crude material was of sufficient purity as judged by $^{1}$HMR to be used directly in the next step. Then, vinyl pyridine was deprotonated by *n*BuLi at -78°C and the crude aldehyde was added. After an aqueous workup, the secondary alcohol was mesylated with mesyl chloride. After another aqueous workup, a E2 elimination was carried out with NaHMDS as base to give vinyl pyridine **129** and **132i** in a 55% and 57% overall yield respectively from the corresponding mono-protected alcohols.

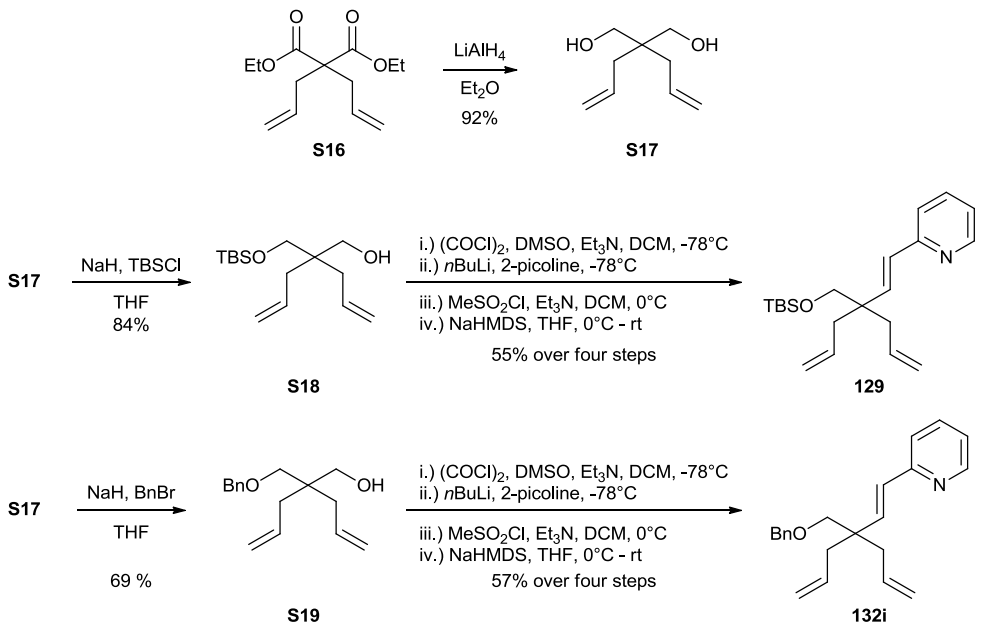


**Scheme 46** Synthesis of **129** and **132i**

The synthesis of **S22** began with the one-pot *bis*-allylation of malonate **S20** to form bis-allylated malonate **S21** (Scheme 47). Afterwards, Krapcho decarboxylation[31] using lithium chloride in DMSO at 160°C gave monoester **S22**.

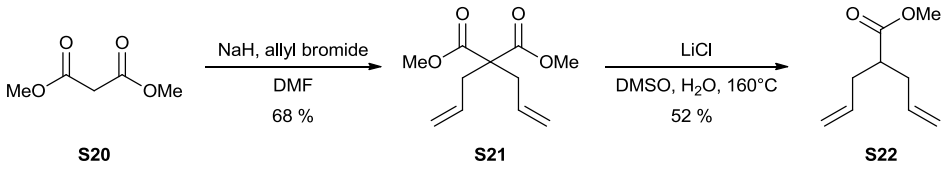


**Scheme 47** Synthesis of **S22**

From the mono-ester **S22**, the synthesis of vinyl pyridine **132j** was achieved (Scheme 48). Due to the volatility of the subsequent intermediates, no attempts on their isolation were made. Therefore, the crude material after the aqueous workup was used directly in the next step until the formation of the secondary alcohol **S23**. The synthesis of secondary **S23** began with the methylation of **S22**. Afterwards, $LiAlH_4$ reduction followed by the Swern oxidation[30] afforded the aldehyde. After a quick filtration over a silica plug, the crude material was of

sufficient purity as judged by $^1$HMR to be used directly in the next step. Then, the aldehyde was added to the vinyl pyridine anion at -78°C to form the secondary alcohol **S23**. **S23** was isolated in a 42% yield over four steps and fully characterised. Finally, mesylation and E2 elimination with NaHMDS as base afforded vinyl pyridine **132j** in 68% yield over two steps.

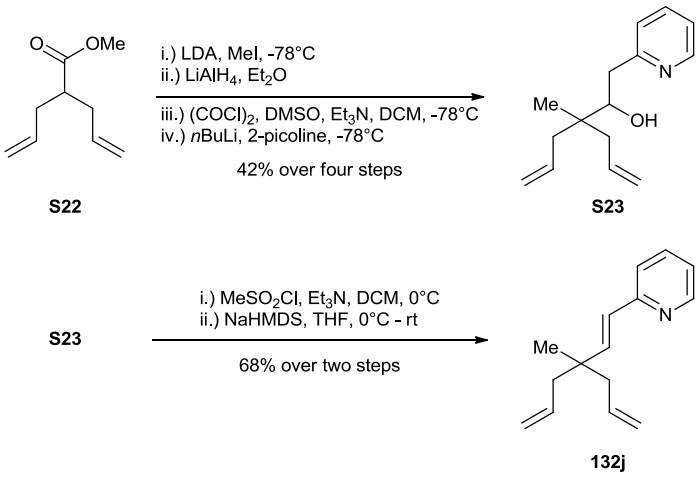


**Scheme 48** Synthesis of vinyl pyridine **132j**

The synthesis of vinyl-imidazole **135** with a *E*-selectivity of >95:1 was achieved by E2 elimination with a strong base (Scheme 49). Swern oxidation[30] of **S4** afforded the aldehyde. After a quick filtration over a silica plug, the crude material was of sufficient purity as judged by $^1$HMR to be used directly in the next step. Aldehyde was added to the vinyl-imidazole anion at -78°C. After purification by aqueous workup to form secondary alcohol **S24** which was isolated in a 86% yield over two steps. Afterwards, mesylation with mesyl chloride in DCM was then carried out. After purification by aqueous workup, the mesylated product was used directly in the next step. To the crude mesylate, E2 elimination was carried out with NaHMDS as base to afford vinyl-imidazole **135** in 58% yield over the two steps.

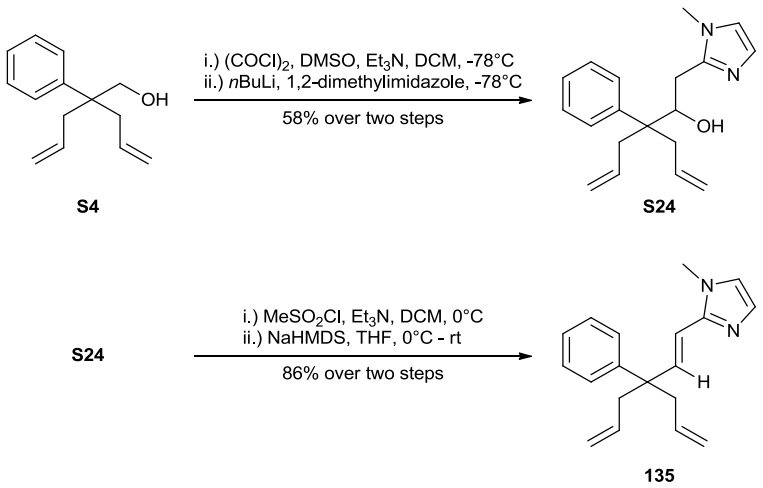


**Scheme 49** Synthesis of the vinyl imidazole **135**

Deuterium labelled vinyl pyridine **139** was synthesised from ester **S3** (Scheme 50). Reduction of the ester with $LiAlD_4$ afforded alcohol **S25** in 94% yield. Afterwards, the Swern oxidation[30] was carried out and was purified by filtration over a small plug of silica. Then the aldehyde was added to the vinyl pyridine anion at -78°C to form the secondary alcohol. Finally, mesylation and E2 elimination with NaHMDS as base afforded vinyl pyridine **139** in 71% yield over four steps.

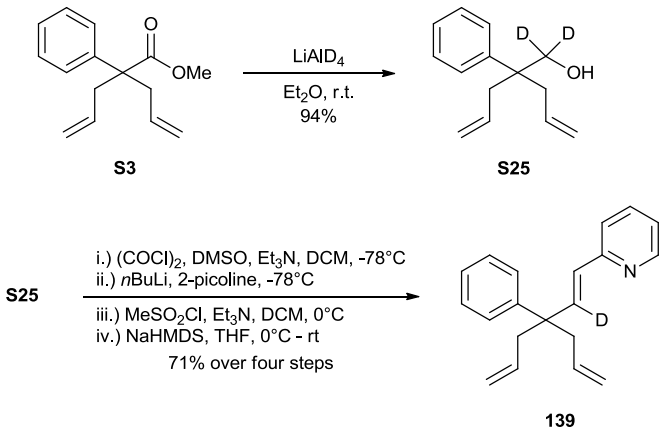


**Scheme 50** Deuterium labelled vinyl pyridine **139** synthesis

## 4.9 Experimental

**General**. Otherwise noted, all reactions were carried out in flame-dried glassware under dry nitrogen atmosphere. The solvents were purified with the solvent purification system Pure Solv MD-6 (THF, $Et_2O$, $CH_2Cl_2$, benzene, toluene, hexane) except otherwise noted. Flash chromatography: Merck silica gel 60 (230-400 mesh). NMR: Spectra were recorded on a Bruker DRX 500 and a Bruker DPX 400 spectrometers in CDCl3; chemical shifts ($\delta$) are given in ppm. The solvent signals were used as references and the chemical shifts converted to the TMS scale ($CDCl_3$: $\delta_C$ = 77.0 ppm; residual $CHCl_3$ in $CDCl_3$: $\delta_H$ = 7.24 ppm). IR: PerkinElmer Spectrum 100 FT-IR spectrometer, wavenumbers ($\tilde{\nu}$) in $cm^{-1}$. HRMS at the University of Liverpool: micromass LCT mass spectrometer (ES+) and Trio-1000 or Agilent QTOF 7200 mass spectrometers (CI). Melting points: Griffin melting point apparatus (not corrected). Elemental analyses: University of Liverpool. X-Ray crystallography: Bruker D8 Venture Photon 100 Dual Microsource diffractometer. All commercially available compounds were used as received.

**Compound S3**

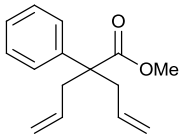


At 0°C, 2.5M of Buli in hexane (11.1 ml, 27.9 mmol) was added to a stirred solution of DIPA (4.3 ml, 30.3 mmol) in THF (36 ml). It was allowed to stir at 0°C for 10 mins. Cooled to -78°C, methyl phenylacetate **S1** (3.5 ml, 24.2 mmol) in THF (70 ml) was added. It was then allowed to stir at -78°C for 40 mins. Afterwards, allyl bromide (2.7 ml, 21.5 mmol) was added. It was then allowed to stir at rt overnight. Afterwards, the reaction was quenched with a saturated solution of $NH_4Cl$. $Et_2O$ was added and extracted two times with $Et_2O$. The organic layer was washed with water and a saturated solution of brine. Dried over $Na_2SO_4$, filtered and

concentrated. Purification by flash column chromatography (PE/DE, 50/1→30/1) gave **S2** as a colourless oil (4.45g, 97%). At 0°C, 2.5M of Buli in hexane (10.8 ml, 26.9 mmol) was added to a stirred solution of DIPA (4.2 ml, 26.2 mmol) in THF (36 ml). It was allowed to stir at 0°C for 10 mins. Cooled to -78°C, **S2** (4.45g, 23.4 mmol) in THF (73 ml) was added. It was then allowed to stir at -78°C for 40 mins. Afterwards, allyl bromide (2.7 ml, 30.4 mmol) and TBAI (864 mg, 2.34 mmol) were added. It was then allowed to stir at rt overnight. Afterwards, the reaction was quenched with a saturated solution of $NH_4Cl$. $Et_2O$ was added and extracted three times with $Et_2O$. The organic layer was washed with water and a saturated solution of brine. Dried over $Na_2SO_4$, filtered and concentrated. Purification by flash column chromatography (PE/DE, 40/1→30/1) gave **S3** as a colourless oil (5.24 g, 97%). This is a known compound. $^1$H NMR (500 MHz, $CDCl_3$): δ = 7.35 – 7.28 (m, 2H), 7.26 – 7.18 (m, 3H), 5.56 – 5.44 (m, 2H), 5.09 – 4.99 (m, 4H), 3.63 (s, 3H), 2.83 – 2.69 (m, 4H)

**Compound S9**

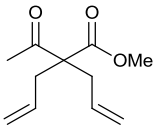


NaH (927 mg, 23.17 mmol, 60% dispersion in mineral oil) and allyl bromide (2 ml, 23.17 mmol) were added to ester **S8** (1 ml, 9.27 mmol) in DMF (19 mL) at 0°C under $N_2$. Then the reaction mixture was warmed to room temperature and stirred for 16 hours. The reaction mixture was re-cooled to 0°C, diluted with $Et_2O$ and quenched carefully with $H_2O$ (initially *via* dropwise addition). The organic layer was separated and washed repeatedly with $H_2O$ to remove excess DMF. The organic phase was dried over $Na_2SO_4$ and the solvent removed under reduced pressure. The crude material was used in the next step without further purification. Pale yellow oil (1.72g, 96%); $^1$H NMR (500 MHz, $CDCl_3$): δ = 5.62 – 5.51 (m, 2H), 5.11 – 5.05 (m, 4H), 3.70 (s, 3H), 2.62 (ddt, *J* = 14.6, 7.4, 1.1 Hz, 2H), 2.56 (ddt, *J* = 14.4, 7.5, 1.1 Hz, 2H), 2.10 (s, 3H); $^{13}$C NMR (125 MHz, $CDCl_3$): δ = 203.9, 172.0, 132.1 (2C), 119.2 (2C), 63.4, 52.3, 36.0 (2C),

27.0; IR (neat): $\tilde{\nu}$ = 3080 (w), 2981 (w), 2953 (w), 1744 (m), 1711 (s), 1641 (w), 1435 (m), 1357 (w), 1321 (w), 1279 (m), 1250 (w), 1211 (s), 1179 (m), 1141 (m), 1052 (w), 993 (m), 919 (s), 871 (w), 844 (w), 794 (w), 750 (w), 697 (w) $cm^{-1}$; MS (CI($CH_4$)): 197 (24) [M + H], 165 (28), 137 (97), 123 (100), 95 (21); HRMS (CI($CH_4$)) calcd for ($C_{11}H_{16}O_3$ + H): 197.1172; found: 197.1170

**Compound S12**

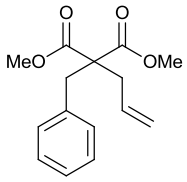


Obtained from dimethyl allylmalonate (1 ml, 6.22 mmol) following the representative procedure except with benzyl bromide (1.1 ml, 9.33 mmol). Colourless oil (1.45 g, 89%). This compound is known. $^1$H NMR (500 MHz, $CDCl_3$): δ = 7.27 – 7.18 (m, 3H), 7.07 (d, *J* = 7.1 Hz), 5.79 – 5.68 (m, 1H), 5.17 – 5.09 (m, 2H), 3.69 (s, 6H), 3.22 (s, 2H), 2.54 (d, *J* = 7.3 Hz, 2H).

**Compound S13**

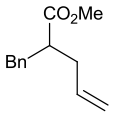


Lithium chloride (231 mg, 5.45 mmol) was added to a solution of **S12** (650 mg, 2.48 mmol) in DMSO (17 mL). Water (15 drops) was added and then the mixture was stirred at 160°C (oil bath temperature) overnight. At room temperature, the mixture was then partitioned between $H_2O$ (10 mL) and $Et_2O$. The organic layer was washed with $H_2O$ (2 x 20 mL), then brine, and dried over $Na_2SO_4$, filtered and concentrated. Purification by flash chromatography (petroleum ether/EtOAc : 20/1) gave **S13** as a colourless oil (348 mg, 72%): $^1$H NMR (500 MHz, $CDCl_3$): δ = 7.28–7.23 (m, 1H), 7.21–7.16 (m, 1H), 7.15–7.12 (m, 2H), 5.73 (ddt, *J* = 17.1, 10.2, 7.0, 1H), 5.08–5.00 (m, 2H), 3.58 (s, 3H), 2.97–2.88 (m, 1H), 2.80–2.69 (m, 2H), 2.40–2.31 (m, 1H), 2.29–2.21 (m, 1H); $^{13}$C NMR (125 MHz, $CDCl_3$): δ = 175.3, 139.1, 135.1, 128.9, 128.4,

126.4, 117.1, 51.4, 47.2, 37.7, 36.0 ; IR (neat): $\tilde{\nu}$ = 3065 (w), 3028 (w), 2950 (w), 1733 (s), 1642 (w), 1604 (w), 1584 (w), 1495 (w), 1455 (w), 1435 (m), 1370 (w), 1262 (w), 1230 (m), 1195 (m), 1161 (s), 1116 (w), 1077 (w), 1031 (w), 994 (w), 915 (m), 832 (w), 762 (w), 743 (m), 698 (s), 656 (w) $cm^{-1}$; MS (CI($CH_4$)): 205 (11) [M + H], 173 (11), 145 (100), 91 (25); HRMS (CI($CH_4$)): calcd for ($C_{13}H_{16}O_2$ + H): 205.1229; found: 205.1224.

**Compound S14**

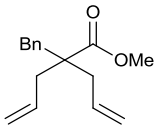


Under $N_2$, a solution of **S13** (150 mg, 0.73 mmol) in THF (0.6 mL) was added to a solution of LDA (0.95 mmol) at -78°C {LDA prepared from 0.38 mL of a 2.5 M of *n*BuLi and 0.14 mL of diisopropylamine in THF (1.4 mL) at 0°C}. The resulting solution was stirred at -78°C for 1.5 hour then allyl bromide (89 µL, 1.03 mmol) was slowly added. The mixture was allowed to warm to room temperature overnight before being quenched with few drops of a saturated solution of $NH_4Cl$. The mixture was diluted with $H_2O$ and extracted three times with diethyl ether. The organic layer was then washed with $H_2O$ and brine and dried over $Na_2SO_4$, then filtered and concentrated. Purification by flash chromatography (petroleum ether/EtOAc: 25/1) afforded **S14** as a colourless oil (179 mg, quant.): $^1$H NMR (500 MHz, $CDCl_3$): δ = 7.26–7.16 (m, 3H), 7.11–7.06 (m, 2H), 5.78 (ddt, *J* = 16.6, 10.6, 7.3 Hz, 2H), 5.14–5.07 (m, 4H), 3.63 (s, 3H), 2.88 (s, 2H), 2.38 (dd, *J* = 14.3, 7.2 Hz, 2H), 2.27 (dd, *J* = 14.3, 7.4 Hz, 2H); $^{13}$C NMR (125 MHz, $CDCl_3$): δ = 175.8, 137.3, 133.6 (2C), 130.0 (2C), 128.1 (2C), 126.5, 118.6 (2C), 51.5, 50.9, 41.4, 38.2 (2C); IR (neat): $\tilde{\nu}$ = 3077(w), 3030 (w), 2980 (w), 2949 (w), 1727 (s), 1639 (w), 1605 (w), 1496 (w), 1435 (m), 1347 (w), 1274 (w), 1200 (m), 1179 (m), 1155 (m), 1079 (w), 1032 (w), 994 (w), 994 (m), 972 (w), 914 (s), 851 (w), 814 (w), 777 (w), 740 (m), 700 (s) $cm^{-1}$; elemental analysis (%) calcd for $C_{16}H_{20}O_2$: C 78.65, H 8.25; found: C 79.17, H 8.36.

**Compound S21**

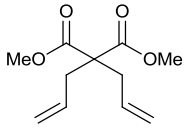


Obtained from dimethyl malonate (2.5 ml, 21.9 mmol) following the representative procedure. Colourless oil (3.2 g, 68%). This compound is known. $^{1}$H NMR (500 MHz, $CDCl_3$): δ = 5.68 – 5.56 (m, 2H), 5.13 – 5.04 (m, 4H), 3.70 (s, 6H), 2.62 (d, *J* = 7.4 Hz, 4H).

**Compound S22**

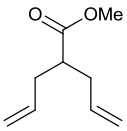


Obtained from **S21** (1.92 mmol, 0.40 mL) following the procedure described for the preparation of **S13**. Colourless oil (155 mg, 52 %): $^{1}$H NMR (500 MHz, $CDCl_3$): δ = 5.71 (ddt, *J* = 17.1, 10.1, 7.0 Hz, 2H), 5.04 (dt, *J* = 17.1, 1.6 Hz, 2H), 5.03–4.98 (m, 2H), 3.64 (s, 3H), 2.51 (tt, *J* = 8.1, 6.1 Hz, 1H), 2.39–2.30 (m, 2H), 2.28–2.19 (m, 2H); $^{13}$C NMR (125 MHz, $CDCl_3$): δ = 135.2 (2C), 117.0 (2C), 51.4, 44.9, 35.8 (2C); IR (neat): $\tilde{\nu}$ = 3080 (w), 2981 (w), 2951 (w), 2846 (w), 1736 (s), 1642 (w), 1437 (m), 1369 (w), 1266 (w), 1236 (m), 1193 (m), 1168 (s), 1139 (m), 994 (m), 914 (s), 862 (w), 833 (w), 763 (w), 702 (w) $cm^{-1}$; elemental analysis (%) calcd for $C_9H_{14}O_2$: C 70.10, H 9.15; found: C 70.18, H 9.28

**Representative procedure for the reduction of esters into alcohols** – A solution of ester **S3** (7.38 mmol, 1.7g) in $Et_2O$ (12 mL) was added under $N_2$ to a suspension of $LiAlH_4$ (4.05 mmol, 150 mg) in $Et_2O$ (24 mL) at 0°C. After stirring at room temperature for 30 minutes, another portion of $LiAlH_4$ (4.05 mmol, 150 mg) was added. After stirring for 30 minutes, the reaction mixture was quenched carefully at 0°C with a saturated aqueous solution of $Na_2SO_4$. After filtration over Celite to remove the white precipitate, the solvent was evaporated under

reduced pressure and the crude material was purified by flash chromatography (petroleum ether/EtOAc = 10:1) to afford **S4** as colourless oil (1.42 g, 95%).

**Compound S4**

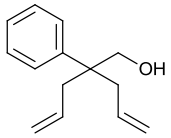


$^{1}$H NMR (500 MHz, $CDCl_3$): δ = 7.36–7.31 (m, 4H), 7.24–7.19 (m, 1H), 5.62 (ddt, *J* = 17.1, 10.1, 7.2 Hz, 2H), 5.11–4.99 (m, 4H), 3.78 (d, *J* = 6.6 Hz, 2H), 2.53 (dd, *J* = 13.9, 7.2 Hz, 2H), 2.45 (dd, *J* = 14.1, 7.2 Hz, 2H), 1.26 (t, *J* = 6.6 Hz, 1H(OH)); $^{13}$C NMR (125 MHz, $CDCl_3$): δ = 143.4, 134.3 (2C), 128.4 (2C), 126.8 (2C), 126.2, 117.8 (2C), 67.8, 45.8, 39.5 (2C); IR (neat): $\tilde{\nu}$ = 3410 (br), 3074 (w), 3006 (w), 2978 (w), 2925 (w), 1638 (w), 1600 (w), 1581 (w), 1498 (m), 1445 (m), 1415 (w), 1385 (w), 1326 (w), 1294 (w), 1218 (w), 1143 (w), 1046 (m), 997 (m), 911 (s), 859 (w), 768 (m), 744 (w), 698 (s), 672 (m) cm$^{-1}$; elemental analysis (%) calcd for $C_{14}H_{18}O$: C 83.12, H 8.97; found: C 83.25, H 9.04.

**Compound S10**

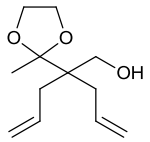


Under $N_2$, TsOH•$H_2O$ (49 mg, 0.25 mmol) was added to a solution of **S9** (508 mg, 2.59 mmol), diethylene glycol (0.567 mmol, 10.19 mmol) and trimethyl orthoformate (0.56 mL, 5.10 mmol) at room temperature. After stirring overnight, the mixture was quenched with a saturated solution of $NaHCO_3$ and extracted with $Et_2O$ (3 x 5 mL). The organic layer was washed with $H_2O$ and then a saturated solution of brine. It was then dried over $Na_2SO4$, filtered and concentrated to give 622 mg of an oil which was dissolved in $Et_2O$ (3 mL) under $N_2$ and added by cannula to a suspension of $LiAlH_4$ (53.0 mg, 1.40 mmol) in $Et_2O$ (10 mL) at 0 °C. After 10

mins at 0 °C, another portion of $LiAlH_4$ (53.0 mg, 1.40 mmol) was added. After 2 hours of stirring at room temperature, the reaction mixture was quenched carefully at 0°C with a saturated aqueous solution of $Na_2SO_4$ which will cause a white precipitate to form. After filtration over Celite to remove the white precipitate, the solvent was evaporated under reduced pressure and the crude material was purified by flash chromatography (petroleum ether/EtOAc: 4/1) to afford **S9** as a colourless oil (284 mg, 52 % over 2 steps). $^1$H NMR (500 MHz, $CDCl_3$): δ = 5.92 (ddt, *J* = 17.1, 10.0, 7.3 Hz, 2H), 5.05 (d, *J* = 17.4 Hz, 2H), 5.04 (d, *J* = 10.0 Hz, 2H), 3.99–3.89 (m, 4H), 3.51 (d, *J* = 5.9 Hz, 2H), 3.08 (t, *J* = 5.9 Hz, 1H(OH)), 2.22 (dd, *J* = 14.4, 7.0 Hz, 2H), 2.15 (dd, *J* = 14.3, 7.6 Hz, 2H), 1.31 (s, 3H); $^{13}$C NMR (125 MHz, $CDCl_3$): δ = 135.0 (2C), 117.3 (2C), 114.7, 66.0, 64.4 (2C), 47.9, 34.9 (2C), 20.0; IR (neat): $\tilde{\nu}$ = 3526 (br), 3074 (w), 2980 (w), 2941 (w), 2888 (m), 1638 (w), 1471 (w), 1436 (w), 1413 (w), 1377 (w), 1334 (w), 1204 (m), 1095 (m), 1038 (s), 998 (m), 950 (m), 912 (s), 874 (m), 765 (w), 693 (w) $cm^{-1}$; HRMS (CI($NH_3$)): calcd for ($C_{12}H_{20}O_3$ + H): 213.1485; found: 213.1490

**Compound S15**

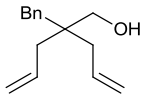


Obtained from **S14** (1.23 mmol, 300 mg) following the representative procedure. Colourless oil (246 mg, 93%): $^1$H NMR (500 MHz, $CDCl_3$): δ = 7.29–7.23 (m, 2H), 7.23–7.17 (m, 3H), 5.98–5.87 (m, 2H), 5.15–5.06 (m, 4H), 3.36 (d, *J* = 6.0 Hz, 2H), 2.63 (s, 2H), 2.04 (d, *J* = 7.4 Hz, 4H), 1.33, (t, *J* = 6.1 Hz, 1H(OH)); $^{13}$C NMR (125 MHz, $CDCl_3$): δ = 138.1, 134.6, 130.6, 128.0, 126.1, 118.0, 66.8, 42.1, 40.4, 38.6; IR (neat): $\tilde{\nu}$ = 3413 (br), 3075 (w), 3029 (w), 2005 (w), 2977 (w), 2923 (m), 1638 (m), 1604 (w), 1496 (w), 1441 (m), 1415 (w), 1328 (w), 1230 (w), 1156 (w), 1048 (m), 1031 (m), 1016 (m), 995 (m), 911 (s), 861 (w), 812 (w), 783 (w), 740 (m), 702 (s), 665 (w) $cm^{-1}$; elemental analysis (%) calcd for $C_{15}H_{20}O$: C 83.28, H 9.32; found: C 83.37, H 9.35.

**Compound S17**

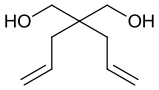


Obtained from diethyl diallylmalonate (2 mL, 8.27 mmol) following the procedure for the synthesis of **S10**. Clear Oil (1.19g, 92%): $^{1}$H NMR (500 MHz, $CDCl_3$): δ = 5.83 (ddt, *J* = 16.8, 10.3, 7.5 Hz, 2H), 5.13 – 5.06 (m, 4H), 3.58 (d, *J* = 4.8 Hz, 4H), 2.08 (dt, *J* = 7.5, 1.1 Hz, 4H), 2.05 – 1.98 (m, 2H); $^{13}$C NMR (125 MHz, $CDCl_3$): δ = 133.8, 118.1, 68.1, 42.0, 36.0; IR (neat): $\tilde{\nu}$ = 3343 (br m), 3076 (w), 3006 (w), 2979 (w), 2924 (w), 1836 (w), 1639 (w), 1465 (w), 1440 (m), 1416 (w), 1333 (w), 1223 (w), 1146 (w), 1057 (m), 1021 (s), 996 (s), 910 (s), 862 (w), 807 (w), 684 (w) $cm^{-1}$; elemental analysis (%) calcd for $C_9H_{16}O_2$: C 69.19, H 10.32; found: C 69.02, H 10.33

**Compound S18**

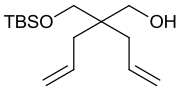


At 0°C, 60 % of NaH (187 mg, 1.24 mmol) was added to a solution of **S17** (194 mg, 1.24 mmol) in THF (12 mL). The ice bath was removed and allowed to stir at rt for 2 hours. The suspension was cooled back down to 0°C and TBSCl (187 mg, 1.24 mmol) was added. The resulting mixture was stirred at rt overnight. The mixture was quenched with a saturated solution of $NH_4Cl$ and extracted three times with diethyl ether. The organic layer was washed with a saturated aqueous solution of brine, dried over $Na_2SO_4$, filtered and concentrated. Purification by flash chromatography (petroleum ether/EtOAc : 9/1) gave **S18** as a clear oil (284 mg, 84%): $^{1}$H NMR (500 MHz, $CDCl_3$): δ = 5.84 – 5.74 (m, 2H), 5.10 – 5.03 (m, 4H), 3.53 – 3.47 (m, 4H), 2.65 (t, *J* = 2.65 Hz, OH), 2.07 (dd, *J* = 13.9, 7.4 Hz, 2H), 2.02 (dd, *J* = 13.9, 7.7 Hz, 2H), 0.88 (s, 9H), 0.05 (s, 6H); $^{13}$C NMR (125 MHz, $CDCl_3$): δ = 134.0, 117.9, 68.9, 68.6, 41.9, 36.0, 25.8, 18.1, -5.7

**Compound S19**

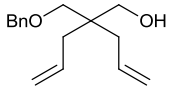


At 0°C, 60 % of NaH (58 mg, 1.44 mmol) was added to a solution of **S17** in THF (6 mL). The ice bath was removed and allowed to stir at rt for 1 hour. The suspension was cooled back down to 0°C and benzyl bromide (172 µL, 1.44 mmol) was added. The resulting mixture was stirred at rt overnight. The mixture was quenched with a saturated solution of $NH_4Cl$ and extracted three times with diethyl ether. The organic layer was washed with a saturated aqueous solution of brine, dried over $Na_2SO_4$, filtered and concentrated. Purification by flash chromatography (petroleum ether/EtOAc : 9/1) gave **S19** as a light yellow oil (244 mg, 69%): $^1$H NMR (500 MHz, $CDCl_3$): δ = 7.38 – 7.25 (m, 5H), 5.85 – 5.72 (m, 2H), 5.12 – 5.00 (m, 4H), 4.48 (s, 2H), 3.52 (d, *J* = 5.4 Hz, 2H), 3.37 (s, 2H), 2.56 (br s, 1H), 2.15 – 2.03 (m, 4H); $^{13}$C NMR (125 MHz, $CDCl_3$): δ = 137.9, 133.9, 128.4, 127.7, 127.5, 118.0, 75.9, 73.6, 68.4, 41.7, 36.2; IR (neat): $\tilde{\nu}$ = 3437 (br w), 3074 (w), 3031 (w), 3005 (w). 2977 (w), 2861 (m), 1639 (m), 1497 (w), 1454 (m), 1441 (m), 1415 (w), 1363 (w), 1330 (w), 1251 (w), 1206 (w), 1096 (s), 1075 (m), 1029 (m), 999 (m), 910 (s), 876 (w), 736 (m), 697 (s) cm$^{-1}$; elemental analysis (%) calcd for $C_{16}H_{22}O_2$: C 78.01, H 9.00; found: C 78.16, H 8.99

**Compound S25**

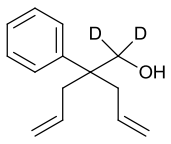


Obtained from **S3** (1.23 mmol, 283 mg) following the representative procedure but using $LiAlD_4$. Colourless oil (237 mg, 94%); $^1$H NMR (500 MHz, $CDCl_3$): δ = 7.38 – 7.29 (m, 4H), 7.24 – 7.18 (m, 1H), 5.62 (ddt, *J* = 17.2, 10.0, 7.3 Hz, 2H), 5.11–5.04 (m, 2H), 5.04–4.99 (m, 2H), 2.53 (dd, *J* = 14.1, 7.2 Hz, 2H), 2.45 (dd, *J* = 13.9, 7.4 Hz, 2H), 1.25 (s, 1H(OH)); $^{13}$C NMR (125 MHz, $CDCl_3$): δ = 143.3, 134.3 (2C), 128.4 (2C), 126.8 (2C), 126.2, 117.8 (2C), 67.0 (pent, *J* = 21.8 Hz),

45.6, 39.5 (2C); IR (neat): $\tilde{\nu}$ = 3399 (br), 3074 (w), 3006 (w), 2978 (w), 2923 (w), 2207 (w), 2101 (w), 1638 (w), 1600 (w), 1580 (w), 1497 (w), 1445 (m), 1415 (w), 1292 (w), 1193 (w), 1158 (w), 1102 (m), 1030 (w), 998 (m), 975 (m), 910 (s), 838 (w), 807 (w), 759 (m), 733 (w), 697 (s), 665 (w) $cm^{-1}$; MS (CI($NH_3$)): *m/z* (rel. intensity): 222 (100) [M + $NH_4$]; HRMS (CI($NH_3$)) calcd for ($C_{14}H_{16}D_2O$ + $NH_4$): 222.1821; found: 222.1824.

**Representative procedure for the Swern oxidation** – Under $N_2$, DMSO (87 µL, 1.20 mmol) in $CH_2Cl_2$ (0.8 mL) was added to a solution of oxalyl chloride (53 µL, 0.61 mmol) in $CH_2Cl_2$ (3.9 mL) at –78°C. After 10 minutes stirring at –78°C, a solution of the **S4** (95 mg, 0.47 mmol) in $CH_2Cl_2$ (0.8 mL) was added. After 20 minutes stirring at –78°C, triethylamine (0.32 mL, 2.34 mmol) was added rapidly and the mixture was stirred at room temperature during 20 minutes. A saturated solution of $NH_4Cl$ was added to the reaction mixture which was then extracted three times with diethyl ether. The organic layer was washed with $H_2O$ and a saturated solution of brine, dried over $Na_2SO_4$, filtered, and concentrated to give 93 mg of aldehyde which was used without further purification in the next step. Under $N_2$, *n*BuLi (0.32 mL, 0.55 mmol, 1.7 M in hexanes) was added to a –78°C solution of 2-Methylpyridine (59 µL, 0.60 mmol) in THF (2.5 mL). After 10 minutes of stirring at –78°C, a solution of the aldehyde (93 mg, 0.46 mmol) in THF (0.8 mL) was added by cannula. After stirring for 10 minutes at –78°C, the reaction was quenched with enough MeOH to turn the deep red solution to yellow and was then allowed to warm to room temperature. The crude mixture was then partitioned between a saturated aqueous solution of $NaHCO_3$, water and $Et_2O$. After three extractions with $Et_2O$ (5 mL), the combined organic layers were dried over $Na_2SO_4$, filtered and concentrated. Purification by flash column chromatography (petroleum ether/EtOAc: 7/1 → 6/1) afforded 133 mg of a clear oil which was dissolved in $CH_2Cl_2$ (0.4 mL) under $N_2$ and cooled to –40°C. $Et_3N$ (193 µL, 1.36 mmol) and methanesulfonyl chloride (53 µL, 0.68 mmol) were added dropwise. After stirring overnight at room temperature, the precipitate thus formed was then filtered off over Celite,

washed with EtOAc, and the filtrate was concentrated under reduce pressure. Under $N_2$, the residue was dissolved in THF (2.4 mL) under $N_2$. At – 20°C, NaHMDS (0.6 mL, 0.61 mmol, 1M in THF) was added. After stirring at room temperature for 1 hour, the reaction mixture was quenched with a saturated solution of $NaHCO_3$ and partitioned between water and EtOAc. After three extractions with $Et_2O$ (5 mL), the combined organic layers were dried over $Na_2SO_4$, filtered and concentrated. Purification by flash column chromatography (petroleum ether/$Et_2O$: 9/1 → 8/1) afforded **126** as a white solid (56 mg, 55% over four steps)

**Compound *E*-126**

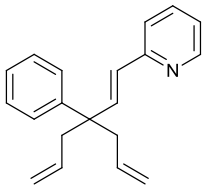


mp.: 27–28°C; $^1$H NMR (500 MHz, $CDCl_3$): δ = 8.53 (d, *J* = 4.6 Hz, 1H), 7.62–7.56 (m, 1H), 7.35–7.26 (m, 5H), 7.22–7.16 (m, 1H), 7.12–7.07 (m, 1H), 6.85 (d, *J* = 16.4 Hz, m1H), 6.53 (d, *J* = 16.2 Hz, 1H), 5.61 (ddt, *J* = 17.2, 10.0, 7.1 Hz, 2H), 5.08–4.97 (m, 4H), 2.68 (d, *J* = 7.1 Hz, 4H); $^{13}$C NMR (125 MHz, $CDCl_3$): δ = 156.0, 149.5, 144.8, 141.8, 136.4, 134.4 (2C), 128.7, 128.1, 127.4, 126.2, 121.8, 121.0, 117.8 (2C), 46.8, 41.9 (2C); IR (neat): $\tilde{\nu}$ = 3059 (w), 3034 (w), 3007 (w), 2922 (w), 2902 (w), 2841 (w), 1953 (w), 1892 (w), 1836 (w), 1650 (m), 1640 (m), 1598 (w), 1585 (m), 1563 (m), 1493 (m), 1469 (m), 1444 (m), 1429 (m), 1322 (w), 1302 (w), 1262 (w). 1243 (w), 1189 (w), 1150 (w), 1127 (w), 1097 (w), 1089 (w), 1049 (w), 1030 (w), 1009 (w), 990 (m), 979 (m), 943 (m), 935 (m), 915 (s), 889 (m), 856 (m), 779 (m), 766 (m), 749 (s), 701 (s), 671 (w), 654 (w) $cm^{-1}$; HRMS (ESI): calcd for ($C_{20}H_{21}N$ + Na): 276.1752; found: 276.1750; elemental analysis (%) calcd for $C_{20}H_{21}N$: C 87.23, H 7.69, N 5.09; found: C 87.71, H 7.69, N 4.87.

**Compound** *E*/*Z*-**126**

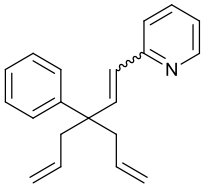

2.5M of *n*Buli in hexane (0.4 ml, 1 mmol) was added to a schlenk containing triphenyl(2-pyridylmethyl)phosphonium chloride hydrochloride (213 mg, 0.50 mmol) in THF (0.1 ml) at -78°C. The mixture was stirred at 35°C for 2 hours. Then, **S5** in THF (0.2 ml) was added at rt. It was then allowed to stir overnight at rt. The reaction was quenched with a saturated solution of $NaHCO_3$. The crude material was partitioned between $H_2O$ and EtOAc. The aqueous layer was then extracted three times with EtOAc. Extracts dried over $Na_2SO_4$ and filtered. Silica was then added, all volatiles were removed and the dry deposit was loaded on to the top of a column. Purification by flash column chromatography (petroleum ether/$Et_2O$: 9/1) afforded **126** as a white solid (29 mg, 43%) with a *E*/*Z* ratio of 91:9 as judged from the $^1$H NMR spectra; Key peaks of *Z*-**126,** $^1$H NMR (500 MHz, $CDCl_3$): δ = 8.36 – 8.33 (m, 1H), 6.63 (d, *J* = 13.0 Hz, 1H), 5.97 (d, *J* = 13.0 Hz, 1H).

**Compound 139**

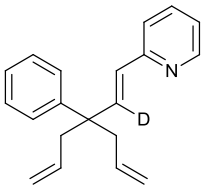

Obtained from **S25** (1.03 mmol, 211 mg) following the representative procedure. Colourless oil (202 mg, 71% over four steps); $^1$H NMR (500 MHz, $CDCl_3$): δ = 8.53 (ddd, *J* = 4.8, 1.7, 0.8 Hz, 1H), 7.59 (dt, *J* = 7.7, 1.8 Hz, 1H), 7.35–7.26 (m, 5H), 7.21–7.16 (m, 1H), 7.09 (ddd, *J* = 7.5, 4.8, 1.1 Hz, 1H), 6.52 (s, 1H), 5.61 (ddt, *J* = 17.2, 10.1, 7.1 Hz, 2H), 5.07–4.97 (m, 4H), 2.70 – 2.66 (m, 4H); $^{13}$C NMR (125 MHz, $CDCl_3$): δ = 156.0, 149.5, 144.8, 141.4 (t, *J* = 22.5 Hz), 136.4, 134.4 (2C), 128.6, 128.1 (2C), 127.4 (2C), 126.2, 121.8, 121.0, 117.8 (2C), 46.7, 41.9 (2C); IR (neat): $\tilde{\nu}$ =

3075 (w), 3003 (w), 2978 (w), 2930 (w), 1638 (m), 1586 (s), 1562 (w), 1494 (w), 1469 (m), 1445 (m), 1429 (m), 1149 (w), 1033 (w), 996 (m), 910 (s), 753 (m), 700 (s) $cm^{-1}$; HRMS ($CI(NH_3)$): calcd for ($C_{20}H_{20}DN$ + H): 277.1815; found: 277.1808.

**Compound 132e**

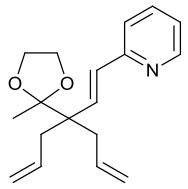

Obtained from **S10** (0.56 mmol, 119 mg) following the representative procedure. Colourless oil (86 mg, 52% over four steps); $^1H$ NMR (500 MHz, $CDCl_3$): δ = 8.53 (ddd, *J* = 4.8, 1.7, 0.8 Hz, 1H), 7.58 (dt, *J* = 7.7, 1.8 Hz, 1H), 7.32 (d, *J* = 7.9 Hz, 1H), 7.07 (ddd, *J* = 7.5, 4.8, 1.1 Hz, 1H), 6.82 (d, *J* = 16.5 Hz, 1H), 6.50 (d, *J* = 16.5 Hz, 1H), 5.94–5.84 (m, 2H), 5.04 (dt, *J* = 17.1, 1.5 Hz, 2H), 5.00 (dt, *J* = 10.2, 1.1 Hz, 2H), 3.97–3.88 (m, 4H), 2.49 (dd, *J* = 14.4, 7.7 Hz, 2H), 2.44 (dd, *J* = 14.4, 6.8 Hz, 2H), 1.28 (s, 3H); $^{13}C$ NMR (125 MHz, $CDCl_3$): δ = 156.1, 149.4, 139.2, 136.3, 135.5 (2C), 130.1, 121.7, 120.9, 116.5 (2C), 113.1, 64.8 (2C), 50.6, 36.6 (2C), 21.1; IR (neat): $\tilde{\nu}$ = 3073 (w), 2979 (m), 2939 (w), 2883 (w), 1638 (w), 1586 (s), 1563 (m), 1469 (m), 1430 (m), 1373 (m), 1304 (w), 1266 (w), 1198 (s), 1149 (m), 1127 (m), 1100 (m), 1083 (m), 1036 (s), 991 (s), 950 (m), 910 (s), 852 (w), 765 (m), 742 (w) $cm^{-1}$; MS ($CI(CH_4)$): *m/z* (rel. intensity): 286 (100) [M + H]; HRMS ($CI(CH_4)$): calcd for ($C_{18}H_{23}NO_2$ + H): 286.1802; found: 286.1804; elemental analysis (%) calcd for $C_{18}H_{23}NO_2$: C 75.76, H 8.12, N 4.91; found: C 76.44, H 8.33, N 4.93.

**Compound 132f**

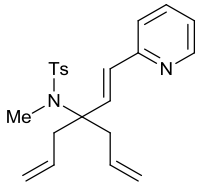


Compound prepared by Daniel J. Tetlow. Yellow oil (320 mg, 60% over four steps); $^{1}$H NMR (500 MHz, $CDCl_3$): δ = 8.50 (d, *J* = 4.6 Hz, 1H), 7.65 (d, *J* = 8.2 Hz, 2H), 7.60 (td, *J* = 7.7, 1.5 Hz, 1H), 7.21–7.15 (m, 3H), 7.11 (dd, *J* = 7.4, 4.9 Hz, 1H), 6.58 (d, *J* = 16.3 Hz, 1H), 6.44 (d, *J* = 16.3 Hz, 1H), 5.72 (ddt, *J* = 17.1, 10.1 and 7.0 Hz, 2H), 5.10 (d, *J* = 16.2 Hz, 2H), 5.09 (d, *J* = 9.7 Hz, 2H), 2.97 (s, 3H), 2.81 (dd, *J* = 14.2, 7.5 Hz, 2H), 2.64 (dd, *J* = 14.2, 6.4 Hz, 2H), 2.37 (s, 3H); $^{13}$C NMR (125 MHz, $CDCl_3$): δ = 154.9, 149.4, 142.7, 139.8, 136.5, 136.4, 133.0 (2C), 130.0, 129.3 (2C), 127.2 (2C), 122.3, 121.6, 118.9 (2C), 66.3, 40.1 (2C), 33.4, 21.4; IR (neat): $\tilde{\nu}$ = 3075 (w), 2977 (w), 2925 (w), 1638 (w), 1584 (m), 1564 (w), 1494 (w), 1469 (m), 1430 (m), 1337 (s), 1304 (m), 1255 (w), 1211 (w), 1153 (s), 1117 (m), 1088 (s), 1049 (w), 1018 (w), 981 (s), 915 (s), 813 (s), 770 (m), 743 (m), 720 (s), 657 (s) $cm^{-1}$; MS (ESI): *m/z* (rel. intensity): 421 (10) [M + K], 405 (72) [M + Na], 383 (100) [M + H]; HRMS (ESI) calcd for ($C_{22}H_{27}N_2O_2S$ + Na): 383.1793; found: 383.1786.

**Compound 132h**

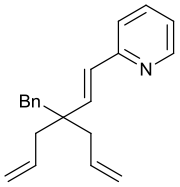


Obtained from **S15** (1.23 mmol, 300 mg) following the representative procedure. Yellow oil (199 mg, 64% over four steps); $^{1}$H NMR (500 MHz, $CDCl_3$): δ = 8.56–8.51 (m, 1H), 7.58 (dt, *J* = 7.7, 1.8 Hz, 1H), 7.23–7.12 (m, 6H), 7.09 (ddd, *J* = 7.4, 4.9, 1.0 Hz, 1H), 6.69 (d, *J* = 16.2 Hz, 1H), 6.28 (d, *J* = 16.2 Hz, 1H), 5.92–5.82 (m, 2H), 5.13– 5.05 (m, 4H), 2.78 (s, 2H), 2.31–2.20 (m, 4H);

$^{13}$C NMR (125 MHz, $CDCl_3$): δ = 155.9, 149.4, 141.6, 137.8, 136.4, 134.5 (2C), 130.8 (2C), 128.6, 127.7 (2C), 126.1, 121.7, 121.0, 117.9 (2C), 44.5, 43.0, 40.6 (2C); IR (neat): $\tilde{\nu}$ = 3074 (w), 3029 9 (w), 3005 (w), 2977 (w), 2922 (w), 2852 (w), 1638 (w)m 1603 (w), 1584 (m), 1563 (w), 1495 (w), 1469 (w), 1454 (w), 1429 (m), 1334 (w), 1304 (w), 1262 (w), 1149 (w), 1088 (w), 1049 (w), 1031 (w), 991 (m), 911 (s), 849 (w), 795 (w), 767 (m), 743 (s), 701 (s), 667 (w) $cm^{-1}$; elemental analysis (%) calcd for $C_{21}H_{23}N$: C 87.15, H 8.01, N 4.84; found: C 86.98, H 8.20, N 4.75.

**Compound 132i**

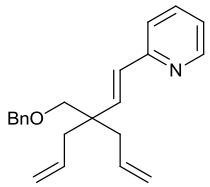


Obtained from **S19** (0.80 mmol, 197 mg) following the representative procedure. Yellow oil (146 mg, 57% over four steps); $^1$H NMR (500 MHz, $CDCl_3$): δ = 8.54–8.50 (m, 1H), 7.58 (dt, *J* = 7.7, 1.8 Hz, 1H), 7.34 – 7.28 (m, 4H), 7.28 – 7.22 (m, 2H), 7.08 (ddd, *J* = 7.4, 4.9, 1.0 Hz, 1H), 6.67 (d, *J* = 16.3 Hz, 1H), 6.42 (d, *J* = 16.3 Hz, 1H), 5.77 (ddt, *J* = 17.1, 10.0, 7.3 Hz, 2H), 5.09–4.99 (m, 4H), 4.50 (s, 2H), 3.41 (s, 2H), 2.38–2.27 (m, 4H); $^{13}$C NMR (125 MHz, $CDCl_3$): δ = 156.0, 149.4, 139.4, 138.7, 136.3, 134.4 (2C), 128.9, 128.3, 127.5 (2C), 127.4 (2C), 121.7, 121.1, 117.7 (2C), 74.1, 73.3, 43.5, 40.0 (2C); IR (neat): $\tilde{\nu}$ = 3074 (w), 3004 (w), 2911 (w), 2857 (m), 1649 (w), 1639 (w), 1585 (s), 1564 (m), 1497 (w), 1470 (m), 1454 (m), 1430 (m), 1363 (w), 1305 (w), 1206 (w), 1095 (s), 1029 (w), 992 (m), 976 (s), 914 (s), 767 (s), 739 (s), 698 (s) $cm^{-1}$; elemental analysis (%) calcd for $C_{22}H_{25}NO$: C 82.72, H 7.89, N 4.38; found: C 83.06, H 7.92, N 4.34.

**Compound 129**

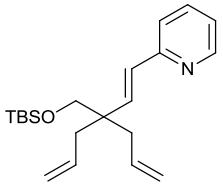


Obtained from **S18** (500mg, 1.85 mmol) following the representative procedure. Colourless oil (347 mg, 55% over four steps); $^{1}$H NMR (500 MHz, $CDCl_3$): δ = 8.51 (d, *J* = 4.2 Hz, 1H), 7.57 (apt dt, *J* = 7.7, 1.8 Hz, 1H), 7.26 – 7.21 (m, 1H), 7.08 – 7.04 (m, 1H), 6.62 (d, *J* = 16.5 Hz, 1H), 6.40 (d, *J* = 16.5 Hz, 1H), 5.78 (ddt, *J* = 15.2, 9.9, 7.3 Hz, 2H), 5.09 – 4.97 (m, 4H), 3.52 (s, 2H), 2.30 (dd, *J* =13.8, 7.5 Hz, 2H), 2.25 (dd, *J* =13.8, 7.2 Hz, 2H), 0.87 (s, 9H), 0.01 (s, 6H) ; $^{13}$C NMR (125 MHz, $CDCl_3$): δ = 156.1, 149.4, 139.3, 136.3, 134.6, 129.0, 121.6, 120.8, 117.5, 66.4, 44.1, 39.5, 25.8, 18.2 , -5.6; IR (neat): $\tilde{\nu}$ = 3075 (w), 3005 (w), 2954 (m), 2928 (m), 2897 (m), 2856 (m), 1639 (w), 1585 (m), 1564 (w), 1470 (m), 1430 (w), 1388 (w), 1361 (w), 1304 (w), 1250 (m), 1147 (w), 1096 (s), 992 (m), 978 (m), 913 (m), 834 (s), 774 (s), 671 (w) $cm^{-1}$; elemental analysis (%) calcd for $C_{21}H_{33}NOSi$: C 73.41, H 9.68, N 4.08; found: C 73.68, H 7.71, N 4.03.

**Compound S23**

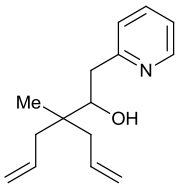


Under $N_2$, a solution of LDA (1.41 mmol) {prepared from 0.67 mL of a 2.5 M of nBuLi and 0.20 mL of diisopropylamine in THF (1.8 mL)} at 0 °C, was added to a solution of **S22** (155 mg, 1.00 mmol) in THF (0.7 mL) at -78°C. The resulting solution was stirred at -78°C for 1.5 hour then methyl iodide (94 µL, 1.51 mmol) was slowly added. The mixture was allowed to warm to room temperature overnight before being quenched with few drops of a saturated aqueous solution of $NH_4Cl$. The mixture was diluted with $H_2O$ and extracted three times with $Et_2O$ (5 mL). The organic layer was then washed with $H_2O$ and a saturated aqueous solution of brine,

dried over $Na_2SO_4$, filtered and concentrated. Purification by flash chromatography (petroleum ether/ $Et_2O$: 29/1) afforded 148 mg of a colourless oil which was dissolved in $Et_2O$ (0.8 mL) and added by cannula to a suspension of $LiAlH_4$ (19 mg, 0.49 mmol) in $Et_2O$ (1.6 mL) at 0°C. After 10 minutes at 0°C another portion of $LiAlH_4$ (19 mg, 0.49 mmol) was added. After stirring for 1 hour at room temperature, the reaction mixture was quenched carefully at 0°C with a saturated aqueous solution of $Na_2SO_4$ which resulted in the formation of a white precipitate. After filtration over Celite to remove the white precipitate, the solvent was evaporated under reduced pressure to give 107 mg of alcohol. Under $N_2$, DMSO (145 µL, 2.04 mmol) in $CH_2Cl_2$ (0.8 mL) was added to a solution of oxalyl chloride (88 µL, 1.02 mmol) in $CH_2Cl_2$ (3.9 mL) at –78°C. After 10 minutes stirring at –78°C, a solution of the alcohol (107 mg, 0.78 mmol) in $CH_2Cl_2$ (0.8 mL) was added. After 20 minutes stirring at –78°C, triethylamine (0.55 mL, 3.92 mmol) was added rapidly and the mixture was stirred at room temperature during 20 minutes. A saturated solution of $NH_4Cl$ was added to the reaction mixture which was then extracted three times with diethyl ether. The organic layer was washed with $H_2O$ and a saturated solution of aqueous brine, dried over $Na_2SO_4$, filtered, and concentrated to give 96 mg of aldehyde. Under $N_2$, *n*BuLi (0.39 mL, 0.81 mmol, 2.1 M in hexanes) was added to a -78°C solution of 2-methylpyridine (80 µL, 0.81 mmol) in THF (2.0 mL). After 10 minutes of stirring at -78°C, a solution of aldehyde (82 mg, 0.60 mmol) in THF (1 mL) was added by cannula. After stirring for 15 minutes at -78°C, the reaction was quenched with enough MeOH to turn the deep red solution to yellow and then allowed to warm to room temperature. The crude mixture was then partitioned between a saturated solution of $NaHCO_3$, water and ethyl acetate and then extracted three times with ethyl acetate (5 mL). The combined organic layers were dried over $Na_2SO_4$, filtered and concentrated. Purification by flash column chromatography (petroleum ether/EtOAc: 5/1) afforded **S23** as a clear oil (98 mg, 42% over four steps): $^1$H NMR (500 MHz, $CDCl_3$): δ = 8.48–8.43 (m, 1H), 7.59 (dt, *J* = 7.6, 1.8 Hz, 1H), 7.15–7.09 (m, 2H), 5.95–5.82 (m, 2H), 5.10–5.00 (m, 4H + 1H(OH)), 3.80 (dd, *J* = 10.5, 1.7 Hz,

1H), 2.90 (dd, *J* = 14.6, 1.7 Hz, 1H), 2.80 (d, *J* = 14.5, 10.4 Hz, 1H), 2.33–2.23 (m, 2H), 2.14 (dd, *J* = 13.9, 7.5 Hz, 1H), 2.03 (dd, *J* = 13.7, 7.8 Hz, 1H), 0.94 (s, 3H); $^{13}$C NMR (125 MHz, $CDCl_3$): δ = 161.0, 148.6, 136.8, 135.4, 135.2, 123.7, 121.4, 117.24, 117.19, 75.7, 40.6, 40.4, 40.2, 37.7, 20.5; IR (neat): $\tilde{\nu}$ = 3351 (br w), 3074 (m), 2975 (m), 2917 (m), 1638 (m), 1597 (s), 1570 (m), 1475 (m), 1438 (s), 1375 (w), 1317 (w), 1145 (w), 1097 (w), 1049 (m), 999 (m), 912 (s), 756 (s) $cm^{-1}$; elemental analysis (%) calcd for $C_{15}H_{21}NO$: C 77.88, H 9.15, N 6.05; found: C 77.79, H 9.17, N 5.88.

**Compound 132j**

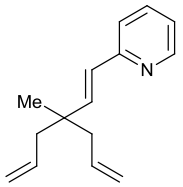


At 0°C, methanesulfonyl chloride (30 µL, 0.39 mmol) was added dropwise to a solution of **S23** (75mg, 0.32 mmol) and $Et_3N$ (68 µL, 0.49 mmol) in $CH_2Cl_2$ (0.64 mL). After stirring at room temperature overnight, the crude mixture was partitioned between a saturated solution of $NaHCO_3$ and ethyl acetate, and extracted three times with ethyl acetate (5 mL). The combined organic layers were washed with water, then a saturated aqueous solution of brine, then dried over $Na_2SO_4$, filtered and concentrated. Under $N_2$, the residue was dissolved in THF (0.32 mL). At 0 °C, NaHMDS (0.5 mL, 0.49 mmol, 1M in THF) was added. After stirring for 2 hours at room temperature, the reaction mixture was quenched with a saturated solution of $NaHCO_3$ and extracted three times with ethyl acetate and the combined extracts were washed with water, followed by a saturated aqueous solution of brine, then dried over $Na_2SO_4$, filtered and concentrated. Purification by flash column chromatography (petroleum ether/Et2O: 6/1 → 4/1) afforded **132j** as a clear oil (47 mg, 68 %): $^1$H NMR (500 MHz, $CDCl_3$): δ = 8.52 (ddd, *J* = 4.9, 1.7, 0.8 Hz, 1H), 7.59 (dt, *J* = 7.7, 1.8 Hz, 1H), 7.27–7.22 (m, 1H), 7.08 (ddd, *J* = 7.5, 4.9, 1.0 Hz,

1H), 6.69 (d, *J* = 16.2 Hz, 1H), 6.37 (d, *J* = 16.1 Hz, 1H), 5.82 – 5.72 (m, 2H), 5.06 – 4.99 (m, 4H), 2.22 (dd, *J* = 13.7, 7.0 Hz, 2H), 2.15 (dd, *J* = 13.7, 7.7 Hz, 2H), 1.08 (s, 3H); $^{13}$C NMR (125 MHz, $CDCl_3$): δ = 156.1, 149.4, 143.0, 136.4, 134.8 (2C), 127.6, 121.6, 121.1, 117.4 (2C), 45.0 (2C), 39.3, 23.3; IR (neat): $\tilde{\nu}$ = 3075 (m), 3004 (w), 2976 (m), 2915 (m), 1640 (m), 1585 (s), 1564 (m), 1471 (m), 1430 (s), 1377 (w), 1321 (w), 1149 (w), 992 (m), 913 (s), 766 (m), 742 (w) $cm^{-1}$; elemental analysis (%) calcd for $C_{15}H_{19}N$: C 84.46, H 8.98, N 6.57; found: C 84.17, H 9.11, N 6.13.

**Compound 135**

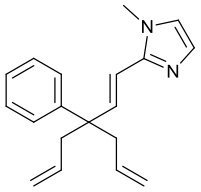

Obtained from **S4** (200mg, 0.99 mmol) following the representative procedure**,** except using 1,2-dimethylimidazole and **S24** was isolated as a yellow oil (254 mg, 86%). Afterwards, methanesulfonyl chloride (37 μL, 0.47 mmol) was added dropwise to a 0°C solution of **S24** (71mg, 0.24 mmol) and triethylamine (66 μL, 0.47 mmol) in DCM (0.50 mL). Afterwards, it was allowed to stir at r.t. for 2 hours. Afterwards, the crude mixture was partitioned between a saturated solution of $NaHCO_3$ and ethyl acetate. Extracted three times with ethyl acetate and the combined extracts was washed with $H_2O$, a saturated solution of brine, dried over $Na_2SO_4$, filtered and concentrated. Under $N_2$, the residue was dissolved in THF (0.5 mL). Cooled to 0$^o$C, NaHMDS (65 mg, 0.35 mmol) was added. It was then allowed to stir overnight at r.t. The reaction mixture was quenched with a saturated solution of $NaHCO_3$. The crude mixture was partitioned between water and ethyl acetate. Extracted three times with ethyl acetate and the combined extracts was washed with $H_2O$, a saturated solution of brine, dried over $Na_2SO_4$, filtered and concentrated. Purification by flash column chromatography (PE/EA : 1/1) afforded compound **135** as a clear oil (39 mg, 58 %): $^1$H NMR (500 MHz, $CDCl_3$): δ = 7.35 – 7.26 (m, 4H),

7.21 – 7.15 (m, 1H), 7.00 (s, 1H), 6.86 (d, *J* = 16.2 Hz, 1H), 6.81 (s, 1H), 6.25 (d, *J* = 16.1 Hz, 1H), 5.61 (ddt, *J* = 17.1, 10.1, 7.1 Hz, 2H), 5.08 – 4.98 (m, 4H), 3.59 (s, 3H), 2.66 (d, *J* = 7.1 Hz, 4H); $^{13}$C NMR (125 MHz, $CDCl_3$): δ = 145.5, 144.5, 141.7, 134.3, 128.3, 128.0, 127.4, 126.1, 121.0, 117.8, 114.9, 46.9, 42.2, 32.7; IR (neat): $\tilde{\nu}$ = 3346 (br w), 3073 (w), 3006 (w), 2977 (w), 2920 (w), 1638 (w), 1598 (w), 1515 (w), 1493 (w), 1483 (m), 1444 (m), 1410 (m), 1284 (m), 1187 (w), 1135 (w), 1082 (w), 1033 (w), 996 (m), 975 (m), 912 (s), 843 (w), 826 (w), 769 (m), 734 (m), 698 (s), 657 (w) cm$^{-1}$; MS (CI): calcd for ($C_{19}H_{22}N_2$ + H): 279.1856; found: 279.1854

**Preparation[32] of [Rh(coe)$_2$Cl]$_2$** – To a 3-neck round-bottomed flask containing $RhCl_3$•$3H_2O$ (175 mg, 0.84 mmol) were sequentially added degassed water (1 mL), degassed *i*PrOH (4 mL) and cyclooctene (0.56 mL, 4.30 mmol). The resulting dark red solution was heated under reflux for 2 hours. Afterwards, the resulting orange suspension was cooled to room temperature. The precipitate was collected by filtration, washed with cold ethanol, washed with petroleum ether and dried *in vacuo* to give $[Rh(coe)_2Cl]_2$ (165 mg, 28 %) as yellow solid. The purity of each batch of this pre-catalyst was assessed by elemental analysis (%) calcd for $C_{32}H_{50}Cl_2Rh_2$: C 53.57, H 7.87; found: C 52.23, H 7.62.

**Representative procedure for the rhodium-catalysed carbocyclisation of 1,6-dienes** – $[Rh(coe)_2Cl]_2$ (2.6 mg, 0.0036 mmol) and P(*p*$MeOC_6H_4)_3$ (5.1 mg, 0.0145 mmol) were added to a flame-dried J-Young Schlenk flask under $N_2$. THF (0.17 mL) was added and the red solution stirred at room temperature for 5 minutes. $AgBF_4$ (1.4 mg, 0.0073 mmol) in THF (0.1 mL) was added and stirred for 5 minutes. Then, under $N_2$, **126** (20 mg, 0.0726 mmol) in THF (0.4 mL) was added via cannula, the tube sealed and the reaction heated at 60°C for 17 hours. The reaction mixture was cooled to room temperature, filtered through a small plug of silica (using $CH_2Cl_2$ to rinse) and the solvent was removed under reduced pressure. Purification by flash

column chromatography (petroleum ether/Et2O, 25:1 → 20:1) afforded **127** as colourless oil (17.7 mg, 89%, **127**/**128** = 98:2).

**Compound 127**

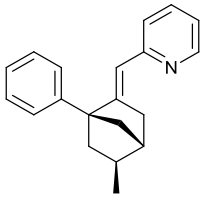

$^{1}$H NMR (500 MHz, $CDCl_3$): δ = 8.48 (ddd, *J* = 4.8, 1.7, 0.8 Hz, 1H), 7.50 (dt, *J* = 7.8, 1.8 Hz, 1H), 7.36–7.31 (m, 4H), 7.25–7.21 (m, 1H), 7.10 (d, *J* = 8.1 Hz, 1H), 6.96 (ddd, *J* = 7.4, 4.9, 0.9 Hz, 1H), 5.75 (t, *J* = 2.3 Hz, 1H), 2.86 (dt, *J* = 17.2, 3.5 Hz, 1H), 2.67 (dt, *J* = 17.2, 2.5 Hz, 1H), 2.23 (d, *J* = 4.2 Hz, 1H), 2.19 (ddd, *J* = 11.6, 8.5, 2.5 Hz, 1H), 1.97 (ddt, *J* = 9.8, 2.1, 1.0 Hz, 1H), 1.93–1.84 (m, 1H), 1.82 (ddd, *J* = 9.7, 3.3, 1.7 Hz, 1H), 1.54 (dd, *J* = 11.8, 4.8 Hz, 1H), 1.02 (d, *J* = 7.0 Hz, 3H); $^{13}$C NMR (125 MHz, $CDCl_3$): δ = 158.2, 157.6, 149.1, 142.8, 135.7, 128.19 (2C), 128.15 (2C), 126.3, 122.7, 120.1, 119.7, 59.6, 43.5, 42.6, 41.2, 40.9, 36.4, 22.3; IR (neat): $\tilde{\nu}$ = 3057 (w), 2951 (m), 2866 (w), 1655 (w), 1585 (s), 1559 (w), 1497 (w), 1471 (m), 1445 (w), 1427 (m), 1375 (w), 1346 (w), 1317 (w), 1260 (w), 1236 (w), 1220 (w), 1184 (w), 1148 (w), 1081 (w), 1061 (w), 1035 (w), 991 (w), 961 (w), 920 (w), 894 (w), 864 (w), 778 (w), 758 (m), 741 (m), 699 (s), 659 (w) $cm^{-1}$; HRMS (ESI): calcd for ($C_{20}H_{21}N$ + H): 276.1752; found: 276.1755.

**Compound 128**

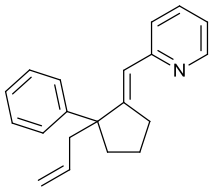

This compound could be isolated by preparative TLC during the optimisation study. Colourless oil; $^{1}$H NMR (500 MHz, $CDCl_3$): δ = 8.60 (ddd, *J* = 4.8, 1.7, 0.8 Hz, 1H), 7.61 (dt, *J* = 7.7, 1.8 Hz, 1H), 7.43–7.38 (m, 2H), 7.30–7.25 (m, 3H), 7.19–7.14 (m, 1H), 7.06 (ddd, *J* = 7.4, 4.9, 0.8 Hz,

1H), 6.44 (t, *J* = 2.5 Hz, 1H), 5.80–5.69 (m, 1H), 5.04 (ddt, *J* = 17.1, 1.9, 1.4 Hz, 1H), 5.00 (ddt, *J* = 10.2, 2.1, 1.0 Hz, 1H), 2.89–2.82 (m, 2H), 2.75 (ddt, *J* = 14.2, 7.4, 1.0 Hz, 1H), 2.64 (ddt, *J* = 14.2, 6.6, 1.3 Hz, 1H), 2.21 (ddd, *J* = 12.6, 6.5, 3.6 Hz, 1H), 1.87 (ddd, *J* = 12.7, 10.1, 7.1 Hz, 1H), 1.80–1.70 (m, 1H), 1.64–1.50 (m, 1H); $^{13}$C NMR (125 MHz, $CDCl_3$): δ = 157.2, 156.1, 149.2, 146.1, 135.9, 135.6, 128.1 (2C), 127.1 (2C), 125.9, 123.5, 123.4, 120.5, 117.2, 55.8, 44.9, 37.7, 32.3, 22.1; HRMS (ESI): calcd for ($C_{20}H_{21}N$ + H): 276.1752; found: 276.1751.

**Compound 140** and **141**

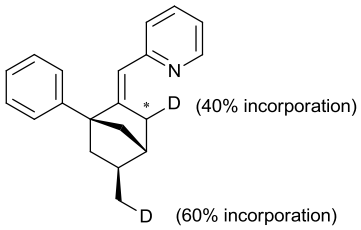


Obtained from **139** (0.071 mmol, 19.6 mg) following the representative procedure. Colourless oil (19.6 mg, quantitative); $^{1}$H NMR (500 MHz, $CDCl_3$): δ = 8.48 (ddd, *J* = 4.8, 1.6, 0.7 Hz, 1H), 7.51 (dt, *J* = 7.8, 1.8 Hz, 1H), 7.37–7.31 (m, 4H), 7.26–7.21 (m, 1H), 7.09 (d, *J* = 8.0 Hz, 1H), 6.96 (ddd, *J* = 7.4, 4.8, 0.9 Hz, 1H), 5.77–5.74 (m, 1H), 2.86 (dt, *J* = 17.3, 3.4 Hz, 0.8H), 2.67 (dt, *J* = 17.3, 2.5 Hz, 0.8H), 2.25–2.21 (m, 1H), 2.18 (ddd, *J* = 11.6, 8.5, 2.5 Hz, 1H), 1.99–1.94 (m, 1H), 1.93–1.84 (m, 1H), 1.82 (ddd, *J* = 9.7, 3.1, 1.5 Hz, 1H), 1.54 (dd, *J* = 11.8, 4.9 Hz, 1H), 1.05–0.98 (m, 2.4H); $^{2}$D NMR (77 MHz, $CDCl_3$): δ = 2.86 (s, 0.2D), 2.78 (s, 0.2D), 1.04 (s, 0.6D); $^{13}$C NMR (125 MHz, $CDCl_3$):^ δ = 158.20, [158.16], 157.6, 149.1, 142.7, 135.7, 128.17 (2C), 128.14 (2C), 126.3, 122.6, 120.1, [119.71], 119.66, 59.6, [43.47], 43.43, 42.51, [42.45], 41.2, 40.9, [40.5 (t, *J* = 20.3 Hz)], [36.32], 36.26, [22.3], 22.0 (t, *J* = 19.2 Hz); IR (neat): $\tilde{\nu}$ = 3057 (w), 3002 (w), 2949 (s), 2866 (w), 2165 (w), 1655 (m), 1602 (w), 1585 (s), 1559 (w), 1497 (w), 1471 (m), 1446 (w), 1427 (s), 1375 (w), 1318 (w), 1257 (w), 1234 (w), 1220 (w), 1148 (w), 1086 (w), 1060 (w), 1036 (w), 990 (w), 958 (w), 890 (w), 864 (w), 776 (w), 758 (s), 741 (m), 699 (s) cm$^{-1}$; MS (CI($CH_4$)):

*m*/*z* (rel. intensity): 277 (70) [M + H], 169 (100); HRMS (CI($CH_4$)): calcd for ($C_{20}H_{20}DN$ + H): 277.1815; found: 277.1805.

^ As easily established by comparison of $^{13}C$ NMR APT, HSQC and HMBC NMR of **127** and the mixture of **140** and **141**, the chemical shifts in brackets correspond to the mono-deuterated isomer for which the deuterium atom is incorporated at the position indicated by a star.

**Hydrochloride salt of compound 127**

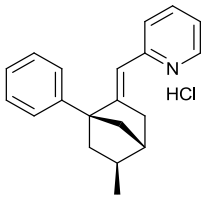


**127** (20 mg, 0.073 mmol) was dissolved in $Et_2O$ (0.2 mL). Then 3 drops of conc. HCl solution were added to give a white suspension. After mixing vigorously for 5 minutes, all volatiles were removed. The residue was dissolved in a vial with $CH_2Cl_2$ (1 mL) and then petroleum ether (5 mL) so that the two layers do not mix. All volatiles evaporated slowly at room temperature at atmospheric pressure to give brown crystals which were washed with diethyl ether to give brown crystals which were suitable for X-ray crystallography (15 mg, 66 %). mp.: 167–174°C (decomposition); $^1H$ NMR (500 MHz, $CDCl_3$): δ = 8.71–8.54 (m, 1H), 8.19–8.06 (m, 1H), 7.67–7.56 (m, 1H), 7.53–7.44 (m, 1H), 7.41 (t, *J* = 7.4 Hz, 2H), 7.34 (d, *J* = 7.6 Hz, 2H), 7.30 (t, *J* = 7.4 Hz, 3H), 6.37–6.29 (m, 1H), 2.94 (d, *J* = 16.1 Hz, 1H), 2.66 (d, *J* = 16.1 Hz, 1H), 2.34 (s, 1H), 2.28–2.19 (m, 1H), 2.06 (d, *J* = 9.7 Hz, 1H), 1.97–1.86 (m, 2H), 1.61 (dd, *J* = 12.0, 4.5 Hz, 1H), 1.05 (d, *J* = 6.8 Hz, 3H); $^{13}C$ NMR (125 MHz, $CDCl_3$): δ = 170.3, 151.6, 144.2, 141.5 (br), 140.1, 128.7 (2C), 128.0 (2C), 127.3, 124.8, 122.7, 111.9, 61.0, 43.3, 42.2, 41.3, 41.1, 35.9, 22.0; IR (neat): $\tilde{\nu}$ = 3086 (w), 3040 (w), 2958 (w), 2916 (w), 2862 (w), 2266 (m), 2209 (m), 2041 (m), 1980 (m), 1933 (m), 1650 (m), 1608 (s), 1528 (m), 1496 (m), 1456 (m), 1444 (m), 1399 (w), 1371 (m), 1323 (w), 1290 (m), 1251 (w), 1233 (w), 1155 (m), 1141 (w), 1096 (w), 1064 (w), 1038 (w), 1025 (w), 988 (m), 961 (w), 950 (w), 923 (w), 896 (w), 882 (w), 871 (w), 847 (w), 827

(w), 814 (w), 772 (s), 763 (s), 702 (s), 659 (w) $cm^{-1}$; elemental analysis (%) calcd for $C_{20}H_{22}ClN$: C 77.03, H 7.11, N 4.49; found: C 76.49, H 7.06, N 4.41.

**Compound 133e**

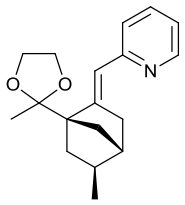


Obtained from **132e** (0.070 mmol, 20 mg) following the representative procedure. Colourless oil (18 mg, 88%); $^{1}H$ NMR (500 MHz, $CDCl_3$): δ = 8.54 (ddd, *J* = 4.8, 1.8, 0.8 Hz, 1H), 7.55 (dt, *J* = 7.7, 1.9 Hz, 1H), 7.22 (d, *J* = 8.1 Hz, 1H), 6.98 (ddd, *J* = 7.4, 4.9, 1.0 Hz, 1H), 6.79 (t, *J* = 2.3 Hz, 1H), 4.07–3.88 (m, 4H), 2.71 (dt, *J* = 17.1, 3.4 Hz, 1H), 2.61 (dt, *J* = 17.1, 2.5 Hz, 1H), 2.04 (d, *J* = 3.9 Hz, 1H), 1.74 (ddd, *J* = 9.6, 3.4, 1.8 Hz, 1H), 1.73–1.67 (m, 1H), 1.62 (ddd, *J* = 11.4, 8.4, 2.4 Hz, 1H), 1.45 (s, 3H), 1.44–1.38 (m, 2H), 0.97 (d, *J* = 6.9 Hz, 3H); $^{13}C$ NMR (125 MHz, $CDCl_3$): δ = 158.1, 152.8, 149.0, 135.7, 123.1, 120.2, 120.0, 110.9, 65.2, 64.5, 63.0, 42.3, 42.0, 38.9, 38.6, 35.8, 22.2, 21.7; IR (neat): $\tilde{\nu}$ = 3052 (w), 2950 (s), 2871 (m), 1650 (m), 1585 (s), 1558 (w), 1470 (m), 1428 (s), 1371 (m), 1321 (w), 1287 (w), 1264 (m), 1239 (w), 1216 (w), 1198 (s), 1161 (s), 1111 (m), 1090 (m), 1075 (w), 1063 (m), 1040 (s), 992 (w), 943 (w), 920 (w), 899 (m), 870 (m), 812 (w), 779 (m), 761 (w), 741 (m), 658 (w) $cm^{-1}$; HRMS ($CI(CH_4)$): calcd for ($C_{18}H_{23}NO_2$ + H): 286.1802; found: 286.1000.

**Compound 133f**

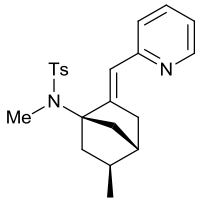


Compound prepared by Daniel J. Tetlow. Obtained from **132f** (0.146 mmol, 56 mg) following the representative procedure. Colourless gum (43 mg, 76%);^ $^{1}$H NMR (500 MHz, $CDCl_3$): δ = 8.54 (dd, *J* = 4.8 and 1.0 Hz, 1H), 7.73 (d, *J* = 8.1 Hz, 2H), 7.55 (td, *J* = 7.8, 1.8 Hz, 1H), 7.26 (d, *J* = 8.1 Hz, 2H), 7.13 (d, *J* = 7.9 Hz, 1H), 7.02 (ddd, *J* = 7.3, 4.8, 0.6 Hz, 1H), 6.38 (t, *J* = 2.2 Hz, 1H), 3.11 (s, 3H), 2.77–2.62 (m, 2H), 2.39 (s, 3H), 2.19 (ddd, *J* = 11.2, 8.4, 2.4 Hz, 1H), 1.97 (d, *J* = 2.6 Hz, 1H), 1.86 (d, *J* = 9.5 Hz, 1H), 1.81–1.72 (m, 1H), 1.58 (dd, *J* = 8.8, 5.0 Hz, 1H), 1.57–1.53 (m, 1H), 0.88 (d, *J* = 6.9 Hz, 3H); $^{13}$C NMR (125 MHz, $CDCl_3$): δ = 159.9, 149.7, 149.0, 142.8, 139.5, 135.9, 129.5 (2C), 126.8 (2C), 123.6, 120.4, 118.4, 74.9, 43.2, 39.81, 39.76, 38.9, 35.7, 35.4, 22.1, 21.4; IR (neat): $\tilde{\nu}$ = 2954 (w), 2923 (w), 2868 (w), 1666 (w), 1585 (m), 1560 (w), 1494 (w), 1470 (m), 1428 (m), 1377 (w), 1336 (s), 1306 (s), 1280 (w), 1225 (w), 1151 (s), 1119 (w), 1089 (s), 1042 (s), 1016 (w), 982 (w), 902 (m), 842 (s), 812 (s), 778 (m), 759 (w), 741 (m), 706 (w), 661 (s) $cm^{-1}$; HRMS (ESI): calcd for ($C_{22}H_{27}N_2O_2S$ + H): 383.1793; found: 383.1783.

^ Over time, we observed a small doublet appearing at 2.64 ppm (*J* = 5.4 Hz) in $^{1}$H NMR which could correspond to the *Me*-N of a minor impurity where the tosyl group is cleaved. A small peak (ESI) with the expected *m*/*z* = 228 [M – Ts + H] also confirms this analysis.

**Compound 133h**

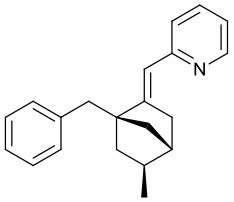


Obtained from **132h** (0.070 mmol, 20.3 mg) following the representative procedure, except that P(*p*MeOC$_6$H$_4$)$_3$ (3.6 mg, 0.0101 mmol) was used. Colourless oil. (17 mg, 83%, **133h**/**134h** = 95:5); $^1$H NMR (500 MHz, $CDCl_3$): δ = 8.55 (ddd, *J* = 4.9, 1.7, 0.8 Hz, 1H), 7.59 (dt, *J* = 7.7, 1.9 Hz, 1H), 7.29– 7.24 (m, 3H), 7.21–7.16 (m, 3H), 7.02 (ddd, *J* = 7.4, 4.9, 1.0 Hz, 1H), 6.44–6.40 (m, 1H), 3.05 (d, *J* = 13.4 Hz, 1H), 2.99 (d, *J* = 13.4 Hz, 1H), 2.67 (dt, *J* = 17.1, 3.4 Hz, 1H), 2.57 (dt, *J* = 16.9, 2.5 Hz, 1H), 1.98 (d, *J* = 4.1 Hz, 1H), 1.72–1.62 (m, 1H), 1.50 (ddd, *J* = 11.7, 8.5, 2.5 Hz, 1H), 1.33 (ddd, *J* = 9.8, 3.1, 1.7 Hz, 1H), 1.26–1.21 (m, 1H), 1.06 (dd, *J* = 11.8, 4.9 Hz, 1H), 0.77 (d, *J* = 6.9 Hz, 3H); $^{13}$C NMR (125 MHz, $CDCl_3$): δ = 157.7, 156.9, 149.2, 139.7, 135.8, 130.3 (2C), 127.8 (2C), 125.8, 122.5, 120.2, 117.7, 55.3, 42.7, 41.8, 41.7, 39.3, 38.2, 36.0, 22.0; IR (neat): $\tilde{\nu}$ = 3061 (w), 3027 (w), 3002 (w), 2950 (m), 2866 (w), 1655 (m), 1603 (w), 1585 (s), 1559 (w), 1496 (w), 1471 (m), 1454 (w), 1428 (m), 1375 (w), 1346 (w), 1308 (w), 1276 (w), 1221 (w), 1149 (w), 1096 (w), 1062 (w), 1031 (w), 991 (w), 889 (w), 858 (w), 804 (w), 771 (w), 754 (m), 741 (w), 702 (s), 658 (w) cm$^{-1}$; HRMS (ESI): calcd for ($C_{21}H_{24}N$ + H): 290.1911; found: 290.1909; elemental analysis (%) calcd for $C_{21}H_{23}N$: C 87.15, H 8.01, N 4.84; found: C 86.55, H 8.13, N 4.63.

**Compound 133i**

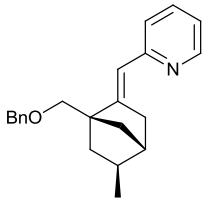


Obtained from **132i** (0.070 mmol, 22.4 mg) following the representative procedure (15.9 mg, 71%, **133i**/**134i** = 2:1). Isomers **133i** and **134i** could be separated by preparative TLC (petroleum ether/EtOAc = 14:1). Colourless oil; $^{1}$H NMR (500 MHz, $CDCl_3$): δ = 8.54–8.49 (m, 1H), 7.56 (dt, *J* = 7.7, 1.8 Hz, 1H), 7.38–7.30 (m, 4H), 7.29–7.24 (m, 1H), 7.21 (d, *J* = 8.0 Hz, 1H), 6.99 (ddd, *J* = 7.4, 4.9, 0.7 Hz, 1H), 6.25–6.23 (m, 1H), 4.60 (s, 2H), 3.77 (d, *J* = 9.6 Hz, 1H), 3.73 (d, *J* = 9.6 Hz, 1H), 2.68 (dt, *J* = 17.1, 3.5 Hz, 1H), 2.53 (dt, *J* = 17.1, 2.5 Hz, 1H), 2.08 (d, *J* = 4.1Hz, 1H), 1.77–1.68 (m, 1H), 1.64 (ddd, *J* = 9.7, 3.2, 1.6 Hz, 1H), 1.56 (ddd, *J* = 11.9, 8.5, 2.4 Hz, 1H), 1.41–1.36 (m, 1H), 1.26 (dd, *J* = 11.9, 4.9 Hz, 1H), 0.98 (d, *J* = 7.0 Hz, 3H); $^{13}$C NMR (125 MHz, $CDCl_3$): δ = 157.6, 154.1, 149.1, 138.8, 135.8, 128.3 (2C), 127.5 (2C), 127.4, 122.5, 120.2, 117.7, 73.4, 71.2, 55.3, 42.5, 41.4, 41.2, 38.8, 36.0, 22.2; IR (neat): $\tilde{\nu}$ = 3058 (w), 303 (w), 3002 (w), 2950 (s), 2864 (m), 1720 (w), 1658 (m), 1585 (s), 1559 (w), 1495 (w), 1470 (m), 1454 (m), 1428 (s), 1364 (w), 1271 (w), 1205 (w), 1148 (w), 1093 (s), 1028 (w), 927 (w), 889 (w), 857 (w), 739 (s), 697 (m) ; MS (ESI): calcd for (C22H25NO + H): 320.2014; found: 320.2013.

**Compound 134i**

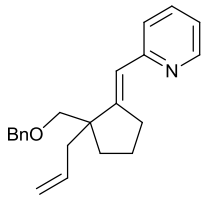


Colourless oil; $^{1}$H NMR (500 MHz, $CDCl_3$): δ = 8.55 (ddd, *J* = 4.7, 1.6, 0.8 Hz, 1H), 7.58 (dt, *J* = 7.8, 1.8 Hz, 1H), 7.33–7.28 (m, 4H), 7.27–7.20 (m, 2H), 7.02 (ddd, *J* = 7.5, 4.8, 1.0 Hz, 1H), 6.37 (t, *J* = 2.4 Hz, 1H), 5.85 – 5.73 (m, 1H), 5.08 – 4.97 (m, 2H), 4.53 (d, *J* = 12.4 Hz, 1H), 4.49 (d, *J* =

12.4 Hz, 1H), 3.36 (s, 2H), 2.90–2.81 (m, 1H), 2.80–2.70 (m, 1H), 2.47 (dd, *J* = 13.8, 8.0 Hz, 1H), 2.35 (dd, *J* = 13.8, 6.6 Hz, 1H), 1.84–1.62 (m, 4H); $^{13}$C NMR (125 MHz, $CDCl_3$): δ = 157.5, 155.2, 149.1, 138.8, 135.8, 135.4, 128.3 (2C), 127.4 (2C), 127.3, 123.2, 122.0, 120.4, 117.3, 76.4, 73.3, 51.5, 41.5, 33.5, 33.4, 23.5; IR (neat): $\tilde{\nu}$ = 3065 (w), 2020 (w), 3004 (w), 2951 (w), 2856 (w), 1647 (w), 1584 (m), 1559 (w), 1496 (w), 1471 (m), 1454 (w), 1427 (m), 1360 (w), 1287 (w), 1218 (w), 1204 (w), 1148 (w), 1094 (s), 1028 (w), 991 (w), 911 (m), 890 (w), 864 (w), 818 (w), 775 (w), 736 (s), 696 (s) cm$^{-1}$; elemental analysis (%) calcd for $C_{22}H_{25}NO$: C 82.72, H 7.89, N 4.38; found: C 82.64, H 7.99, N 4.12.

**Compound 133j**

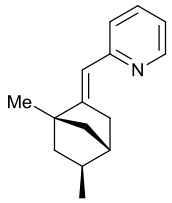


Obtained from **132j** (0.080 mmol, 17.1 mg) following the representative procedure, except that P(*p*MeO$C_6H_4$)$_3$ (3.6 mg, 0.0101 mmol) was used. Colourless oil (12.3 mg, 72%, **133j**/**134j** = 3:1, not separable);^ $^1$H NMR (500 MHz, $CDCl_3$): δ = 8.53–8.50 (m, 1H), 7.56 (dt, *J* = 7.8, 1.8 Hz, 1H), 7.27–7.22 (m, 1H), 6.98 (ddd, *J* = 7.4, 4.9, 0.9 Hz, 1H), 6.27–6.24 (m, 1H), 2.64 (dt, *J* = 17.1, 3.5 Hz, 1H), 2.50 (dt, *J* = 17.1, 2.5 Hz, 1H), 2.04 (d, *J* = 4.2 Hz, 1H), 1.76–1.62 (m, 1H), 1.57 (ddd, *J* = 11.8, 8.5, 2.5, 1H), 1.52 (ddd, *J* = 9.6, 3.1, 1.5 Hz, 1H), 1.31 (s, 3H), 1.27–1.22 (m, 1H), 1.04 (dd, *J* = 11.9, 4.9 Hz, 1H), 0.96 (d, *J* = 7.1 Hz, 3H); $^{13}$C NMR (125 MHz, $CDCl_3$): δ = 157.8, 157.5, 149.1, 135.8, 122.3, 120.0, 117.0, 51.0, 46.0, 42.7, 42.6, 41.0, 36.8, 22.3, 18.1; IR (neat): $\tilde{\nu}$ = 3073 (w), 3003 (w), 2950 (s), 2868 (w), 1731 (w), 1657 (m), 1585 (s), 1559 (w), 1471 (m), 1463 (m), 1427 (s), 1375 (w), 1316 (w), 1279 (w), 1265 (w), 1227 (w), 1149 (w), 1088 (w), 1061 (w), 989 (w), 966 (w), 912 (w), 887 (w), 858 (w), 823 (w), 775 (m), 740 (m) cm$^{-1}$; HRMS (CI($CH_4$)): calcd for ($C_{15}H_{19}N$ + H): 214.1590; found: 214.1594.

^IR recorded and HRMS recorder on the **133j**/**134j mixture**

**Compound 134j**

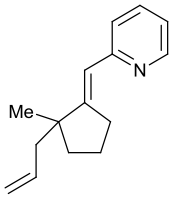


$^{1}$H NMR (500 MHz, $CDCl_3$): δ = 8.57–8.53 (m, 1H), 7.61 – 7.54 (m, 1H), 7.27 – 7.22 (m, 1H), 7.00 (ddd, *J* = 7.5, 5.0, 0.9 Hz, 1H), 6.29 (t, *J* = 2.4 Hz, 1H), 5.84–5.73 (m, 1H), 5.06–4.98 (m, 2H), 2.92–2.82 (m, 1H), 2.80–2.69 (m, 1H), 2.26 – 2.15 (m, 2H), 1.80–1.63 (m, 3H), 1.48–1.41 (m, 1H), 1.13 (s, 3H); $^{13}$C NMR (125 MHz, $CDCl_3$): δ = 159.3, 157.7, 149.1, 135.8, 135.6, 122.9, 120.5, 120.2, 116.9, 47.1, 45.4, 38.0, 32.6, 26.6, 23.0.

**Compound 137**

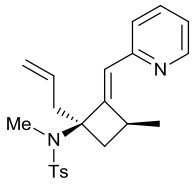


Compound prepared by Daniel J. Tetlow. Obtained from **132f** (0.117 mmol, 45 mg) using the representative procedure for the Rh(I)- catalysed cycloisomerisation, except that the reaction was stopped after 30 minutes heating. Purification by flash column chromatography (petroleum ether/EtOAc, 10:1) yielded the title compound as colourless oil (15 mg, 33%). $^{1}$H NMR (500 MHz, $CDCl_3$): δ = 8.53 (ddd, *J* = 4.7, 1.6 and 0.7 Hz, 1H), 7.72 (d, *J* = 8.2 Hz, 2H), 7.59 (td, *J* = 7.7, 1.6 Hz, 1H), 7.25 (d, *J* = 8.0 Hz, 2H), 7.18 (d, *J* = 7.8 Hz, 1H), 7.06 (ddd, *J* = 7.5, 4.7, 0.8 Hz, 1H), 6.50 (d, *J* = 2.2 Hz, 1H), 5.90–5.79 (m, 1H), 5.18–5.12 (m, 1H), 5.09 (dt, *J* = 10.2, 0.8 Hz, 1H), 3.26–3.15 (m, 1H), 2.92 (s, 3H), 2.94–2.86 (m, 1H), 2.77 (dd, *J* = 13.9, 8.5 Hz, 1H), 2.55 (dd, *J* = 12.8, 9.0 Hz, 1H), 2.38 (s, 3H), 2.27 (dd, *J* = 12.8, 5.3 Hz, 1H), 1.12 (d, *J* = 7.0 Hz, 3H); $^{13}$C NMR (125 MHz, $CDCl_3$): δ = 155.2, 152.0, 149.5, 143.0, 138.6, 136.1, 133.8, 129.4 (2C), 127.3 (2C), 127.1, 123.0, 121.4, 118.9, 68.6, 42.5, 37.0, 34.6, 33.6, 21.5, 18.5; IR (neat) $\tilde{\nu}$ = 3074 (w),

2958 (w), 2869 (w), 1665 (w), 1638 (w), 1584 (m), 1563 (w), 1494 (w), 1469 (m), 1430 (m), 1329 (s), 1304 (m), 1289 (m), 1270 (w), 1214 (w), 1184 (w), 1150 (s), 1086 (s), 1018 (w), 993 (w), 893 (s), 846 (m), 813 (s), 743 (s), 707 (m), 688 (w), 658 (s) $cm^{-1}$; MS (ESI): *m/z* (rel. intensity): 421 (12) [M + K], 405 (27) [M + Na], 383 (100) [M + H]; HRMS (ESI) calcd for ($C_{22}H_{26}N_2O_2S$ + H): 383.1793, found: 383.1792.

Table 14 Crystal data and structure refinement for Hydrochloride salt of **127**

| | | |
|---|---|---|
| Empirical formula | $C_{20}H_{22}NCl$ | |
| Formula weight | 311.84 | |
| Temperature | 100.01°K | |
| Crystal system | orthorhombic | |
| Space group | $Pca2_1$ | |
| Unit cell dimensions | a = 7.0429(4) Å | α = 90.00° |
| | b = 14.2625(9) Å | β = 90.00° |
| | c = 16.0706(10) Å | γ = 90.00° |
| Volume | 1614.28(17) $Å^3$ | |
| Z | 4 | |
| Density (calculated) | 1.283 $mg/mm^3$ | |
| Absorption coefficient | 2.038 $mm^{-1}$ | |
| F(000) | 664.0 | |
| Crystal size | 0.3 × 0.145 × 0.045 $mm^3$ | |
| Radiation | Cu Kα (λ = 1.54178) | |
| 2Θ range for data collection | 6.2 to 144.52° | |
| Index ranges | $-7 \leq h \leq 8$, $-17 \leq k \leq 17$, $-19 \leq l \leq 19$ | |
| Reflections collected | 17764 | |
| Independent reflections | 3082[R(int) = 0.0205] | |
| Data/restraints/parameters | 3082/1/200 | |
| Goodness-of-fit on $F^2$ | 1.065 | |
| Final R indexes [I>=2σ (I)] | $R_1$ = 0.0259, $wR_2$ = 0.0693 | |
| Final R indexes [all data] | $R_1$ = 0.0259, $wR_2$ = 0.0693 | |
| Largest diff. peak/hole | 0.24/-0.27 e.$Å^{-3}$ | |
| Flack parameter | 0.040(10) | |

## 4.10 References


1.) For examples in most recent reviews, see: a) X. Chen, K. M. Engle, D.H. Wang, J. Q. Yu, *Angew. Chem. Int. Ed*. **2009**, *48*, 5094; b) L. Ackermann, R. Vicente, A. R. Kapdi, *Angew. Chem. Int. Ed.* **2009**, *48*, 9792; c) K. Fagnou, *Top. Curr. Chem*. **2010**, *292*, 35; d) D. A. Colby, R.G. Bergman, J. A. Ellman, *Chem. Rev*. **2010**, *110*, 624; e) T.W. Lyons,M. S. Sanford, *Chem. Rev.* **2010**, *110*, 1147; f) C.-L. Sun, B.-J. Li, Z.-J. Shi, *Chem. Commun*. **2010**, *46*, 677; g) C. S. Yeung, V.M. Dong, *Chem. Rev*. **2011**, *111*, 1215; h) P. B. Arockiam, C. Bruneau, P. H. Dixneuf, *Chem. Rev.* **2012**, *112*, 5879; i) N. Kuhl, M. N. Hopkinson, J. Wencel-Delord, F. Glorius, *Angew. Chem. Int. Ed.* **2012**, *51*, 10236; j) J. Yamaguchi, A.D. Yamaguchi, K. Itami, *Angew. Chem. Int. Ed.* **2012**, *51*, 8960; k)G. Song, F. Wang, X. Li, *Chem. Soc. Rev*. **2012**, *41*, 3651.

2a.) T. V. Rajanbabu, *Chem. Rev*. **2003**, *103*, 2845; b) T. V. Rajanbabu, *Synlett* **2009**, 853; c) G. Hilt, *Eur. J. Org. Chem*. **2012**, 4441.

3.) M. Brookhart, S. Sabo-Etiennel, *J. Am. Chem. Soc.* **1991**, *113*, 2777–2779.

4.) Y. Ura, H. Tsujita, K. Wada, T. Kondo, T. Mitsudo, *J. Org. Chem.* **2005**, *70*, 6623–6628.

5.) Y. Hiroi, N. Komine, S. Komiya, M. Hirano, *Org. Lett.* **2013**, *15*, 2486–2489.

6.) S. Ogoshi, T. Haba, M. Ohashi, *J. Am. Chem. Soc.* **2009**, *131*, 10350–10351.

7.) H. Tsujita, Y. Ura, S. Matsuki, K. Wada, T. Mitsudo, T. Kondo, *Angew. Chem. Int. Ed.* **2007**, *46*, 5160–5163.

8.) Q.-S. Wang, J.-H. Xie, L.-C. Guo, Q.-L. Zhou, *Org. Biomol. Chem.* **2012**, *10*, 43–45.

9.) Y. Hatamoto, S. Sakaguchi, Y. Ishii, *Org. Lett.* **2004**, *6*, 4623–4625.

10.) Y.-H. Xu, J. Lu, T.-P. Loh, *J. Am. Chem. Soc.* **2009**, *131*, 1372–1373.

11.) Y.-H. Xu, W.-J. Wang, Z.-K. Wen, J. J. Hartley, T.-P. Loh, *Tetrahedron Lett.* **2010**, *51*, 3504–3507.

12.) S. Mochida, K. Hirano, T. Satoh, M. Miura, *J. Org. Chem.* **2009**, *74*, 6295–6298.

13a.) S. Komiya, A. Yamamoto, *Chem. Lett.* **1975**, 475–478; b) S. Komiya, T. Ito, M. Cowie, A. Yamamoto, J. A. Ibers, *J. Am. Chem. Soc.* **1976**, *98*, 3874–3884.

14.) B. M. Trost, K. Imi, I. W. Davies, *J. Am. Chem. Soc.* **1995**, *117*, 5371–5372.

15a.) F. Kakiuchi, Y. Tanaka, T. Sato, N. Chatani, S. Murai, *Chem. Lett.* **1995**, 679–680; b) T. Sato, F. Kakiuchi, N. Chatani, S. Murai, *Chem. Lett.* **1998**, 893–894.

16.) F. Kakiuchi, T. Sato, K. Igi, N. Chatani, S. Murai, *Chem. Lett.* **2001**, 386–387.

17.) a) M.-O. Simon, R. Martinez, J.-P. Genêt, S. Darses, *Adv. Synth. Catal.* **2009**, *351*, 153–157; b) M.-O. Simon, J.-P. Genet, S. Darses, *Org. Lett.* **2010**, *12*, 3038–3041.

18.) C.-H. Jun, C. W. Moon, Y.-M. Kim, H. Lee, J. H. Lee, *Tetrahedron Lett.* **2002**, *43*, 4233–4236.

19.) D. A. Colby, R. G. Bergman, J. A. Ellman, *J. Am. Chem. Soc.* **2006**, *128*, 5604–5605.

20.) A. S. Tsai, R. G. Bergman, J. A. Ellman, *J. Am. Chem. Soc.* **2008**, *130*, 6316–6317.

21.) F. Mo, G. Dong, *Science* **2014**, *345*, 68–72.

22.) Y.-G. Lim, J.-B. Kang, Y. H. Kim, *Chem. Commun.* **1996**, 585–586; (b) Y.-G. Lim, J.-B. Kang, Y. H. Kim, *J. Chem. Soc., Perkin Trans. 1* **1998**, 699–707.

23.) Y.-G. Lim, J.-S. Han, J.-B. Kang, *Bull. Korean Chem. Soc.* **1998**, *19*, 1143–1145.

24.) Y.-G. Lim, J.-S. Han, B. T. Koo, J.-B. Kang, *Bull. Korean Chem. Soc.* **1999**, *20*, 1097–1100.

25.) Y.-G. Lim, J.-B. Kang, B. T. Tak, *Tetrahedron Lett.* **1999**, *40*, 7691–7694.

26.) a) N. Fujii, F. Kakiuchi, N. Chatani, S. Murai, *Chem. Lett.* **1996**, 939–940; b) N. Fujii, F. Kakiuchi, A. Yamada, N. Chatani, S. Murai, *Chem. Lett.* **1997**, 425–426; c) N. Fujii, F. Kakiuchi, A. Yamada, N. Chatani, S. Murai, *Bull. Chem. Soc. Jpn.* **1998**, *71*, 285–298.

27.) C. Aïssa, A. Fürstner, *J. Am. Chem. Soc.* **2007**, *129*, 14836–14837.

28.) N. Fujii, F. Kakiuchi, A. Yamada, N. Chatani, S. Murai, *Bull. Chem. Soc. Jpn.* **1998**, *71*, 285–298.

29a.) T. Hayashi, *Acc. Chem. Res.* **2000**, *33*, 354–362; b.) Z. Hua, V. C. Vassar, H. Choi, I. Ojima, *Proc. Natl. Acad. Sci. U. S. A.* **2004**, *101*, 5411–5416; c.) R. Martin, S. L. Buchwald, *Acc. Chem.*

*Res.* **2008**, *41*, 1461–1473; d.) J. Jover, N. Fey, J. N. Harvey, G. C. Lloyd-Jones, A. G. Orpen, G. J. J. Owen-Smith, P. Murray, D. R. J. Hose, R. Osborne, M. Purdie, *Organometallics* **2010**, *29*, 6245–6258; e.) I. G. Rios, A. Rosas-Hernandez, E. Martin, *Molecules* **2011**, *16*, 970–1010; f.) D. S. Surry, S. L. Buchwald, *Chem. Sci.* **2011**, *2*, 27–50; g.) T. Saget, S. J. Lemouzy, N. Cramer, *Angew. Chem. Int. Ed.* **2012**, *51*, 2238–2242.

30.) S. L. Huang, K. Omura, D. Swern, *J. Org. Chem.* **1976**, *41*, 3329–3331.

31a.) A. P. Krapcho, *Synthesis* **1982**, 805–822; b.) A. P. Krapcho, *Synthesis* **1982**, 893–914.

32.) Adapted from I. Ojima, A. T. Vu, D. Bonafoux, *Science of Synthesis* **2001**, Georg Thieme Verlag KG.